National Aeronautics and Space Administration

Program Annual Technology Report

Cosmic Origins Program Office
Astrophysics Division
Science Mission Directorate

October 2017

COR Program

Program Office

Program Manager: *Mansoor Ahmed (mansoor.ahmed@nasa.gov)*
Deputy Program Manager: *Azita Valinia (azita.valinia-1@nasa.gov)*
Chief Scientist: *Susan Neff (susan.g.neff@nasa.gov)*
Deputy Chief Scientist: *Erin Smith (erin.c.smith@nasa.gov)*
Chief Technologist: *Harley Thronson (harley.a.thronson@nasa.gov)*
Technology Development Manager: *Thai Pham (thai.pham@nasa.gov)*
PATR Production Lead and Editor: *Opher Ganel (opher.ganel@nasa.gov)*
PATR Co-Editor: *Russell Werneth (russell.l.werneth@nasa.gov)*
PATR Graphics: *Herbert Eaton (herbert.e.eaton@nasa.gov)*
DeLee Smith (delee.i.smith@nasa.gov)
PATR Admin Support: *Kay Deere (kay.m.deere@nasa.gov)*

Headquarters

Program Executive: *Shahid Habib (shahid.habib-1@nasa.gov)*
Program Scientist: *Mario Perez (mario.perez@nasa.gov)*
Deputy Program Scientist: *Kartik Sheth (kartik.sheth@nasa.gov)*

http://cor.gsfc.nasa.gov

The report cover reflects the breadth of science topics pursued by the Cosmic Origins Program. Modern astronomy has expanded far beyond objects visible to the naked eye. For example, the Hubble Space Telescope has captured countless images of distant objects, seen on the top surfaces of the three-dimensional "COR" letters on the cover, including e.g. the Eagle Nebula, some 7000 light-years from Earth shown on the "C." The Cosmic Web, the large-scale filamentary structure of the universe seen at the top half of the cover, is believed to contain about half of the "ordinary" matter in the universe. Stellar jets, such as the one seen at the middle right of the cover, are also of great interest to COR science.

The Strategic Astrophysics Technology (SAT) project images, shown on the edges of the three-dimensional letters, demonstrate our ongoing efforts to identify and develop the technologies that will advance humankind's ability to observe and understand our universe.

Table of Contents

COR 2017 PATR Executive Summary

What is the Cosmic Origins (COR) Program?

From ancient times, humans have looked up at the night sky and wondered: Are we alone? **How did the universe come to be?** How does the universe work? COR focuses on the second question. Scientists investigating this broad theme seek to understand the origin and evolution of the universe from the Big Bang to the present day, determining how the expanding universe grew into a grand cosmic web of dark matter enmeshed with galaxies and pristine gas, forming, merging, and evolving over time. COR also seeks to understand how stars and planets form from clouds in these galaxies to create the heavy elements that are essential to life, starting with the first generation of stars to seed the universe, and continuing through the birth and eventual death of all subsequent generations of stars. The COR Program's purview includes the majority of the field known as astronomy.

In 2015, the Laser Interferometer Gravitational-Wave Observatory (LIGO) recorded the first direct measurement of long-theorized gravitational waves (GWs). Another surprising recent discovery is that the universe is expanding at an ever-accelerating rate, the first hint of so-called "dark energy," estimated to account for 75% of mass-energy in the universe. Dark matter, so called because we only observe its effects on regular matter, accounts for another 20%, leaving only 5% for regular matter and energy. Scientists now also search for so-called "B-mode" polarization in the cosmic microwave background to support the notion that in the split-second after the Big Bang, the universe inflated faster than the speed of light! The most exciting aspect of this grand enterprise today is the extraordinary rate at which we can harness technologies to enable these key discoveries.

Why is COR Technology Development Critical?

A 2008 Space Review paper noted that robust technology development and maturation is crucial to reducing flight project schedule and cost over-runs: "*…in the mid-1980s, NASA's budget office found that during the first 30 years of the civil space program, no project enjoyed less than a 40% cost overrun unless it was preceded by an investment in studies and technology of at least 5 to 10% of the actual project budget that eventually occurred*" [1]. Such technology maturation program is most efficiently addressed through focused R&D projects, rather than in flight projects, where "marching armies" make the cost of delays unacceptably high. The National Academies of Science 2010 Decadal Survey, "*New Worlds, New Horizons in Astronomy and Astrophysics*" (NWNH) stressed that "*Technology development is the engine powering advances in astronomy and astrophysics… Failure to develop adequately mature technology prior to a program start also leads to cost and schedule overruns*" [2].

NASA requires flight projects to demonstrate technology readiness level (TRL) 6* for required technologies by their preliminary design review. However, this can only occur if we correctly identify and adequately fund development of relevant "blue sky" technologies to TR 3†, and then mature them to TRL 5‡ or 6, across the so-called "mid-TRL gap," where sustained funding frequently falls short.

---

* TRLs are fully described in NPR 7123.1B, Appendix E, with TRL definitions reproduced in Appendix A below; TRL 6 is defined as: *"System/sub-system model or prototype demonstration in a relevant environment."*

† TRL 3 is defined as: "*Analytical and experimental critical function and/or characteristic proof-of-concept.*"

‡ TRL 5 is defined as: "*Component and/or breadboard validation in relevant environment.*"

What's in this Report? What's New?

This seventh Program Annual Technology Report (PATR) summarizes the Program's technology development activities for fiscal year (FY) 2017. It lists technology gaps identified by the COR community and two mission-concept studies with priorities assigned by the COR Technology Management Board (TMB; see p. 22). Following this year's prioritization, the Program Office recommends that NASA Astrophysics Division at HQ solicit and fund the maturation of the following technologies with the highest priority:

- High-reflectivity broadband far-ultraviolet (Far-UV) to near-infrared (Near-IR) mirror coatings;
- Large-format, low-noise and ultralow-noise far-infrared (Far-IR) direct detectors;
- High-performance, sub-Kelvin coolers;
- Heterodyne Far-IR detector arrays and related technologies;
- Large-format, high-dynamic-range UV detectors;
- Cryogenic readouts for large-format Far-IR detectors;
- Warm readout electronics for large-format Far-IR detectors; and
- Large cryogenic optics for the Far IR.

These recommendations represent technologies most critical for substantive near-term progress on strategic priorities. They take into account technology development needs identified by the Science and Technology Definition Teams (STDTs) studying the Origins Space Telescope (OST, formerly the Far-IR Surveyor) and the Large UV/Optical/IR (LUVOIR) Surveyor. These STDTs, along with those studying Lynx (formerly the X-Ray Surveyor) and a Habitable Exoplanet (HabEx) imaging mission, were charged by the Astrophysics Division Director to develop the science case, technology assessment, design reference mission with strawman payload, and cost assessment. This is being done in preparation for the upcoming 2020 Astronomy and Astrophysics Decadal Survey. These Surveyors are three of five described in the Astrophysics Roadmap, "*Enduring Quests, Daring Visions*," released in December 2013, while HabEx was described in the NWNH.

Meanwhile, the Program is pleased to announce four newly awarded COR Strategic Astrophysics Technology (SAT) projects for FY-2018 start (alphabetically, by Principal Investigator, PI):

- "Ultrasensitive Bolometers for Far-IR Spectroscopy at the Background Limit," Charles Bradford, JPL;
- "Development of Digital Micromirror Devices for Far-UV Applications," Zoran Ninkov, RIT;
- "High Performance Sealed Tube Cross Strip Photon Counting Sensors for UV-Vis Astrophysics Instruments," Oswald Siegmund, U.C. Berkeley; and
- "Development of a Robust, Efficient Process to Produce Scalable, Superconducting kilopixel Far-IR Detector Arrays," Johannes Staguhn, JHU.

Including these, the Astrophysics Division has awarded 22 COR SAT projects to date, funded by COR Supporting Research and Technology (SR&T), and intended to develop telescopes, optics, coatings, and detectors from the Far-IR to the Far-UV, applicable to strategic COR missions. Eight projects continue from previous years, each reporting significant progress. Along with two new projects begun in FY 2017 that continue previous efforts, this PATR reports on the progress, current status, and planned activities for 10 projects funded in FY 2017. We thank the PIs for their informative progress reports (Appendix B – Quad Charts, p. 64; Appendix C – Development Status, p. 75), and welcome our new awardees, one of whom is a returning SAT PI (abstracts of the new SATs are included at the end of Appendix C).

The following are examples where COR-funded technologies were infused, or are planned to be infused, into projects and missions:

- TES bolometer detector was selected to support the Stratospheric Observatory for Infrared Astronomy (SOFIA) High-resolution Airborne Wide-bandwidth Camera (HAWC) instrument (deployed 2015);
- High-efficiency Solid-state Photon-counting Ultraviolet Detector (SPUD) will be flight-tested on the Faint Intergalactic medium Redshifted Emission Balloon (FIREBall) (2017 launch);
- High-reflectivity UV coatings were used to coat optics for Ionospheric Connection (ICON) and Global-scale Observations of the Limb and Disk (GOLD) missions (2017 planned launches);
- COR technology funding made possible the selection of the HIgh-Resolution Mid-infrarEd Spectrometer (HIRMES) for development as a third-generation facility for SOFIA (2019 deployment); and
- The Wide-Field Infrared Survey Telescope (WFIRST) project adopted the H4RG Near-IR detector to address some of the most enduring questions in astrophysics (mid-2020s launch).

1. Program Science Overview

The goal of the COR Program is to understand the origin and evolution of the universe from the Big Bang to the present day. On the largest scale, COR's broad-reaching science question is to determine how the expanding universe grew into a grand cosmic web of dark matter enmeshed with galaxies and pristine gas, forming, merging, and evolving over time. COR also seeks to understand how stars and planets form from clouds in these galaxies; how stars create the heavy elements essential to life – starting with the first generation of stars to seed the universe, and continuing through the birth and death of stars to today. Many of the topics thought of throughout history as astronomy fall within the purview of the COR Program.

Background

The Program encompasses multiple scientific missions aimed at meeting Program objectives, each with unique scientific capabilities and goals. The Program was established to integrate those space, suborbital, and ground activities into a cohesive effort that enables each project to build on the technological and scientific legacy of its contemporaries and predecessors. Each project operates independently to achieve its unique set of mission objectives, which contribute to the overall Program objectives.

Currently Operating COR missions:

Hubble Space Telescope (HST)

The *Hubble Space Telescope's* launch in 1990 began one of NASA's most successful and long-lasting science missions. Now into its 28th year of operations, including five highly successful servicing missions, HST relayed over a million observations back to Earth, shedding light on many of the great mysteries of astronomy. HST has helped determine the age of the universe, peered into the hearts of quasars, studied galaxies in all stages of evolution, found protoplanetary disks where gas and dust around young stars serve as birthing grounds for new planets, and provided key evidence for the existence of dark energy.

Spitzer Space Telescope

Spitzer, which is approaching the 14th anniversary of its launch, provides sensitive IR observations that allow scientists to peer into cosmic regions hidden from optical telescopes, such as dusty stellar nurseries, centers of galaxies, and still-forming planetary systems. Many of its investigations have focused on objects that emit very little visible light, including brown dwarf stars, extra-solar planets, and giant molecular clouds. Although the primary phase of Spitzer's mission ended in 2009 with the exhaustion of its onboard cryogen, the Spitzer "warm" mission continues valuable work on COR science goals.

Stratospheric Observatory for Infrared Astronomy (SOFIA)

SOFIA, the world's largest airborne observatory is operated as a partnership between NASA and the German Aerospace Research Center (DLR), performing imaging and spectroscopy across the IR spectrum. SOFIA was declared fully operational in May 2014. The SOFIA Program Office and aircraft are based at NASA's Armstrong Flight Research Center (AFRC), with science mission operations based at NASA's Ames Research Center (ARC). SOFIA is managed outside the COR program; however, because SOFIA science is well-aligned with COR science, with SOFIA representing an important platform for maturing COR technologies that may be applicable to future space missions, certain SOFIA science objectives are considered strategic in relation to applicable prioritization criteria described in Section 3.

Herschel Space Observatory (HSO)

The European Space Agency (ESA) *Herschel Space Observatory* has revealed new information about the earliest, most distant stars and galaxies, as well as those forming and evolving closer to home. NASA contributed significant portions of HSO's instrumentation, data processing, and science analyses. HSO was decommissioned in June 2013, but data refinement and analysis continues through 2017.

Explorer Missions:

The NWNH rightfully called NASA's Explorer program "a crown jewel of NASA space sciences." Explorers play an important role in furthering COR science goals and training future instrumentalists. Past Explorers relevant primarily to COR science include the Far-Ultraviolet Spectroscopic Explorer (FUSE), the Galaxy Evolution Explorer (GALEX), and the Wide-field Infrared Survey Explorer (WISE). Explorer missions do not have the resources or schedule for technology development, and are not considered "strategic" when setting technology-development priorities. However, Explorers can and do take advantage of technologies whose development is supported by the COR program through the Strategic Astrophysics Technology (SAT) program.

COR Development Portfolio 2017

The COR Program Office manages the investment of SR&T funds in a variety of avenues to advance COR technology needs. Appendix C details recent progress of projects supported during FY 2017. In 2017, the COR Program development portfolio includes:

Wide-Field Infrared Survey Telescope–Mission in Development

WFIRST is a NASA observatory project within the astrophysics Exoplanet Exploration Program (ExEP) designed to perform wide-field imaging and slitless spectroscopic surveys of the Near-IR sky. It was the top-ranked large space mission in NWNH, and is expected to launch in the mid-2020s. Because WFIRST survey data will address major COR science questions such as galaxy evolution, the COR Program supported pre-formulation studies and technology development until late 2013, when they were moved into the WFIRST study. The Program continues to follow WFIRST development with specific attention to COR science goals.

James Webb Space Telescope (JWST)

A partnership between NASA and ESA, *JWST* is the largest science mission under development, and will address important COR science objectives. JWST will collect Near-IR and mid-IR data, allowing investigations of the earliest observable objects in the universe, tracing the evolution of galaxies, and probing obscured star-formation regions in our own and other galaxies. JWST is currently managed outside the COR Program. However, JWST operations will be managed under the COR Program when the mission transitions to Phase E after launch and commissioning in 2018/19.

Technology Development

The COR Program is responsible for ensuring that NASA is technologically ready to continue mission development into the future and to advance the broad scope of COR science goals. Accordingly, the Program Office is charged with overseeing the science of missions in formulation, implementation, and operations, as well as the maturation of technologies in development for these missions.

US astrophysics priorities were last refined in 2010 when the National Research Council (NRC) released the NWNH report. The priorities were confirmed in 2016, by the Decadal Survey Mid-term Assessment. Following the NWNH recommendations, the COR Program has supported focused technology development and mission-concept studies. In NWNH, the NRC placed high value on COR missions relating to Cosmic Dawn (the science theme most closely identifiable with COR). With JWST still in development, the NRC-prioritized recommendations did not include a new specific NASA-led mission that fit solely within COR. However, several of the NWNH recommendations are directly relevant to the COR Program.

- The NWNH report's first priority space recommendation, WFIRST, will address many key COR science goals, such as the formation and evolution of cosmic structure and galaxy growth.
- The report gave high priority to technology development in support of a future 4-m UV/Visible-band space telescope.
- The recommendations include a NASA instrument contribution to the Japanese Aerospace Exploration Agency (JAXA) Space Infrared Telescope for Cosmology and Astrophysics (SPICA) mission, if affordable. The Astrophysics Division's "*Astrophysics Implementation Plan*" (AIP), released in December 2012 and updated in 2014 and 2016, clarified that the desired contribution would exceed available NASA budgets.
- The report also strongly recommended an augmentation to the Explorers Program that supports astrophysics with rapid, targeted, competed investigations, that are selected largely based on scientific merit and technological readiness. Explorer missions provide an additional robust way to accomplish COR science: four of the six Medium-Class Explorer (MIDEX)/Small Explorer (SMEX) missions launched in the past 15 years primarily support COR objectives.

Since the COR Program was formulated in 2009 and the NWNH report was released in 2010, fiscal constraints have been significantly more restrictive than anticipated. The Program manages available funds strategically to foster COR science objectives to the extent possible.

The COR Program is committed to preparing for the next UV/Visible astrophysics mission. NWNH recommends developing technology for a large UV/Visible mission that will continue and extend HST's science accomplishments, through a 4-m-class mission covering wavelengths shorter than HST's primary range. However, the COR Program has chosen to consider a broader range of possible future endeavors.

A 2012 Request for Information (RFI) regarding science objectives and requirements for future UV/Visible astrophysics mission(s) led to a September 2012 community workshop based on 34 responses, which are posted on the COR website. A second community workshop in June 2015 continued working toward community consensus on science objectives and technology needs. Further, two independent (non-Program-sponsored) studies considering a future large UV/Visible observatory developed requirements that are likely to help guide the prioritization of COR SR&T technology development needs. Most technology development toward future strategic UV/Visible missions is also expected to benefit the Explorer Program.

In 2012, the Program also studied the feasibility of an instrument contribution to SPICA, then slated for launch around 2022. The Program concluded that based on the readiness level and development risk of possible NASA-provided SPICA instruments, all possible instrument contributions required funding beyond what was available, and could not meet JAXA's schedule constraints. Two Program-

sponsored workshops on the future of Far-IR space astrophysics were held in May 2014 and June 2015, to identify the most pressing science questions that can be addressed with Far-IR techniques, to determine technologies needed, and to build community consensus regarding future possible Far-IR astrophysics missions. As in the UV/Visible range, technology development toward future strategic Far-IR missions will also benefit Explorers.

SOFIA, which provides a platform for observations across the IR spectrum, with the possibility of frequent instrument upgrades, started Science Cycle 4 in early 2016. The recent upgrade to SOFIA's HAWC instrument offers observers polarimetric optics and new Far-IR detectors. The new HAWC+ detectors were matured with COR funding in prior years, an example of how COR technology development investment can be handed off to a flight project once the appropriate TRL is reached. A new third-generation instrument for SOFIA, the High Resolution Mid-infrarEd Spectrometer (HIRMES) was selected in fall 2016, for which early COR SR&T funding was key in enabling technology maturation and readiness. New technology will continue to be infused into SOFIA though future instrument calls.

The activity given first priority in NWNH for a future large space mission, WFIRST, is currently in formulation (Phase A), with a Mission Definition Review planned for late 2017. WFIRST is managed by the ExEP at the Jet Propulsion Laboratory (JPL), so it is not formally within the COR Program's suite of future missions. However, it still holds great relevance to COR science. The mission will use a 2.4-m repurposed telescope, and is expected to launch in the mid-2020s. The COR Program supported this high-priority mission activity through SAT-funded detector development until the work was moved into the WFIRST study office in 2014. The COR Program continues to pay attention to WFIRST planned capabilities that will serve COR science.

Planning for the Future

In early 2016, in preparation for the 2020 Decadal Survey of Astronomy and Astrophysics, NASA's Astrophysics Division initiated four community-based concept studies for possible future strategic missions (for information about the study teams' activities and progress, click on the mission links below). If selected, these would explore the nature of the universe from its earliest moments, in its most extreme conditions, and at the largest scales. Two of the possible missions address science topics largely within the COR program's purview: *Origins Space Telescope* (OST, formerly Far-IR Surveyor) and *LUVOIR*. Both of these study teams are developing ambitious and challenging mission concepts, which will require substantial technology advances. The technology needs of these studies will help guide the COR Program's technology development over the next few year, possibly longer. The other two mission studies, *HabEx Imaging Mission* and *Lynx* (formerly X-ray Surveyor), are expected to have significant interest for COR science as well, though they do not directly influence COR Program technology planning. Most of the technology development needed for these large missions will also strongly benefit the Explorer Program. As explained in Section 3, these studies play a major role in determining the Astrophysics Division's technology development priorities.

In early 2017, also in preparation for the 2020 Decadal Survey, the Astrophysics Division initiated 10 community-based concept studies for astrophysics Probe missions, defined as costing between $0.4B and $1.0B. The probes, like Explorers, have the potential for significant advancement in COR science. However, at this point they are expected to be competed PI missions, with little or no technology innovation required in development. Thus, they do not drive COR strategic technology development priorities, although like Explorers, they will likely benefit from such development.

2. Strategic Technology Development Process and Portfolio

The COR, Physics of the Cosmos (PCOS), and ExEP Program Offices were set up by NASA HQ Science Mission Directorate (SMD) Astrophysics Division to manage all aspects of these focused astrophysics programs. The Program Offices shepherd critical technologies toward infusion into Program-relevant flight projects. The Offices follow Astrophysics Division guidance, and base their recommendations on science community input, ensuring the most relevant technologies are solicited and developed. The COR Program Office, located at NASA GSFC, serves as HQ's implementation arm for COR Program-related matters. The Astrophysics Division achieves efficiency by having the same staff and physical facilities serve both the COR and PCOS Program Offices. The Astrophysics Division funds technology development at all TRLs. Early-stage development (TRL ≤3) and technologies related to non-strategic missions and suborbital projects are typically funded by Astrophysics Research and Analysis (APRA). Final maturation (TRL ≥6) is mission-specific and thus handled by flight missions. The SAT program, launched in 2009, funds maturation of technologies across the mid-TRL gap (3≤TRL <6).

The COR Technology Development Process

The COR Program Office is charged to develop and administer a technology development and maturation program, moving innovative technologies across the mid-TRL gap to enable strategic COR missions. The Program Office facilitates, manages, and implements the technology policies of the Program. Our goal is to facilitate technology infusion into COR missions, including the crucial phase of transitioning nascent technologies into targeted projects' technology programs during mission formulation. COR SAT projects are funded by the COR SR&T budget. Our work is guided by the priorities set forth in the AIP, the Astrophysics Roadmap, and other current strategic guidance. The AIP describes the Astrophysics Division's planned implementation of space-based priority missions and activities identified in NWNH, updated due to more recent budgetary developments. The Roadmap strives to inspire and challenge the community to pursue the missions and technologies needed over the next three decades to address NWNH-identified science goals.

Our technology development process (Fig. 2-1) places the science community's inputs at the center of our efforts through the Decadal Survey process and ongoing identification of technology gaps. The community is encouraged to submit gaps at any time via the COR Program Analysis Group (COPAG) or directly through the COR Technology website. The recently established COPAG Technology Interest Group (TIG) reviews gaps submitted before the annual June 1 cutoff date, consolidating, enhancing, and adding to them as needed to create a complete, accurate, and compelling set of gaps for TMB evaluation. The Program Office charges its TMB annually to evaluate and determine which of the submitted technology developments would meet Program objectives, and to prioritize them for further development consideration. The TMB ranks gaps based on Program objectives, strategic ranking of relevant science/missions, benefits and impacts, and urgency. The TMB, a Program-level functional group, thus provides a formal mechanism for input to, and review of, COR technology development activities.

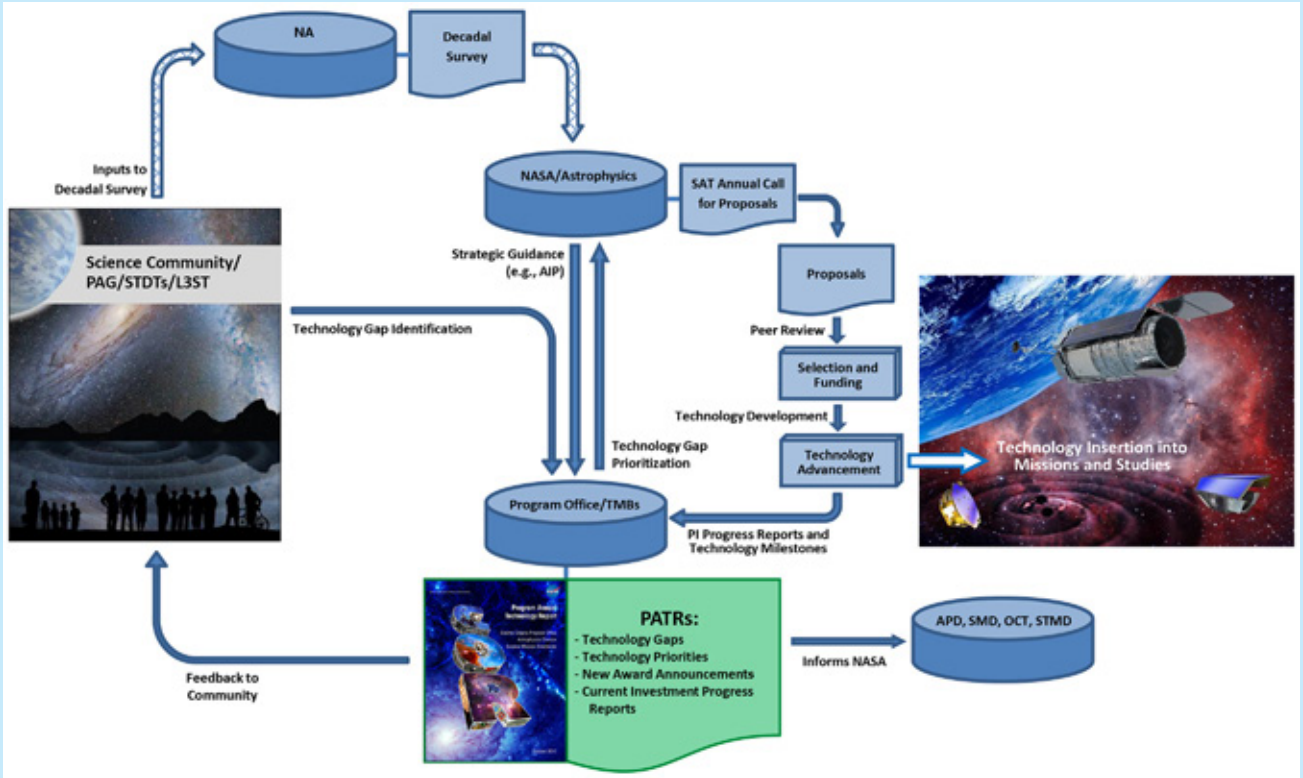

Fig. 2-1. *The COR technology development process receives community input on technology gaps, recommends priorities, manages SAT-funded activities, and informs NASA and the science community about progress (NA, National Academies; PAG, Program Analysis Group; APD, Astrophysics Division; OCT, Office of the Chief Technologist; STMD, Space Technology Mission Directorate).*

TMB priority recommendations inform Astrophysics Division decisions on what technologies to solicit in the upcoming annual SAT call for proposals, and help guide proposal selections. HQ's investment considerations are made within a broader context, with programmatic factors apparent at the time of selection affecting funding decisions. HQ evaluates submitted technology development proposals, considering overall scientific and technical merit, programmatic relevance, and cost reasonableness given the scope of work. Awardees work to mature their technologies from their initial TRL, normally 3 or 4[§], through TRL 5. PIs report progress and plans to the Program Office periodically, and submit their technologies for TRL advancement review as appropriate. Progress in these projects allows infusion of newly mature technologies into NASA missions and studies, enabling and enhancing their capabilities with acceptable programmatic costs and risks.

As seen in Fig. 2-1, the PATR plays an important role in our process. Through PI reports and quad charts, it describes the status of all current investments in strategic COR technologies. It reports technology gaps articulated by the scientific community and the large-mission-concept study teams, with a prioritized list of technologies for future solicitation and funding. The PATR is an open source for the public, academia, industry, and the government to learn about the status of enabling technologies required to fulfill COR science objectives. The report informs NASA organizations, including but not limited to the Astrophysics Division, and updates the community regarding technology development

[§] TRL 4 is defined as: "*Component and/or breadboard validation in laboratory environment.*"

progress, as input for future technology-gap submissions. Technological progress and programmatic decisions change the landscape of requirements for COR needs; therefore, the process is repeated annually to ensure continued relevance of priority ranking. Indeed, in any given year, new SAT award decisions are informed by PATRs published over the prior two years, a new SAT solicitation is informed by the prior-year PATR and the current year's TMB priority ranking, and the current PATR provides recommendations for next year's SAT.

This technology development and maturation process identifies existing and emerging needs in a transparent manner, improves the relevance of COR technology investments, provides the community a voice in the process, and promotes targeted external technology investments by defining needs and identifying NASA as a potential customer for innovative technologies. It also identifies providers of technologies and expertise, the Program PIs, to potential customers and collaborators within and beyond NASA. This encourages industry and other players to invest in enabling technologies for future missions, and promotes formation of productive collaborations. Beyond involvement in the Decadal Survey process and technology gap submission, the science and technical community is a key stakeholder in Program technology development activities. The community provides feedback and inputs to the technology development process; and participates in COPAG and other committees and workshops, ad-hoc studies, and in technology development by responding to SAT solicitations.

TRL Vetting

SAT funding helps mature technologies expected to enable and/or significantly enhance future strategic astrophysics missions. These technologies typically enter the SAT program at TRLs 3 or 4, and are intended to progress toward higher TRLs. TRL assertions above a technology's approved entry level are not official until a TRL-vetting TMB concurs with the development team's assessment. When PIs believe their team has demonstrated the required progress, they may request a review to present their case for TRL update. The Program Office then convenes a TMB consisting of Program Office and HQ senior staff along with subject matter experts to assess the request and, when warranted, approve the new TRL. The typical forum for such a request is during the PI's end-of-year presentation to the Program Office, but it can be made at any time. One COR SAT project has already gone through this process, and the PIs of several more are considering TRL vetting this coming year.

Why review TRLs?

TRLs are used throughout the agency to help assess the maturity of technologies. The Program Office's charge includes a requirement that it monitor the progress of the Astrophysics Division's investments in technology maturation through SAT projects relative to the TRL plan and milestones submitted by the PI in the SAT proposal. A key indicator of such progress is TRL advancement as vetted by the Program Office, providing a consistent method of assessing progress across our full portfolio of projects.

What does our vetting mean?

When the Program's TMB approves a higher TRL asserted by the PI, it provides an independent assessment and verification that the project has achieved that TRL. The TMB consists of scientists, technologists, and systems engineers from the Program; and subject matter experts from the community and Aerospace Corporation; who provide an objective and informed assessment. The primary purpose for issuing this assessment is to inform the Program Office of significant progress in preparing the technology for possible infusion into strategic missions. It also informs the community of an improved state of readiness.

What is expected?

The TRL vetting process is initiated when a PI notifies the Program Office that the milestones necessary for TRL advancement have been met. The PI team prepares a brief but compelling presentation that makes the case for the higher TRL, and the PI presents it to the TRL-vetting TMB which considers the TRL assertion. The TMB is guided by TRL definitions in *NASA Systems Engineering Processes and Requirements*, also known as NASA Procedural Requirement (NPR) 7123.1B. Recognizing that PI teams are busy and must concentrate their efforts on the work of maturing their technology, the Program Office is satisfied to rely on a cogent exposition of the same reports, graphs, and test results the team captures for its own records.

The Program Office has tools to help PIs assess their progress and is available to provide information on the TRL process. Finally, if the project is still ongoing, we recommend the PI present a plan for further TRL advances, if any, allowing the TMB to offer feedback and make recommendations.

What are the benefits for the PI and the Program?

The Program Office's TRL-vetting process serves as an opportunity to capture and collect the needed documentary evidence and present it to a group of independent experts. This can strengthen a potential future TRL case presentation, whether in person or in writing, to flight projects, proposal teams considering adding the technology to their mission, and/or proposal reviewers. Another leveraging opportunity might be in collaboration opportunities. As alluded to above, the TMB can help the PI team fine-tune its plan for future work to achieve the claimed TRL if the current claim was not vetted, or for the next TRL if it was.

Finally, TRLs are NASA's technology-development-assessment language, and TRL advancement is one of the key success criteria for SAT projects. Our TRL vetting is an objective process, rendering an independent verification of achievement, increasing the credibility of the technology's maturity and its potential for continued funding, infusion into flight missions, and consideration by community assessments such as STDT studies and Decadal Surveys.

The COR Technology Development Portfolio as of 2017

For FY 2017, the driving objective is to maintain progress in key enabling technologies for OST and LUVOIR, to enable compelling cases for both in the upcoming 2020 Decadal Survey.

Twenty COR SAT grants have been awarded to date. Table 2-1 provides top-level information on the 10 projects that received funding in FY 2017, including where each is described in detail in the appendices. Appendix B provides one-page "quad chart" project summaries, while Appendix C provides in-depth reports detailing development status, progress over the past year, and planned near-term development activities. Abstracts for the four recently awarded projects, slated to begin in FY 2018, are included at the end of Appendix C. The appendices provide technology overviews and status, not flight implementation details. For additional information, please contact the COR Program Office or the PIs directly. Contact information for each PI appears at the end of his or her report.

Technology Development Title	PI	Institution	Start Year & Duration	Current TRL	Quad Chart & Status Report Page Locations
Ultraviolet Coatings, Materials, and Processes for Advanced Telescope Optics	K. 'Bala' Balasubramanian	JPL	FY13; 3 yrs	3-4	65, 76
Advanced Far-UV/UV/Visible Photon-Counting and Ultralow-Noise Detectors	Shouleh Nikzad	JPL	FY16; 3 yrs	3-4	66, 92
Development of Digital Micro-mirror Device (DMD) Arrays for use in Future Space Missions	Zoran Ninkov	RIT	FY14; 3 yrs	4	67, 99
Ultra-Stable Structures: Development and Characterization Using Spatial Dynamic Metrology	Babak Saif	GSFC	FY16; 4 yrs	3	68, 105
Improving UV Coatings and Filters using Innovative Materials Deposited by ALD	Paul Scowen	ASU	FY16; 3 yrs	3	69, 108
Advanced UVOIR Mirror Technology Development for Very Large Space Telescopes	H. Philip Stahl	MSFC	FY14; 3 yrs	3	70, 117
Predictive Thermal Control Technology to Enable Thermally Stable Telescopes	H. Philip Stahl	MSFC	FY17; 3 yrs	3	71, 127
Development of Large-Area (100 cm2) Photon-Counting UV Detectors	John Vallerga	UC Berkeley	FY16; 3 yrs	4	72, 134
Raising the Technology Readiness Level of 4.7-THz Local Oscillators	Qing Hu	MIT	FY16; 3 yrs	3	73, 154
High-Efficiency Continuous Cooling for Cryogenic Instruments and sub-Kelvin Detectors	James Tuttle	GSFC	FY17; 3 yrs	3-5	74, 157

Table 2-1. *COR Technology Development Portfolio as of FY 2017 (organized by science topic and PI name). Project durations include approved no-cost extensions.*

The Astrophysics Division collaborated with STMD in certain solicitations, developments, proposal reviews, and technology co-funding. The Division is open to collaboration efforts when possible, as this leverages limited funding to advance technologies that meet the respective goals of the collaborating organizations. Such joint investments are "win-win-win" opportunities for the Astrophysics Division, STMD (or other organizations), and the PI. The COR Program looks forward to continued relationship with STMD, creating more such opportunities in the future.

Strategic Astrophysics Technology Selection for FY 2017 Start

The COR Program funds SAT projects to advance the maturation of key technologies to make feasible their implementation in future flight missions. The Program focuses on advancing those technologies most critical for substantive near-term progress on strategic priorities. The COR SAT proposals selected for FY 2018 start, announced in September 2017, advance four technologies in the areas of Far-UV optics, and detectors from the Far-IR to the Far-UV (Table 2-2).

Technology Development Title	PI	Institution	Duration	Initial TRL	Abstract Page Locations
Ultrasensitive Bolometers for Far-IR Spectroscopy at the Background Limit	Charles Bradford	JPL	3 years	4	164
Development of Digital Micromirror Devices for Far-UV Applications	Zoran Ninkov	RIT	2 years	5	165
High Performance Sealed Tube Cross Strip Photon Counting Sensors for UV-Vis Astrophysics Instruments	Oswald Siegmund	UC Berkeley	3 years	4	166
Development of a Robust, Efficient Process to Produce Scalable, Superconducting kilopixel Far-IR Detector Arrays	Johannes Staguhn	JHU	2 years	5	167

Table 2-2. *COR SAT Development Starts in FY 2017 (alphabetically by PI).*

These new SAT selections were based on the following factors:

- Overall scientific and technical merit;
- Programmatic relevance of the proposed work, including urgency; and
- Cost reasonableness of the proposed work.

Since these projects have only recently been selected for funding, their status is not presented yet. First-year progress for each will appear in the 2018 COR PATR.

Large-Mission-Concept Studies toward the 2020 Decadal Survey

As mentioned in Section 1, the Astrophysics Division has set up STDTs to study four large-mission concepts – OST, HabEx, LUVOIR, and Lynx. The STDTs are each charged to develop the science case and design reference mission, assess technology development needs, and estimate the cost of their mission concept. These studies will guide our efforts to mature technology components and architectures required to offer four equally compelling cases for the 2020 Decadal Survey's consideration. Similarly, the L3 Study Team (L3ST) was chartered to help us understand how NASA might participate in ESA's LISA mission, inform our engagement through its earliest stages, and prepare for the 2020 Decadal Survey.

Each of these ambitious mission concepts promises breakthrough science results, but implementing them will require us to overcome daunting technology development challenges. The SAT program is certain to play a major role in funding these technology development efforts. We encourage all members of the community to support our efforts to identify the highest-priority technology gaps we need to close to make these missions feasible, and continue to submit proposals in response to SAT solicitations. As of this writing, notices of intent to submit for the next SAT round are due January 18, 2018, with proposals due March 15, 2018.

As described in Section 3, the OST and LUVOIR Surveyor STDTs provide their own technology gap lists to the COR Program Office. The Program Office combines these lists with the one reviewed by the COPAG TIG, and submits the resulting list to the TMB for prioritization.

Historical Record of TCOR Proposals and Awards

As shown in Table 2-3, the Technology Development for Cosmic Origins (TCOR) section of the SAT program received 14 proposals in response to the 2010 solicitation, its first year. This was followed by 24 for 2011, 13 for 2012, none for 2013 as the Program did not solicit SATs that year, 14 for 2014, 12 for

2015, and 19 for 2016. Three proposals were selected out of the first set, with five more the following year, three in the third year, five in 2014, two in 2015, and four selected in the latest round. This makes the historical selection rate for COR SAT proposals 23%, with the three most recent rounds hitting 36%, 17%, and 21%, respectively.

Solicitation Year	TCOR Proposals		Proposal Success Ratio
	Submitted	Awarded	
2010	14	3	21%
2011	24	5	21%
2012	13	3	23%
2013	Not solicited	N/A	N/A
2014	14	5	36%
2015	12	2	17%
2016	19	4	21%
Total to Date	96	22	23%

Table 2-3. *Number of TCOR SAT Proposals and Awards.*

3. Technology Gaps, Priorities, and Recommendations

Enabling strategic astrophysics missions that are decades away requires identifying and closing gaps between state-of-the-art (SOTA) performance and that required for those missions. As current technologies develop and mature, and as our understanding of the missions' concept designs mature, those gaps evolve.

As shown in Fig. 2-1, we solicit technology gaps from the community on an ongoing basis. Anyone may submit a technology gap directly to the Program Office, *downloading a form* from the COR website, or through the COPAG. Gaps may be submitted throughout the year; however, since gaps are assessed and prioritized annually in late July or early August, the Program Office set a June 1 cutoff date for consideration in the same year. This allows the COPAG TIG to review the gaps for completeness, merge overlapping ones, and complete and improve entries where the submission did not adequately address the requested information. Then, the TIG returns the list to the Program Office for final preparation for TMB assessment.

To maximize the likelihood of high priority ranking, the Program Office encourages submitters to include as much of the information requested as possible. Importantly, we ask submitters to describe a capability gap, not a specific implementation process or methodology. The goals and objectives should be clear and quantified. Additionally, a complete description of the needed capability with specific performance goals based on mission needs is very valuable. Such information serves several important purposes:

1. The TMB is best able to understand and thus correctly assess the identified technology gap.
2. NASA HQ is best able to develop accurate technology development proposal calls.
3. The community is clearly informed and best able to match candidate technologies to mission needs.

Aside from submitter information, the technology gap form requests the following information:

- **Technology gap name:** Identifies the gap, and optimally the type of mission filling it would enable;
- **Brief description:** Summarizes the technology gap and associated key performance criteria; in general, well-defined technology gaps receive higher priority than vague ones;
- **Assessment of current SOTA and TRL:** Describes the SOTA with justification, allowing the TMB to appreciate the gap between what's available and what's needed; **SOTA TRL** specifies the current TRL per NPR 7123.1B Appendix E of relevant SOTA technology; and **Full-Solution TRL** specifies the current TRL of candidate technologies that could provide a full solution; the SAT program funds projects to advance technologies from TRL 3 up through TRL 5, so those with full solutions already at TRL 6 rank lower unless the existing technology is significantly deficient in some way (e.g., cost, complexity, yield, etc.); note that full-solution TRL can never exceed the SOTA TRL, else this full-solution technology would be the SOTA;
- **Target goals and objectives:** Details the quantifiable goals and/or objectives for a candidate technology to fill the described gap. For example, "*The goal is to produce a detector with a sensitivity of X over a wavelength of Y to Z nm*"—technology gaps with clearly quantified objectives may receive higher priority than those without quantified objectives;
- **Scientific, engineering, and/or programmatic benefits:** Describes the benefits of closing the technology gap; for enabling technology, this describes how and why it is such; for an enhancing technology, it describes, and if possible quantifies, the impact; benefits could be better science, lower resource requirements (e.g., mass, power, etc.), and/or programmatic (e.g., reduced risk, cost, or schedule); for example, "*Material X is 50% stronger than the current state of the art and will enable the optical subsystem for a 2-m telescope to be Y kg lighter*;" technology gaps with greater potential mission benefits receive higher scores;

- **Application and potential relevant missions:** Technologies enabling or enhancing missions ranked highly by the AIP, Astrophysics Roadmap, or NWNH, will score higher; technologies applicable to a wide range of COR missions, as well as PCOS and/or ExEP missions will rank better; and
- **Urgency:** Specifies when the strategic mission enabled or enhanced by the technology is planned to launch; in cases where there is a more immediate driving need (e.g., demonstrating credibility in time for consideration by the 2020 Decadal Survey), this driving requirement is also considered; technology gaps with shorter time windows relative to required development times receive higher priority.

Technology Gaps Submitted to the 2017 TMB

As in prior years, the COPAG EC agreed to review the list of technology gaps compiled by the Program Office, assigning the task starting this year to their newly established TIG. The Program Office forwarded to the TIG 18 gaps from the 2016 TMB list plus 16 new entries, some of which simply suggested edits to 2016 gaps. We thank the community for their engagement in this process and for their meaningful gap submissions. The TIG returned to the Program Office a gaps list with notes indicating concurrences or disagreement as to strategic relevance of gaps and suggestions to merge similar/overlapping gaps or drop duplicate ones. In parallel, the LUVOIR STDT submitted 13 gaps; while the OST STDT submitted 11. To facilitate and streamline the TMB prioritization process, a subset of the full TMB consolidated the three lists into 37 unique gaps. At the start of its meeting, the full TMB decided to further merge gaps, reducing the list to 35 gaps. Of the 13 LUVOIR gaps, four were deemed outside the scope of COR science and with the concurrence of the ExEP Program Office moved from the COR TMB list to the ExEP list. Two entries submitted by the general community were similarly handed off to the ExEP Program Office. As a result, the COR TMB scored 29 technology gaps for 2017 (see below).

Almost all technologies developed to close these gaps would enable and/or enhance high-priority strategic missions per the AIP, the Astrophysics Roadmap, and/or NWNH. We deeply appreciate the efforts of the TIG, LUVOIR STDT, and OST STDT, and look forward to continued collaboration in the future. Having the TIG and study teams review gap entries and propose new ones where appropriate, prior to TMB prioritization, serves several important purposes:

- Providing a set of expert-vetted, unique, and compelling technology gaps, such that the resulting entries potentially merit higher priority ranking;
- Ensuring the gaps accurately reflect the current situation per the community and study teams; and
- Making the process of generating unique technology gaps more transparent to the community.

Prioritizing Technology Gaps

In its prioritization meeting, the TMB followed an agreed-upon set of evaluation criteria, resulting in the priorities shown below. TMB membership included senior staff from NASA HQ Astrophysics Division, the Program Office, STMD, and the Aerospace Corporation. The TMB used a prioritization approach similar to that used in prior years, with a streamlined set of four criteria. These included strategic alignment, benefits and impacts, scope of applicability, and urgency.

- **Strategic alignment:** How well does the technology align with COR science and programmatic priorities of current programmatic guidance (i.e., AIP, Roadmap, and NWNH)?
- **Benefits and impacts:** How much impact does the technology have on COR-relevant science in applicable mission(s)? To what degree does the technology enable and/or enhance achievable science objectives, reduce cost, and/or reduce mission risks?

- **Scope of applicability:** How crosscutting is the technology? How many Astrophysics programs and/or mission concepts could it benefit?
- **Urgency:** When are launches and/or other schedule drivers of missions enhanced or enabled by this technology anticipated?

The TMB assigned weighting factors, reflecting the relative importance of each criterion. Each gap received a score of 0 to 4 for each criterion. The scores were multiplied by their respective weights, and the products were summed. Technologies that could be scored based on several missions or mission classes were scored for each scenario independently, assigning the highest overall score (e.g., if a gap could receive an overall score of 91 for one mission and 75 for another, it would be assigned the higher score). Table 3-1 details the criteria descriptions, weighting factors, and TMB scoring guidelines.

Criterion	Weight	Max Score	Max Weighted Score	General Description/ Question	4	3	2	1	0
Strategic Alignment	10	4	40	How well does the technology align with COR science and programmatic priorities of current programmatic guidance (i.e., AIP, Roadmap, NWNH)?	Technology enables COR-relevant science within mission concept receiving highest current programmatic consideration	Technology enables COR-relevant science within mission concept receiving mid to high current programmatic consideration in AIP or Roadmap	Technology enables COR-relevant science within mission concept receiving low current programmatic consideration in AIP or Roadmap	Technology enables COR-relevant science within mission concept not considered in AIP or Roadmap, but positively addressed in NWNH	Technology does not enable COR-relevant science within any mission concept considered by current programmatic guidance
Benefits and Impacts	8	4	32	How much impact does the technology have on COR-relevant science in applicable mission(s)? To what degree does the technology enable and/or enhance achievable science objectives, reduce cost, and/or reduce mission risks?	Critical and key enabling technology; required to meet COR-science-relevant mission concept objectives; without this technology mission would not launch or COR science return would be significantly impaired	Highly desirable; not mission-critical to COR-science-relevant objectives, but significantly enhances COR science capability, reduces critical resources needed, and/or reduces mission risks; without it, missions may launch, but COR science return would be compromised	Desirable - not required for COR-relevant mission success, but offers moderate COR-relevant science or implementation benefits; if technology is available, would almost certainly be implemented in missions for COR purposes	Minor COR-relevant science impact or implementation improvements; if technology is available would be considered for implementation in missions for COR purposes	No COR-relevant science impact or implementation improvement; even if available, technology would not be implemented in missions for COR purposes
Scope of Applicability	3	4	12	How cross-cutting is the technology? How many Astrophysics programs and/or mission concepts (including Explorers and Probes) could it benefit?	Applies widely to COR mission concepts and both PCOS and ExoPlanet mission concepts	Applies widely to COR mission concepts and either PCOS or ExoPlanet mission concepts	Applies widely to COR mission concepts	Applies to a single COR mission concept	No known applicable COR mission concept
Urgency	4	4	16	When are launches and/or other schedule drivers of missions enhanced or enabled by this technology anticipated?	Launch anticipated in next 4-8 years (2021-2025) or other schedule driver requires progress in 2-3 years (2019-2020)	Launch anticipated in next 9-13 years (2026-2030) or other schedule driver requires progress in 4-8 years (2021-2025)	Launch anticipated in next 14-18 years (2031-2035)	Launch anticipated in next 19-23 years (2036-2040)	Launch anticipated in 24 or more years (2041 or later)

Table 3-1. *Clear, strategic criteria provide a rigorous, transparent process for prioritizing technology gaps.*

This process provides a systematic and transparent ranking of technology gaps based on the Program's goals, community scientific rankings of relevant missions, Astrophysics Division priorities as outlined in the AIP and Astrophysics Roadmap, and the external programmatic environment. Since the SAT program is intended to promote development and maturation of technologies relevant to missions and concepts identified as strategic, the strategic alignment criterion is driven by strategic documents such as the AIP, the Astrophysics Roadmap, and the NWNH. The AIP details highly ranked science missions and technology development, which for COR include instruments to be flown on SOFIA and technologies for future UV/Vis/Far-IR missions; and prioritizes those based on current budget realities. This year, the TMB considered technologies identified by the OST and LUVOIR STDTs as having the highest strategic alignment, and SOFIA instrument technologies considered highly aligned.

Prioritization Results

As mentioned above, in 2017, the COR TMB scored 29 technology gap entries. Reviewing the scores, the TMB binned the technology gaps into three groups based on a number of factors, including primarily a natural grouping of overall scores. As described below, the TMB established a fourth priority tier, though no gaps were assigned to this new tier at this time.

Priority Tier 1: Technologies the TMB determined to be of the highest interest to the COR Program. Advancing these key enabling technologies is judged to be most critical to making substantive near-term COR-science-relevant progress on the highest-priority strategic astrophysics missions, including OST and LUVOIR. The TMB recommends SAT calls and award decisions address these technology gaps first.
Priority Tier 2: Typically, technologies the TMB believes would be highly desirable or desirable for a variety of strategic missions. The TMB recommends that should sufficient funding be available, SAT calls and award decisions address closing these technology gaps as well.
Priority Tier 3: Technologies the TMB deemed supportive of COR objectives, but scoring lower than Priority 1 and 2 technology gaps.
Priority Tier 4: Recognizing that a reasonable way of "sunsetting" gaps that have no strategic alignment may become necessary, the TMB created a new "Priority Tier 4." Gaps that the TMB deems legitimate COR technology gaps, but that are not currently aligned with any strategic mission, will be assigned to this new tier and will not be reprioritized in following years. The Program Office will contact submitters of such gaps to inform them of what happened, why, and what changes are needed before their gap can be resubmitted.

Table 3-2 lists the gaps prioritized by the TMB, including 2017 assigned priorities, gap names, science topics addressed, gap submission sources, and where in Appendix A you can find detailed gap entries.

2017 Priority	Technology Gap Name	Science Addressed	Submitted By	Gap Detail Page Location
Priority 1	High-reflectivity broadband Far-UV-to-Near-IR mirror coatings	UVOIR	LUVOIR STDT	45
	Large-format, low-noise and ultralow-noise Far-IR direct detectors	Far-IR	OST STDT	46
	High-performance, sub-Kelvin coolers	Far-IR/X Ray	OST STDT	54
	Heterodyne Far-IR detector arrays and related technologies	Far-IR	OST STDT	49
	Large-format, high-dynamic-range UV detectors	UV/Far-UV	LUVOIR STDT	39
	Cryogenic readouts for large-format Far-IR detectors	Far-IR	OST STDT	47
	Warm readout electronics for large-format Far-IR detectors	Far-IR	OST STDT	48
	Large cryogenic optics for the Far IR	Far-IR	OST STDT	52
Priority 2	Mid-IR detectors	Mid IR	OST STDT	59
	Lightweight, large-aperture, high-performance telescope mirror systems for UVOIR	UVOIR	General Community	32
	Lightweight, large-aperture, high-performance telescope mirror systems for Far-IR	Far-IR	General Community	34
	Compact, integrated spectrometers for 100 to 1000 μm	Far-IR	OST STDT	56
	High-efficiency UV multi-object spectrometers	UV	General Community	31
	Band-shaping and dichroic filters for the UV/Vis	UV/Vis	General Community	43
	Advanced cryocoolers	Far-IR/X Ray	OST STDT	55
	Advanced adaptive optics	UVOIR/HabEx	General Community	60
	High-performance spectral dispersion component/device	UVOIR/ Far-IR	General Community	42
	Cryogenic deformable mirror	Mid IR	OST STDT	58
Priority 3	Mid-IR coronagraph optics and architecture	Mid IR	OST STDT	57
	Ultra-stable opto-mechanical systems architecture	UVOIR/HabEx	LUVOIR STDT	38
	UV/Opt/Near-IR tunable narrow-band filters	UVOIR	General Community	63
	Segment phasing and control	UVOIR/HabEx	LUVOIR STDT	39
	Dynamic isolation systems	UVOIR/HabEx	LUVOIR STDT	40
	Segmented-aperture coronagraph architecture	UVOIR/HabEx	LUVOIR STDT	36
	High-contrast imaging post-processing	UVOIR/HabEx	LUVOIR STDT	37
	Mirror segment systems	UVOIR/HabEx	LUVOIR STDT	41
	Wide-bandwidth, high-spectral-dynamic-range receiving system	Cosmic Dawn	General Community	51
	High-precision low-frequency radio spectrometers and interferometers	Cosmic Dawn	General Community	61
	Far-IR interferometry	Far-IR	General Community	53

Table 3-2. *Summary of 2017 COR technology gaps and their TMB-assigned priorities. Gaps shown by priority tier and science theme. All gaps within a specific tier have equal priority. Although a fourth tier was created, no 2017 gap was assigned to it.*

From 2011 through 2017, nearly all gaps achieving Priority 1 maintained that rank or changed by one level due to minor shifts in how priority scores break up naturally into groups. In addition, funded projects have addressed high-priority gaps, mostly Priority 1, and occasionally Priority 2. For example, four of the eight 2017 Priority 1 gaps have already been addressed by SAT projects or will be addressed by 2018-start SATs, as have two of the 10 Priority 2 gaps.

The Program Office continues to solicit and compile technology gap submissions from the community, and as was done this year, will maintain its collaboration with the TIG and study teams to ensure the gaps ranked by the TMB continue to be complete, distinct, and compelling. As mentioned above, the next cutoff date for community gap submissions is June 1, 2018. Notices of intent to submit SAT proposals are due January 18, 2018, with proposals due March 15, 2018.

4. Benefits and Successes Enabled by the COR SAT Program

The main benefit of the SAT program is in maturing technologies across the mid-TRL gap, so they can be infused into strategic COR missions and/or international collaborative missions relevant to Program goals, as part of a US contribution. All SAT projects have made significant progress in maturing their technologies, with several claiming TRL advances in at least some aspects of their technologies. These have yet to be vetted by a TMB.

Where appropriate, newly matured technologies may also be implemented in ground-based projects, suborbital experiments, Explorers, and Probe-class missions. These often extend beyond the COR Program to PCOS, ExEP, and even beyond missions managed by Astrophysics Division.

The following are examples of COR-funded project developments contributing to missions and projects:

- TES bolometer detector was selected to support the SOFIA *HAWC* instrument (PI, S. Harvey Moseley);
- Advanced high-efficiency, photon-counting CCD detectors, matured with SAT support, were implemented into the *FIREBall* long-duration balloon mission, the Guide and Focus CCDs for Wafer-Scale Imager for Prime instrument (WaSP) at Palomar, and for Caltech Optical Observatory's Zwiki Transient Facility (PI, Shouleh Nikzad).
- Advanced UV-reflective coatings, matured with SAT support, were implemented on the *ICON* and *GOLD* missions (PI, Manuel Quijada);
- HIRMES was selected as a third-generation facility for SOFIA (PI, S. Harvey Moseley);
- H4RG Near-IR detectors matured with SAT support were adopted by *WFIRST* (PI, Bernard Rauscher);
- Heterodyne detector technology matured with SAT support was incorporated into the *Stratospheric Terahertz Observatory* (STO) balloon experiment (PI, Imran Mehdi); and
- A 4.74-THz local oscillator was flown on the STO-2 balloon experiment. Unfortunately, due to sun damage to the control electronics, no data was obtained.

As in prior years, the Program Office surveyed current PIs about additional benefits resulting from their SAT funding. Of the nine PIs represented in this PATR, six provided information about collateral benefits. Of these, three reported they were able to leverage SAT funding to generate other support, (e.g., co-funding from a project at the Defense Advanced Research Projects Agency, DARPA; the National Science Foundation, NSF; and a Caltech Summer Undergraduate Research Fellowship), set up collaborations with researchers at other institutions on proposals and new programs, and generate industry interest in their technologies. All six PIs report having hired students and/or post-doctoral fellows to assist their technology development work (on average three undergraduate students and two graduate students per project, with half the projects also hiring a post-doctoral fellow), helping train the next generation of researchers and technologists needed to support future missions (Fig. 4-1). The PIs reported that former students and post-docs have proceeded to PhD programs, and positions at other institutions and high-tech industry; proving that the SAT Program is helping train and shape the future astrophysics work force as well as the wider technological work force. Several PIs went on to successfully propose additional technology development projects through the SAT and APRA programs, including one of the four new COR SATs selected for FY 2018 start, as well as non-astrophysics programs.

Fig. 4-1. *SAT projects hire many students and post-doctoral fellows, helping train the future astrophysics workforce.*

In 2017, the Program presented a poster of COR and PCOS technology development at the AAS meeting in Grapevine, TX (Fig. 4-2), displaying the breadth of scope of our SAT investment and placing it visually in the progression of astronomy and astrophysics from ancient times to the coming decades. The poster explained the Programs' technology development priorities, and how the four large-mission-concept STDTs are involved in technology development.

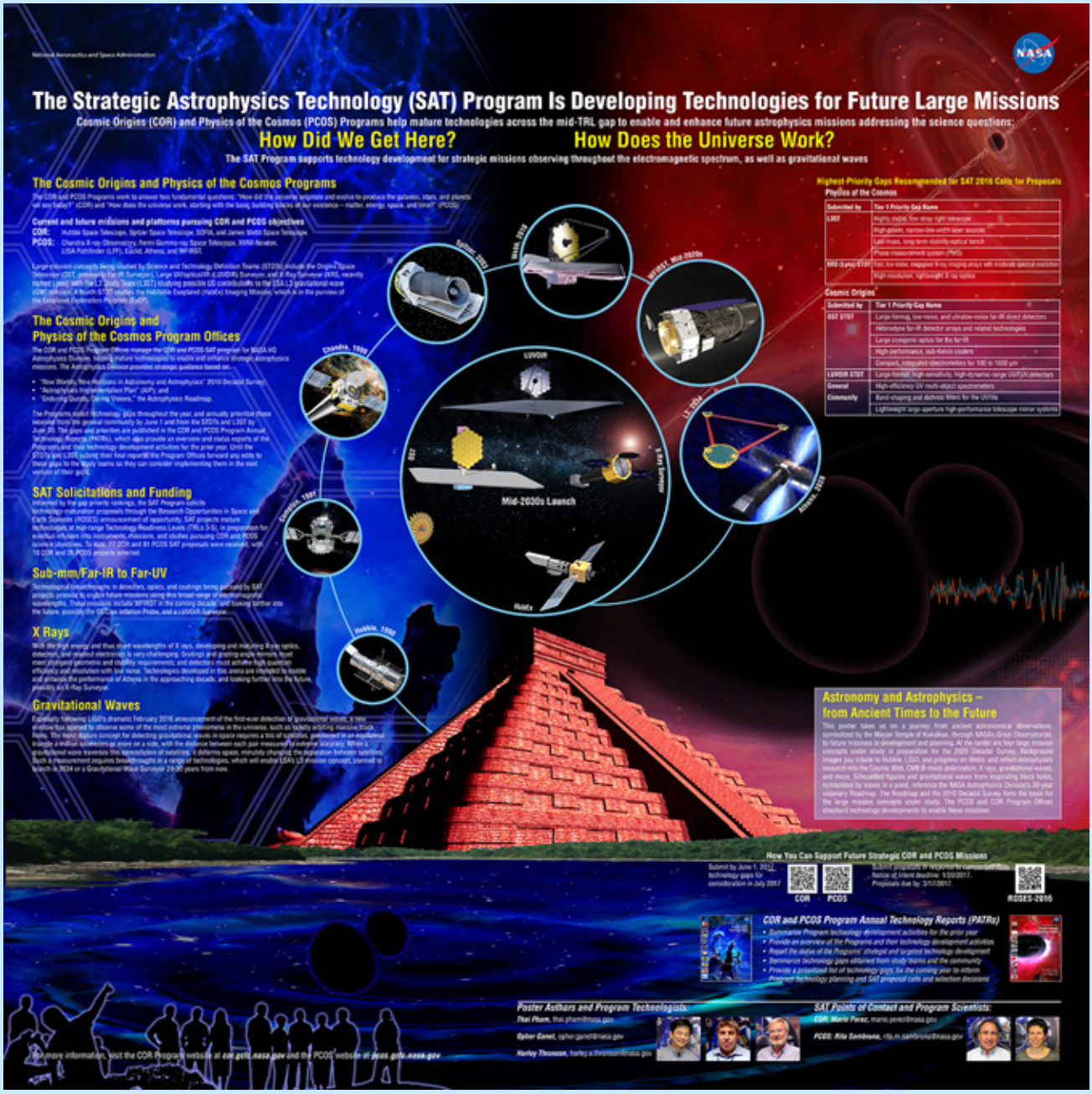

Fig. 4-2. *Poster presented at the January 2017 AAS meeting in Grapevine, TX. The Program promotes exposure of current technology developments and investment priorities at national and international meetings, and informs the community of upcoming SAT funding opportunities.*

The Broad Impacts of the SAT Program

Figure 4-3 depicts the geographic breadth of SAT program (both COR and PCOS) impacts, showing the locations of our PI institutions, their collaborators and partners, and the universities and colleges where the students and post-doctoral fellows involved in SAT projects attend school and work.

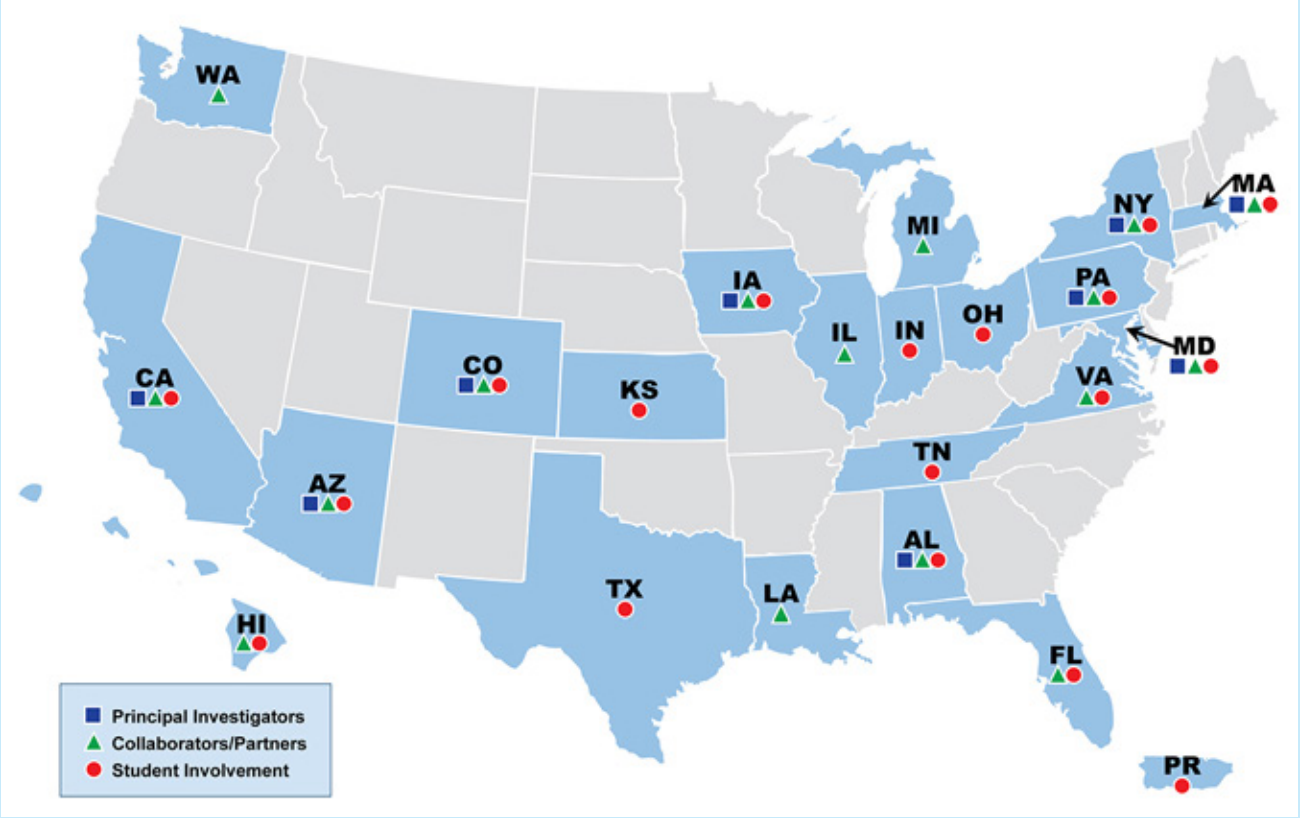

Fig. 4-3. *SAT Program Impacts Map. The Program supports research efforts of PIs and collaborators/partners, and develops our future astrophysics workforce through student involvement (locations shown for both COR and PCOS Programs).*

5. Closing Remarks

This 2017 COR PATR serves as a snapshot of the dynamic state of technology development managed by the Program Office and provides future directions for technology planning and maturation. As we complete another year of COR technology development activities, we see many positive developments.

Our technology development portfolio is growing, and continues to deliver significant advancements. All funded technologies are maturing toward higher TRLs, with several providing direct benefit to ground-based experiments and flight missions. New SAT awards slated to start in FY 2018 will fund development of Far-UV optics and UV/Vis detectors. COR SAT investments are also generating benefits beyond direct advancement of strategic technologies. This includes leveraging internal and external (including non-NASA) funding; using contributed materials, parts, and facility/equipment; hiring students and post-docs, thereby training our future astrophysics workforce; and generating research collaborations and industry partnerships, in support of COR science goals.

Our technology gap prioritization process continues to adhere to strategic guidance based on the AIP; Astrophysics Roadmap "Surveyor" concepts, especially those being studied by STDTs; and NWNH; with the TMB assigning the most significant weight in technology gap prioritization to strategic alignment. As a result, the Astrophysics Division is likely to continue to fund SAT proposals addressing technology gaps identified by the TMB as having the highest priority. The latest set of highest-priority TMB recommendations, submitted to the Astrophysics Division and reported here, include technology developments related to OST and LUVOIR.

To support the ever-evolving technology needs of the COR community, we continue to interact with the broad scientific and technical communities through the COPAG, through various workshops, via public outreach activities, and at scientific conferences. These activities identify and incorporate the astrophysics community's ideas about new science, current technology progress, and new needs for technology in an open and accessible process. Each year, we incorporate new lessons learned and make appropriate improvements to our process. In parallel, we incorporate the technology needs identified by the large-mission-concept study teams into our technology gaps identification and prioritization process.

We would like to thank the COR scientific and technical communities, the PIs and their teams, the COPAG TIG, and the large-mission-concept STDTs for their efforts and inputs that make this annual report current and meaningful. We welcome continued feedback and inputs from the community in developing next year's PATR, which should be sent to *Program Office Technology Development Manager*. For more information about the COR Program and its activities, please visit the *COR website*.

References

[1] J. Mankins, "*The critical role of advanced technology investments in preventing spaceflight program cost overrun*," The Space Review, December 1, 2008. Available at *http://www.thespacereview.com/article/1262/1*. Accessed May 2014

[2] National Research Council, "*New Worlds, New Horizons in Astronomy and Astrophysics*," Washington, DC: The National Academies Press, 2010. Available at *http://ww.nap.edu/catalog.php?record_id=12951*. Accessed May 2014

Appendix A
Technology Gaps Evaluated by the TMB in 2017

This appendix details the technology gaps prioritized by the Cosmic Origins (COR) Program Technology Management Board (TMB) in 2017. These are gaps between the current state-of-the-art (SOTA) technologies, as assessed by technology readiness levels (TRLs, see Table A-1) and capabilities needed for future missions.

The order of the gaps is similar to that of prior-year Program Annual Technology Reports (PATRs). Specifically, we've grouped the gaps by science topic and technology type. Where submitted gaps had significant overlap, they were merged into a single gap by the TMB. Gap priority ranking is shown on p. 22 above. Submitted entries not ranked may have been merged into others; deemed outside the purview of the COR program (e.g., better addressed by Strategic Astrophysics Technology, SAT, programs other than COR; or associated with launch vehicles, rovers, avionics, spacecraft systems, etc.); deemed as not being technology gaps (i.e., specific implementations or not technologies at all); or deemed too mature for the SAT program.

Each entry lists the source of the gap next to the gap name. Sources include the general community or a large-mission-concept study team. We thank the TIG, the Origins Space Telescope (OST) Science and Technology Definition Team (STDT), the Large UV/Optical/IR (LUVOIR) STDT, and the general community for their engagement in and support of our technology gap identification process.

The Program Office considers gaps submitted by a study team as "owned" by the study team until the team submits its final report. In practical terms, this means that the Program Office will forward to the study team any edits to such a gap that are submitted by the general community by the June 1 deadline. The study team will then consider these edits for possible inclusion into the following-year version of the gap. The study teams' unmatched expertise in the technology needs of their respective mission concepts gives great credibility to their opinions on such technologies; increasing the likelihood of higher priority ranking for gaps owned by the teams.

TRL	Definition
1	Basic principles observed and reported.
2	Technology concept and/or application formulated.
3	Analytical and experimental critical function and/or characteristic proof-of-concept.
4	Component and/or breadboard validation in laboratory environment.
5	Component and/or breadboard validation in relevant environment.
6	System/subsystem model or prototype demonstration in a relevant environment.
7	System prototype demonstration in an operational environment.
8	Actual system completed and "flight qualified" through test and demonstration.
9	Actual system flight proven through successful mission operations.

Table A-1. *TRL definitions from NASA Procedural Requirements (NPR) 7123.1B Appendix E, which provides a full description of the TRLs.*

Gap Name		Large-format, high-dynamic-range UV detectors *Submitted by LUVOIR STDT*
Description		Micro-channel Plate (MCP) detectors that are 200 x 200 mm or larger in format are needed to enable large field-of-view UV instruments. Additional improvements in FUV sensitivity and count rates further enhance the science yield of LUVOIR.
Current State-of-the-Art (SOTA)		SISTINE, FORTIS, CHESS: Suborbital sounding rocket missions that have incrementally matured aspects of MCP detector technology, including array size, photocathode sensitivity, and read-out electronics count rates (TRL 9) Delta-doped silicon-based detectors such as CCD, EMCCD, and CMOS arrays offer new options in terms of format and dynamic range, but are less mature, less solar blind, and less radiation tolerant than MCP detectors. (TRL 4) A principal goal for all technologies is the development of a large-format detector with high pixel count to allow for wide-field imaging and multi-object spectroscopy (MOS) in the UV. All technologies need additional development to achieve these high fill-factor focal planes with a large pixel count, while maintaining other capability requirements. Curved detectors that have the potential to simplify relay optics and reduce the number of reflections for wide-field of view performance should also be considered.
TRL	**SOTA**	4 – 9
	Solution	4
Performance Goals and Objectives		TRL 5: Incorporate all aspects of the sounding rocket development program into a single MCP detector demonstration that achieves the LUVOIR format, sensitivity, and count-rate requirements. Thorough flight qualification would further improve the TRL to 6. Continue developing delta-doped silicon based detectors to improve sensitivity, radiation tolerance, and solar blindness. Flight qualify large-format arrays.
Scientific, Engineering, and/or Programmatic Benefits		MCPs have long been the “gold standard” for UV science observations. Continued improvement of these detectors would have science and programmatic benefits for any mission operating in the UV. Development of silicon-based UV detectors will offer new options for future UV science missions.
COR Applications and Potential Relevant Missions		LUVOIR, HabEx, any mission with UV science.
Time to Anticipated Need		TRL 6 would be necessary by mission PDR in the mid-2020s.

Gap Name		High-efficiency UV multi-object spectrometers *Submitted by General Community*
Description		Future NASA UV missions devoted to spectroscopy require high-throughput (> 50%), multi-object spectrometer (> 100 sources; R~3000 or greater) architectures and components for operation at 100-400 nm or broader band (e.g., digital micro-mirror device, DMD; advanced diffraction gratings; micro-shutter arrays; fiber-fed spectrographs; and integral-field spectrometers).
Current State-of-the-Art (SOTA)		DMD is at TRL 5, based on European studies for Euclid, and particle-radiation tests at LBL. Micro-shutters for longer wavelengths (> 0.6 microns) are at TRL 6 from JWST testing. Microshutters for the FUV have been flown on a sounding rocket. There are currently no technologies proven by prototyping or flight for multiplexed integral field spectroscopy without spectral confusion limitations in the far-UV. Low-scatter Echelle gratings are currently at TRL 2.
TRL	**SOTA**	2–6
	Solution	
Performance Goals and Objectives		Routinely produce large-format, high-throughput, moderate-resolution systems that can be used in a variety of Explorer, medium, and strategic missions. Key performance criteria for customization, maturation, and characterization of object-selection components (such as DMDs, micro-shutters, or reconfigurable fibers) for UV/Vis/NIR space astronomy include: • Sensitivity over the spectral interval 0.10-1.7 μm, • Effective sky background blockage (e.g., zodiacal light) • Source multiplexing without spectral confusion limitations • Low instrumental background (optical scattering, thermal background). Low-scatter Echelle gratings are required for high-resolution far-UV (λ = 90-180 nm) spectroscopy. Performance goals for gratings include scattered-light control comparable to the best first-order diffraction grating currently flying (HST-COS), ~10^{-5} of peak intensity at $\Delta\lambda$ = 10 Å from fiducial wavelength λ_0. In the short term, scattering < 10^{-3} would enable deeper, high-resolution UV spectroscopy than currently available with HST, in an Explorer-class mission.
Scientific, Engineering, and/or Programmatic Benefits		High-performance multi-object spectrometers can increase the science impact of missions by orders of magnitude. Space telescopes today can obtain slit spectra of a single object or slit-less spectra of a field, but not slit spectra of multiple objects in a field, nor can they reconfigure the focal plane (like a fiber fed spectrograph) for integral field spectroscopy in the far-UV. A UV/visible slit selector (DMD, micro-shutter array, or multi-fiber) would enable multi-object source selection and block unwanted background (e.g., zodiacal light). Better gratings improve contrast and thereby sensitivity. New technologies that would eliminate spectral confusion would enable efficient spectroscopic mapping of extended sources in the UV. Enabling technology for small, wide-field telescopes appropriate for an Explorer mission.
COR Applications and Potential Relevant Missions		UV/Vis/IR multiplexing technologies have a broad application to astrophysics, heliospheric, and Earth-science missions.
Time to Anticipated Need		As early as possible since mission definition and capabilities are built around instrument performance. Development for space astronomy is needed in time to respond to an expected announcement of opportunity for an Explorer-class mission in 2019.

Gap Name		Lightweight, large-aperture, high-performance telescope mirror systems for UVOIR *Submitted by General Community*
Description		Potential UVO missions require 4 to 8-m monolithic or 10 to 16-m (or larger) segmented mirrors with 5 nm RMS surface figure error to achieve diffraction limited system performance at wavelengths less than 500 nm. This SFE can be achieved via active or passive technology. Active technology includes alignment and wavefront sense and control. Passive technology includes ultra-stiff, damped, mirror substrates and support structure. Areal density depends upon aperture diameter and intended launch vehicle, but large apertures required areal densities of less than 25 kg/m^2. Areal cost also depends on aperture diameter, but for UVOIR the goal should be less than $1M per m2 ($0.5M per m^2 desired). Key technologies to enable such a mirror include new and improved: • Mirror substrate materials and/or architectural designs • Processes to rapidly fabricate and test UVO quality mirrors • Mirror support structures that are ultra-stable at the desired scale • Mirror support structures with low-mass that can survive launch at the desired scale • Mechanisms and sensors to align segmented mirrors to < 1 nm RMS precisions Also needed is ability to fully characterize surface errors and predict optical performance via integrated STOP (structure thermal optical performance) modeling.
Current State-of-the-Art (SOTA)		The SOA for UVO is defined by the 2.5-meter Hubble primary mirror and 1.4-m Kepler primary mirror. Both are at TRL9. However, the Hubble mirror was made by a technology that is no longer used. Kepler was manufactured via the ULE® frit process. This process is scalable to sizes as large as 4 meters. The 2.4-m WFIRST primary mirror is at TRL6. It is manufactured via the ULE® low-temperature fusion process. This process is scalable to sizes as large as 4-meters. AMDS and MMSD projects demonstrated 1.4-m, 200-Hz first mode,< 10 nm rms surface figure error, < 5 Å micro-roughness (projected) and < 25 kg/m^2 mirrors manufactured via the ULE® low-temperature-fusion/ low-temperature slumping (LTF/LTS) process. This technology is at TRL5. The AMTD project has demonstrated a 1.5-m × 200-mm, 450-Hz first mode, 40-kg/m^2 mirror manufactured via the stacked core ULE® LTF/LTS process. This technology is at TRL3/4. The areal cost of this mirror is approximately $1M/m^2. Additionally, an extreme-lightweighted Zerodur® mirror has been demonstrated at 1.2 m and thermally characterized via the AMTD project. This technology is assessed to be TRL4.
TRL	**SOTA**	3 – 4
	Solution	3
Performance Goals and Objectives		Development is required to fabricate components and systems to achieve the following: • Monolithic: 1 to 8 meters • Segmented: > 12 meters • Surface Figure: < 5 nm RMS • Slope: < 0.1 micro-radian • First Mode Frequency: >200 Hz • Actuator Resolution: < 1 nm rms • Areal Cost: < $1M/m^2 • Areal Density: < 25 kg/m^2

Scientific, Engineering, and/ or Programmatic Benefits	Closing this technology gap may enable rigid monolithic primary mirrors, or affordable but reliable deployment techniques for segmented apertures; either would provide increased capabilities. Scientific: greater collecting area increases sensitivity; larger diameter enables greater angular resolution. Both enable important new science for COR and exoplanets. Engineering: lower-mass primary allows lighter structure, larger margins; simplified deployment concepts and mechanisms allow larger apertures in smaller launch vehicles. Programmatic: A lighter and cheaper telescope allows greater allocation of mass and money for the science instrument, and could enable smaller missions.
COR Applications and Potential Relevant Missions	This is an enabling technology all potential Astrophysics UVOIR missions, including but not limited to HabEx, LUVOIR, or an Astro-Probe mission. This technology development will enable (current) MIDEX-class science with a SMEX, Astrophysics Probe-class science with a MIDEX, and more ambitions larger-mission science with an Astrophysics Probe-class implementation. Development of inexpensive 1-3-m monolithic lightweight stiff mirrors will benefit suborbital, Explorer, and Astrophysics Probe missions.
Time to Anticipated Need	Need to demonstrate credibility before the 2020 Decadal Survey, and would require TRL 6 by mission PDR anticipated in the mid-2020s.

Gap Name		Lightweight, large-aperture, high-performance telescope mirror systems for Far-IR *Submitted by General Community*
Description		Potential Far-IR missions require 4 to 8-m monolithic or 10 to 16-m (or larger) segmented mirrors with 100 nm RMS surface figure error AT TEMPERATURE to achieve diffraction limited system performance at wavelengths less than 10 micrometers. This SFE can be achieved via active or passive technology. Active technology includes alignment and wavefront sense and control. Passive technology includes stiff, damped, mirror substrates and support structure. Areal density depends upon aperture diameter and intended launch vehicle, but large apertures required areal densities of less than 25 kg/m^2. Areal cost also depends on aperture diameter, but for Far-IR the goal should be less than $0.5M per m2 ($0.25M desired). Key technologies to enable such a mirror include new and improved: • Mirror substrate materials and/or architectural designs • Processes to rapidly fabricate and test cryogenic mirrors • Mirror support structures that are stable at the desired scale • Mirror support structures with low-mass that can survive launch at the desired scale Also needed is ability to fully characterize surface errors and predict optical performance via integrated STOP (structure thermal optical performance) modeling. NOTE: to achieve ultimate sensitivity, emission must be minimized, which requires Far-IR telescopes to be operated at temperatures (depending on the application) as low as 4 K.
Current State-of-the-Art (SOTA)		The 6.5-meter Beryllium JWST Primary Mirror Assembly meets all the performance requirements for Far-IR operating at < 50K. JWST Be mirror segment technology is TRL6. But: • JWST technology is unaffordable for larger aperture telescopes. JWST areal cost is ~$6M/m^2 or $150M for a 25 m^2 collecting area. For a 16-m (200 m^2 collecting area) telescope, an areal cost of $1M/m^2 yields a $200M primary mirror cost. • Monolithic aperture Beryllium mirrors cannot be made larger than approximately 1.4-meters. The MMSD program has produced 1.35-m JWST class SiC actuated hybrid mirror segments with < 14 nm rms surface figure error, < 10 Å micro-roughness (projected), and < 25 kg/m^2 total. This technology is at TRL5. The 3.5-meter SiC Herschel Primary Mirror meets all requirements except diffraction limited performance. The Herschel primary mirror is diffraction limited at 80 micrometers. Herschel SiC mirror technology is TRL9. Cryogenic low-dissipation actuators exist at TRL 3-5. The balloon BLAST program is developing a 2.5-meter Carbon Fiber Resin Epoxy (CFRP) or Graphite Composite mirror. Apertures of up to ~10 meters are undergoing ground-based tests, including the phase 1 study for the Large Balloon Reflector
TRL	**SOTA**	3 – 4
	Solution	3
Performance Goals and Objectives		Development is required to fabricate components and systems to achieve the following: • Monolithic: 1 to 8 meters • Segmented: > 12 meters • Surface Figure: < 150 nm RMS AT TEMPERATURE • Cryo-Deformation: < 100 nm RMS (surface) • First Mode Frequency: > 200 Hz • Areal Cost: < $1/m^2 • Areal Density: < 25 kg/m^2

Scientific, Engineering, and/ or Programmatic Benefits	Low-cost, lightweight cryogenic optics at reasonable cost are required to enable development of large-aperture FIR telescopes in the 2020s. Large apertures are required to provide the spatial resolution and sensitivity needed to follow up on discoveries from the current generation of space telescopes. A high altitude, long duration observing platform with a mirror factors of 2-5 larger than on either SOFIA or Herschel has the potential to increase sensitivity in the far-infrared by factors of several in particular wavelength regimes over either facility, at relatively low cost. This enables scientific breakthroughs in the far-infrared including (1) detecting the dusty progenitors to 'ordinary' local galaxies at redshifts up to z = 3, and (2) high sensitivity mapping of debris disks around young stars. This technology is also relevant to e.g. Earth observation.
COR Applications and Potential Relevant Missions	This is enabling technology all potential Astrophysics Far-IR missions, including but not limited to OST, or an Astro-Probe mission. Additionally this is enhancing technology for a potential FIR interferometer. This technology development will enable (current) MIDEX-class science with a SMEX, Astrophysics Probe-class science with a MIDEX, and more ambitions larger-mission science with an Astrophysics Probe-class implementation. Development of inexpensive 1-3-m monolithic lightweight stiff mirrors will benefit suborbital, Explorer, and Astrophysics Probe missions. This technology is of particular relevance to ultra-long duration balloon projects, which are maturing as a viable and attractive platform for multiple astrophysics missions.
Time to Anticipated Need	Need to demonstrate credibility before the 2020 Decadal Survey, and would require TRL 6 by mission PDR anticipated in the mid-2020s.

Gap Name		Segmented-aperture coronagraph architecture *Submitted by LUVOIR STDT*
Description		The design of coronagraph masks (apodizers, occulters, Lyot stops) and architectures fundamentally determines what contrast will ultimately be achievable by the coronagraph, and over what spatial frequencies and bandpasses. The coronagraph design also has a large impact on the overall throughput and sensitivity of the coronagraph to wavefront error instability. Additional coronagraph backend architectures (integral field spectrometers, fiber fed spectrometers, etc.) can enable observational efficiencies by allowing multiplexed object characterization.
Current State-of-the-Art (SOTA)		**APLC:** The SCDA study resulted in several designs that achieve the necessary contrast, IWA, bandpass, and throughput to enable the LUVOIR science, but require additional modeling to understand the impact of wavefront instability and stellar diameter (TRL 3) **VVC:** The SCDA study resulted in several designs that achieve the necessary contrast, IWA, and bandpass to enable the LUVOIR science, but throughput was significantly impacted by the on-axis obscuration. Additional optimization is needed to improve design throughput, as well as understand the impact of wavefront instability and stellar diameter (TRL 3) **VNC:** A lateral shearing VNC was demonstrated at 10^{-9} contrast at the necessary IWA, but narrowband and with no shear implemented. This demonstration was performed with a segmented DM at a pupil, thus constitutes a demonstration with a segmented aperture (TRL 3) **HL / SPC:** WFIRST CGI has demonstrated 10^{-8} contrast as part of the WFIRST CGI technology development program, with a significantly obscured aperture (TRL 6)
TRL	**SOTA**	3–6
	Solution	3
Performance Goals and Objectives		TRL 4: Continue the SCDA study to model coronagraph performance with realistic noise inputs, including dynamic disturbances and stellar diameter. Perform testbed demonstrations of the coronagraph designs and achieve moderate contrasts (10^{-8} or better) over 15% bandpass at relevant inner working angles. Correlate the testbed demonstration with the models that predict 10^{-10} contrasts. TRL 5/6: Perform testbed demonstrations of coronagraph designs that achieve flight requirements on contrast, bandpass, IWA, and throughput, using flight-traceable components for masks and DMs.
Scientific, Engineering, and/or Programmatic Benefits		This technology fundamentally enables a full exoplanet survey using a large-aperture segmented space telescope. Such a survey would statistically bound the frequency of habitable exoplanets, while simultaneously exploring the full diversity of all exoplanets around sunlike stars.
COR Applications and Potential Relevant Missions		Although the high-contrast coronagraph is fundamentally an exoplanet science instrument, it has two potentially relevant COR impacts. First, the coronagraph can enable a small number of important COR observations such as debris disks and active galactic nuclei. Secondly, this technology fundamentally enables the LUVOIR mission, which itself enables a wide variety of general astrophysics observations. Thus, this technology indirectly enables groundbreaking general astrophysics science.
Time to Anticipated Need		A TRL 4 demonstration prior to the 2020 Decadal Survey would improve credibility of the overall LUVOIR mission concept. TRL 5 and 6 demonstrations would be necessary prior to mission PDR in the mid-2020s.

Gap Name		High-contrast imaging post-processing *Submitted by LUVOIR STDT*
Description		Calibration and post-processing techniques allow the additional subtraction of stellar flux from an image, after data collection. This is a process necessary to achieve the highest contrast, thus defining the exoplanet detection floor.
Current State-of-the-Art (SOTA)		**HST:** Post-processing techniques have been used routinely on archival NICMOS coronagraphic images to improve contrast from raw levels of 10^{-5} by an average of 300×, with detection of point sources 50× below the mean speckle intensity (TRL 9) For ground based systems, additional factors of ~10× in contrast have been achieved for moderate contrast coronagraph systems (10^{-5} – 10^{-6}) (TRL 4) WFIRST is baselining a factor of 30× improvement in contrast via post-processing (TRL 4)
TRL	**SOTA**	4 – 9
	Solution	4
Performance Goals and Objectives		TRL 5/6: Post-processing techniques and algorithms need to be tested on simulated and/or real data with raw contrasts on the order of 10^{-8} – 10^{-10}, that include realistic background and noise fluxes. Achieving additional contrast factors of 10×-100× would enable significant improvements in the science yield of LUVOIR.
Scientific, Engineering, and/or Programmatic Benefits		Contrast enhancement via PSF calibration and subtraction (or deconvolution) can be useful for any imaging application to improve image quality after data collection.
COR Applications and Potential Relevant Missions		Any imaging mission.
Time to Anticipated Need		TRL 6 by mission PDR in the mid-2020s would enhance the LUVOIR science goals.

Gap Name		Ultra-stable opto-mechanical systems architecture *Submitted by LUVOIR STDT*
Description		High-contrast (10^{-10}) imaging and spectroscopy for exoplanet science is critically dependent on telescope optics and wavefront stability. A challenging requirement on the opto-mechanical system is that of wavefront error stability on the order of 10 pm RMS per wavefront control step (~10s of minutes), within the specific spatial frequencies that correspond to the dark-hole region of the focal plane. For the LUVOIR segmented aperture architecture(s), several key technologies are required to enable sufficient thermal and dynamic stability. These technologies are detailed in subgaps 1(a) through 1(c), below.
Current State-of-the-Art (SOTA)		**Lisa Pathfinder:** The LISA pathfinder mission is an existence proof of a spaceflight opto-mechanical system capable of achieving picometer-level stability (1 pm/rt-Hz on mHz bandwidths) (TRL 9). However, the demonstrated stability was not over the spatial or temporal frequencies required by LUVOIR. **JWST:** When launched, JWST will exhibit the state-of-the-art for large aperture space telescopes in just about every area of performance, including wavefront stability. The expected wavefront stability is ~50 nm RMS per 14 day control period (TRL > 6) **WFIRST:** The WFIRST Coronagraph Instrument (CGI) will be the first on-orbit demonstration of a high-contrast imaging system operating at ~10^{-8} contrasts. While the level of wavefront stability to achieve this contrast is not sufficient for LUVOIR, WFIRST CGI will be a critical precursor technology demonstration for all future missions with a high-contrast coronagraph, providing invaluable experience in the design, integration, test, and operation of a large space telescope with single-digit nanometer, or sub-nanometer wavefront stability (TRL 6)
TRL	**SOTA**	6–9
	Solution	2
Performance Goals and Objectives		TRL 3: Perform model-based systems-level studies that predict component technologies working together in an architecture to deliver the required stability. Such models can include integrated structural, thermal, optical models of the system with relevant thermal and dynamic inputs. End-to-end telescope-coronagraph optical models can also be used to verify stability requirements at specific spatial frequencies, relaxation of stability requirements, as well as closed-loop control system architectures using different wavefront sensing and metrology inputs. TRL 4: Perform hardware demonstrations of key technology components that indicate those components working at the required performance predicted by the above models. TRL 5/6: Systems-level h/w demonstrations showing the technology components working together on scale testbeds traceable to the LUVOIR architecture(s), and achieving performance predicted by validated models.
Scientific, Engineering, and/or Programmatic Benefits		An ultra-stable opto-mechanical system directly benefits any science program that requires precision optical measurements. The objectives laid out here are directly applicable to any high-contrast imaging system, though other missions performing ultra-precise astrometry or photometry, as well as metrology-based measurement such as eLISA, would benefit from large-scale opto-mechanical systems with picometer-level stability. The development of such systems will likely include the development of new materials, metrology systems, control architectures, isolation systems, and optical components. These individual technology components will have cross-cutting engineering and programmatic benefits.
COR Applications and Potential Relevant Missions		Any coronagraph-based mission can benefit from the development of this technology, including WFIRST, LUVOIR, HabEx, and OST. Any other mission requiring ultra-precise optical performance, such as diffraction-limited UV imaging or highly consistent PSF morphology, will benefit from this technology as well. It is important to note that being able to perform high-contrast imaging on a large segmented aperture system fundamentally enables the LUVOIR mission, which itself enables a wide variety of general astrophysics observations. Thus this technology indirectly enables groundbreaking general astrophysics science.
Time to Anticipated Need		TRL 3 and 4 demonstrations prior to the 2020 Decadal Survey would improve credibility of the overall LUVOIR mission concept. TRL 5 and 6 demonstrations would be necessary prior to mission PDR in the mid-2020s.

Gap Name		Segment phasing and control *Submitted by LUVOIR STDT*
Description		Both LUVOIR architectures are expected to use large, deployable, segmented primary mirrors to enable a large collecting aperture. Diffraction-limited phasing of such segmented systems using image-based phase retrieval will be demonstrated by JWST in 2018. However, maintaining picometer-level phasing between segments during long-duration coronagraph observations will require new sensing and control architectures, including: edge sensors (capacitive, inductive, or optical), laser metrology, artificial guide stars, and picometer-level actuators for both rigid body and surface figure correction.
Current State-of-the-Art (SOTA)		**JWST:** 6 nm RMS rigid body positioning error and ~50 nm RMS stability over a 14-day period using image-based phase retrieval (> TRL 6). Capacitive gap sensors operating at 450 Hz with ~10pm sensitivity, feeding back to PZT control of an etalon cavity (TRL 4). **LISA Pathfinder:** Laser metrology systems exceeded requirement of 1 pm/rt-Hz on mHz bandwidths (TRL 9). **SIM:** Demonstrated picometer-level laser metrology, but not in a configuration traceable to the LUVOIR architecture (TRL 5). Lab demonstrations of laser metrology systems with nanometer-level performance in a configuration similar to what might be needed by LUVOIR, consistent with high-contrast imaging applications (TRL 4). **HST:** PZT actuators with necessary stroke and precision have flight heritage on WFC3, though custom control electronics are likely necessary for LUVOIR applications (TRL 9). Ground-based edge sensor systems demonstrate basic control system architecture; additional work is needed to develop edge sensor geometry for efficiently measuring six degrees of freedom of segment position (TRL 4).
TRL	**SOTA**	4 – 9
	Solution	3
Performance Goals and Objectives		TRL 4: demonstrate a closed-loop sense & control architecture between (at least) two subscale segments, operating at appropriate bandwidths and resolutions. The performance requirements of the sensors and actuators should be tied to predictions from the over-arching system-level TRL 3 demonstration. TRL 5/6: demonstration on a sub-scale or full-scale segmented system that is traceable to the LUVOIR architecture with relevant dynamic and thermal inputs.
Scientific, Engineering, and/or Programmatic Benefits		As demonstrated by the range of state-of-the-art heritage, new metrology and control systems can have cross-cutting scientific, engineering, and programmatic benefits.
COR Applications and Potential Relevant Missions		LUVOIR, segmented aperture HabEx, future large segmented aperture systems, future interferometric systems.
Time to Anticipated Need		A TRL 4 demonstration prior to the 2020 Decadal Survey would improve credibility of the overall LUVOIR mission concept. TRL 5 and 6 demonstrations would be necessary prior to mission PDR in the mid-2020s.

Gap Name		Dynamic isolation systems *Submitted by LUVOIR STDT*
Description		Passive and active isolation and damping of dynamic disturbance sources on the spacecraft and/or payload.
Current State-of-the-Art (SOTA)		**JWST:** 80 dB attenuation at frequencies > 40 Hz (> TRL 6) Disturbance-free payload demonstrated broadband isolation at better than 60 dB (all frequencies), and better than 80 dB at many frequencies between 1 and 20 Hz (TRL 4). These measurements have been used in integrated modeling studies of the Advanced Technology Large Aperture Space Telescope (ATLAST, a precursor study to LUVOIR) and indicate these levels of isolation are acceptable, when coupled with TRL 9 passive isolators at the disturbance sources (reaction wheels).
TRL	**SOTA**	4–6
	Solution	4
Performance Goals and Objectives		TRL 5/6: update testbed demonstrations that were used for TRL 4 to use flight-traceable control electronics. Demonstrate the required pointing control authority necessary for the LUVOIR architecture(s).
Scientific, Engineering, and/or Programmatic Benefits		Passive and active isolation systems can be used to provide dynamically stable platforms for many science measurements.
COR Applications and Potential Relevant Missions		LUVOIR, HabEx, any COR mission requiring a dynamically stable platform.
Time to Anticipated Need		A TRL 5 demonstration prior to the 2020 Decadal Survey would improve credibility of the overall LUVOIR mission concept. A TRL 6 demonstration would be necessary prior to mission PDR in the mid-2020s.

Gap Name		Mirror-segment systems *Submitted by LUVOIR STDT*
Description		Mirror segments achieving diffraction-limited performance at 500 nm, high stiffness (> 200 Hz), and thermal stability consistent with the overarching picometer-level wavefront stability requirement.
Current State-of-the-Art (SOTA)		**JWST:** Beryllium mirror segments, 1.32-m flat-to-flat with 25 nm surface figure error (TRL 6). Multiple Mirror System Demonstrator (MMSD) demonstrated fabrication or partial fabrication of five, 1.4-meter point-to-point ULE mirror segment substrates, achieving 10 kg/m^2 areal density and a production schedule of 3 mirrors on three-week centers. One of the five mirror segment substrates was flight qualified. Thermal modeling performed with as-measured CTE distributions indicate that these fabricated mirrors can achieve the necessary thermal stability for LUVOIR when properly controlled. ULE segment substrate is TRL 5; fully integrated ULE segments are TRL 4. Multiple fully integrated actuated 1.35-m SiC substrate mirror segment systems have been demonstrated for visible applications, and one has been flight qualified at TRL 6. Adding the necessary polished Si cladding would lower this TRL to 4.
TRL	**SOTA**	4–6
	Solution	5
Performance Goals and Objectives		TRL 5/6: Demonstrate fully integrated mirror segment system (including mounts, thermal control, actuators, and support structure) that meets mirror figure requirements, including segment-to-segment figure matching. TRL 6: demonstrate thermal and dynamic stability of a fully integrated mirror segment system that is traceable to the LUVOIR architecture and tested in relevant dynamic and thermal environments. To fully explore mirror architecture trades, a competitive, industry-driven mirror development program should be pursued, wherein 2 or 3 mirror architectures are developed, eventually downselecting to a flight candidate architecture.
Scientific, Engineering, and/or Programmatic Benefits		Enables a LUVOIR or segmented HabEx mission.
COR Applications and Potential Relevant Missions		LUVOIR, segmented HabEx, or any future large segmented aperture telescope operating at room temperature in the UV/O/IR bandpass.
Time to Anticipated Need		A TRL 6 demonstration would be necessary by mission PDR in the mid-2020s.

Gap Name		High-performance spectral dispersion component/device *Submitted by General Community*
Description		1. A highly spectral-dispersive compact component/device can be inserted into a converging beam before the telescope focus as a slitless spectrograph or grism. Note: a presently promising solution to this gap is Freeform Diffractive Optical Surfaces. 2. High-efficiency gratings with a relatively flat diffraction efficiency over the grating free spectral range (minimum > 85% over the free spectral range; 90% is preferred; the higher, the better). Note: a presently promising solution is to modify the groove profile from blazed grating. Transmissive or reflective hologram optical element technology performs a similar function. Geometric wavefront aberrations can be corrected at the same time as the diffraction to reduce the number of surfaces and maintain high transmittance.
Current State-of-the-Art (SOTA)		For Item 1 above: Current SOTA slitless spectrometer in Euclid mission is being designed and built as a standalone instrument, including corrector, imager, and grism assembly, to cover the requirement indicated in Item 1 [Proc. of SPIE **9143**, 91430K-1 (2014)]. For Item 2 above: Current SOTA diffraction efficiency reaches high 90%. It is achieved with blazed transmission grating. However, the diffraction efficiency quickly drops to 70% at the edges.
TRL	**SOTA**	3
	Solution	3
Performance Goals and Objectives		The technical goal is as follows: • Compact enough to be installed in the spectral-filter wheel as one filter element; • Accommodate large FOV (> 0.25 square degrees in sky); • Diffraction limited (or nearly so) in the wavelength range; • Relatively high spectral resolution (> 600 λ); • Dispersion wavelength range reaches, or is close to, the grating free spectral range. It can be used between 600 to 2400 nm; • High diffraction efficiency (> 95% at peak wavelength); • Par-focal with other filter elements; and • Spread the unwanted orders on the detector so much as to be buried in detector noise. The objective is to develop a compact spectral dispersive device/component that can be simply inserted into a converging beam as a slitless spectrograph. The technical goal is also to develop a transmission grating with a high and relatively uniform diffraction efficiency. The objective is to ease spectral-intensity calibration and shorten exposure time.
Scientific, Engineering, and/or Programmatic Benefits		Science benefit: dramatically reduce ghost-spectra intensity, increase element throughput (transmittance), and shorten exposure time for larger survey area. Engineering benefit: Make a standalone instrument into a component greatly simplifying the entire engineering process and saving precious spacecraft volume for other applications. Programmatic benefit: Reduce risk and lower cost, as well as shorten delivery time.
COR Applications and Potential Relevant Missions		Any mission that needs a spectrograph, e.g., LUVOIR and its Probe, as well as OST. Can also be used for heliophysics, planetary, and Earth science. Beyond that, the technique will be very useful to many commercial applications.
Time to Anticipated Need		As soon as possible.

Gap Name		Band-shaping and dichroic filters for the UV/Vis *Submitted by General Community*
Description		Bandpass filters are employed throughout astronomy, and efficient transmissive designs are standard in the Vis/NIR. There is a pressing need for high-efficiency UV-transmitting filters. Because some classes of UV detectors have significant visible-light sensitivity, UV-transmitting "red-blocking" filters are also of high value. This includes narrowband (bandpass) or band-selectable (dichroic, long-pass) imaging applications, or spectroscopic applications where multiple UV channels or order-sorting is required. Detector-integrated filters of various types (bandpass, visible blocking, and graded thickness) can offer improved performance over stand-alone optical components by improving overall system throughput and reducing the total number of optical surfaces in an instrument. Finally, UV/Vis/NIR dichroic filters are useful in creating multiple channels in an instrument, allowing simultaneous observation using band-optimized instrumentation and detectors over the widest possible FOV. Reflecting optical filters have been shown to have high extinction in the red ~10^{-6}, and excellent UV reflectivity.
Current State-of-the-Art (SOTA)		Commercial optical filters are mature and widely available for visible and NUV wavelengths (> 250 nm). Current state of the art UV-transmission filters have efficiencies of < 10-20% below 180 nm and < 50% for 180-280 nm. Robust commercial high-efficiency UV-transmitting filter solutions are not frequently available. Red-blocking "Woods filters" with low efficiency (< 10-15%) and lifetime issues have been employed for solar-blind imaging. All dielectric designs are less commonly available at shorter FUV wavelengths due in part to the lack of transparent high-refractive-index materials in this wavelength. Dichroic filters have been designed for the UV, for example the FUV/NUV split in the GALEX instrument, but efficiency in each channel (50/80%) and effective bandwidth in each channel (< 50 nm) is limited at current SOTA. In the FUV, metal-dielectric structures have been successfully implemented as bandpass filters for broadband detector systems (e.g., HST, Swift) but with low throughput (< 20% below 200 nm). Similar designs have been implemented in laboratory settings directly on silicon FPAs to provide integrated red rejection capabilities with increased throughput (> 50% below 200 nm).
TRL	**SOTA**	4
	Solution	
Performance Goals and Objectives		• Filter transmittance in UV for R~5 bandpass filter: > 50% (80%) FUV (NUV); • Red-blocking transmittance: > 50-75% (UV), < 0.0001%-0.01% Vis-NIR; • Dichroic: Mid-UV Split: R (FUV) > 0.8, T (NUV) > 0.9; • Bandwidth: FUV (100 nm), NUV (100-200 nm); • Minimum wavelength: 100-105 nm; • Improved dielectric designs (dichroics, edge filters); dichroic: UV/Vis Split: R (UV) > 0.9, T (Vis) > 0.9; and • Detector-integrated filters (red rejection, narrowband, or broadband AR) on large scale.
Scientific, Engineering, and/or Programmatic Benefits		High efficiency and low noise resulting from out-of-band rejection, and multi-channel instruments using dichroics allow deep astronomical surveys to be conducted with space-based telescopes on much shorter, feasible timescales, and enable instrument designs that exploit the aperture size (geometrical area) and full working FOV of the telescope. The integration of UV-filtering elements directly on a sensor system has the potential to improve in-band sensitivity while providing out-of-band rejection. Eliminating discrete optical component can reduce instrument complexity. Relevant experience with UV, Vis, and/or NIR filters and dichroics that achieve the technical goals set forth above is essential for maximizing the return of future space observatories. This technology is crosscutting, with applications across astrophysics, planetary, and space sciences. Commercial applications similarly benefit from high throughput and band-rejection.

COR Applications and Potential Relevant Missions	COR science requires deep multi-wavelength measurements of galaxies and AGN to study their evolution from the formation of the first stars and black holes to structures observed on all scales in the present-day universe. High priority for observations of unseen phenomena such as the cosmic web of intergalactic and circumgalactic gas and resolved light from stellar populations in a representative sample of the universe. Potentially relevant missions include a LUVOIR space telescope, Explorer and Probe-class missions that can conduct wide-field surveys, and small-sat experiments that can advance technology while addressing one or more COR science objectives.
Time to Anticipated Need	Need to demonstrate credibility before the 2020 Decadal Survey, and would require TRL 6 by mission PDR anticipated in the mid-2020s.

Gap Name		High-reflectivity broadband FUV-to-NIR mirror coatings *Submitted by LUVOIR STDT*
Description		General astrophysics and exoplanet science require high-throughput observations between 100 nm and 2.5 μm. Coating should achieve > 50% reflectivity at 105 nm while not compromising performance at wavelengths > 200 nm compared to existing state-of-the-art. Coating process must be scalable to meter-class segments and repeatable to ensure uniform performance across an aperture comprised of > 100 segments.
Current State-of-the-Art (SOTA)		State-of-the-art Al+LiF coatings demonstrated on coupons exhibit the desired performance but suffer from environmental degradation (hygroscopicity). Investments in improving deposition processes is needed, to provide repeatable, large scale results. The ability to deposit an additional thin capping layer of MgF_2 or AlF_3 would provide environmental stability while not affecting performance. Coating characterization is needed to perform polarization performance modeling and its impact on high-contrast imaging. As to mirror cleaning, existing approaches (e.g., CO_2 snow, or electrostatic wands with AC excitation), do not remove molecular contamination. Promising methods (e.g., electron or ion beams) could clean off molecular layers as well as dust on substrates.
TRL	**SOTA**	3
	Solution	3
Performance Goals and Objectives		TRL 4: Demonstrate the deposition of a protected Al+LiF+MgF_2 or Al+LiF+AlF_3 FUV-optimized coating on glass substrates and separate coating runs to verify repeatability of the coating process. Characterize coating reflectivity, uniformity, and polarization performance to verify the coatings achieve LUVOIR requirements. TRL 5/6: Verify coating stability over time in ambient environments, as well as in a relevant radiation environment. Demonstrate coating process on meter-class segments. Techniques for last-minute ground or in-flight cleaning technology to remove molecular coatings as well as dust.
Scientific, Engineering, and/or Programmatic Benefits		Improved coating reflectivity can have cross-cutting benefits for any missions with broadband UVOIR science. Stable coatings that maintain performance in ambient environments can have programmatic benefits by simplifying I&T and handling procedures.
COR Applications and Potential Relevant Missions		NWNH noted the importance of technology development for a future ≥ 4-m class UV/Vis mission for spectroscopy and imaging. This technology would also support the next generation of UV missions, including Explorers, Probes, and large (> 4-m apertures) future UV/Optical/IR telescopes, and is key for a LUVOIR Surveyor. All future missions with optics, particularly missions with an important FUV or UV component, will benefit from improved coatings. Benefits will also accrue to planetary, heliospheric, and Earth missions utilizing the UV band.
Time to Anticipated Need		A TRL 4 demonstration prior to the 2020 Decadal Survey would improve credibility of the overall LUVOIR mission concept. TRL 5 and 6 demonstrations would be necessary prior to mission PDR in the mid-2020s. Mirror cleaning technologies would be immediately useful for missions already in development.

Gap Name		Large-format, low-noise and ultralow-noise Far-IR direct detectors *Submitted by OST STDT*
Description		The most important technology for the FIR/submillimeter is large-format detectors that operate with high efficiency (≥ 80%), low noise, and relatively fast time constant. Arrays containing thousands of pixels are needed to take full advantage of spectral information content. Arrays containing tens of thousands of pixels are needed to take full advantage of the focal plane available on a large, cryogenic telescope. Detector sensitivity is required to achieve background-limited performance, using direct (incoherent) detectors to avoid quantum-limited sensitivity.
Current State-of-the-Art (SOTA)		Single detectors are at TRL ~5, but demonstrated array architectures are lagging at TRL ~3. Sensitive (NEP low 10^{-19} W/√Hz), fast detectors (TES bolometers, and MKIDs in kilo pixel arrays) are at TRL 3.
TRL	**SOTA**	3
	Solution	3
Performance Goals and Objectives		Detector format of at least 10^4 pixels with high fill-factor and sensitivity (noise-equivalent power, NEP) of ~1×10^{-19} W/√Hz are needed for wide-band photometry. **(enabling)** Detector sensitivities with NEP of ≈ 3×10^{-20} W/√Hz are needed for spectroscopy (enabling), available in a close-packed configuration in at least one direction. NEPs of 3×10^{-21} W/√Hz would enable near background-limited sensitivity **(enhancing)** The detector system should be scalable to enable ~million-pixel total format (10k~50k pixels per sensor) in a large mission. Array size of 1×10^4 is **enabling** and 5×10^4 is **enhancing** Fast detector time constant (~200 μs) is needed for Fourier-transform spectroscopy.
Scientific, Engineering, and/or Programmatic Benefits		Sensitivity reduces observing times from many hours to a few minutes (≈ 100 × faster), while array format increases areal coverage by × 10-100. Overall mapping speed can increase by factors of thousands. Sensitivity enables measurement of low-surface-brightness debris disks and protogalaxies with an interferometer. This is enabling technology. Suborbital and ground-based platforms can be used to validate technologies and advance TRL of new detectors.
COR Applications and Potential Relevant Missions		FIR detector technology is an enabling aspect of all future FIR mission concepts, and is essential for future progress. This technology can improve science capability at a fixed cost much more rapidly than larger telescope sizes. This development serves Astrophysics almost exclusively (with some impact on planetary and Earth studies).
Time to Anticipated Need		Need to demonstrate credibility before the 2020 Decadal Survey, and would require TRL 6 by mission PDR anticipated in the mid-2020s.

Gap Name		Cryogenic readouts for large-format Far-IR detectors *Submitted by OST STDT*
Description		Readout schemes including cryogenic multiplexing for arrays of large-format Far-IR detectors need to be developed.
Current State-of-the-Art (SOTA)		Readout schemes using HEMT or SiGe amplifiers and frequency-multiplexed resonant circuits are currently in development.
TRL	**SOTA**	
	Solution	2
Performance Goals and Objectives		Near-term, this scheme should result in 1000 pixels per amplifier channel **(enabling)**; however, 3000 pixels/channel is preferred **(enhancing)**.
Scientific, Engineering, and/or Programmatic Benefits		Sensitivity reduces observing times from many hours to a few minutes (≈ 100 × faster), while array format increases areal coverage by × 10-100. Overall mapping speed can increase by factors of thousands. Sensitivity enables measurement of low-surface-brightness debris disks and protogalaxies with an interferometer. This is enabling technology. Suborbital and ground-based platforms can be used to validate technologies and advance TRL of new detectors.
COR Applications and Potential Relevant Missions		FIR detector technology is an enabling aspect of all future FIR mission concepts, and is essential for future progress. This technology can improve science capability at a fixed cost much more rapidly than larger telescope sizes. This development serves Astrophysics almost exclusively (with some impact on planetary and Earth studies). Many synergies exist with similar developments for x-ray microcalorimeters.
Time to Anticipated Need		Need to demonstrate credibility before the 2020 Decadal Survey, and would require TRL 6 by mission PDR anticipated in the mid-2020s.

Gap Name		Warm readout electronics for large-format Far-IR detectors *Submitted by OST STDT*
Description		Readout schemes compatible with cryogenic multiplexing and room temperature ADCs and RF electronics for these arrays need to be developed. The cryogenic electronics are covered in a separate gap.
Current State-of-the-Art (SOTA)		Room temperature readout of cryogenic amplifier outputs currently use FPGAs and ADCs for bandwidths up to 4 GHz having power dissipation of about 30W per channel. Dedicated ASICs would potentially lower the input power requirement by a factor of 10.
TRL	**SOTA**	
	Solution	4
Performance Goals and Objectives		Recovering the signal to noise with lower-power room-temperature electronics needs to lower the input power by up to a factor of 10.
Scientific, Engineering, and/or Programmatic Benefits		Sensitivity reduces observing times from many hours to a few minutes (≈ 100 × faster), while array format increases areal coverage by × 10-100. Overall mapping speed can increase by factors of thousands. Sensitivity enables measurement of low-surface-brightness debris disks and protogalaxies with an interferometer. This is enabling technology. Suborbital and ground-based platforms can be used to validate technologies and advance TRL of new detectors.
COR Applications and Potential Relevant Missions		FIR detector technology is an enabling aspect of all future FIR mission concepts, and is essential for future progress. This technology can improve science capability at a fixed cost much more rapidly than larger telescope sizes. This development serves Astrophysics almost exclusively (with some impact on planetary and Earth studies).
Time to Anticipated Need		Need to demonstrate credibility before the 2020 Decadal Survey, and would require TRL 6 by mission PDR anticipated in the mid-2020s.

Gap Name		Heterodyne FIR detector arrays and related technologies *Submitted by OST STDT*
Description		Heterodyne FPAs are needed for high-sensitivity, spectrally resolved mapping of interstellar clouds, star-forming regions, and solar system objects including comets. These arrays require mixers with low noise-temperature and wide intermediate frequency (IF) bandwidth, local oscillators (LOs) that are tunable but which can be phase-locked, and accompanying system technology including optics and low-cost, low-power digital spectrometers. Specifically, LO sources at frequencies above 2 THz that can generate ≥ 10 μW of power will be essential for large-format heterodyne receiver arrays to observe many spectral lines important for COR (e.g., HD at 2.7 THz and OI at 4.7 THz).
Current State-of-the-Art (SOTA)		For SOFIA, 10-pixel receivers have been developed for flight; arrays of 64 pixels are approaching TRL ~4. LOs above 2 THz are at TRL 2. Far IR SIG: Heterodyne arrays are used routinely for infrared observations in platforms including SOFIA and Herschel. The largest arrays that have been used in these settings (such as upGREAT on SOFIA) contain fewer than 20 pixels. Existing systems have good performance but power requirements far exceed what is available in spacecraft, especially if there are more pixels in arrays than currently employed. Currently LOs located at 4 K dissipate 4 mW per pixel. Near term this is expected to decrease to 1 mW per pixel.
TRL	**SOTA**	4
	Solution	3
Performance Goals and Objectives		Tunable-bandwidth array receivers for operation at frequencies of 1-5 THz. Arrays of 10 to 100 pixels are required to build on the discoveries of Herschel and exploit the sub-millimeter/FIR region for astronomy. Should include optics and accompanying system components. For mixers, IF bandwidths of 8 GHz at shorter wavelengths (< 100 microns) are essential to analyze entire galactic spectrum in one observation. Sensitive mixers not requiring cooling to 4 K (e.g., based on high critical temperature superconductors) will be essential for application on space platforms, especially with the benefit of increased IF bandwidth. For LOs, sources with output power levels ≥ 10 μW at frequencies above 2 THz. For digital spectrometers, 8 GHz bandwidth with > 8000 spectral channels, and < 1W power per pixel will be necessary for large arrays used in space missions. Cryogenic IF amplifiers with reduced power dissipation also needed, e.g. 0.5 mW for 8 GHz bandwidth. SIS- and HEB-based mixer arrays with up to hundreds of pixels, coupled with low power, broadly tunable local oscillators. Increased IF bandwidth of mixers, with minimum of 8 GHz bandwidth required at frequencies about 3 THz. Low-power digital spectrometer systems with frequency coverage of 4 GHz in general, and up to 8 GHz for higher-frequency systems.
Scientific, Engineering, and/or Programmatic Benefits		Ability to observe and map spectral lines (such as OI at 4.774 THz) to study star formation and galactic chemical evolution. Observations of transitions of water are necessary to probe the early phases of planet formation, and to determine the origin of the Earth's oceans. Development of such systems and associated technology will make imaging observations over 10 × faster. They will also significantly benefit laboratory spectroscopy and biomedical imaging. Increasing the pixel count by 1-2 orders of magnitude over existing instruments will dramatically increase imaging efficiency for high spectral resolution observations. Increased instantaneous bandwidth will enable simultaneous observation of multiple lines, further improving efficiency and relative calibration accuracy.

COR Applications and Potential Relevant Missions	Potential use in OST. Needed for future sub-millimeter/FIR suborbital missions (instruments for SOFIA and balloon missions such as Stratospheric Terahertz Observatory, STO and Galactic/Xtragalactic ULDB Spectroscopic Stratospheric Terahertz Observatory, GUSSTO) and for potential small-sat and Explorer missions beyond Herschel. Solar system studies of planetary atmospheres will directly benefit. For Earth observing, FPAs will improve coverage speed and provide small spot sizes with reasonably sized antennas. Heterodyne arrays are used in existing and upcoming SOFIA instrumentation, as well as in planned instruments for OST.
Time to Anticipated Need	Need to demonstrate credibility before the 2020 Decadal Survey, and would require TRL 6 by mission PDR anticipated in the mid-2020s. The next round of SOFIA instruments will need to reach TRL 6 by the end of the decade (i.e., 3-5 years). Will be needed in 2-4 years for deployment on SOFIA and balloon-based platforms.

Gap Name		Wide-bandwidth, high-spectral-dynamic-range receiving system *Submitted by General Community*
Description		Receiving systems consisting of an antenna and associated electronics to amplify, filter, and sample the highly redshifted neutral hydrogen signals from Cosmic Dawn, i.e., at redshifts $z > 10$. The desired signals of interest have amplitudes of milli-Kelvins to potentially a few hundred milli-Kelvin (measured as brightness temperatures), relative to galactic and other foreground emissions at the level of 1000 to 10,000 K, implying spectral dynamic ranges of order 1 million or more (60 dB). Further, signals of interest are generated over a wavelength range comparable to their central wavelength. Finally, given signal weakness, the antenna and associated electronics either must not introduce spectral features at levels comparable to those expected from the signals of interest or the spectral behavior of the antenna and associated electronics must be stable and allow sufficient characterization to enable calibration to remove any such spectral features. The technology development required is specifically for a wide-band antenna and receiver system that are functional in the space environment.
Current State-of-the-Art (SOTA)		Notional designs exist for full systems; proof-of-concept subsystems have been demonstrated in laboratory environments, and the individual components likely to be used in a full system have been demonstrated in relevant environments. A demonstration of subsystems and a full system in a relevant environment has not yet been accomplished.
TRL	**SOTA**	4
	Solution	
Performance Goals and Objectives		The goals of a program to address this gap are two-fold: demonstrate capability to make measurements of sky-averaged highly redshifted neutral-hydrogen signals; and demonstrate capability to collect highly redshifted neutral-hydrogen signals in a manner allowing later imaging. If the first goal can be met, the technology capability required for the second goal will also be met. A system capable of fulfilling the first goal can be divided into three key sub-systems: I. Antenna: Proof-of-concept antennas able to receive signals over at least a 3:1 wavelength range have been constructed; the objective is to construct an antenna with a sufficiently stable frequency response that it changes by only a small amount over range of temperatures expected for a space-based antenna; II. Analog receiver: The receiver amplifies and, if needed, filters and conditions for further processing signals collected by the antenna; the receiver must allow characterization at a level sufficient to allow extraction of the cosmological hydrogen signal at a level of 1 ppm of signals received by antenna; designs for such receivers exist; the objective is to construct one in a lab environment, demonstrate its performance, and then construct one for the thermally controlled environment expected for a spacecraft; and III. Digital spectrometer: The spectrometer converts analog signals to digital, and forms them into spectra with sufficient spectral resolution to detect the cosmological hydrogen signal; digital spectrometers with the required performance have been developed in a lab environment; the objective is to implement a spectrometer with flight-qualified hardware in the thermally controlled environment of a spacecraft.
Scientific, Engineering, and/or Programmatic Benefits		This technology capability would benefit studies of "Cosmic Dawn," one of the three science objectives for this decade as identified by the NWNH report. Studies of the highly redshifted neutral-hydrogen signals will probe the Epoch of Reionization (EoR) NWNH science frontier discovery area, and address the science frontier question "What were the first objects to light up the universe and when did they do it?" from the Origins theme. Studies of highly redshifted neutral-hydrogen signals may also be able to probe into the true Dark Ages, before any stars had formed. Such studies would complement COR objectives, and address goals of the PCOS Program.
COR Applications and Potential Relevant Missions		The application is for space- and lunar-based missions designed to find highly redshifted ($z > 10$) signals from neutral hydrogen. Potentially relevant missions described in the Astrophysics Roadmap include a precursor lunar orbiter mission (Introduction to Chapter 6 of the Astrophysics Roadmap) and an eventual Cosmic Dawn Mapper.
Time to Anticipated Need		Two to three years for a precursor lunar orbiter mission.

Gap Name		Large cryogenic optics for the Far IR *Submitted by OST STDT*
Description		Large telescopes (of order 10 m in diameter) provide both light-gathering power to see the faintest targets, and spatial resolution to see the most detail and reduce source confusion. To achieve the ultimate sensitivity, their emission must be minimized, which requires these telescopes to be operated at temperatures (depending on the application) as low as 4 K. These telescopes will probably need in-orbit adjustability and should be designed for low-cost optical-performance verification before launch. Some material properties, such as damping for telescope structures, are also needed.
Current State-of-the-Art (SOTA)		JWST Be mirror segments may meet requirements now, so TRL 5 with an extremely expensive technology; TRL 3 exists for other materials like SiC. Cryogenic low-dissipation actuators exist at TRL 3-5.
TRL	**SOTA**	5
	Solution	4
Performance Goals and Objectives		Develop a feasible and affordable (suggestion received to be more specific about areal cost objective) approach to producing a 10-m-class telescope with sufficiently high specific stiffness, strength, and low areal density to be launched; while maintaining compatibility with cryogenic cooling and FIR surface quality/figure of ~1μm rms. Material property measurements at cryogenic temperatures for structures and optics such as damping, emissivity, thermal conductivity, etc. (suggestion received to be more specific about optical performance requirements).
Scientific, Engineering, and/or Programmatic Benefits		Low-cost, lightweight cryogenic optics at reasonable cost are required to enable development of large-aperture FIR telescopes in the 2020s. Large apertures are required to provide the spatial resolution and sensitivity needed to follow up on discoveries from the current generation of space telescopes.
COR Applications and Potential Relevant Missions		This is a key enabling technology for any future single-aperture FIR telescope, and an enhancing technology for a FIR interferometer.
Time to Anticipated Need		Need to demonstrate credibility before the 2020 Decadal Survey, and would require TRL 6 by mission PDR anticipated in the mid-2020s.

Gap Name		Far-IR interferometry *Submitted by General Community*
Description		Interferometry in the FIR provides sensitive integral field spectroscopy with sub-arcsec angular resolution and R ~ 3000 spectral resolution. It could resolve proto-planetary and debris disks; and measure the spectra of individual high-z galaxies, at resolutions beyond what is currently envisioned for single-dish FIR telescopes. A structurally connected interferometer would have these capabilities. Telescopes need to operate at temperatures as low as 4 K.
Current State-of-the-Art (SOTA)		Wide-FOV spatio-spectral interferometry has been demonstrated in the lab at visible wavelengths with a test-bed that is functionally and operationally equivalent to a space-based FIR interferometer, the error terms are well understood, and experiments have been conducted with an astronomically realistic test scene. Further, single-pixel spatio-spectral interferometry has been demonstrated in the lab at THz frequencies, demonstrating the desired broadband far-IR wavelength response of the beam combiner.
TRL	**SOTA**	4
	Solution	4
Performance Goals and Objectives		Interferometric baselines in the tens of meters, up to ~100 m, are required to provide the spatial resolution needed to follow up on discoveries made with the Spitzer and Herschel space telescopes, and to provide information complementary to that attainable with ALMA and JWST. Develop a single science instrument providing both dense coverage of the u-v plane for high-quality, sub-arcsec imaging and Fourier Transform Spectroscopy over the entire spectral range, 25-400 microns, in an instantaneous FOV > 1 arc minute.
Scientific, Engineering, and/or Programmatic Benefits		Experimentation with and simulation of data acquisition with a rotating interferometer, “single dish” (standard FTS) mode, and further development of spatio-spectral reconstruction software will close the gap. This is enabling technology for a space-based far-IR interferometer.
COR Applications and Potential Relevant Missions		Wide-field spatio-spectral interferometry is a key technology for a FIR astrophysics mission, consistently given high priority by the FIR astrophysics community since the 2000 Decadal Survey. Applicable to OST, currently under study. Will be used in balloon experiments such as BETTII, and potentially in a Probe-class FIR mission. Potential applications also exist in NASA’s planetary and Earth science programs.
Time to Anticipated Need		Need to demonstrate credibility before the 2020 Decadal Survey, and would require TRL 6 by mission PDR anticipated in the mid-2020s. Continuation of prototype efforts expected to yield mature technique in time for the BETTII balloon experiment (engineering test flight scheduled in June 2017). In addition to BETTII, this technology is potentially applicable to a Probe-class mission and to the OST.

Gap Name		High-performance, sub-Kelvin coolers *Submitted by OST STDT*
Description		Optics and detectors for FIR, sub-millimeter, and certain X-ray missions require very low temperatures of operation, typically in the tens of milli-Kelvins. Compact, low-power, lightweight coolers suitable for space-flight are needed to provide this cooling. Both evolutionary improvements in conventional cooling technologies (adiabatic demagnetization and dilution refrigerators) with higher cooling power, and novel cooling architectures are desirable. Novel cooling approaches include optical, microwave, and solid-state techniques.
Current State-of-the-Art (SOTA)		Existing adiabatic demagnetization refrigerators with low cooling power at 50 mK are at TRL 7-9 (Hitomi/SXS) but high-cooling-power versions are at TRL 4. Dilution refrigerators and solid-state cooling approach based on quantum tunneling through normal-insulator-superconductor (NIS) junctions are both at TRL 3. Currently funded technology development is expected to result in a TRL 5 or 6 ADR for use over the temperature range of 10 to 0.030K with high efficiency and cooling power of 6 micro-W at 0.05 K.
TRL	**SOTA**	4
	Solution	4
Performance Goals and Objectives		A sub-Kelvin cooler operating from a base temperature of ~4 K and cooling to 30 mK with a continuous heat lift of 5 μW at 50 mK and 1 μW at 30 mK is required. Features such as compactness, low input power, low vibration, intermediate cooling, and other impact-reducing design aspects are desired.
Scientific, Engineering, and/or Programmatic Benefits		Sub-Kelvin cryocoolers are required to achieve astrophysical photon-background-limited sensitivity in the FIR and high-resolution sensitive X-ray microcalorimetry. Techniques to lower cooling costs and improve reliability will aid the emergence of powerful scientific missions in the FIR and X-ray.
COR Applications and Potential Relevant Missions		This technology is a key enabling technology for any future FIR mission, including OST. Sensors operating near 100 mK are envisioned for future missions for X-ray astrophysics, measurements of the CMB, and FIR imaging and spectroscopy. Applicable to missions of all classes (balloons, Explorers, Probes, and flagship observatories). High synergy with X-ray missions using microcalorimeters.
Time to Anticipated Need		Need to demonstrate credibility before the 2020 Decadal Survey, and would require TRL 6 by mission PDR anticipated in the mid-2020s.

Gap Name		Advanced cryocoolers *Submitted by OST STDT*
Description		Cryocoolers are required for achieving very low temperatures (e.g., ~4 K) for optics and as pre-coolers for sub-Kelvin detector coolers for COR missions. Eliminating the need for expendable materials (cryogens) will increase achievable lifetime and reduce system mass and volume. Improvements are needed in terms of performance, especially low power consumption and low vibration levels.
Current State-of-the-Art (SOTA)		For several-Kelvin temperature designs, the current SOTA includes pulse-tube, Stirling, and Joule-Thomson coolers which are at high TRL but are expensive, and do not yet have good enough performance. Changes in the working fluid have been shown to produce temperatures in the 4.0 K range as required for OST.
TRL	**SOTA**	3–6
	Solution	4
Performance Goals and Objectives		Several mission concepts require sustaining temperatures of a few Kelvin, with continuous heat-lift levels of a few dozen to ~200 mW at temperatures ranging from 4 to 18K. Other concepts could benefit from greater heat lifts at somewhat higher temperatures. All this needs to be accomplished with < 200 W input power. Such coolers need to be compact, and impose only low levels of vibration on the spacecraft. In some applications, a sub-Kelvin cooler will be implemented, and an advanced few- Kelvin cryo-cooler able to maintain the sub-Kelvin cooler's hot zone at a steady (e.g.) 4 K will be very beneficial.
Scientific, Engineering, and/or Programmatic Benefits		Cryocoolers able to operate near 4 K, cooling detectors and optics directly, as well as serving as a backing stage for ultra-low-temperature (sub-Kelvin) coolers will enable large FIR telescopes, as well as ultra-low-noise operation of cryogenic detectors for other bands. Increased heat lift, lower mass, lower volume, increased operational lifetime, and reduced cost will enable such missions to fly extended durations without wasting critical resources on cooling. Large-capacity cryocoolers are required to achieve astrophysical photon-background-limited sensitivity in the FIR and meet sensitivity requirements to achieve the science goals for future FIR telescopes or interferometers.
COR Applications and Potential Relevant Missions		This technology is a key enabling technology for any future FIR mission, including OST. It is also applicable to balloons, airborne platforms, Explorers, and Probes. For example, it would improve performance of STO2 long/ultra-long duration balloon and SOFIA instruments. Explorer missions would also be very positively impacted
Time to Anticipated Need		Need to demonstrate credibility before the 2020 Decadal Survey, and would require TRL 6 by mission PDR anticipated in the mid-2020s.

Gap Name		Compact, integrated spectrometers for 100 to 1000 μm *Submitted by OST STDT*
Description		Compact, integrated spectrometers operating in the 100 μm to 1 mm band which can provide a wide (e.g., 1:1.6) instantaneous bandwidth at resolving power ($R = \lambda/\Delta\lambda = \nu/\Delta\nu$) ~500 with high efficiency in a compact (~10 cm) package that could be arrayed in a focal plane to provide integral-field mapping or multi-object spectroscopy capability. Si immersion technology can provide increased spectrometric capability ($R \sim 1 \times 10^5$) with smaller size (factor of 3) over standard Eshelle gratings.
Current State-of-the-Art (SOTA)		Multiple compact spectrometers are under development: including compact silicon gratings and grating analogs, as well as superconducting filter banks. These systems are promising, and in some cases are approaching photon-noise limited performance suitable for ground-based observations, but have not yet been demonstrated in a scientific application.
TRL	**SOTA**	3
	Solution	3
Performance Goals and Objectives		An integrated spectrometer + detector array system would demonstrate 1:1.7 bandwidth (or greater), high efficiency (> 50%, including detector absorption), resolving power > 400, and a coupling scheme compatible with a telescope beam e.g., an f/4 Gaussian beam. To enable the observatories with hundreds of spectrometers, a single spectrometer + detector array would be a packaged on a silicon wafer on order tens of square cm in size (i.e., less than one 4" wafer).
Scientific, Engineering, and/or Programmatic Benefits		Large-format spectrometers in the far-IR through millimeter enable 3-D spatial-spectral surveys over large areas. The combination of large spatial coverage (many to tens of square degrees) and spectral bandwidth (giving redshift, or line-of-sight distance) will simultaneously find galaxies and measure their redshifts in large numbers (e.g., on order millions with OST). This measurement addresses key questions in galaxy evolution and the reionization epoch. This is enabling technology.
COR Applications and Potential Relevant Missions		Compact spectrometers are key for a future far-IR flagship such as OST, but they also enable interim opportunities such as involvement with SPICA, balloon-borne far-IR experiments which are being proposed, and SOFIA.
Time to Anticipated Need		Need to demonstrate credibility before the 2020 Decadal Survey, and would require TRL 6 by mission PDR anticipated in the mid-2020s.

Gap Name		Mid-IR coronagraph optics and architecture *Submitted by OST STDT*
Description		Characterization of the atmospheres of cool exoplanets in wide orbits (> 5 AU, ice giants and more massive) requires spectrally dispersed coronagraphy in the 7-30 micron range with contrasts of 10^{-6} and IWA of 0.1" at the shortest wavelength. The spectral resolving power should be moderate (R~100-500).
Current State-of-the-Art (SOTA)		The current state of the art for mid-infrared coronagraphs are the three four-quadrant phase masks of JWST-MIRI. These provide narrow-band imaging with contrasts up to 1E-4 in three narrow bands from 10.65-15.5 micron with inner working angles of 0.33-0.49". The MIRI coronagraphs do not offer spectral dispersion.
TRL	**SOTA**	
	Solution	3
Performance Goals and Objectives		A spectro-imaging instrument with and inner working angle of 0.1" at 10 micron. This is likely less than 2 λ/D for the available aperture. The best IWA is needed to detect a 300 K Neptune-sized planet at 10 pc at a 1-2 AU separation, and the contrast should be 1E-6 to detect Saturn at 10 pc (~1 microJy @ 24 micron, 3 λ/D for 16m aperture) with R~10. The maximum spectral dispersion should be sufficient to resolve the 15 micron CO2 band (R~500).
Scientific, Engineering, and/or Programmatic Benefits		Mid-IR coronagraphic spectroscopy would support a variety of COR science cases, including resolved studies of solid-state features indicative of amorphous or crystalline grain mineralogy in protostellar, protoplanetary, and debris disks, as well as studies of dust and gas around evolved stars and AGN. The low mid-IR contrast ratio between hot central stars and warm surrounding dust make circumstellar dust investigations especially interesting in this wavelength range.
COR Applications and Potential Relevant Missions		OST.
Time to Anticipated Need		Need to demonstrate credibility before the 2020 Decadal Survey, and would require TRL 6 by mission PDR anticipated in the mid-2020s.

Gap Name		Cryogenic deformable mirror *Submitted by OST STDT*
Description		Characterization of the atmospheres of cool exoplanets in wide orbits (> 5 AU, ice giants and more massive) requires spectrally dispersed coronagraphy in the 7-30 micron range with contrasts of 10^{-6} and IWA of 0.1" at the shortest wavelength. The spectral resolving power should be moderate (R~100-500). Such a system is likely to require adaptive optics, but to operate in the mid-IR must function at cryogenic temperatures.
Current State-of-the-Art (SOTA)		The current state of the art for mid-infrared coronagraphs are the three four-quadrant phase masks of JWST-MIRI. These provide narrow-band imaging with contrasts up to 10^{-4} in three narrow bands from 10.65-15.5 micron with inner working angles of 0.33-0.49". The MIRI coronagraphs do not offer spectral dispersion.
TRL	**SOTA**	
	Solution	2
Performance Goals and Objectives		TBD: Requirements need to be set on actuator stroke length and resolution, actuator density, heat dissipation. Must be operable at cryogenic temperatures.
Scientific, Engineering, and/or Programmatic Benefits		Mid-IR coronagraphic spectroscopy would support a variety of COR science cases, including resolved studies of solid-state features indicative of amorphous or crystalline grain mineralogy in protostellar, protoplanetary, and debris disks, as well as studies of dust and gas around evolved stars and AGN. The low mid-IR contrast ratio between hot central stars and warm surrounding dust make circumstellar dust investigations especially interesting in this wavelength range.
COR Applications and Potential Relevant Missions		OST.
Time to Anticipated Need		Need to demonstrate credibility before the 2020 Decadal Survey, and would require TRL 6 by mission PDR anticipated in the mid-2020s.

Gap Name		Mid-IR detectors *Submitted by OST STDT*
Description		Characterization of the atmospheres of cool exoplanets in wide orbits (> 5 AU, ice giants and more massive) requires spectrally dispersed coronagraphy in the 7-30 micron range with contrasts of 10^{-6} and IWA of 0.1" at the shortest wavelength. The spectral resolving power should be moderate (R~100-500). Direct imaging and spectroscopy of exoplanets will have strict requirements on the detectors. A mid-IR coronagraph will require detectors that have very low dark current and read noise. High stability, high sensitivity (~ 10 × better than JWST/MIRI) mid-IR detectors are need for exoplanet spectroscopy. (enabling)
Current State-of-the-Art (SOTA)		The current state-of-the-art for mid-IR coronagraphs are the three four-quadrant phase masks of JWST-MIRI. These provide narrow-band imaging with contrasts up to 10^{-4} in three narrow bands from 10.65-15.5 micron with inner working angles of 0.33-0.49". The MIRI coronagraphs do not offer spectral dispersion.
TRL	**SOTA**	
	Solution	3
Performance Goals and Objectives		TBD: noise levels must be compatible with coronagraphy Mid-IR detectors with ~10 × better sensitivity and stability as the JWST/MIRI detectors, and/or schemes to improve the instrument sensitivity with existing detectors.
Scientific, Engineering, and/or Programmatic Benefits		Mid-IR coronagraphic spectroscopy would support a variety of COR science cases, including resolved studies of solid-state features indicative of amorphous or crystalline grain mineralogy in protostellar, protoplanetary, and debris disks, as well as studies of dust and gas around evolved stars and AGN. The low mid-IR contrast ratio between hot central stars and warm surrounding dust make circumstellar dust investigations especially interesting in this wavelength range.
COR Applications and Potential Relevant Missions		OST.
Time to Anticipated Need		Need to demonstrate credibility before the 2020 Decadal Survey, and would require TRL 6 by mission PDR anticipated in the mid-2020s.

Gap Name		Advanced adaptive optics *Submitted by General Community*
Description		Exoplanet characterization and high sensitivity general astrophysics requires optical systems with large apertures to obtain the highest angular resolution and a large radiation gathering capability, along with the ability to optically process and transmit the maximum radiation to the focal plane detector. Assigning multiple functions to a single optical surface (i.e. focus the optical beam while simultaneously apodizing the beam for coronagraphic suppression) can reduce the number of space optics components improving throughput and science yield while potentially reducing instrument complexity and cost.
Current State-of-the-Art (SOTA)		To reduce their number of surfaces, Xinetics combines' Integrated Wavefront Corrector Xinetics has combined a typical Deformable Mirror (DM) with a tip-tilt mechanism device in their Integrated Wavefront Corrector to reduce the number of surfaces. Analysis in Groff, et al., Proc. SPIE 9904, 990421 shows that combining DM capabilities with focusing optics can reduce the overall number of actuators in a system while improving coronagraph performance. Freeform optics allow for multiple wavefront error components to be corrected with a single optic, reducing the number of elements in an optical system and improving throughput, while increasing complexity and cost of the individual elements With fewer optical surfaces there is less work for thermal, dynamics, vibration, structural, and mechanical engineers. Therefore reducing instrument cost risk.
TRL	**SOTA**	2–4
	Solution	2–4
Performance Goals and Objectives		Develop adaptive optics technology to correct both phase and amplitude in large aperture telescope systems using concave or convex surfaces. This will combine the function of a powered optical element with wavefront correction capability and, possibly, with tip/tilt error correction. Develop technology that enables coating active optical components (DMs, etc.) with very high reflectivity optical coatings. Develop A/O technology to enable a single integrated device to compensate for tip-tilt, while at the same time correcting for wavefront surface deformation errors. In most implementations, these two functions require separate optical surfaces.
Scientific, Engineering, and/or Programmatic Benefits		**Scientific benefits:** Successful development of this technology has the potential to increase the scientific yield of currently planned missions and, if the science measurement objective is at the threshold of measurement, this technology will enable it to be achieved. **Engineering benefits:** Reducing the number of optical elements will decrease the engineering time to design, specify, procure, integrate and test optical devices; increase development schedule confidence or reduce development schedule risk; and increase system reliability. **Programmatic benefits:** By integrating more optical functions (focus, collimate, fold, filter, etc.) into a smaller set of integrated devices, mission cost and schedule may be reduced, while increasing performance.
COR Applications and Potential Relevant Missions		This important technology will be applied to the telescopes and instruments needed for both Large-aperture ultra-violet, optical infrared (LUVOIR) observations and for the Exoplanet explorer (ExEP) missions. It is also applicable to all optical systems that use Deformable Mirrors (DMs) for wavefront control.
Time to Anticipated Need		All missions that are launched in the mid-2020's and beyond would likely use this technology to increase their science yield. All missions in the UV and visible will benefit from technology developed to reduce mission cost and schedule, while increasing performance.

Gap Name		High-precision low-frequency radio spectrometers and interferometers *Submitted by General Community*
Description		Radio spectrometers and interferometers are needed for lunar surface and orbital missions that operate below 100 MHz (> 3 meters wavelength) over fractional bandwidths of 100% (e.g. 25-75 MHz) with spectral resolution of R > 10^4. Relative accuracy must exceed 0.001% (1 part in 10^5) between any two channels within the band, but overall absolute accuracy is acceptable at 1%. Antennas/feeds must exhibit low reflection coefficients below -10dB across the full fractional bandwidth. Antenna/feed radiation patterns must be achromatic over the full bandwidth such that residuals to a 5th-order fit of observed Galactic sky noise are less than 0.01%. Low-power signal processing for interferometric arrays of radio systems is needed that achieves < 10 pJ per CMAC. Full systems are needed that can operate through the 14-day lunar night and that meet functional requirements for robotic and/or human deployment. The technology development here is different from #12 in that the requirements are for multiple dipole antennas that must be deployed on the lunar surface and the correlation of these signals to measure the power spectrum of the first structures in the early Universe. So, #10 and #22 are sufficiently different to stand independently.
Current State-of-the-Art (SOTA)		Existing flight radiometers (e.g. JUNO Microwave Radiometer, GPM Microwave Imager) have < 10% fractional bandwidths and accuracy of order 1-10% across only ~10 spectral channels. Radio receivers meeting the bandwidth and resolution requirements are used on ground arrays (e.g. Tingay et al. 2013, DeBoer et al. 2017). Radio receivers meeting the accuracy requirement have been demonstrated in the laboratory and deployed for ground-based measurements (Bowman & Rogers 2010, Rogers & Bowman 2012, Monsalve 2016, 2017). Techniques have been designed to improve accuracy (Nhan et al. 2017). Existing receivers are limited by design choices not suitable for flight, including use of mechanical radio-frequency switches. Antennas meeting the requirements have been demonstrated in simulation and validated in ground-based measurements (Mozdzen et al. 2016, 2017). Low-power cross-correlation ASICs have been designed (D'Addario & Wang 2016) and more-efficient correlator algorithms have been demonstrated on data from ground arrays (Thyagarajan et al. 2017).
TRL	**SOTA**	4
	Solution	3
Performance Goals and Objectives		1. Produce a radio receiver with bandwidth 33-99 MHz, 10 kHz spectral channels, and relative accuracy of 0.001% at the antenna input plane. 2. Produce an achromatic antenna with reflection coefficient less than -10dB across bandwidth 33-99 MHz and thermal stability sufficient to meet the requirement across temperature variations of 100 degrees C. 3. Produce an end-to-end low-power digital signal processing using ASICs that requires less than 10pJ per CMAC for interferometric correlation of 16 receiver systems with 100 MHz bandwidth. 4. Produce a deployable surface antenna suitable for use with robotic deployment platforms designed to assemble an array of 16 systems on the lunar farside. 5. Produce full system design capable of operating on lunar surface through the full lunar day/night cycle (specifically addressing power and thermal constraints during lunar night).
Scientific, Engineering, and/or Programmatic Benefits		The desired radio spectrometer performance is two orders of magnitude better than existing systems and enables missions that support NASA key science on "The History of Galaxies" and "Originals and Fate of the Universe" (Astrophysics Roadmap 2013), including the Cosmic Dawn Mapper (Astrophysics Roadmap 2013, p. 90). The desired low-power correlator reduces mass and cost of a lunar interferometer compared to baseline estimates (Lazio et al. 2011). The desired technology further enables detection of exoplanet auroral radio emission/space weather in the key band below the Earth's ionospheric cutoff (< 20 MHz) from orbital or lunar surface platforms, thus enhancing future science opportunities for "Characterizing other worlds" and "Our Nearest Neighbors and the Search for Life" by improving understanding of exoplanet habitability.

COR Applications and Potential Relevant Missions	Dark Ages Radio Explorer (Burns et al. 2012) Cosmic Dawn Mapper (Astrophysics Roadmap 2013, p. 90)
Time to Anticipated Need	Early 2020s for a lunar orbiter demonstrator, e.g. Dark Ages Radio Explorer (DARE; Burns et al. 2012) 2025 for lunar surface array pathfinder, e.g. Radio Observatory on the Lunar Surface for Solar studies (ROLSS; MacDowall et al. 2011, Lazio et al. 2011) and coordination with Human Exploration planning 2030 for full lunar surface array, e.g. Lunar Radio Array (LRA; Lazio et al. 2009, 2011).

Gap Name		UV/Opt/NIR tunable narrow-band filters *Submitted by General Community*
Description		High throughput UV, Optical and Near Infra-red narrow-band filters ($\Delta\lambda/\lambda$~2-3 %) with continuously selectable central wavelength capable of covering an un-vignetted and un-aberrated FOV of several arcmin (linear size) or better.
Current State-of-the-Art (SOTA)		Some technology development was done to flight certify filters for JWST but were not completed. ABSTRACT: Space environment challenges with the tunable Fabry-Pérot etalon for the JWST fine guidance sensor. The Fine Guidance Sensor (FGS) on the James Webb Space Telescope (JWST) has a science observing capability that was to be provided by a tunable Fabry-Pérot etalon incorporating dielectric coated etalon plates with a small vacuum gap and piezoelectric actuators (PZTs). The JWST etalon was more challenging than our existing ground-based operational systems due to the low-order gap, the extremely wide waveband and the environmental specifications. Difficulties were encountered in providing the required performance due to variability in the mechanical gap after exposure to the vibration, shock and cryogenic cycling environments required for the JWST mission. The risks associated with operating the flight model etalon in the space environment, along with changes in scientific priorities, resulted in the etalon being replaced by the grism-based Near-Infrared Imager and Slitless Spectrograph (NIRISS). We describe here the performance of the etalon system and the unresolved risks that contributed to the decision to change the flight instrument. Space environment challenges with the tunable Fabry-Pérot etalon for the JWST fine guidance sensor. Available from: https://www.researchgate.net/publication/258718456_Space_environment_challenges_with_the_tunable_Fabry-Perot_etalon_for_the_JWST_fine_guidance_sensor [accessed Jul 4, 2017].
TRL	**SOTA**	
	Solution	
Performance Goals and Objectives		High throughput UV, Optical and Near Infra-red narrow-band filters ($\Delta\lambda/\lambda$~2-3 %) with continuously selectable central wavelength capable of covering an un-vignetted and un-aberrated FOV of several arcmin (linear size) or better.
Scientific, Engineering, and/or Programmatic Benefits		The availability of variable narrow band filters at UV, Optical and Near Infrared wavelengths will enable systematic studies of a broad range of astrophysical problems in galaxy evolution that are core to the Cosmic Origins program that currently can either not be done or are done very sub-optimally (with grism/slitless spectroscopy, which partially destroys spatial information) or can only be done in few, very lucky cases when the targeted emission line is fortuitously redshifted to the wavelength of available onboard fixed filters.
COR Applications and Potential Relevant Missions		Tunable narrow band filters will allow us to study the formation and evolution of the proto-cluster environment, the proto-galaxy environment and star-formation in the cosmic web. The device will enable high-angular resolution, large-scale spatial tomography of line-emission processes from galaxies, globular clusters and gaseous nebulae in general. This capability is key, and currently unavailable to address a broad range of problems, from spatial reconstruction of the cosmic web, to satellite star-formation and quenching in massive halos, to the formation of globular clusters, to gas accretion and expulsion in galaxies. These physical processes are key to the Cosmic Origins program and currently cannot be addressed in a systematic way.
Time to Anticipated Need		

Appendix B
Program Technology Development Quad Charts

UV/Vis/IR

Far-IR

Ultraviolet Coatings, Materials, and Processes for Advanced Telescope Optics

PI: K. 'Bala' Balasubramanian / JPL

Objectives and Key Challenges:

- Development of UV coatings with high reflectivity (>90-95%), high uniformity (<1-0.1%), and wide bandpasses (~100 nm to 300-1000 nm) is a major technical challenge; this project aims to address this key challenge and develop feasible technical solutions
- Materials and process technology are the main challenges; improvements in existing technology base and significant innovations in coating technology such as Atomic Layer Deposition (ALD) are to be developed

Significance of Work:

- This is a key requirement for future Cosmic Origins and ExoPlanet missions, such as LUVOIR and HabEx.

ALD chamber at JPL

1.2-m coating chamber at Zecoat Corp.

Approach:

- Develop a set of experimental data with MgF_2-, AlF_3-, and LiF-protected Al mirrors in the wavelength range 100-1000 nm for a comprehensive base of measurements, enabling full-scale developments with chosen materials and processes
- Investigate and develop enhanced coating processes including ALD
- Improve characterization and measurement techniques

Key Collaborators:

- John Hennessey, Shouleh Nikzad, Nasrat Raouf, Stuart Shaklan (JPL)
- Paul Scowen (ASU)
- Manuel Quijada (GSFC)

Current Funded Period of Performance:

Jan 2013 – Dec 2015 with no-cost-extension in 2016

Recent Accomplishments:

- ✓ Upgraded coating chamber with sources, temperature controllers, and other monitors to produce various coatings
- ✓ Upgraded measurement tools at JPL and GSFC
- ✓ Produced and tested several coatings with MgF_2, AlF_3, and LiF
- ✓ Fabricated several iterations of protective coatings on Al mirrors
- ✓ Developed ALD coating processes for MgF_2, AlF_3, and LiF at JPL
- ✓ Developed and studied Atomic Layer Etching (ALE) techniques
- ✓ Produced and characterized first set of test coupons representing 1m-class mirror to assess uniformity

Further Research Needed:

- Enhancements to conventional coating techniques and ALD and ALE processes to advance the TRL status depending on further funding

Applications:

- Future astrophysics and exoplanet missions such as LUVOIR and HabEx intended to capture key spectral features from far-UV to near-IR

$TRL_{In} = 2 - 3$ $TRL_{PI\text{-}Asserted} = 3 - 4$ $TRL_{Target} = 5$

Advanced FUV/UV/Visible Photon-Counting and Ultralow-Noise Detectors

PI: Shouleh Nikzad / JPL

Objectives and Key Challenges:

- Develop and advance TRL of solar-blind (SB), high-efficiency, photon-counting, and ultralow-noise solid-state detectors, especially in FUV (λ < 200 nm)
- SB silicon, large-format arrays, reliable and stable high response in FUV

Significance of Work:

- Key innovation are high and stable UV response through atomic-level control of surface and interfaces; the breakthrough in rendering Si detectors with optimized in-band response and out-of-band rejection; versatility with CMOS and CCD

Edge of conduction band for SL doped silicon

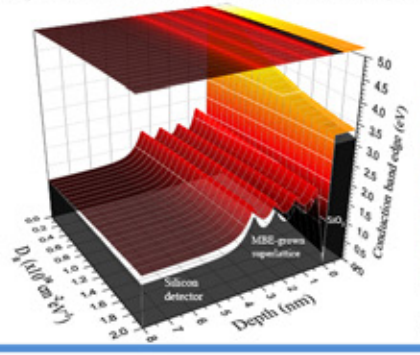

Superlattice doped EMCCD

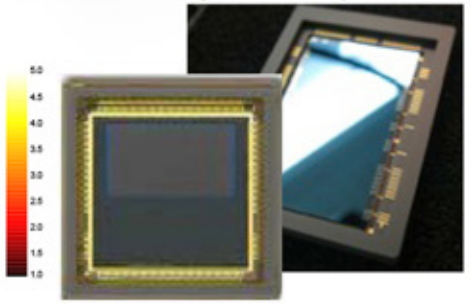

sCMOS example of ultralow-noise CMOS

Approach:

- Fabricate and process UV detectors by superlattice (SL) doping Electron Multiplying CCDs (EMCCDs) and ultralow-noise CMOS wafers
- Develop multi-stack, integrated, SB filters using atomic-layer deposition (ALD)
- Combine integrated SB filters and SL with sCMOS and EMCCDs
- Characterize and validate

Key Collaborators:

- Chris Martin (Caltech)
- David Schiminovich (Columbia University)
- Michael Hoenk (JPL)
- e2v and potentially Andor

Current Funded Period of Performance:

Dec 2015 – Dec 2018

Recent Accomplishments:

- ✓ EMCCD wafers that were procured were processed by SL-doping and coatings.
- ✓ Several devices taken to Palomar Observatory.
- ✓ Designs of visible-blind filters performed and measurements on blank silicon agree with model.
- ✓ Filters implemented on non-functional SL-doped EMCCDs to check and address mechanical issues
- ✓ Delivered SL-doped and tri-layer-coated EMCCD FIREBall detector (flight planned for Sep 2017)

Next Milestones:

- Resume conversations with vendor(s) for ultralow-noise CMOS to select design and procure wafers (Jun 2017)
- Implement detector-integrated filters into functional SL-doped EMCCDs (Jul 2017)
- Complete processing next batch of SL-doped EMCCDs (Aug 2017)
- Characterize devices under thermal cycling (Sep 2017)

Applications:

- LUVOIR, HDST, HabEx, Probes, Explorers

sCMOS $TRL_{In} = 3$ $TRL_{PI\text{-}Asserted} = 3$ $TRL_{Target} = 4\text{-}5$

EMCCD $TRL_{In} = 4$ $TRL_{PI\text{-}Asserted} = 4$ $TRL_{Target} = 5/6$

Note: TRLs assessed for 2-D, w/integrated filters

Development of DMD Arrays for Use in Future Space Missions

PI: Zoran Ninkov / Rochester Institute of Technology

Objectives and Key Challenges:

- A technology is needed that allows target selection in a field of view that can be input to an imaging spectrometer for remote sensing and astronomy
- We are looking to modify and develop Digital Micro-mirror Devices (DMDs) for this application

Significance of Work:

- Existing DMDs need to have the commercial windows replaced with appropriate windows for the scientific application desired
- The devices need to be evaluated for survivability in a space environment

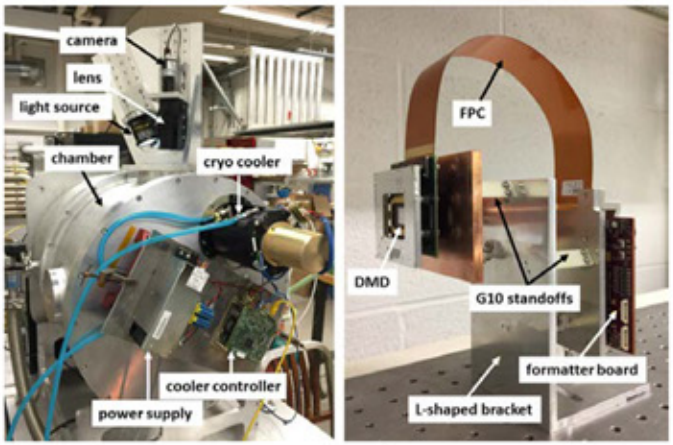

Low-temperature testing of DMDs at APL/JHU

Approach:

- Use available 0.7 XGA DMDs to develop window removal procedures, and then replace delivered window with a hermetically sealed UV-transmissive window of Magnesium Fluoride, HEM sapphire, and fused silica
- Test and evaluate such devices and as well as Cinema DMDs

Key Collaborators:

- Sally Heap, Manuel Quijada, Jonny Pellish, and Tim Schwartz (NASA/GSFC)
- Massimo Robberto (STScI)
- Alan Raisanen (RIT)

Current Funded Period of Performance:

May 2014 – May 2018

Recent Accomplishments:

- ✓ 0.7 XGA DMD and 1.2 DC2K DMDs delivered
- ✓ XGA devices re-windowed with MgF_2, Sapphire, and fused silica
- ✓ Proton and heavy-ion testing show good results (only SEUs)
- ✓ Contrast measurements indicate high contrast (>5000:1)

Next Milestones:

- Analysis and publication of gamma-ray testing (Dec 2017)
- Measurement, analysis, and publication of UV scattering measurements (Feb 2018)
- Low-temperature long-hold-time testing (Apr 2018)

Applications:

- Can be used in any hyper-spectral imaging mission
- Galaxy Evolution Spectroscopic Probe

$TRL_{In} = 4$ $TRL_{Current} = 4$ $TRL_{Target} = 5$

Ultra-Stable Structures: Development and Characterization Using Spatial Dynamic Metrology

PI: Babak N. Saif / GSFC

Objectives and Key Challenges:

- Developing surface picometer metrology of mirrors and structures
- Developing stimuli system for picometer excitations
- Developing structures and mirrors with controlled dynamics at picometer levels

Significance of Work:

- Stability and dynamics of large structures and mirrors are requirements for large space missions such as ATLAST and Exoplanet missions

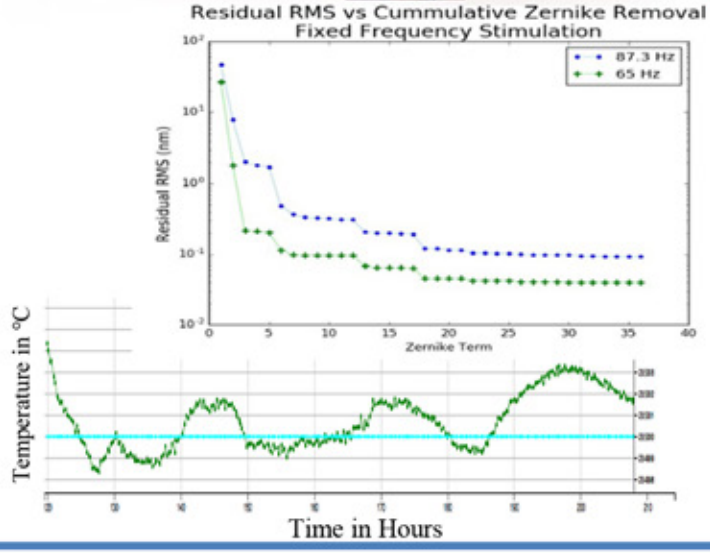

Approach:

- Work with a vendor to develop a Dynamical Digital Speckle Pattern Interferometer with picometer precision
- Develop an isolated tabletop setup to measure dynamics and drift of material and small structures
- Redesign and model dynamics of the measured material/structures

Key Collaborators:

- Babak Saif and Lee Feinberg (GSFC)
- Dave Chaney (Ball Aerospace)
- Marcel Bluth (SGT)
- Perry Greenfield (STScI)

Current Funded Period of Performance:

2016 - 2018

Recent Accomplishments:

- ✓ Picometer dynamics measurements on reflective surfaces
- ✓ Thermal-vacuum chamber control to fraction of a milliKelvin over 80 hours

Next Milestones:

- Speckle interferometer delivery (Oct 2017)
- Speckle interferometer Characterization (Jan 2018)
- Measurements of components reflective and diffuse (Mar 2018)

Applications:

- Future large astronomy/astrophysics missions
- Exoplanet missions

$TRL_{In} = 3$ $TRL_{Current} = 3$ $TRL_{Target} = 4$

Improving Ultraviolet Coatings and Filters Using Innovative Materials Deposited by ALD

PI: Paul Scowen / ASU

Objectives and Key Challenges:

- Use a range of oxide and fluoride materials to build stable optical layers using Plasma-Enhanced Atomic Layer Deposition (PEALD) to reduce adsorption, scattering, and impurities
- Layers will be suitable for protective overcoats with high UV reflectivity and unprecedented uniformity (compared to thermal Atomic Layer Deposition, ALD)
- Development of single-chamber system to deposit metal oxide and dielectric layers without breaking vacuum

Significance of Work:

- The improved ALD capability can help leverage innovative UV/optical filter construction

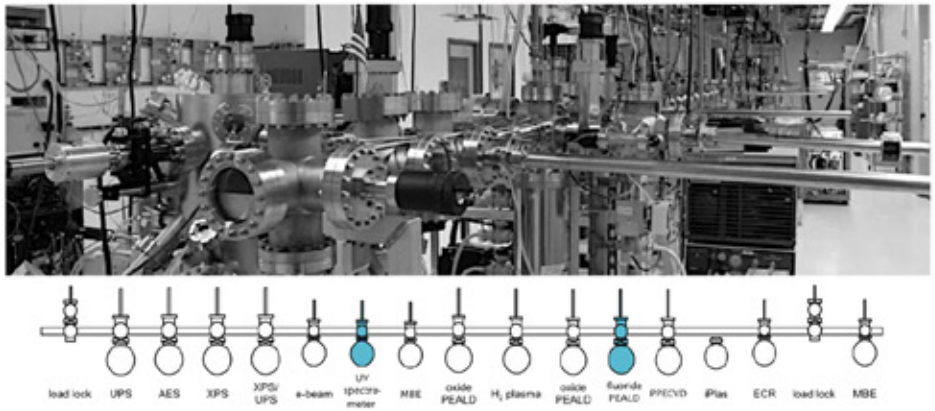

Photograph and schematic of UHV system. The chamber highlighted in blue and the chambers currently being built, which will support oxygen-free deposition and processing.

Approach:

- Develop existing PEALD system to a single-chamber model
- Demonstrate Al-film deposition
- Demonstrate fluoride deposition on top of Al films
- Demonstrate VUV reflectivity, uniformity, and stability

Key Collaborators:

- Paul Scowen, Robert Nemanich, Brianna Eller, Franz Koeck, Hongbin Yu (ASU)
- Tom Mooney (Materion)
- Matt Beasley (Planetary Resources, Inc.)

Current Funded Period of Performance:

Dec 2015 – Nov 2018

Recent Accomplishments:

- ✓ Installed in-situ VUV spectrometer to measure performance <120 nm – calibrated performance using NIST-calibrated UV detector
- ✓ Demonstrated deposition of low-loss oxides on evaporated Al surfaces – providing surface for reflection <190 nm

Next Milestone:

- Demonstrate deposition of metal fluoride films using PEALD and measure UV reflectivity to accuracy better than 3% (Dec 2017)

Applications:

- LUVOIR / HDST / ATLAST / HabEx

$TRL_{In} = 3$ $TRL_{Current} = 3$ $TRL_{Target} = 4$

Advanced UVOIR Mirror Technology Development for Very Large Space Telescopes

PI: H. Philip Stahl / MSFC

Objectives and Key Challenges:

- Advance TRL of key technology challenges for the primary mirror of future large-aperture Cosmic Origins UVOIR space telescopes
- Include monolithic and segmented optics design paths
- Conduct prototype development, testing, and modeling
- Trace metrics to science mission error budget

Significance of Work:

- Deep-core manufacturing method enables 4-m-class mirrors with 20-30% lower cost and risk
- Design tools increase speed and reduce cost of trade studies
- Integrated modeling tools enable better definition of system and component engineering specifications

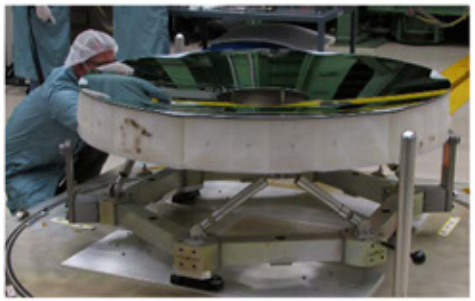

1.5m Harris and support structure

Schott mirror testing in XRCF

Approach:

- Science-driven systems engineering
- Mature technologies required to enable highest-priority science and result in high-performance, low-cost, low-risk system
- Provide options to science community by developing technology enabling both monolithic- and segmented-aperture telescopes
- Mature technology in support of 2020 Decadal process

Key Collaborators:

- AMTD team at MSFC
- Stuart Shaklan (JPL)
- Carl Rosati, Rob Egerman, and Katie Hannon (Harris)
- Steve Sokach (Schott)
- Tony Hull (UNM)
- Martin Valente (AOS)
- Gary Mosier (GSFC)

Current Funded Period of Performance:

Sep 2011 – Sep 2017

Recent Accomplishments:

- ✓ Conducted XRCF thermal cycling and modal testing of Schott mirror
- ✓ Validated thermal & mechanical Schott model predictions by test
- ✓ Fabricated and assembled 1.5-meter Harris ULE© mirror
- ✓ Increased Arnold Mirror Modeler capability
- ✓ Analyzed interaction between optical telescope wavefront stability and coronagraph contrast leakage

Next Milestones:

- Harris mirror XRCF optical and modal testing (Aug 2017)
- Thermal and Mechanical model predictions of Harris optical testing (Sep 2017)

Applications:

- Flagship optical missions; Explorer-type optical missions
- Department of Defense and commercial observations

$TRL_{In} = 3 - 5$ $TRL_{Current} = 3 - 5$ $TRL_{Target} = 4 - 5$

(values depend on specific technology)

Predictive Thermal Control Technology to Enable Thermally Stable Telescopes

PI: H. Philip Stahl / MSFC

Objectives and Key Challenges:

- Validate models that predict thermal optical performance of real mirrors and structure based on their structural designs and constituent material properties, i.e. CTE distribution, thermal conductivity, thermal mass, etc.
- Derive thermal system stability specifications from science-driven wavefront-stability requirement
- Demonstrate utility of PTC system for achieving thermal stability

Significance of Work:

- Thermally stable space telescopes enable the desired science of potential HabEx and LUVOIR missions
- Integrated modeling tools enable better definition of system and component engineering specifications

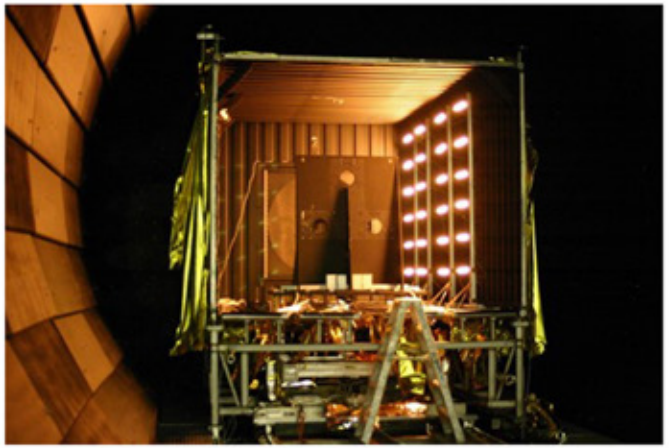

Lateral lamp array for simulating solar heat on mirror inside X-Ray & Cryogenic Facility (XRCF)

Approach:

- Science-driven systems engineering
- Mature technologies required to enable highest-priority science and result in high-performance, low-cost, low-risk system
- Mature technology in support of 2020 Decadal process

Key Collaborators:

- PTC team (MSFC)
- Carl Rosati and Rob Egerman (Harris)

Current Funded Period of Performance:

Jan 2017 – Sep 2019

Recent Accomplishments:

- ✓ Coated Harris 1.5-m mirror with protected aluminum coating
- ✓ Fabricated, installed, and characterized lamp array in XRCF

Next Milestones:

- Image Harris mirror with Computed Tomography and generate as-built design model (Aug 2017)
- Design and fabricate forward cold sink (Dec 2017)
- High-fidelity CTE map of as-built 1.5-m ULE AMTD-2 mirror (Mar 2018)

Applications:

- Flagship optical missions
- Explorer-type optical missions
- Department of Defense and commercial observations

$TRL_{In} = 3$ $TRL_{Current} = 3$ $TRL_{Target} = 4 - 5$

(values depend on specific technology)

Development of Large-Area (100 cm²) Photon-Counting UV Detectors

PI: John Vallerga / U.C. Berkeley

Objectives and Key Challenges:

- A 50 mm x 50 mm XS MCP photon-counting UV detector was previously developed, achieving high spatial resolution (15 µm) at low gain (500k) and high input flux (MHz). The detector was then environmentally qualified. Two ASICs (CSAv3 and HG2) were also fabricated to improve this performance. This program continues development by scaling the detector format to 100 mm x 100 mm while updating the ASICs for lower power and simpler layout.
- Combining our two existing ASIC designs into one ASIC ("GRAPH") using 130-nm CMOS technology
- Maintaining noise performance with analog and digital circuits on same die
- Developing a new 100 mm x 100 mm MCP detector with the new electronics and testing it environmentally

Significance of Work:

- Allow high-speed, photon-counting UV detection in package small enough and low enough power and mass to be usable in space

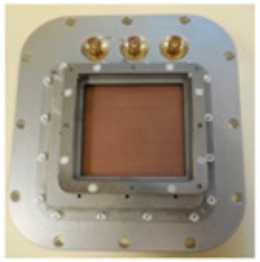

Existing 50-mm detector (without MCPs)

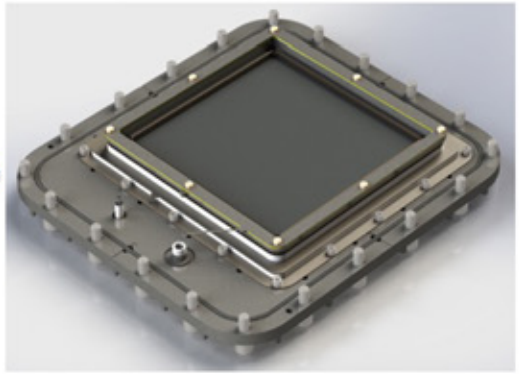

100-mm MCP detector with ASIC electronics qualified for flight

Approach:

- Scale up the 50 mm x 50 mm detector design by a factor of two to create a flight-qualified 100 mm x 100 mm design that can be environmentally tested for thermal and vibration stability
- Test the sensitivity of both ASICs to radiation, both total ionizing dose and single event upsets
- Convert the HG2 ASIC design into 130-nm CMOS technology and combine with the existing CSAv3 design into a single die
- In parallel, design and construct an FPGA readout circuit for these new ASICs

Key Collaborators:

- Prof. Gary Varner (U. Hawaii)
- Dr. Oswald Siegmund (U.C. Berkeley)

Current Funded Period of Performance:

Apr 2016 – Mar 2019

Recent Accomplishments:

- ✓ 100-mm detector fabricated
- ✓ Detector imaging performance with PXS electronics

Next Milestones:

- Convert HG2 design to GRAPH in 130-nm CMOS (Aug 2017)
- Submit GRAPH ASIC to foundry (fall 2017)
- Fabrication and performance testing of GRAPH (early 2018)
- GRAPH ASIC integration with control FPGA boards (spring 2018)
- Test full ASIC electronics with detector (summer 2018)
- Environmental tests of 100-mm detector + ASICs (fall 2018)

Applications:

- High performance UV (1-300 nm) detector for astrophysics (LUVOIR, ANUBIS, CETUS), planetary, solar, heliospheric, or aeronomy missions
- Particle or time-of-flight detector for space physics missions
- Neutron radiography/tomography for material science

$TRL_{In} = 4$ $TRL_{Current} = 4$ $TRL_{Target} = 5$

Raising the Technology Readiness Level of 4.7-THz Local Oscillators

PI: Qing Hu / MIT

Objectives and Key Challenges:

- This project seeks to raise the TRL of 4.7-THz local oscillators (LOs) based on THz quantum-cascade lasers
- The key challenges are to increase the output power level from the current level of <1 mW to 5 mW, and to increase the operating temperature from a lab-demonstrated ~10 K to ~40 K that can be provided in a space-based or suborbital observatory

Significance of Work:

- The 4.744 THz [OI] fine-structure line is the dominant cooling line of warm, dense, neutral atomic gas. Observation of this line will provide valuable information for studies of cosmic origins.
- This project will be important to the proposed GUSTO project.

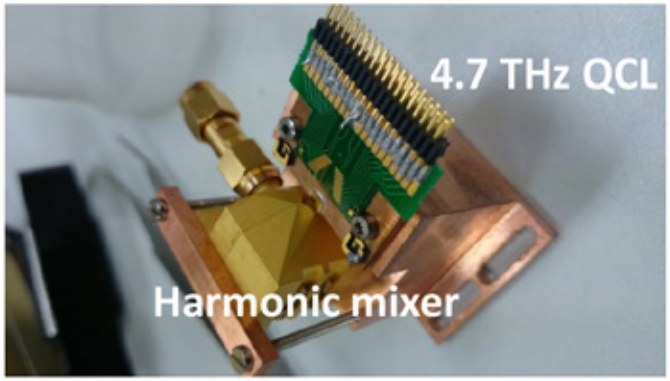

Array of DFB lasers at ~4.7 THz. The harmonic mixer is used to phase-lock the QCL LO.

Approach:

- Develop perfectly phase-matched 3rd-order DFB structures at 4.7 THz with robust single-mode operations with good beam patterns.
- Develop phase-matched 3rd-order DFB structures coupled with integrated antennae to increase the output power level to ~5 mW, and to increase the wall-plug power efficiency to 0.5%.

Key Collaborators:

- J.L. Reno (Sandia Nat'l Lab)
- J.R. Gao (SRON/Delft)

Current Funded Period of Performance:

Mar 2016 – Feb 2019

Recent Accomplishments:

- ✓ Complete the design of perfectly phase-matched 3rd-order DFB lasers aimed for ~4.7 THz
- ✓ Develop a high-yield dry-etching process using ICP (inductive-coupled plasma) to achieve clean and smooth side walls with high aspect ratios
- ✓ Grow ~3 MBE wafers based on improved QCL designs

Next Milestones:

- Fabricate devices using a combination of dry and wet etching (Feb 2018)
- Characterize the power, frequency, and beam patterns of the fabricated devices (Feb 2018)

Application:

- GUSTO (The Gal/xgal U/LDB Spectroscopic/Stratospheric THz Observatory)

$TRL_{In} = 3$ $TRL_{Current} = 3$ $TRL_{Target} = 5$

High-Efficiency Continuous Cooling for Cryogenic Instruments and sub-Kelvin Detectors

PI: Jim Tuttle / GSFC

Objectives and Key Challenges:

- Bring to TRL 6 a cooling system that provides:
  - Continuous cooling at T < 50 mK; rejecting heat at 10 K
  - Cooling power > 10 times that of current flight Adiabatic Demagnetization Refrigerator (ADR) at 50 mK
  - Continuous cooling at 4 K for telescopes, optics, etc.
  - Low external magnetic field: |B| < 5 μT
  - Simple, efficient, vibration-free operation
  - Proven reliability; no moving parts

Significance of Work:

- System will exceed requirements of currently-conceived cryogenic detector arrays

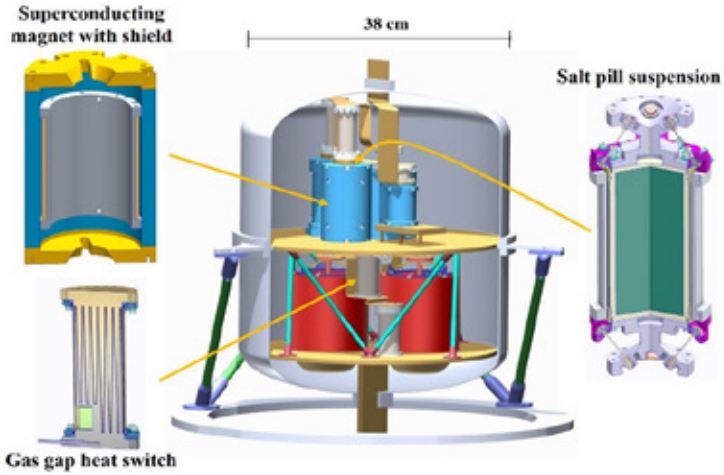

Approach:

- Adiabatic Demagnetization Refrigerator
  - Paramagnetic salts heated/cooled by changing magnetic field
  - Heat pumped between stages separated by heat switches
  - Control of heat transfer provides continuous cooling at selected stages (50 mK, 4 K)
  - Advanced magnetic shielding eliminates stray fields

Key Collaborators:

- Amir Jahromi, Ed Canavan, Hudson DeLee, Mike DiPirro, Mark Kimball, Peter Shirron, Dan Sullivan, and Eric Switzer (NASA/GSFC)

Current Funded Period of Performance:

Jan 2017 – Dec 2019

Recent Accomplishments:

- ✓ Completed analysis and detailed design of one-stage 10-to-4-K ADR
- ✓ Fully analyzed and tested 10-K Nb_3Sn magnet for this ADR
- ✓ Determined optimum heat switch pressure via testing
- ✓ Filled heat switch and verified its performance
- ✓ Initiated long-lead procurements of magnets and salt pills

Next Milestones:

- Demonstrate one-stage 10-to-4-K ADR (Dec 2017)
- Demonstrate 10-to-4-K CADR (Dec 2018)
- Demonstrate pre-vibe 10-to-0.05-K CADR (Sep 2019)
- Demonstrate post-vibe 10-to-0.05-K CADR (Dec 2019)

Applications:

- Origins Space Telescope, Inflation Probe, X-ray Surveyor
- Possibly HabEx and LUVOIR

$TRL_{In} = 3 - 5$ $TRL_{Current} = 3 - 5$ $TRL_{Target} = 6$

Appendix C
Program Technology Development Status

UV/Vis/IR

Far-IR

Abstracts of SAT Projects Starting in 2018

Ultraviolet Coatings, Materials, and Processes for Advanced Telescope Optics

Prepared by: K. 'Bala' Balasubramanian (PI; JPL/Caltech); John Hennessy, Nasrat Raouf, Shouleh Nikzad, and Stuart Shaklan (JPL/Caltech); Paul Scowen (Arizona State University); and Manuel Quijada (NASA/GSFC)

Summary

NASA's Cosmic Origins (COR) program and the astrophysics community seek to develop and advance coating technologies for telescope optics needed for large missions such as the Large UV/Optical/IR (LUVOIR) Surveyor and the Habitable Exoplanet Imaging Mission (HabEx) in the upcoming decades. Development of high-reflectivity coatings, particularly for the ultraviolet (UV) part of the spectrum, is considered a technology challenge requiring significant materials research and process development.

A successful pathway to achieve the objectives, namely to develop durable mirror coatings that will provide high reflectance over the extended spectral band in the Far-UV (FUV) to near-infrared (NIR), requires the best choice of materials and processes. Void-free thin films of absorption-free materials are required to protect and maintain high reflectivity and durability of aluminum mirrors in laboratory and pre-launch environments. A precisely controllable and scalable deposition process is also required to produce such coatings on large telescope mirrors.

During the first year of our three-year project commencing in 2013, we investigated the applicability of common materials and known processes, and identified promising candidates [1-3]. MgF_2, LiF, and AlF_3 stand out as the most promising materials for protective coatings while GdF_3, LaF_3, and LuF_2 are other potential materials to be considered. Coatings of some of these materials using conventional vacuum deposition processes were produced and characterized. Our initial results were reported in a poster paper presented at the American Astronomical Society (AAS) meeting in Baltimore, MD [4]. Preliminary results with coating experiments on Al mirrors protected with MgF_2 and AlF_3 were also reported in our reports in the 2014, 2015, and 2016 COR Program Annual Technology Reports (PATRs).

Our recent experiments focused on Atomic Layer Deposition (ALD) to produce thin MgF_2, AlF_3, and LiF protective coatings in addition to conventional techniques. With the 1.2-m coating chamber at our sub-contract vendor, ZeCoat Corp. of Torrance, CA, we produced a number of samples with chosen recipes with conventional evaporation techniques as detailed in the sections below. Similarly, several samples of newly developed ALD protective coatings on Al were produced at JPL. A PerkinElmer UV/Vis spectrophotometer at JPL and an ACTON FUV spectrophotometer at the NASA Goddard Space Flight Center (GSFC) were employed to measure the reflectance properties of these samples. A spectroscopic ellipsometer was also employed at JPL to characterize the films. Theoretical model fits of measured characteristics were analyzed. Key advances were made this year on the ALD front with successful process development for AlF_3 and LiF coatings at faster rates and lower temperatures. Further process development for protected Al coatings with these chosen materials is in progress. Papers [5, 6] on the recent ALD results were presented at the ALD conference in Portland, OR on June 29, 2015 and at the 2015 SPIE Annual Conference in San Diego in July 2015. Comprehensive refereed papers [7-9] have been published in the Journal of Vacuum Science and Technology (JVST) and in the Journal of Astronomical Telescopes, Instruments, and Systems (JATIS).

Background

It has been recognized that in the Far-UV to Mid-UV wavelengths ($90 < \lambda < 300$ nm), it is possible to detect and measure important astrophysical processes, which can shed light on the physical conditions of many environments of interest in the universe. For example, in the local interstellar medium (LISM), all but two of the key diagnostic resonance lines (Ca II H and K lines) are in the UV [10]. In addition to the fruitful science areas that UV spectroscopy has contributed since the early 1970s, France et al. [11] have emphasized the role of UV photons in the photo-dissociation and photochemistry of H_2O and CO_2 in terrestrial planet atmospheres, which can influence their atmospheric chemistry, and subsequently the habitability of Earth-like planets. However, only limited spectroscopic data are available for exoplanets and their host stars, especially in the case of M-type stars. Similarly, new areas of scientific interest are in the detection and characterization of the hot gas between galaxies and the role of the intergalactic medium (IGM) in galaxy evolution [12].

The 2011 COR PATR (Technology Needs, Table 7, Item 8.1.3., page 43, Oct 2011) [13] defined the primary goal that we have adopted for this project: "*Development of UV coatings with high reflectivity (>90-95%), high uniformity (<1-0.1%), and wide bandpasses (~100 nm to 300-1000 nm).*" The Advanced Technology Large-Aperture Space Telescope (ATLAST) technology team assessed and stressed the technology development for maturing mirror coatings for the Far-UV spectral range [14]. A comprehensive summary of the Far-UV science requirements (a Science Traceability Matrix, STM) was compiled by our Co-I Paul Scowen [15]. Table 1 lists some of the important spectral lines in the FUV region for general astrophysics. The NASA Astrophysics 30-year roadmap, "*Enduring Quests, Daring Visions*" [16], lists broadband coatings as one of the key technologies needed for LUVOIR to address a broad range of astrophysical questions "*from cosmic birth to living Earth*," combining general astrophysics and direct imaging and spectroscopy of exoplanets. High-reflectivity coatings covering the 100-300-nm spectral range are considered important for studying intergalactic matter. The COR Program Analysis Group (COPAG) pointed to telescope coatings as a technology needed to make general astrophysics and exoplanet measurements compatible within the same observatory, "*The COPAG is considering a future large UVOIR [UV/Optical/Infrared] mission for general astrophysics that would also perform exoplanet imaging and characterization. Some technologies may be specifically required to make these two missions compatible, for example telescope coatings*" [17, p. 5]. COPAG assessed the degree of difficulty to achieving this as very high, and it is indeed very challenging. Bolcar et al. [18] identified mirror coatings as one of five key technology areas needed to enable a LUVOIR mission.

Objectives and Milestones

The main objectives of the three-year project were: a) to explore materials and processes to produce protective coatings for Al mirrors providing high reflectivity over a wide spectral range from the Far-UV to NIR, and b) to demonstrate fabrication of durable mirror coatings with chosen processes on distributed coupons representing a meter-class mirror. Conventional coating processes and advanced ALD processes are pursued and investigated to achieve these goals. During the reporting period, from June 2016 to May 2017, following research conducted over previous years, the primary objectives were:

1. Optimize ALD process for absorption-free thin AlF_3 and LiF coatings and characterize them.
2. Conduct coating experiments with AlF_3-protected and LiF-protected Al mirrors.
3. Measure changes in the reflectance characteristics of these mirror samples over time.
4. Investigate Atomic Layer Etching (ALE) of surface oxide to reduce FUV absorption.
5. Develop and perform environmental tests of mirror samples, measure reflectance before and after environmental tests, and characterize the surface microscopically.

Wavelength (nm)	Species	Significance	Bodies of Interest
68.1, 69.4	Na IX	Coronal-gas (>10^6 K) diagnostic (density, ionization state, etc.)	IGM, quasi-stellar object (QSO) sight lines
77.0	Ne VIII	Warm-hot-gas (5×10^5 - 10^6 K) diagnostic (density, ionization state, etc.)	IGM, QSO sight lines
99.1, 175.0	N III	Gas-temperature diagnostic	Stellar-atmosphere abundances
102.6	H, Ly-α	Lyman Series H recombination line	Plasma diagnostics for ionized gas in astrophysical contexts
103.2, 103.8	O VI	Recombination-line doublet	Diagnostic for presence of coronal gas and the boundaries between such gas and cooler gas envelopes or media
108.5, 164.0	He II	Balmer line for He	Stellar-atmosphere diagnostic used to trace flares and coronal-mass ejections (CMEs)
117.5	C III	Gas-electron-density diagnostic	Stellar atmospheres and stellar winds
120.6	Si III	Optically thin emission line of silicon	Used as a diagnostic line sensitive to time-variability in emitted or ionizing flux
121.6	H, Ly-α	Lyman Series H recombination line	Plasma diagnostics for ionized gas in astrophysical contexts – especially used for cosmological targets such as reionization-era galaxies and stars
123.8, 124.3	N V	Gas-emission diagnostic	Used to study extended stellar coronae
133.5	C II	Absorption line for ionized carbon	Used as a diagnostic and tracer for stellar chromospheres and planetary atmospheres
139.4, 140.3	Si IV	Emission line of silicon	Used to perform diagnostics of stellar coronae including density, temperature, and abundance
140.7	O IV	Gas-density-sensitive doublet	Used to study upper chromospheres in stars
148.8	N IV	Gas diagnostic line – sensitive in particular to electron collision strengths	Used to study stellar coronae and changes in their emission and bulk motion
154.8, 155.1	C IV	Gas-density-sensitive doublet	Used to diagnose most ionized-gas phases including stellar atmospheres and nebulae
166.3	O III	Gas-temperature and density-sensitive diagnostic	Used to diagnose nebula-gas emission
175.0	N III	Gas-temperature-sensitive diagnostic	Used for stellar-plasma observations and diagnosis
189.5	Si III	Gas-density-sensitive diagnostic	Used to study astrophysical plasmas
190.9	O III	Gas-temperature and density-sensitive diagnostic	Used to diagnose nebula-gas emission
232.6	C II	Absorption line for ionized carbon	Used as a diagnostic and tracer for stellar chromospheres and planetary atmospheres
233.6	Si II	Gas-density-sensitive diagnostic	Magnetic-field diagnostic in stellar atmospheres; density diagnostic in stellar chromospheres

Table 1. *Significant diagnostic spectral lines in the UV (50-250 nm) (Courtesy: Paul Scowen).*

Progress and Accomplishments

Single-layer coatings of applicable transparent protective materials by conventional deposition process. Single-layer coatings of MgF_2, LiF, AlF_3, LaF_3, Na_3AlF_6, and GdF_3 were produced initially with conventional coating processes in a 1.2-m chamber. The chamber was fitted with resistive sources, electron gun, ion gun, heater lamps, liquid nitrogen (LN) traps, cryo-pumps, residual-gas analyzers, and computer controls, at pressures in the range of 2×10^{-7} to 1×10^{-6} Torr and temperatures in the range

of 20° to 200°C. Figure 1 shows the coating chamber used for this purpose at ZeCoat Corp. A sample transport with masking mechanism was installed in the chamber. This enabled multiple coatings on different samples without breaking vacuum. An FUV optical monitoring system was also installed in the chamber to measure reflected signal from the growing film during deposition and post-deposition while monitoring varying total pressure, water vapor and oxygen content, etc. for diagnostic purposes.

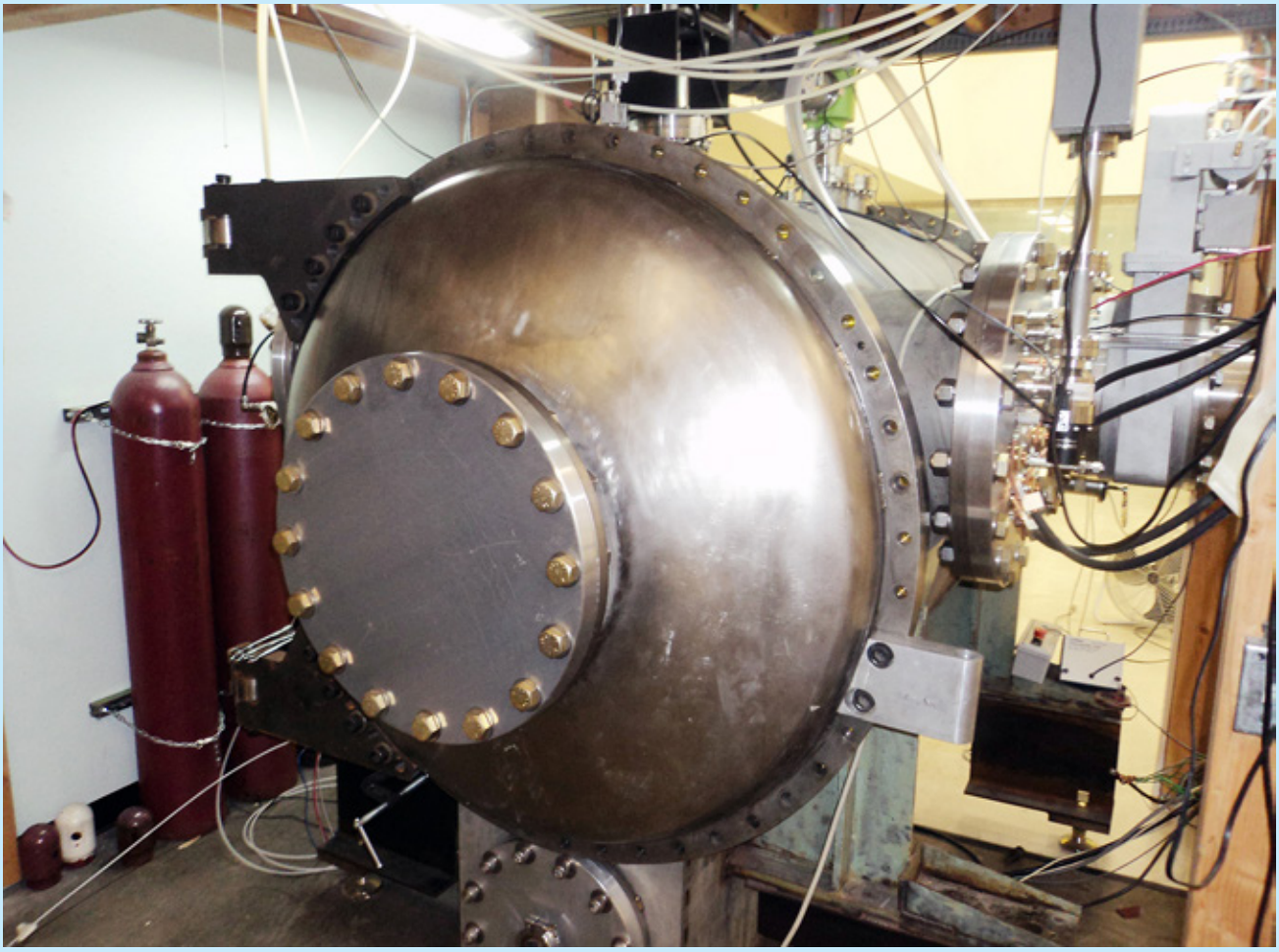

Fig. 1. *A 1.2-m coating chamber fitted with process controllers, thickness monitor, and gas analyzer (Courtesy: ZeCoat Corp).*

MgF_2, LiF, and AlF_3 are considered the most promising coatings based on their UV transparency, as evidenced by results from these initial experiments. Other materials, particularly high-index fluorides, could be employed in other multilayer devices such as filters and beam splitters. Several coatings were prepared on fused silica and silicon substrates. Spectral performance characteristics of these coatings were measured with a state-of-the-art UV/Vis spectrophotometer (PerkinElmer Lambda 1050) as well as with an ACTON FUV spectrometer at GSFC.

Protected Al mirror coatings. MgF_2, AlF_3, and LiF single-layer- and bi-layer-protected Al mirror samples were produced in 2014 and 2015 with a conventional deposition process in the chamber described above. Figure 2 shows the reflectance of bi-layer-protected Al mirror samples from initial experimental runs in the same chamber. These samples remained in the lab in a dry-nitrogen flow-box except during

measurements involving a few days of exposure to normal lab environment with ~30 to 50% humidity. Figure 3 shows the spectral reflectance performance of a bi-layer-protected ($LiF+AlF_3$) Al mirror sample for FUV to NIR, measured over a period of ~14 months after fabrication. The data show excellent stability. Figure 4 shows the details of the spectral reflectance performance of the same sample in the FUV range after 3 years. While the UV to NIR (200 to 1000 nm) reflectance measurements were made at JPL, FUV (50 to 200 nm) measurements with an ACTON FUV spectrophotometer and more recently with McPherson spectrophotometer were made at GSFC under the guidance of Dr. Manuel Quijada. These samples were produced using conventional deposition techniques. Optimization and enhancement of reflectance in the 100-to-200-nm range is a subject of further experimental investigation of process conditions and layer structures. In this context, research done at GSFC has also been reported [19, 20] at an SPIE conference and at the AAS meeting in Baltimore, MD. ALD deposition of such coatings is now in progress at JPL.

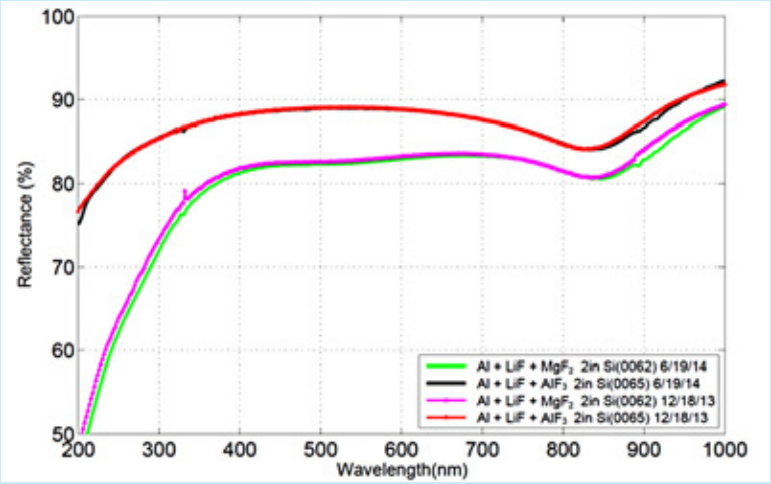

Fig. 2. *Reflectivity of Al+LiF mirror samples with MgF_2 and AlF_3 protective layers. Measured six months after fabrication, these samples showed little degradation.*

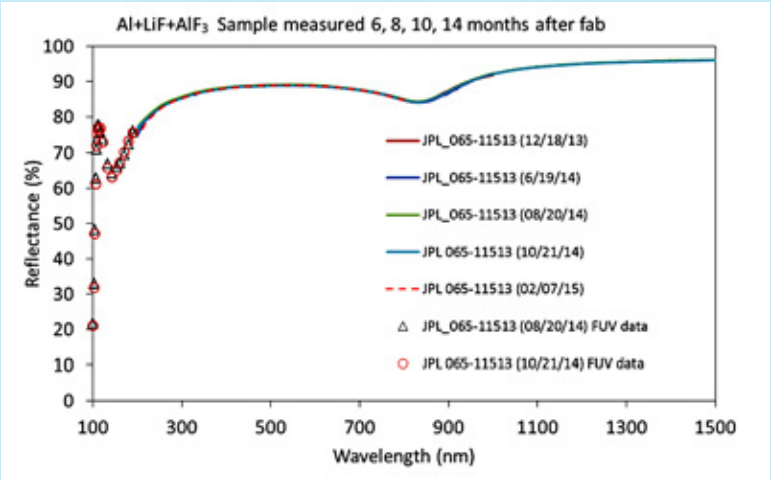

Fig. 3. *Measured reflectance of bi-layer-protected Al-mirror sample 065 (AlF_3+LiF on Al) measured 6, 8, 10, and 14 months after fabrication showing excellent stability. Results over the FUV to NIR spectral range.*

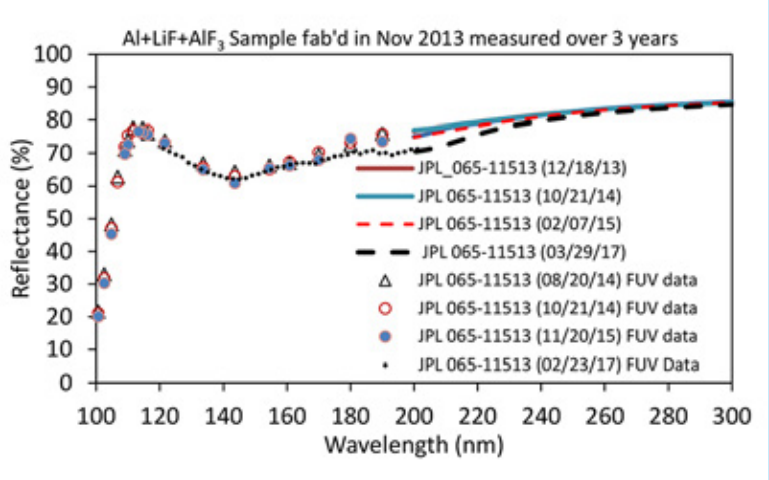

Fig. 4. *Measured reflectance (expanded view showing the FUV spectral range) of bi-layer-protected Al-mirror sample 065 (AlF_3+LiF on Al) measured over a three-year period after fabrication, showing excellent stability.*

With further refinement of process controls in the conventional coating chamber, we prepared another set of samples of MgF_2- and AlF_3-protected mirrors with Al and LiF layers. The outermost layers were only about 4 to 5 nm thick. FUV measurements of such tri-layer samples indicate a reflectance greater than 75% achievable at 110 nm and greater than 50% at 100 nm (Fig. 5). Further optimization of coating thicknesses and process parameters is expected to enhance the FUV reflectance.

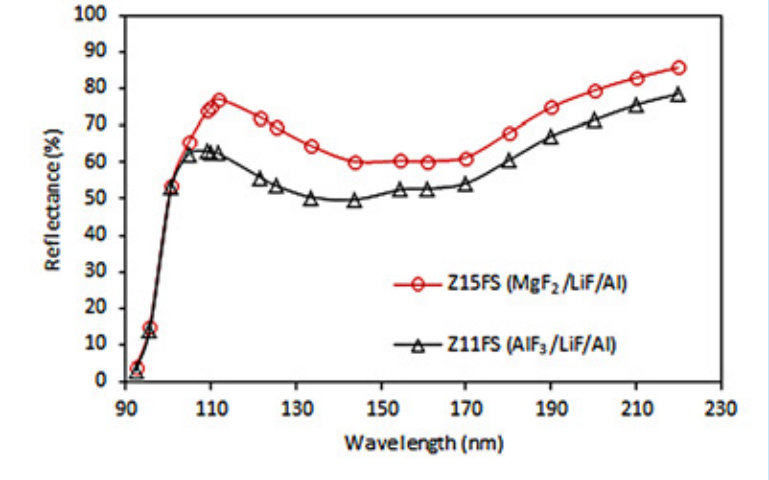

Fig. 5. *FUV reflectance of tri-layer mirror samples from conventional evaporation.*

Atomic Layer Deposition. ALD processes are under development at JPL to produce MgF_2 and AlF_3 protective coatings for high-reflectivity mirrors using an Oxford OpAl showerhead-style ALD reactor and a Beneq ALD system (Fig. 6).

Fig. 6. *ALD systems at JPL.* Left: *Oxford OpAl showerhead-style ALD reactor with gas feedthroughs and process controls enabling AlF_3 and MgF_2 coatings development.* Right: *Beneq ALD deposition system.*

ALD films were deposited using bis(ethylcyclopentadienyl) magnesium ($Mg(EtCp)_2$) and trimethylaluminum (TMA) as the metal-containing precursors and anhydrous hydrogen fluoride (HF) as the fluorine-containing precursor in our Oxford reactor. Although metal fluorides are not common ALD materials, there have been several previous reports of their deposition using metal fluorides such as TaF_5 or TiF_4 as the fluorine-containing source [21, 22]. This tends to result in residual metal contamination that degrades the absorption properties in the FUV and results in a process which can only be performed at substrate temperatures greater than 250°C. As a result of this high deposition temperature, the fluoride films deposited with this method tend to crystallize readily, resulting in significant surface morphology which is undesirable for many optical applications. In contrast, the JPL-developed ALD process using HF results in fluorides with lower residual contamination that can also be deposited at low temperature, resulting in smoother, denser films.

As part of this effort, MgF_2 and AlF_3 were deposited at substrate temperatures ranging from 100°C to 250°C. Film thickness and refractive index were measured by spectroscopic ellipsometry and monitored as a function of process conditions such as process purge times and substrate temperature. Recent reports on the same JPL ALD materials have also shown good optical performance at wavelengths down to 90 nm [5, 23].

Typical ALD conditions involve heating the $Mg(EtCP)_2$ precursor, which is then bubbled with Ar into the process chamber with exposure times of approximately 1 s. TMA and HF are delivered by vapor draw at room temperature with shorter exposure times of 15-30 ms. The chamber is purged with Ar between each half-cycle exposure in the ALD process to ensure saturated, self-limiting deposition. We have demonstrated both MgF_2 and AlF_3 with thickness uniformities better than 1% over six inches. Initial X-ray Photoelectron Spectroscopy (XPS) measurements suggest the films are approximately stoichiometric and future studies will investigate how material composition changes as a function of process conditions. A key goal in the development of an ALD process is to optimize the process at acceptably low temperatures, i.e., below 100°C, in order to enable large mirror coatings in high vacuum. Our recent experiments indicate the feasibility to produce ALD coatings of the relevant fluoride materials.

Reflectance degradation of Al with an oxide formation: evaporation rate, surface roughness, and reflectance stability. To assess the nature and progression of oxide formation on fresh Al coating, we conducted a series of control experiments with Al coatings of different thicknesses deposited at different rates at a high vacuum of ~2×10^{-9} Torr in an ultra-high vacuum (UHV) chamber at JPL. Figure 7 shows the measured (symbols) and modeled (lines) performance of an unprotected Al mirror in the wavelength range from 190 to 290 nm over a period of about 1500 minutes after deposition. A very thin layer of oxide formation (only about 10 Å thick) is estimated to be sufficient to degrade the reflectance as shown.

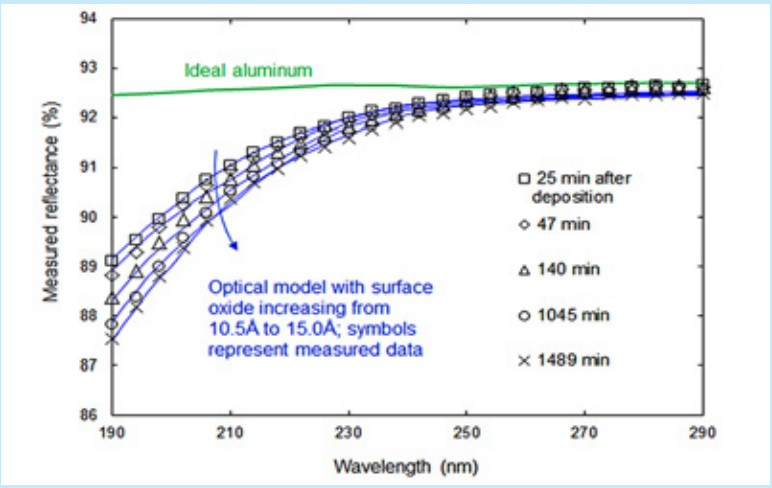

Fig. 7. *Oxidation-induced near-UV reflectance reduction of Al mirror samples; model fits match a progressive increase of oxide formation.*

Figure 8 shows the measured FUV reflectance of an unprotected Al mirror and its model fit with an oxide formation of different thicknesses. These measurements and simulations show that an oxide layer of less than 2-nm thickness affects the FUV reflectance dramatically.

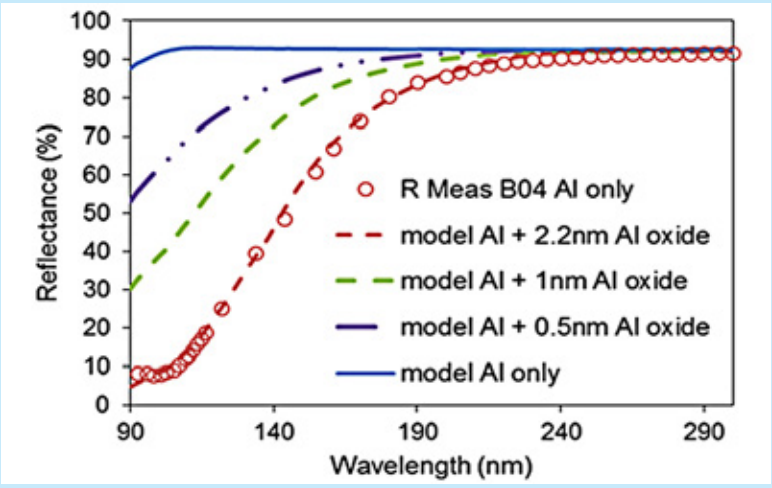

Fig. 8. *Unprotected Al reflectance per models with a thin oxide layer in comparison with measured characteristics (sample B04) in the FUV spectral range.*

Unprotected and protected samples with ALD coatings were also fabricated and measured within about 20 minutes and thereafter for several days to assess the nature of degradation and the effectiveness of a thin protective layer.

Rate of deposition of the Al layer is a critical parameter that affects the reflectance as well as its stability over time. Samples were fabricated at different rates in high vacuum. Initial measurements clearly indicated (Fig. 9 and Table 2) that a rate of about 20 Å/sec or higher (could be as high as 100 Å/sec) is favorable for obtaining better reflectance in the FUV due to denser microstructure and lower oxidation in the bulk of the layer compared to lower-rate samples.

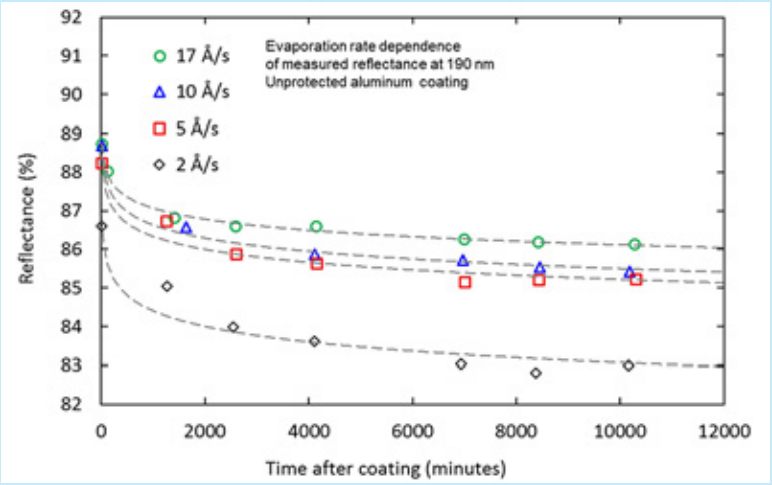

Fig. 9. *Measured reflectance at 190 nm vs. elapsed time of unprotected Al mirror samples produced at different evaporation rates at a base pressure of 2× 10^{-9} Torr. Initial reflectance, as well as rate of degradation, are better with higher deposition rate. Dashed lines indicate an approximate power law dependence.*

Evaporation Rate (Å/s)	Micro-Roughness 1 µm × 1 µm (nm rms)	XPS [O 1s] / [Al 2p] ratio	Reflectance After 1 Week at 190 nm (%)
2	2.05 (±0.14)	1.3 (±0.2)	83.0
5	1.45 (±0.09)	1.3 (±0.2)	85.2
10	1.30 (±0.08)	1.3 (±0.2)	85.5
17	1.18 (±0.03)	1.1 (±0.2)	86.1

Table 2. *The influence of evaporation rate on the UV reflectance at 190 nm for Al thin films deposited by electron beam evaporation at a base pressure of ~2×10^{-9} Torr. The mean root-mean-square (rms) roughness and standard deviation are averaged over five scans for each of the four samples analyzed in Fig. 9.*

We examined the surface roughness of the Al samples deposited in UHV conditions at different rates. Figure 10 shows Atomic Force Microscopic (AFM) images of samples deposited at 1 Å/s and 17 Å/s clearly indicating improved smoothness is achievable with higher deposition rates.

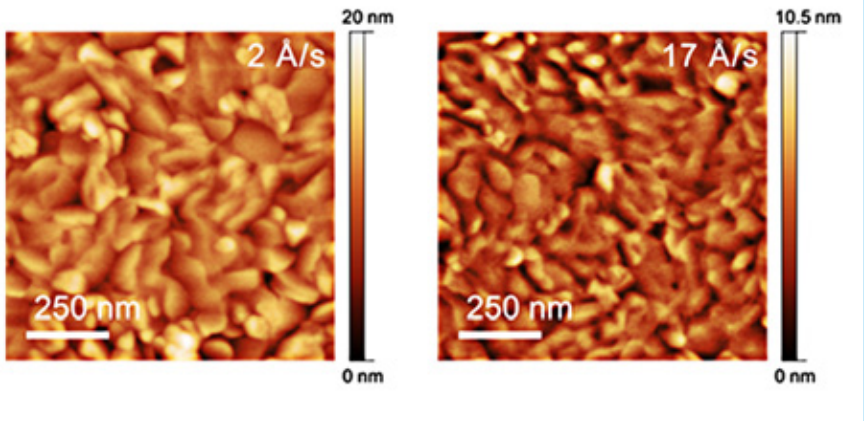

Fig. 10. *AFM images at a length scale of 1 µm× 1 µm of UHV electron beam evaporated Al films (60 nm thickness) at deposition rates of 2 Å/s (left) and 17 Å/s (right).*

A phenomenological refractive index model to estimate the optical properties of the surface oxide was developed to assess the performance impact of a brief air exposure prior to deposition of a protective layer. Details of this model and analysis can be found in Hennessy et al., 2016 [9]. The n and k derived from such a model are plotted in Fig. 11 (adopted from [9]).

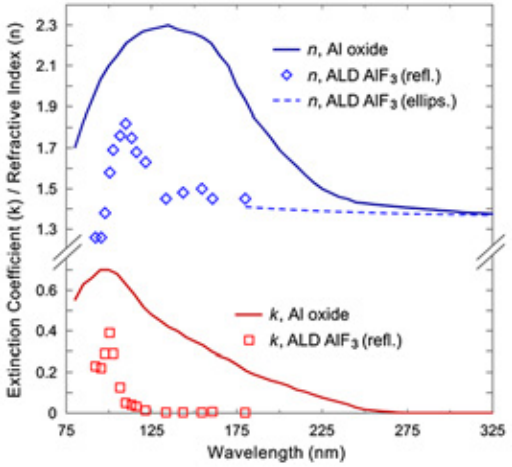

Fig. 11. *Phenomenological refractive index model for the interfacial native oxide on evaporated Al thin films, and the refractive index model for ALD AlF_3 derived from isoreflectance analysis in the FUV.*

Protected Al mirrors. A series of AlF_3-coated Al mirror samples were prepared with different thicknesses of the protective fluoride coated with the ALD process. The UV reflectance of five of these samples with different thicknesses of the protective layer was measured over several days and reported in the 2016 COR PATR. It was inferred that a very thin layer (~3 to 5 nm thick) of AlF_3 is optimum to protect the LiF-coated Al mirror.

FUV performance of ALD AlF_3-protected Al samples. Figure 12 shows the measured FUV reflectance of the ALD AlF_3-protected Al mirrors in comparison with a commercial Physical Vapor Deposition (PVD) MgF_2-protected Al mirror. Model fits indicate a smaller level of oxide formation in the Al layer when a thicker protective coating is applied.

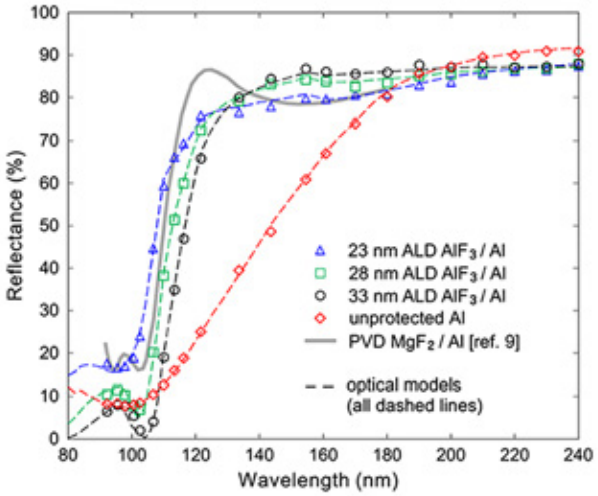

Fig. 12. *Measured FUV reflectance (symbols) and the corresponding calculated optical model (dashed lines) of ALD AlF_3 protective coatings of various thickness deposited on e-beam-evaporated Al thin films, compared to an unprotected Al coating and a typical high-performance PVD MgF_2-protected mirror.*

Figure 13 compares the performance of protected Al samples produced by conventional evaporation techniques and by e-beam followed by ALD. Moving the absorption edge to the FUV end towards 90 nm is the subject of further optimization of layer structures and thicknesses. While a LiF layer allows moving the edge to shorter wavelengths, it reduces the reflectance in the mid-range of FUV when these typical structures are employed. Hence, thinner layers are considered necessary if adequate protection can be ensured.

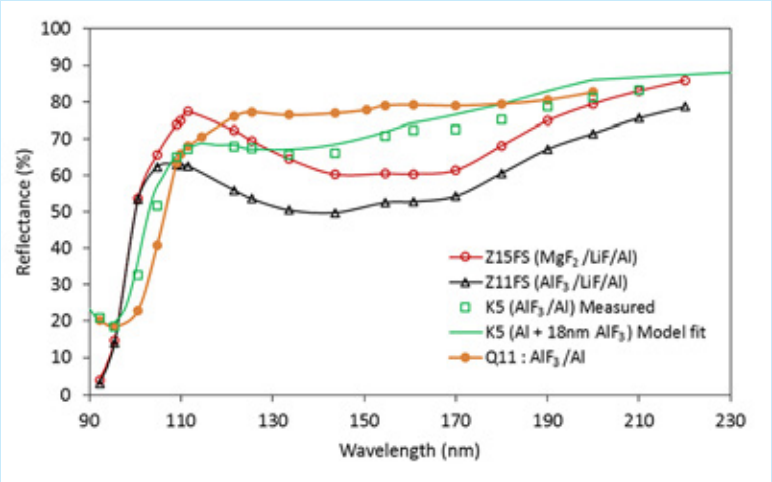

Fig. 13. *FUV reflectance of tri-layer mirror samples produced by conventional thermal evaporation (samples Z11 and Z15); bi-layer mirror samples produced by e-beam of Al and ALD of AlF_3 (samples K5 and Q11).*

Environmental tests. Samples Z11 and Z15 (Figs. 5 and 13), produced by conventional deposition processes early in 2015, were measured repeatedly over the past two years at GSFC. The main difference between these samples is that the outermost protective layer is either MgF_2 or AlF_3 with nearly same physical thicknesses, around 4 to 5 nm. The measurements plotted in Fig. 14 show that the MgF_2-protected sample is more stable over the years compared to the AlF_3-protected sample. However, as it indicates stabilization after the initial drop, we continue to monitor the performance of these samples.

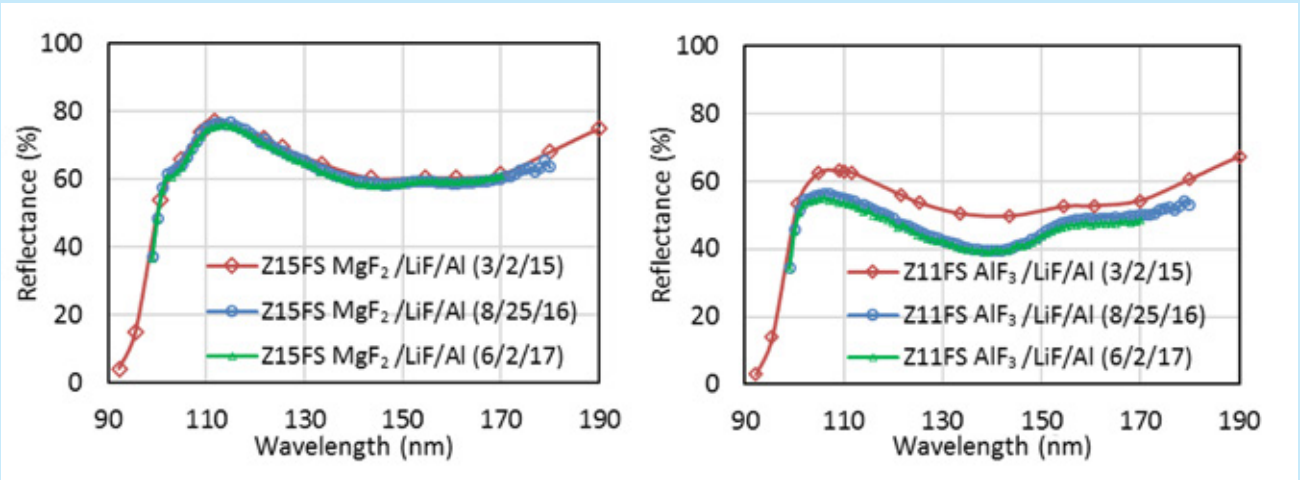

Fig 14 . *Environmental stability of samples Z11 and Z15 over two years of normal storage in lab at 30 to 50% relative humidity (RH) and 25°C temperature except during sample transport and measurements.*

We also prepared a few Al mirror samples with ALD AlF_3 protective layers for environmental tests. Preliminary test of one of the samples subjected to 24 hours in 96% RH at 50° C shows a drop in reflectance in the near-UV (Fig. 15). This silicon substrate sample P04 was coated with Al by conventional e-beam technique and overcoated with a thin ~3-nm layer of AlF_3 by ALD. More detailed tests are necessary to confirm these preliminary results. As discussed above, a sample of AlF_3+LiF-protected Al coated by conventional technique has shown little degradation over two years (Fig. 4) in normal laboratory conditions. Further work is therefore needed in this area to arrive at conclusions and to improve performance and stability.

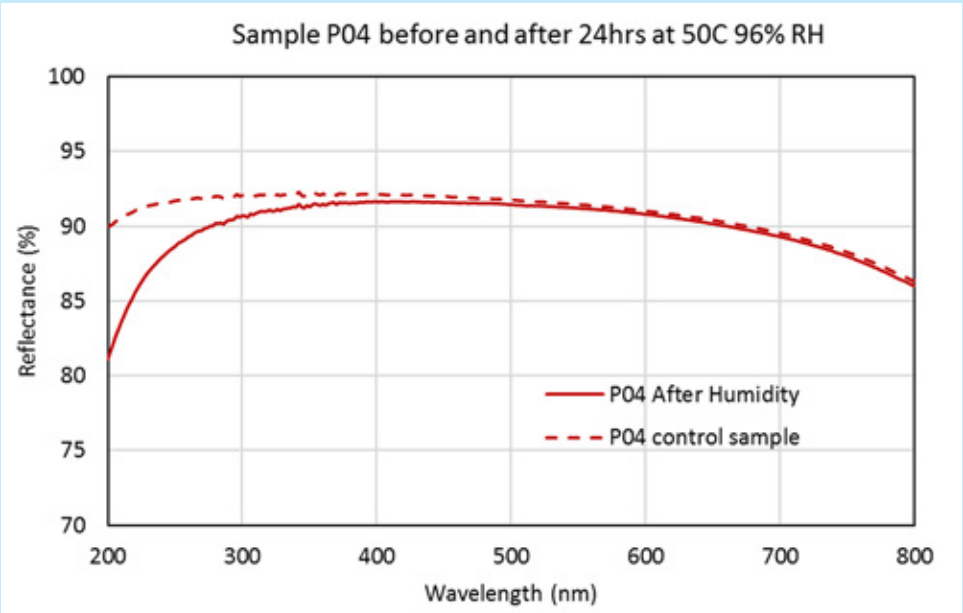

Fig. 15. *Measured reflectance of an Al+ALD AlF_3-coated Si wafer sample subjected to 96% RH at 50° C for 24 hours in an oven, with K_2SO_4 salt to produce and maintain RH. While this sample, made in Sep 2015, showed no noticeable change in reflectance after ~1 year of storage in the laboratory, it suffers when subjected to high humidity at elevated temperature as seen above. The drop in reflectance at 200 nm observed in this preliminary test suggests that further tests are needed, besides optimization of the process conditions and layer thickness.*

Early experiments with ALD AlF_3 protective coatings gave promising results on performance and stability of Al mirrors in laboratory environment as shown in our earlier reports [5]. Recent experiments with ALD coating of a protective fluoride layer after ALE of the surface oxide on Al surface improves the reflectivity significantly. Measurements of reflectivity of ALE + ALD coatings under controlled conditions and high humidity exposures are shown in Fig. 16.

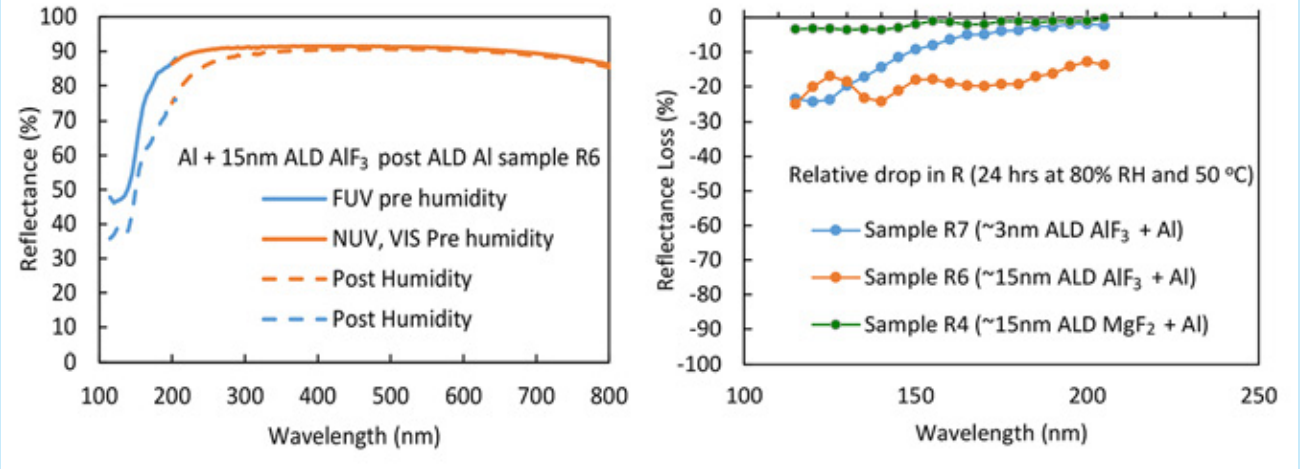

Fig. 16 . Left: *Measured reflectivity (before and after 24 hours at 80% RH at 50°C) of a sample with ~15 nm AlF_3 ALD layer on Al after ALE procedure to remove surface oxide.* Right: *Relative change in reflectivity of similar samples of different thicknesses of AlF_3 and MgF_2 on Al after ALE process indicating the superior stability of MgF_2-protected sample.*

The observed drop of about 10 to 20% with AlF_3 layers relative to unexposed control sample suggests the need for further optimization. Without the ALE process, the drop in reflectivity would have been much greater as we observed in our earlier experiments. While this experiment shows improved reflectivity of such a coating, it reveals that the AlF_3 layer has some vulnerability to moisture attack and hence needs further improvement and protection. Optimization of thickness and process conditions are needed. The ALE procedure greatly reduces the extreme care needed with load lock transport of samples for ALD coating after Al evaporation.

Uniformity tests with conventional evaporation. To test the uniformity of the Al coating on a meter-class optic with conventional e-beam evaporation techniques, a preliminary study was conducted with a number of small coupons placed along the diameter of the coating chamber at ZeCoat Corp, which was fitted with a moving e-gun source. The results are plotted in Fig. 17. The process was not optimized for the UV range, leading to a larger variation of reflectance in UV than in the visible range. However, this is a subject to further process optimization to achieve better than 1% uniformity across a 1-m-diameter optic. In contrast, the ALD process is inherently uniform, as it is not based on a line-of-sight deposition. Thermal conditions and gas flow over the area of the optic will determine the uniformity achievable with ALD. Significant research and engineering effort is needed to accomplish high uniformity of coating reflectivity and phase across the larger mirrors envisioned for the LUVOIR and HabEx mission concepts.

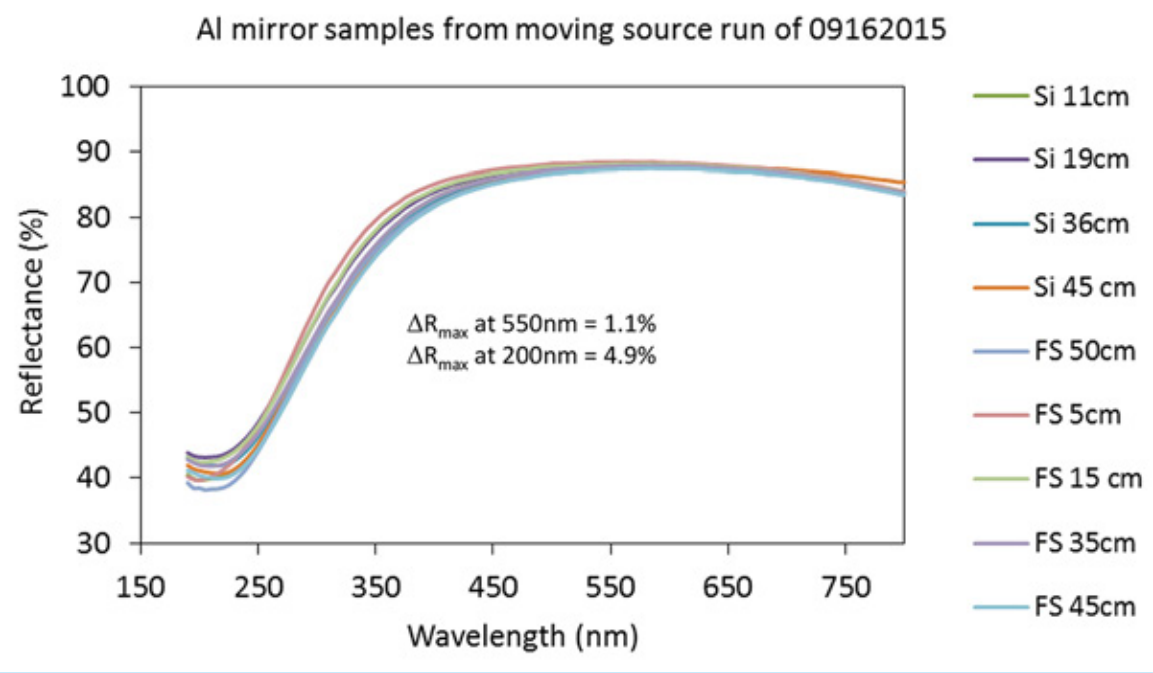

Fig. 17. *Uniformity tests: Coating experiment done with a moving source in a 1.2-m chamber at ZeCoat Corp. Legends indicate distance of the samples from the center of the substrate holder geometry. Further optimization of process conditions and geometry is feasible to achieve better results, particularly in the UV.*

Path Forward

In the years ahead, we will focus on further optimizing deposition parameters of the ALD process, and prepare samples of protected Al mirrors for reflectivity measurements. Lower-temperature processes with faster cycle times are being developed in the new Beneq ALD system now. Our models predict that very thin protective layers deposited by ALD process can accomplish higher reflectance in the FUV as shown in Fig. 18. Details of these models can be found in [9]. Similarly, conventional deposition techniques also require further investigation, particularly with regard to improving reflectivity and uniformity over large-area mirrors.

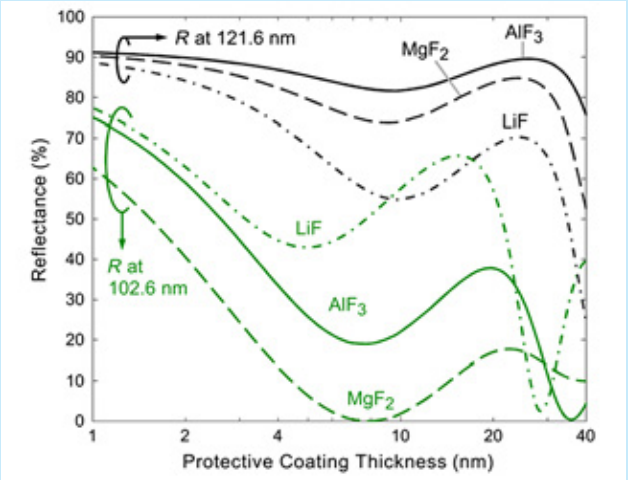

Fig. 18. *The calculated reflectance at 121.6 and 102.6 nm as a function of coating thickness for films of MgF_2, AlF_3, and LiF on ideal Al.*

Acknowledgements

The research reported here was performed at the Jet Propulsion Laboratory, California Institute of Technology under a grant from the NASA Cosmic Origins Program.

References

[1] F. Bridou et al., "*Experimental determination of optical constants of MgF_2 and AlF_3 thin films in the vacuum ultraviolet wavelength region (60–124 nm), and its application to optical designs*," Opt. Communications, **283**, 1351-1358 (2010)

[2] R.A.M. Keski-Kuha et al., "*Optical coatings and applications for ultraviolet space applications*," (NASA GSFC) ASP Conference Series, **164**, J.A. Morse et al.; eds. (1999)

[3] M. Yang, A. Gatto, and N. Kaiser, "*Aluminum-enhanced optical coatings for the VUV spectral range*," Proc. SPIE, **5963** (2005)

[4] K. Balasubramanian et al., "*Protective coatings for FUV to NIR advanced telescope mirrors*," AAS 223 Poster paper on the progress presented at the AAS meeting in Baltimore, MD (Jan 2014)

[5] J. Hennessy et al., "*Thin ALD fluoride films to protect and enhance Al mirrors in Far UV*," 15th International Conference on Atomic Layer Deposition, Portland, OR (June 28th – July 1st 2015)

[6] K. Balasubramanian et al., "*Coatings for UVOIR telescope mirrors*," presented at the SPIE Optics + Photonics conference, San Diego, CA, Aug 9-13, 2015; Proc SPIE **9602** (2015) and see also K. Balasubramanian et al., "*Mirror coatings for large aperture UV optical infrared telescope optics*," presented at the UV/Optical/IR Space Telescopes and Instruments Innovative Technologies and Concepts VIII, conference paper 10398-33 (Aug 7, 2017)

[7] J. Hennessy, A.D. Jewell, F. Greer, M.C. Lee, and S. Nikzad, "*Atomic layer deposition of magnesium fluoride via bis(ethylcyclopentadienyl) magnesium and anhydrous hydrogen fluoride*," JVST **A 33**, no. 1, 01A125 (2015)

[8] J. Hennessy, A.D. Jewell, K. Balasubramanian, and S. Nikzad, "*Ultraviolet optical properties of aluminum fluoride thin films deposited by atomic layer deposition*," JVST **A 34**, 01A120 (2016)

[9] J. Hennessy, K. Balasubramanian, C.S. Moore, A.D. Jewell, S. Nikzad, K. France, and M. Quijada, "*Performance and prospects of far ultraviolet aluminum mirrors protected by atomic layer deposition*," J. Astron. Telesc. Instrum. Syst. 2(4), 041206, doi: 10.1117/1.JATIS.2.4.041206 (2016) and see also J. Hennessy et al., "*Atomic layer deposition and etching methods for ultraviolet aluminum mirrors*," presented at the SPIE Engineering + Applications, paper 10401-40 (Aug 10, 2017)

[10] S. Redfield, "*The Local Interstellar Medium*," in ASP Conference Series 352, New Horizons in Astronomy, **79**, arXiv:astro-ph/0601117v1 (2006)

[11] K. France et al., "*From Protoplanetary Disks to Extrasolar Planets: Understanding the Life Cycle of Circumstellar Gas with Ultraviolet Spectroscopy*," arXiv:1208.2270 [astro-ph.SR] (2012)

[12] J.M. Shull et al., "*The baryon census in a multiphase intergalactic medium: 30% of the baryons may still be missing*," The Astrophysical Journal, **759**:23 (2012)

[13] Cosmic Origins Program Annual Technology Report and Space Telescope Science Institute Cosmic Origins Program Analysis Group (COPAG) Workshop (2011)

[14] C. Stahle et al., "*The Advanced Technology Large-Aperture Space Telescope (ATLAST)*," 224th AAS Meeting, Boston (June 4, 2014)

[15] P. Scowen, in *http://cor.gsfc.nasa.gov/RFI2012/rfi2012-responses.php*

[16] NASA Astrophysics Roadmap Team, C. Kouveliutou, Chair, "*Enduring Quests, Daring Visions: NASA Astrophysics in the Next Three Decades*" (2013)

[17] J. Dalcanton, L. Hillenbrand, K. Sembach, J. Gardner, C. Lillie, P. Goldsmith, D. Leisawitz, and C. Martin (Chair), "*COPAG Technology Assessment*," v.1.3 (Nov 10, 2011)

[18] M. Bolcar et al., "*A Technology Gap Assessment for a Future Large-Aperture Ultraviolet-Optical-Infrared Space Telescope*," submitted to the Journal of Astronomical Telescopes, Instruments, and Systems (JATIS) 2016, and Proc. SPIE **9602** (2015)

[19] M. Quijada et al., "*Enhanced MgF_2 and LiF Over-coated Al Mirrors for FUV Space Astronomy*," Proc. SPIE **8450** (2012)

[20] M. Quijada et al., "*Enhanced Fluoride Over-coated Al Mirrors for FUV Space Astronomy*," Poster paper presented at the AAS meeting in Baltimore, MD (Jan 2014)

[21] T. Pilvi et al., "*Study of a novel ALD process for depositing MgF_2 thin films*," J. Mater. Chem., **17**, 5077 (2007)

[22] M. Mantymaki et al., "*Atomic Layer Deposition of LiF Thin Films from Lithd, $Mg(thd)_2$, and TiF_4 Precursors*," Chem. Mater. **25**, 1656 (2013)

[23] C. Moore et al., "*Recent developments and results of new ultraviolet reflective mirror coatings*," presented at SPIE Astronomical Telescopes + Instrumentation, Montreal, Proc. SPIE **9144** (2014)

For additional information, contact K. Balasubramanian: *kbala@jpl.nasa.gov*

Advanced FUV/UV/Visible Photon-Counting and Ultralow-Noise Detectors

Prepared by: Shouleh Nikzad (PI; JPL), Chris Martin (Caltech), David Schiminovich (Columbia University), and Michael Hoenk (JPL)

Summary

In this three-year Strategic Astrophysics Technology (SAT) effort that began in January 2016, we develop and advance the Technology Readiness Level (TRL) of solar-blind (SB), high-efficiency, photon-counting, and ultralow-noise solid-state detectors especially in the far ultraviolet (FUV) with $\lambda < 200$ nm. We will combine superlattice (SL) doping (Fig. 1) integrated SB filters (Fig. 2), and anti-reflection (AR) coatings with ultralow-noise scientific CMOS (sCMOS) and large-format Electron-Multiplying CCDs (EMCCDs). We will fabricate, characterize, and validate these detectors in a relevant space environment.

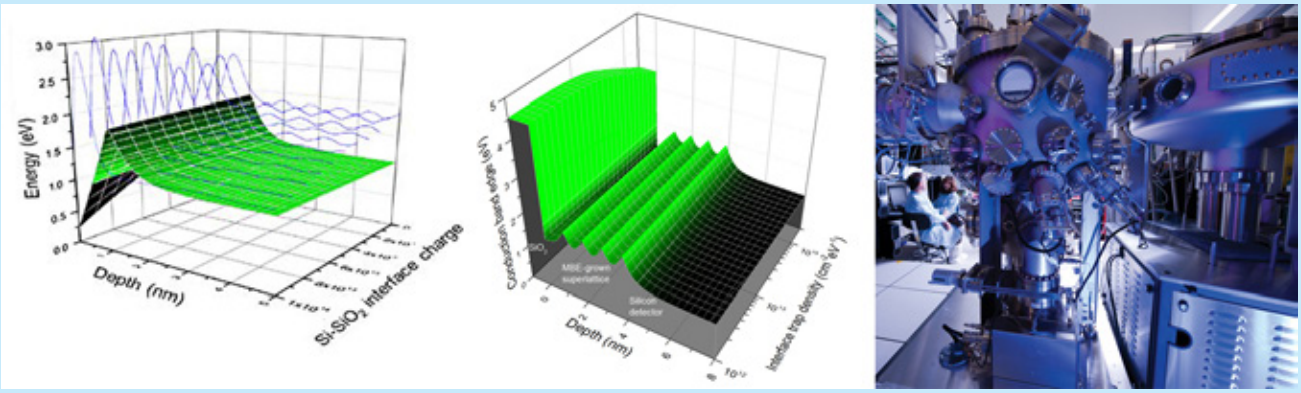

Fig. 1. Left and Middle: *Band diagram of delta-doped and SL-doped silicon surface.* Right: *JPL 8"-wafer-capacity silicon molecular beam epitaxy (MBE) used for superlattice doping.*

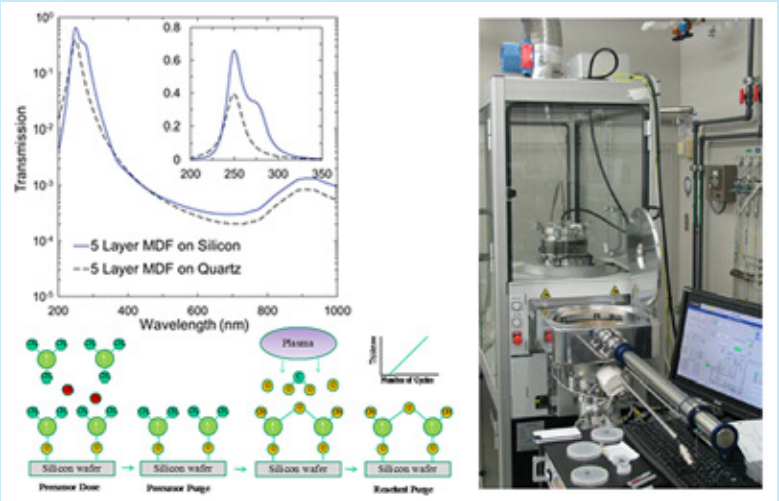

Fig. 2. Top Left: *Calculated performance of a five-layer metal-dielectric filter on silicon or quartz substrates, showing in-band QE >60% and out-of-band rejection approaching 10^{-4}, an example of detector-integrated filters that can render silicon "solar blind".* Bottom Left: *Diagram of Atomic-Layer-Deposition (ALD) process showing layer-by-layer control.* Right: *JPL ALD system used for deposition of these metal-dielectric layers.*

The detectors under development in this effort offer potentially game-changing performance and capabilities, directly addressing the Technology development for Cosmic Origins (TCOR) requirements outlined in the SAT call for detectors with high quantum efficiency (QE) for $\lambda < 200$ nm, large format, photon-counting capability, and ultralow noise. High-performance ultraviolet (UV) detector and coating technologies will be an essential part of the Large UV/Optical/Infrared (LUVOIR) Surveyor, a leading contender to be one of the next flagship missions. Additionally, the photon-counting capability and ultralow noise in either UV or visible bands will have a high impact on a Habitable Exoplanet Imaging Mission (HabEx). Because of the dramatic efficiency increase in the detector, flagship-class science will be possible with smaller-size apertures, offering great impact on future Probe- and Explorer-class missions. Our coating processes, with films prepared by ALD, also advance UV coatings for optics.

SL doping (or multilayer delta doping; Fig. 1) was invented at JPL [1], and has been proven to achieve high internal QE on EMCCDs and CMOS arrays [2-6]. SL-doped EMCCDs and SL-doped CMOS are at TRL 4. Integrated visible-rejection filters have been demonstrated and proven on avalanche photodiodes (APDs) and extensively tested [7]; they are at TRL 3. The resulting combination of these SL-doped, AR-coated (SLAR), and SB EMCCD [8, 9] and sCMOS arrays are at TRL 3. Furthermore, we will extend the capability to $\lambda < 200$ nm. Devices will be produced to meet our QE, noise, and visible-rejection requirements; and will be thermally cycled, and characterized and validated in a relevant radiation environment, advancing them to TRL 4-5 by the end of this three-year effort.

Our team includes members with complementary expertise in materials, detectors, instrument building, and observational science. The team is uniquely qualified to carry out this project. By forming alliances between technology developers, instrument builders, and mission Principal Investigators (PIs)—Profs. D. Schiminovich and C. Martin are PIs of Galaxy Evolution Explorer (GALEX) as well as suborbital missions such as Faint Intergalactic medium-Redshifted Emission Balloon (FIREBall)—our team has a natural path for TRL advancement and flight insertion.

Background

The 2010 Decadal Survey, "*New Worlds, New Horizons in Astronomy and Astrophysics*" (NWNH) [10] set a priority for path-finding work toward a 4m+ UV/Optical flagship mission as a successor to the Hubble Space Telescope (HST). Great emphasis on Explorer missions is also anticipated in this decade.

Recently, mid-decadal studies have been ongoing that build on the work of the NWNH. These studies have consistently set forth technology-development goals aimed at enabling a future LUVOIR flagship mission, and increasing the scientific reach of smaller missions in this decade. The Cosmic Origins Program Analysis Group (COPAG) is now evaluating and recommending technology investments toward these goals through Science Interest Groups (SIGs). A new Technology Interest Group (TIG) is reviewing technology gaps. In these scientific focus areas, single-photon-counting or ultra-low-noise detectors are a priority. Furthermore, these recommendations set as a goal very-large-format (100 Megapixel to Gigapixel), high-QE, UV-sensitive detectors. These recommendations reflect the new understanding of the scientific opportunities enabled by technological breakthroughs in large-scale detector fabrication.

Our objectives are tied to the needs of and recommendations for future NASA missions in the NWNH, guided by the mid-decadal studies being carried out by COPAG and the Association of Universities for Research in Astronomy (AURA); and is updated with the needs of flagship concepts such as the LUVOIR Surveyor and HabEx.

Frontier astrophysical investigations are necessarily conducted at the limits of resolution, etendue, and sensitivity. A future 10-m UV/Optical telescope mission will require significant detector advances beyond HST, GALEX, and Far Ultraviolet Spectroscopic Explorer (FUSE) detector technologies, particularly in QE, spectral responsivity in the UV, resolution, and pixel count. Our primary performance metric, detector QE in the UV, represents a dramatic increase (5- to 10-fold) over previous missions. Dramatically increasing the efficiency of the detectors could allow Explorer-class or Probe-class missions to perform flagship-mission science.

A solid-state detector with high efficiency and photon counting offers scalability and reliability that are necessary and attractive features for reliable, high-performance, and cost-effective instruments. The LUVOIR requirements are directly applicable to the objectives of this effort. Additionally, detectors developed under this SAT, optimized for visible light, would have a high impact on the HabEx mission.

Objectives and Milestones

Table 1 shows the project's milestones and schedule.

Milestone	Year 1				Year 2	Year 3
	Q1	Q2	Q3	Q4		
Demonstrate SB SLAR EMCCD						
Procure wafers of standard larger-format EMCCDs	Δ					
Thin, bond, SL-dope wafers		—	Δ	Δ	Δ	Δ
Incorporate advanced ALD filters (200-240 nm)				—	Δ	
Demonstrate SB SLAR Low-noise CMOS						
Select low-noise CMOS design		—	—	—	Δ	
Procure wafers of low-noise CMOS (e.g., sCMOS)					Δ	
Thin, bond, SL-dope sCMOS					—	Δ
Incorporate advanced ALD filters (200-240 nm)					—	Δ
Extend visible-blind filter to FUV						
Extend multilayer design to center at 140 or 150 nm				—	—	Δ
Integrate with SLAR EMCCD				—	—	Δ
Integrate with SLAR sCMOS					—	Δ
Validation and environmental testing						
Test noise and QE in temperature, illumination; test lifetime					—	Δ

Table 1. *Project milestones and schedule.*

Progress and Accomplishments

Although the funding for 2017 was received incrementally, necessarily slowing down the procurement of low-noise CMOS wafers, we have made excellent progress in the task objectives, including development of processes for high-QE CMOS arrays.

EMCCD wafers that were previously procured and received were bonded to "handle" or "support" wafers prior to thinning. Discussions with e2v resulted in final thickness decisions. Superlattice doping and single-layer Al_2O_3 coating designed for FIREBall were implemented on one wafer.

Several devices were produced by dicing and packaging. Detailed characterization was performed to determine optimal performance. Testing and characterizations were performed at both JPL and Caltech (in photon-counting mode) cross-checking the results, as well as verifying performance tested on previously SL-doped devices at e2v.

Multiple trips were made to Palomar Observatory to collect on-sky data using the Cosmic Web Imager (CWI). Photon-counting, low-noise, and QE performance were verified (Fig. 3).

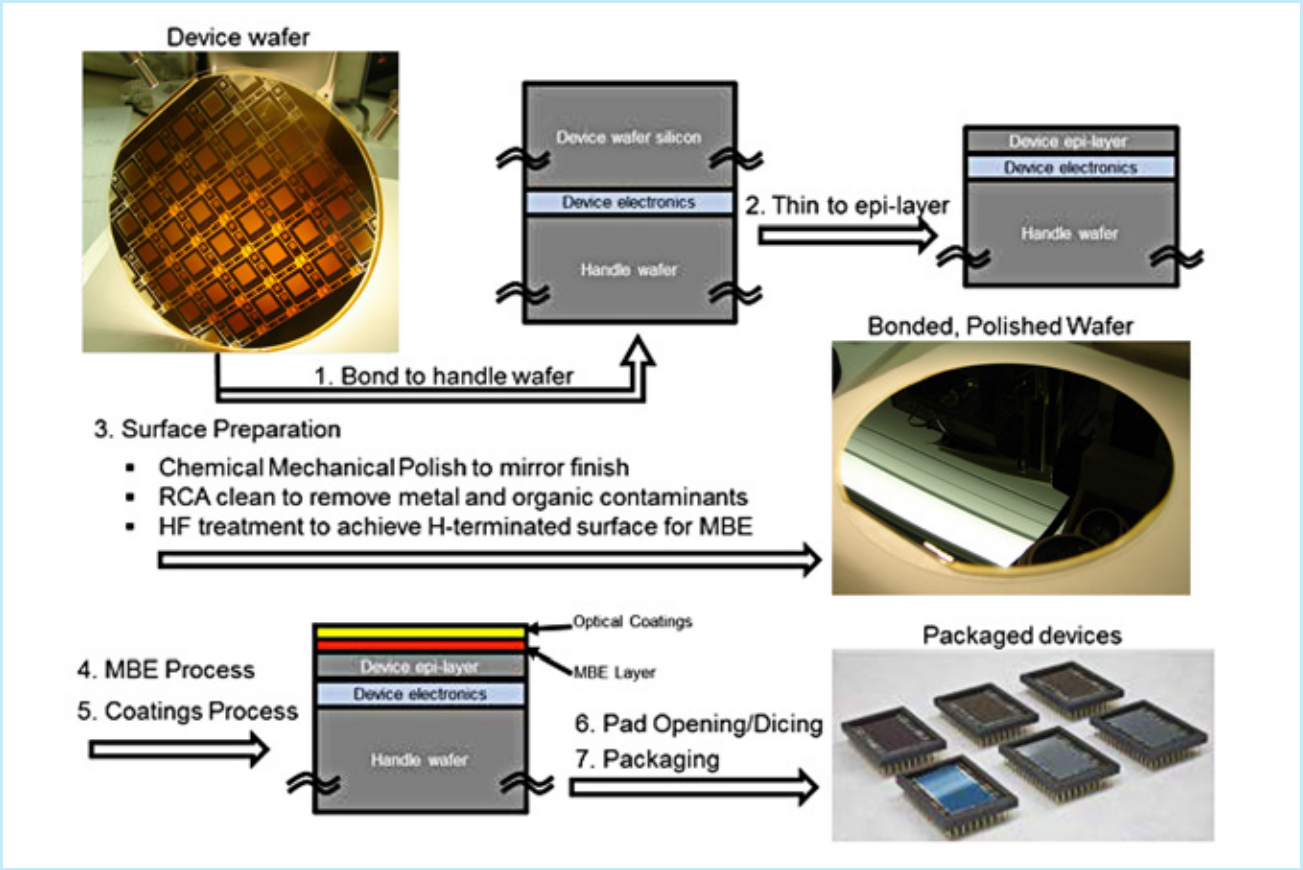

Fig. 3. *End-to-end post-fabrication processing for an EMCCD wafer. Results for some of these have been published recently [11, 12].*

The FIREBall EMCCD was tested post-delivery at Caltech and Palomar for photon-counting capability. It was also tested to show nearly 60% QE, five-fold better than the FIREBall micro-channel plate (MCP) detector response (Figs. 4, 5). Three coatings designs were considered for FIREBall, with five layers, three layers, and a single layer (Fig. 5). The three-layer design was selected for flight.

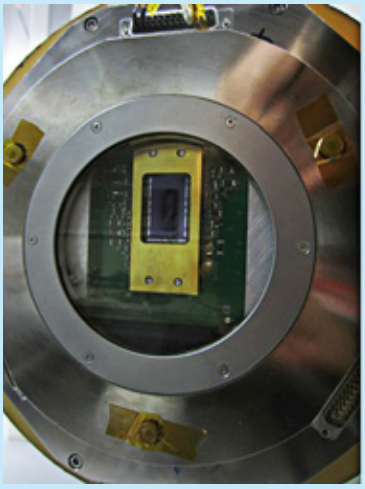

Fig. 4. Left: *Delta-doped and AR-Coated EMCCD (CCD201), optimized for 200 nm, in the dewar at Palomar's CWI.* Right: *CCD in FIREBall spectrometer with Zn lines around 200 nm indicating good performance for FIREBall's atmospheric window at 205 nm.*

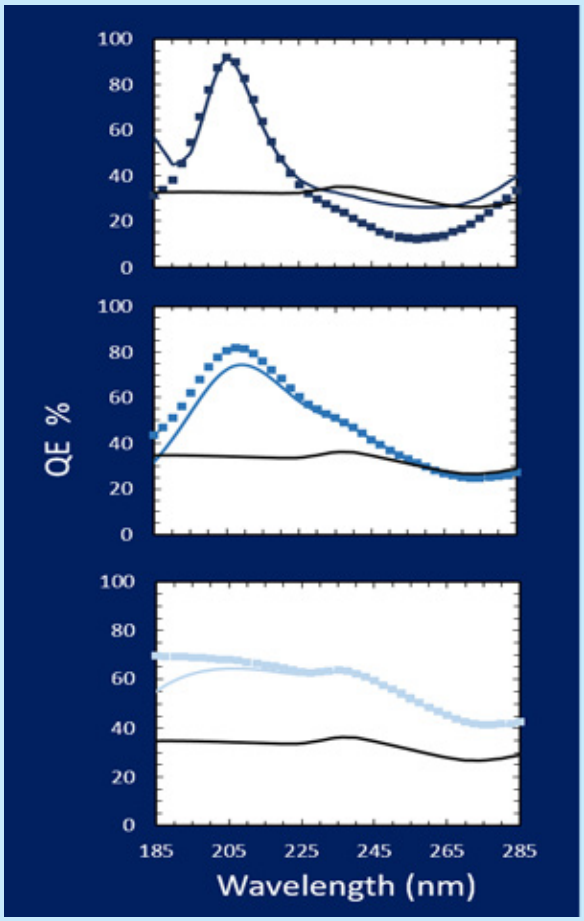

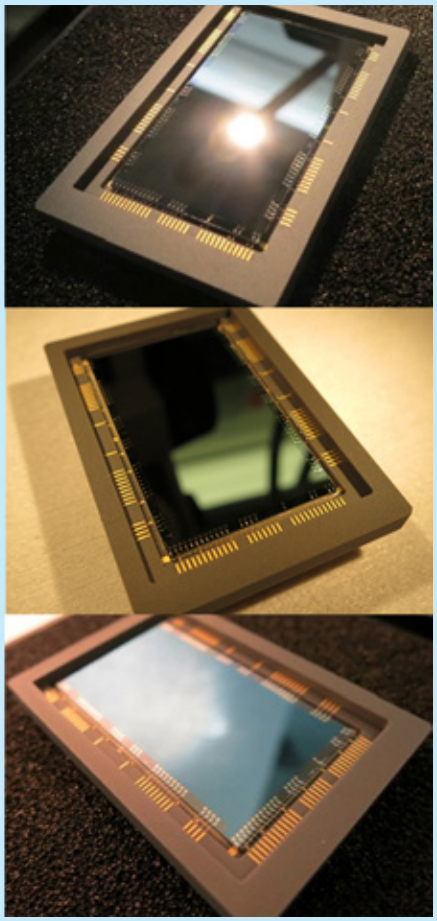

Fig. 5. Left: *QE performance in the UV with (top to bottom) five-layer, three-layer, and single-layer dielectric designs.* Right: *CCD201s processed by superlattice doping and ALD coating for the same three designs. The middle option was selected for flight.*

Upon receipt of full funding for 2017, discussions with Andor, Sarnoff, and potentially e2v regarding acquiring wafers containing sCMOS or other low-noise CMOS will resume. We had previously contacted top groups in ultralow-noise CMOS development such as Fairchild (for sCMOS), Celeaste, e2v, Sarnoff, CMOSIS-AMS, and Rutherford Appleton Laboratory (RAL) regarding wafer procurement and collaboration. Non-disclosure agreements (NDAs) are in process with Andor-Fairchild and Sarnoff as potential CMOS suppliers (already executed with Sarnoff, and far along with Andor-Fairchild). Andor-Fairchild currently appears to be the most likely collaborator.

Metal dielectric filters for enhancement in the 140-150-nm band were designed. In collaboration with end users, another band was identified, 150-175 nm. The latter design was implemented in silicon wafer. The designed layers were also implemented in non-functional SL-doped EMCCDs to check for and address mechanical issues. These designs are now ready for integration into functional SL-doped EMCCDs.

Two papers (by S. Nikzad and M. Hoenk) were accepted for oral presentation at the 2017 International Image Sensor Workshop (2017 IISW) with papers submitted for the workshop proceedings. S. Nikzad also served as an IISW technical program committee member.

A revision to the paper, "*High Efficiency UV/Optical/NIR Detectors for Large Aperture Telescopes and UV Explorer Missions: Development of and Field Observations with Delta-doped Arrays*," by S. Nikzad et al. is nearly complete and will be submitted in the next reporting period. An invited paper by S. Nikzad on space technology for medicine was published in SPIE Professional.

S. Nikzad also served as Senior Guest Editor for a special issue of Neurophotonics, where emphasis was given to technology (e.g., space technology) for neuroscience and neurosurgery.

Path Forward

We plan several activities during the coming year:

- Complete further wafer processing and produce several 2-megapixel arrays in preparation for radiation testing and draft a radiation-testing plan;
- Evaluate and characterize the QE, dark noise, and uniformity of devices from those processed in these subsequent wafers;
- Implement the design of metal dielectric films into EMCCDs that are superlatticed; further optimization might be necessary once the filters are integrated into the detector;
- To approach as close as possible to the absolute QE value, we are verifying the measured QE in other systems;
- The Caltech group will continue to also characterize devices in photon-counting mode; and
- Resume discussions with CMOS vendors and work on procuring wafers from our selected vendors.

References

[1] M.E. Hoenk, P.J. Grunthaner, F.J. Grunthaner, M. Fattahi, H-F. Tseng, and R.W. Terhune, "*Growth of a Delta-Doped Silicon Layer by Molecular-Beam Epitaxy on a Charge-Coupled Device for Reflection-Limited Ultraviolet Quantum Efficiency*," Appl. Phys. Lett., **61**, 1084 (1992)

[2] S. Nikzad, M.E. Hoenk, P.J. Grunthaner, R.W. Terhune, F.J. Grunthaner, R. Winzenread, M. Fattahi, and H-F. Tseng, "*Delta-doped CCDs: High QE with Long-term Stability at UV and Visible Wavelengths*," Proc. SPIE, **2198**, 907 (1994)

[3] J. Blacksberg, S. Nikzad, M.E. Hoenk, S.E. Holland, and W. Kolbe, "*Near-100% Quantum Efficiency of Delta Doped Large-Format UV-NIR Silicon Imagers*," IEEE Trans. on Electron Devices, **55**, 3402, (2008)

[4] M.E. Hoenk, T.J. Jones, M.R. Dickie, F. Greer, T.J. Cunningham, E.R. Blazejewski, and S. Nikzad, "*Delta-doped back-illuminated CMOS imaging arrays: Progress and prospects*," Proc. SPIE, **74190**, 74190-74115 (2009)

[5] S. Nikzad, M.E. Hoenk, F. Greer, E. Hamden, J. Blacksberg, B. Jacquot, S. Monacos, C. Martin, D. Schiminovich, and P. Morrissey, "*Silicon Detector Arrays with Absolute Quantum Efficiency over 50% in the Far Ultraviolet for Single Photon Counting Applications*," Applied Optics, **51**, 365 (2012)

[6] S. Nikzad, M.E. Hoenk, P.J. Grunthaner, R.W. Terhune, R. Winzenread, M. Fattahi, H-F. Tseng, and F.J. Grunthaner, "*Delta-doped CCDs As Stable, High Sensitivity, High Resolution UV Imaging Arrays*," Proc. SPIE, **2217**, 355 (1994)

[7] E. Hamden, F. Greer, M.E. Hoenk, J. Blacksberg, T.J. Jones, M. Dickie, B. Jacquot, S. Monacos, C. Martin, P. Morrissey, D. Schiminovich, and S. Nikzad, "*Antireflection Coatings Designs for use in UV Imagers*," Applied Optics, **50**, 4180-4188 (2011)

[8] P. Jarram, P. Pool, R. Bell, D. Burt, S. Bowring, and S. Spencer, "*LLLCCD—Low Light Level Imaging without the need for an intensifier*," Proc. SPIE, **4306**, 178 (2001)

[9] J. Hynecek, "*Impactron–A New Solid State Image Intensifier*," IEEE Transaction on Electron Devices, **48** No. 10, 2238-2241 (2001)

[10] Blandford et al., "*New Worlds, New Horizons in Astronomy and Astrophysics*," National Academy of Sciences (2010)

[11] E. Hamden, D. Schiminovich, S. Nikzad, and C. Martin "*UV photon-counting CCD detectors that enable the next generation of UV spectroscopy missions: AR coatings that can achieve 80-90% QE*," Proc. SPIE, **8453**, High Energy, Optical, and Infrared Detectors for Astronomy V, 845309 (2012)

[12] S. Nikzad, M.E. Hoenk, F. Greer, B. Jacquot, S. Monacos, T. Jones, J. Blacksberg, E. Hamden, D. Schiminovich, C. Martin, and P. Morrissey, "*Delta doped Electron Multiplied CCD with Absolute Quantum Efficiency over 50% in the near to far Ultraviolet Range for Single Photon Counting Applications*," Applied Optics, **51**, 365 (2012)

For additional information, contact Shouleh Nikzad: *Shouleh.Nikzad@jpl.nasa.gov*

Development of DMD Arrays for Use in Future Space Missions

Prepared by: Zoran Ninkov (PI; Rochester Institute of Technology, RIT); Sally Heap and Manuel Quijada (NASA/GSFC); Massimo Robberto (STScI); and Alan Raisanen, Dmitry Vorobiev, and Anton Travinsky (RIT)

Summary

This NASA Strategic Astrophysics Technology (SAT) project began in May 2014. The project seeks to investigate the feasibility of using a digital micro-mirror device (DMD) as the slit mask for a multi-object spectrograph (MOS) system for a variety of future NASA space missions. In particular, we are investigating a number of key operating parameters for Texas Instruments (TI) commercial-off-the-shelf DMDs including: replacing the borosilicate window with windows transmissive at ultraviolet (UV) and infrared (IR) wavelengths, tolerance to particle-radiation effects, ability to survive the vibrational conditions of launch, and non-specular scattering properties of the DMDs. The team includes Sally Heap at NASA/GSFC, who provides us with insight into the connection between astronomical measurement requirements and our laboratory testing; Massimo Robberto at the Space Telescope Science Institute (STScI), who provides test design guidance and has previous experience with proposed DMD used by the European Space Agency (ESA); Manuel Quijada at GSFC, who provides considerable optics experience and the use of the Carey 5000 Spectrometer at GSFC; and Alan Raisanen at RIT, who provides the necessary microsystems experience to allow for replacement of DMD windows in the RIT cleanroom. Additionally, we have worked with Jonny Pellish (GSFC Code 561) to conduct heavy-ion radiation testing of DMDs at Texas A&M and Tim Schwartz (GSFC Code 549) for vibration and shock testing. The project has made significant progress this year, including an improved measurement of light scattering from the TI DMD, a second round of heavy-ion testing on the DMDs at the Texas A&M University Cyclotron, vibrational and shock testing of DMDs in re-windowed and standard packages, extensive low-temperature testing with our collaborators at Johns Hopkins University (JHU), and re-coating a DMD with high-purity aluminum at GSFC.

Background

Our ultimate objective is to address two key questions of NASA's Cosmic Origins (COR) Program:

1. How did galaxies evolve from the very first systems to the elliptical and spiral types we observe today?
2. How did super-massive black holes affect the lives of galaxies in which they reside, and vice versa?

Ground-based telescopes and the Hubble Space Telescope (HST) have shown us that the Hubble sequence of elliptical and spiral galaxies was in place by redshift $z=1$. However, what physical processes drove $z > 1$ galaxies to join the Hubble sequence? To understand galaxy evolution, we need to carry out a large spectroscopic survey of the sky with a particular focus on galaxies at redshifts of $z=1\sim2$. Experience with the Sloan Digital Sky Survey [1] indicates that several hundred thousand galaxies need be observed in order to distinguish among the many possible drivers of galaxy evolution (e.g., accretion, mergers, star formation, stellar evolution and feedback, growth of black holes, etc.).

A large spectroscopic survey requires a MOS able to record the spectra of hundreds of galaxies in a single exposure. The MOS must have adjustable slits to eliminate confusion with nearby sources and to block out unwanted zodiacal background, which would otherwise swamp the light from these faint galaxies. The MOS should have access to the far UV (1200 - 2000 Å) radiation emitted by a z~1 galaxy because this spectral region has a rich set of diagnostics of stars, gas, and dust in the galaxy. Access to the blue-red spectral regions (2000 - 8000 Å) is also essential for determining the precise redshift of a galaxy, its stellar mass, and its elemental abundances; and for characterizing dust extinction. Because the light from a z~1 galaxy is redshifted before reaching us, a large spectroscopic survey should be sensitive over the spectral interval 2000 - 16000 Å.

The Problem: No existing MOS has such a wide spectral range, let alone access to the UV. TI's DMD would make an excellent slit selector for a spectrograph if it were sensitive in the UV. However, commercial DMD windows block UV light.

Scientific Impact: A UV-transmitting DMD window enables a breakthrough in observational power sufficient to address two key COR science issues. No other telescope, ground- or space-based, present or planned, can accomplish this investigation, because it can't observe all the spectral diagnostics from Ly α (~1200 Å) to Hα + [N II] (~6600 Å) in the same high-redshift galaxy.

Our project intends to investigate the applicability of DMDs to this and other space-based applications by testing the radiation hardness and light-scattering properties of these devices. In addition, our project will look at approaches to replacing the commercially provided windows on DMDs.

The Solution: We therefore propose to optimize the performance of DMDs for the UV region. This requires replacing the DMD window with a UV-transmitting window (> 2000 Å) with an anti-reflection coating on each side, optimized for the UV, optical, and IR. Because the target galaxies are at a redshift of z~1, the observed spectrum of a galaxy over 0.2–1.6 μm records the light emitted by the galaxy in the spectral range 0.1 – 0.8 μm. This wavelength region contains virtually all the important spectral diagnostics of stars, gas, and dust in the galaxy.

Objectives and Milestones

Table 1 provides the major milestones of this project. Our project started more slowly than expected, principally because it took longer than expected to identify vendors for the needed components (e.g., windows, DMDs) and services (L-1 Standards & Technology). There was also a long delay in getting purchase orders through the GSFC system. Finally, although we received a quote from a US-based distributor to acquire TI Cinema DMDs when we submitted the proposal, it turned out they could not resell those in the US. The only way to get these DMDs was through TI's European distributor, at a higher-than-budgeted cost. STScI provided the additional funds, but there was a delay in placing the sub-contract and thus the order.

Milestone	Vendor/Work Location	Dates	Comments
Proton-testing of DMD and data analysis	LBNL 88" Cyclotron	Completed 2014	Results published
Receipt of MgF_2 and Heat Exchanger Method (HEM) Sapphire windows	Photonics Solutions Group, Blue Ridge Optics, GT Crystal Systems	Received Sep 2015	After many delays from vendors, we received all of the windows; all windows met our specifications
Replacement of TI DMDs window	L-1 Standards & Technology	Received Dec 2015	Devices all accepted
Receipt of Cinema DMDs + drive electronics	VISITECH, Germany	Received Jan 2016	Final quote for these items was higher than budgeted; supplemental funding allowed order to proceed
Replacement of TI DMD windows with custom windows	Semiconductor & Microsystem Fabrication Laboratory, RIT	Aug 2015 & Jan 2016	DMDs with Sapphire and MgF_2 windows have been fabricated as have devices with Kapton and Mica windows for heavy-ion testing
Vibration and shock testing	NASA GSFC Code 549	Testing completed May 2016; Analysis completed Feb 2017	Results accepted by Journal of Astronomical Telescopes, Instruments, and Systems
Measurement of light scattering from eXtended Graphics Array (XGA) DMD	RIT, Carey 5000 at GSFC Code 551	May 2016 Mar 2017	High signal-to-noise ratio (SNR) measurements of standard DMDs; Final measurements of bare DMDs with original coating and new Al coating
Heavy-ion testing of DMD and data analysis	Texas A&M Radiation Effects Facility	Tests Aug 2015 & Apr 2016; Analysis completed Feb 2017	On-orbit event rates estimated; Results accepted by Journal of Astronomical Telescopes, Instruments, and Systems
Recoating of DMDs with high-reflectivity aluminum	NASA GSFC Code 551	Feb 2017	Coated a section of a functioning XGA DMD with high reflectivity aluminum; DMD remained operational
Low-temperature testing of DMDs	Instrument Development Group at JHU	May 2017	Supplied DMDs with re-windowed & original packages for testing at 77 K
Gamma-ray testing	NASA GSFC	October 2017	Tests of multiple DMD devices
Extended-time low-temperature testing	JHU/APL	November 2017	Hold DMD patterns for typical astronomical observation times at low temperature
Optical modeling module	RIT	February 2018	Permit inclusion of DMD scattering in standard software packages

Table 1. *Milestones of this SAT project.*

Progress and Accomplishments

For DMD arrays to be suitable for future NASA missions, a number of performance issues must be addressed. This project attempts to investigate these questions, and to improve DMDs to make them more suitable for such instrumentation requirements. The two commercially available DMDs we will be evaluating are the 0.7 XGA 1024×768 13.6-µm pixel pitch and the Cinema 2048×1080 13.6-µm pixel pitch DMD.

Radiation Testing: The heavy-ion radiation testing was performed at the Cyclotron Institute of the Texas A&M University. The facility is equipped with three beam types: 15, 25, and 40 MeV/amu. Over the two rounds of testing, we used the 25 MeV/amu beam with four different ions – neon, argon, krypton, and xenon. DMDs were re-windowed with 2-µm-thick pellicle and tested under accelerated heavy-ion radiation (control electronics shielded from radiation), focusing on detection of single-event effects

(SEEs) including latch-up events. Testing showed that while DMDs are sensitive to non-destructive ion-induced state changes, all SEEs were cleared with a soft reset (that is, sending a new pattern to the device). The DMDs did not experience single-event-induced permanent damage or functional changes that required a hard reset (power cycle), even at high ion fluence. The proton and heavy-ion testing suggests that the SEE-rate burden will be manageable for a DMD-based instrument when exposed to solar-particle fluxes and cosmic rays in orbit. Using the 95% confidence bounds obtained from the fitted model (Fig. 1) we calculate lower and upper values for the predicted worst-case in-orbit single-event upset (SEU) rate to be 3.42 and 11.7 micromirrors in 24 hours, for an XGA DMD with 1024×768 mirrors.

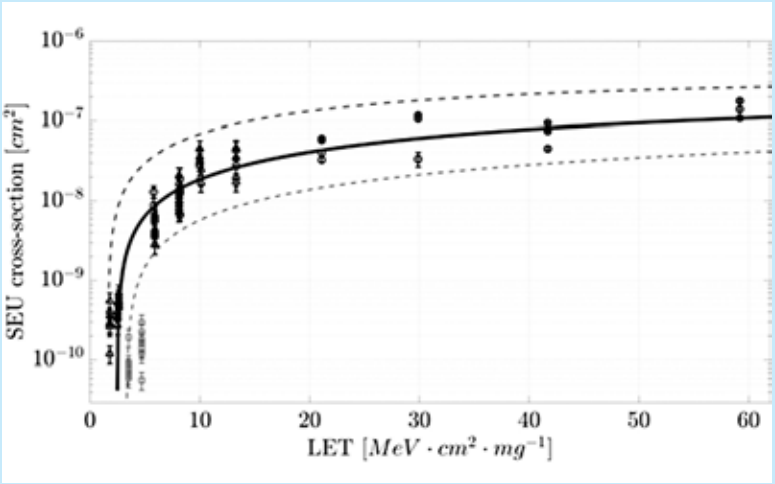

Fig. 1. *Measured SEU cross-section as a function of linear energy transfer (LET) of incident ions from both runs. The Weibull cumulative distribution fit and 95%-confidence-level bounds are represented by solid and dotted lines, respectively.*

Low-Temperature Testing: In the past year, we have collaborated with colleagues at the Instrument Development Group at JHU to build on our previous efforts to test DMD performance at cryogenic temperatures. At RIT, we used a modified Infrared Laboratories liquid nitrogen dewar to test the DMD at temperatures as low as 130 K [2]. This is the lowest temperature we could achieve, because the DMD control electronics had to be housed in the dewar. The commercial formatter board dissipated too much heat to allow us to reach 77 K.

At JHU, our collaborators used a much larger dewar with a cryo-cooler (Fig. 2), which allowed them to reach a temperature of 77K, even while using the same formatter board. We supplied several XGA DMDs with HEM Sapphire, fused silica, and original TI windows for a round of extensive testing. Among the tests we are performing are high-duty-cycle tests (where the DMD mirrors are flipped many times, rapidly at low temperature) and "operational conditions" tests (where the DMD mirrors are latched in the same state for about 20 minutes at a time, as would be done in a spectrograph). We are currently finishing up this round of testing and preparing to present our results at the SPIE Photonics West conference, and potentially in a refereed journal.

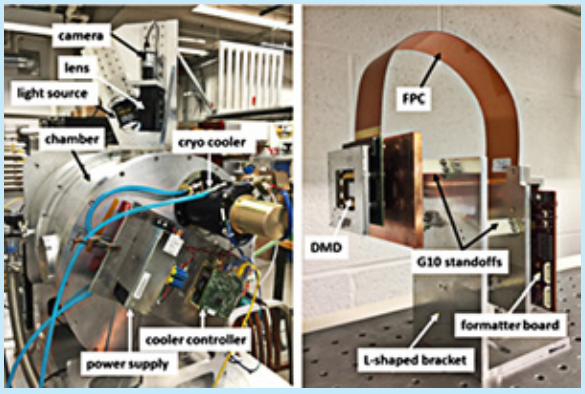

Fig. 2. Left: *Test chamber and optical setup used for cryogenic DMD operability testing.* Right: *DMD and formatter board mounted to the chamber interface bracket (FPC, Flexible Printed Circuit).*

Re-Coating DMDs with Al: Replacing the standard borosilicate window with a UV-transmissive material (MgF_2, HEM Sapphire, fused silica) extends the operational range of the DMD to approximately 200 nm. The UV reflectance of the DMD (ignoring losses due to fill factor and diffraction) is less than that of pure aluminum, because the DMD mirrors are made with an aluminum alloy. Below about 200 nm, the DMD reflectance drops rapidly (Fig. 3, Right). This decrease is seen for all aluminum (and aluminum-alloy) mirrors if they are not protected against the formation of an aluminum oxide layer. In the last year, we attempted to extend the use of the DMD to approximately 100 nm, by recoating the DMD with high-purity aluminum and protecting it with a thin film of LiF or AlF_3.

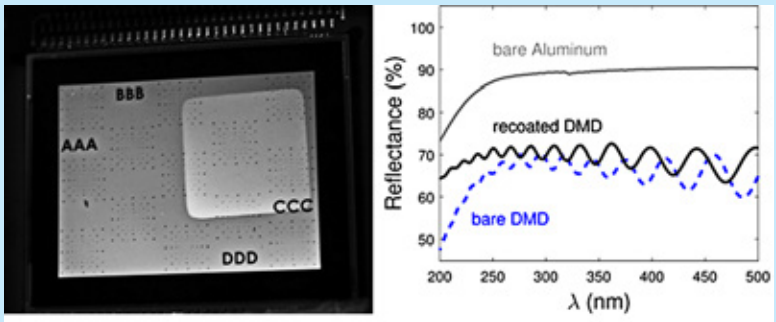

Fig. 3. Left: *We re-coated a section of a TI XGA DMD with high-purity aluminum at NASA GSFC (lighter-color square). The DMD remained operational after the coating process.* Right: *Reflectance of the re-coated region increased across the visible range, with significant improvements in the UV.*

The re-coated DMD remained operational (Fig. 3, Left), with no obvious differences between the coated and original regions, except improved reflectance. The re-coated region showed a reflectance improvement of several percent across the visible range, with more significant gains in the UV; at 200 nm, the reflectance increased from 48% to 65%. At this wavelength, the reflectance difference between the re-coated DMD and a standard aluminum mirror is due to the 92% fill-factor of the DMD. At longer wavelengths, diffraction creates additional losses, as well as the "ringing" structure seen in the blue curve. Neither the re-coated DMD nor the witness mirror sample was protected against oxidation in this experiment, so the reflectance drop-off near 200 nm persists. However, our initial tests show that DMDs can survive this type of re-coating, suggesting that DMDs can be made usable in the 100–400 nm range, if the coating is protected with a fluoride film. Lithium fluoride windows can be

used to protect the DMD using the re-windowing techniques we developed as part of this SAT program, to allow operation in the 108–3000 nm range. Furthermore, we are investigating the use of DMDs without protective windows, to extend the usable range to 91.2 nm (rest-frame Lyman limit), which is near the current state-of-the-art aluminum coatings [3, 4].

Path Forward

Several items remain to be done on this project, specifically:

1. Complete radiation testing of DMDs with gamma-ray irradiation at GSFC, and then use the numbers derived to determine in-orbit upset rates.
2. Complete scattering measurements on the re-windowed XGA devices. We want to extend the measurements to 200 nm in the UV. In addition, we want to complete optical DMD modeling and compare results to measurements, verifying our understanding.
3. Use scattering results to build a model for scattering that can be included in various popular optical modeling software packages, so that system designers can use our results easily to perform accurate signal-to-noise estimation.
4. Complete a new process for re-windowing the DMDs without epoxy, producing devices that are as hermetic as the original devices from TI.
5. Complete low-temperature testing of the DMD devices. In particular, holding patterns on the DMDs for longer times (i.e., simulating astronomical exposures).
6. Complete publication summarizing these results and disseminate scattering software module to interested parties. Assemble this information for a TRL review early next year. Complete Anton Travinsky's PhD thesis.

References

[1] J.E. Gunn et al., "*The 2.5-m Telescope of the Sloan Digital Sky Survey*," The Astronomical Journal, **131**, Issue 4, 2332-2359 (2006)

[2] K. Fourspring, Z. Ninkov, S. Heap, M. Robberto, and A. Kim, "*Testing of digital micromirror devices for space-based applications*," Proc. SPIE, **8618**, Emerging Digital Micromirror Device Based Systems and Applications V, id. 86180B (2013)

[3] M.A. Quijada, J. Del Hoyo, and S. Rice, "*Enhanced far-ultraviolet reflectance of MgF_2 and LiF over-coated Al mirrors*," Proc. SPIE **9144**, 91444G (2014)

[4] K. Balasubramanian, J. Hennessy, N. Raouf, S. Nikzad, M. Ayala, S. Shaklan, P. Scowen, J. Del Hoyo, and M. Quijada, "*Aluminum mirror coatings for UVOIR telescope optics including the far UV*," Proc. SPIE **9602**, 96020I (2015)

Publications

1. A. Travinsky, D. Vorobiev, Z. Ninkov, A.D. Raisanen, J. Pellish, M. Robberto, and S. Heap, "*Effects of heavy ion radiation on digital micromirror device performance*," Optical Engineering **55** (9), 094107 (2016)
2. A. Travinsky, D. Vorobiev, Z. Ninkov, A.D. Raisanen, M. Quijada, S. Smee, J. Pellish, T. Schwartz, M. Robberto, S. Heap, D. Conley, C. Benavides, N. Garcia, Z. Bredl, and S. Yllanes, "*Evaluation of Digital Micromirror Devices for use in space-based Multi-Object Spectrometer application*," J. Astron. Telesc. Syst. **3** (3), 035003, doi:10.1117/1.JATIS.3.3.035003 (2017)

For additional information, contact Zoran Ninkov: *ninkov@cis.rit.edu*

Ultra-Stable Structures: Development and Characterization Using Spatial Dynamic Metrology

Prepared by: Babak Saif (PI; NASA/GSFC) and Lee Feinberg (NASA/GSFC)

Summary

One possible successor to the James Webb Space Telescope (JWST) is an observatory that combines general ultraviolet-optical-infrared (UVOIR) astrophysics with the search for life on habitable Earth-like exoplanets using a large-aperture segmented telescope. Work on this problem began in 2009 as a potential Advanced Technology Large-Aperture Space Telescope (ATLAST) architecture. Early work focused on a scalable 9.2-m segmented telescope that could be launched on a Delta IV Heavy vehicle. More recently, this has progressed to a 12-m segmented telescope architecture. The most significant architectural driver beyond the aperture size is the 10^{-10} contrast required to block out the bright stars sufficiently to detect dim Earth-like planets orbiting within their habitable zones. Achieving this requires a combination of a high-throughput coronagraph with sufficient bandpass and wavelength range to perform spectroscopic surveys, and an ultra-stable telescope that maintains better-than-10-picometer stability for most observations. Achieving few-picometers stability, thermal and dynamics, requires both passive and active means in a system with multi-level hierarchies.

Background

Picometer Interferometry of Reflective Surfaces

An important first step in achieving this level of stability is achieving picometer-level metrology that can characterize the thermal and dynamic behavior of an optical system being designed and built, starting from the smallest components, through subsystems, up to the system as a whole. This requires a metrology system capable of measuring thermal and dynamical changes of both diffuse and reflective surfaces of system elements to picometer accuracy. One cannot assume that the system stability scales linearly with levels of stimulus over orders of magnitude. More precisely, the transfer function of a system is not constant over orders of magnitude in stimulus level.

At what level of accuracy is it possible to measure dynamics components? Our principal approach is to compare the amplitude of measured Zernike terms when the structure is stimulated mechanically to what was measured without stimulus. Different Zernike terms have different phases, and their contribution to surface variance vary over a cycle of stimulus. However, since these are orthogonal functions, the time-averaged total surface variance is the sum of individual-surface Zernike variances. The relative contributions of each term can be illustrated by showing how the residual root mean square (rms) varies with the Zernike term, by successively removing Zernike components from the net dynamic figure as a function of Zernike term, and computing the resulting rms.

Objectives and Milestones

Our objective is to develop picometer surface metrology of mirrors and structures. To this end, we work with a vendor to develop a dynamical digital speckle-pattern interferometer with picometer precision. In parallel, we develop an isolated tabletop setup to measure dynamics and drift of material and

small structures, including a stimuli system able to exert picometer-level excitations. We then develop structures and mirrors with dynamics controlled at picometer levels. Finally, we redesign and model the dynamics of the measured material/structures.

Initially, we use a spare JWST primary-mirror segment to characterize picometer dynamical response. Figure 1 shows residual rms vs. Zernike terms. The background plot shows that above Zernike 3, the remaining rms is under 30 picometers, dropping slowly to under 20 picometers above Zernike 30.

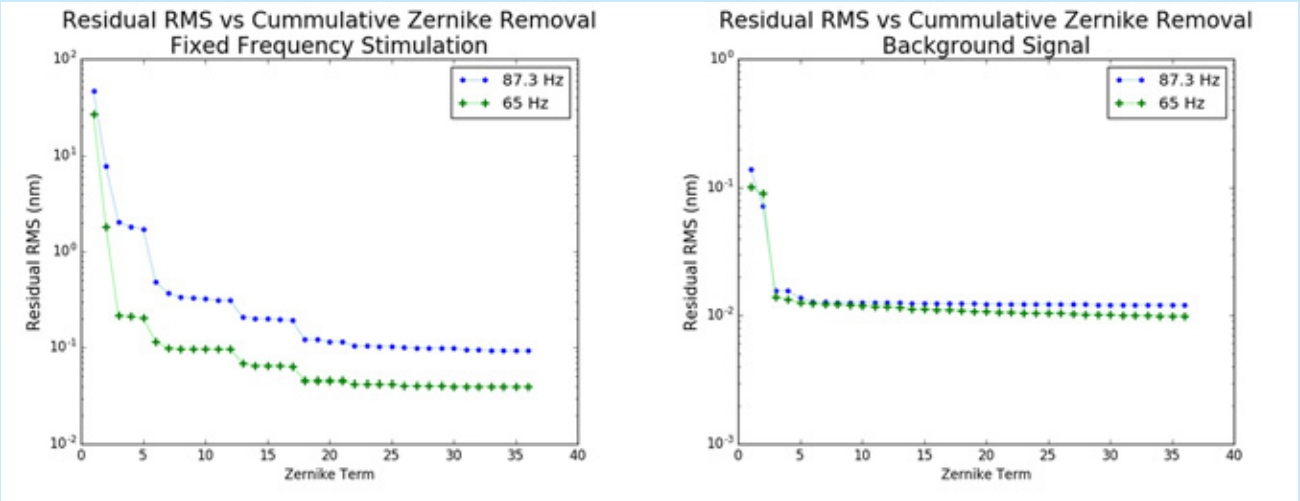

Fig. 1. Left: *The change in Zernikes in higher terms for 87.3- and 65-Hz stimulation is measured in tens of picometers.* Right: *No change is seen in background measurements for the same Zernikes.*

Progress and Accomplishments

This year's accomplishments are on two fronts. The first is picometer dynamics measurements of reflective surfaces. The second is fabricating a thermal-vacuum chamber capable of fraction-of-a-milliKelvin stability over many hours. These are two major components of our picometer-metrology test bed. We expect to receive a new interferometer next year that should enable speckle measurements at picometer levels. The interferometer is needed because not all subsystem components have specular characteristics. Interferometry of diffuse light to picometer levels is challenging, but required to enable design and fabrication of subsystems and systems with picometer stability. Characterizing the test bed with reflective and speckle capability enables dynamics and drift measurements facilitating the ultimate goal of demonstrating picometer stability of a minimal segmented-mirror system, comprised of two segments.

Temperature Stability to MilliKelvins

The Large UVOIR (LUVOIR) ultra-stable thermal-vacuum chamber system (Fig. 2) was fully assembled and integrated at the Smithsonian Astrophysical Observatory (SAO). The aluminum vacuum chamber is 30" in diameter and 30" in length. The assembly includes two bolt-on aluminum doors (35" outer diameter, OD) with Viton O-ring seals and handles to facilitate door mounting. One door includes a 10"-diameter fused-silica viewport, and the other door has provision for mounting a second 10" viewport. Three heater zones maintain high stability for the test article within the chamber. The heater pads are adhered to the external surfaces of the cylinder. Thermal and acoustical barrier foam panels surround the chamber to dampen local ambient acoustical noise and ambient temperature.

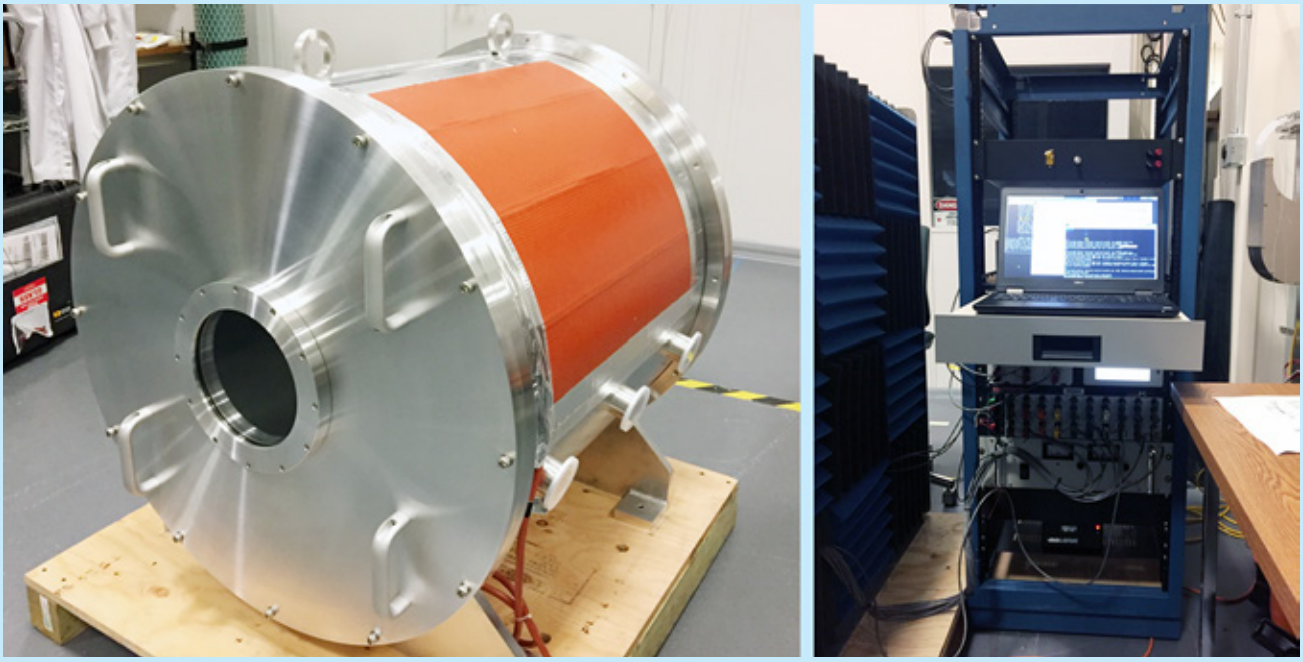

Fig. 2. Left: *Thermal-vacuum chamber.* Right: *Chamber electronics control rack.*

The high-precision thermal-control system functions as expected. The thermal control electronics rack (Fig. 2) includes a control laptop with SAO's nested-heater control-loop-logic software, a heater-power drive module, a high-precision thermometry system, and a power supply.

The functional test has been completed with a nominal set-point of 23.5°C during this functional test. An average test-article thermal stability of +0.4/-0.2 milliKelvin (23.5 +0.0004/-0.0002°C) was achieved for a period of over 80 hours (Fig. 3).

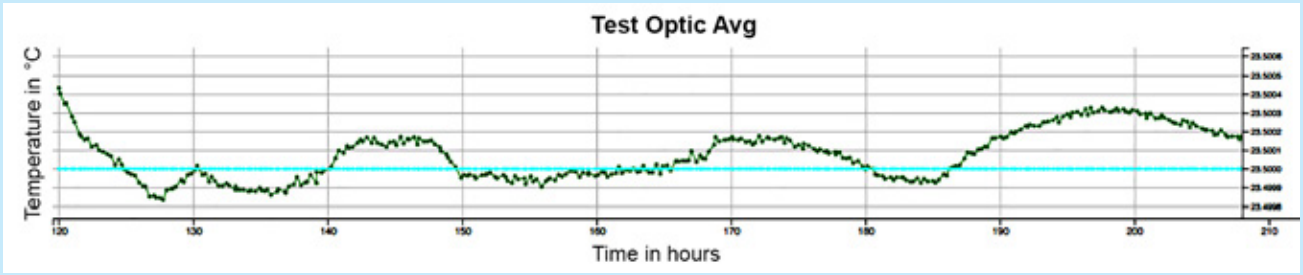

Fig. 3. *Test results: 23.5 +0.0004/-0.0002°C thermal stability achieved for over 80 hours.*

Path Forward

We expect the speckle interferometer to be delivered in October 2017, with interferometer characterization to be completed by January 2018. We will then use this setup to expand our measurements to include both reflective and diffuse components.

For additional information, contact Babak Saif: *babak.n.saif@nasa.gov*

Improving Ultraviolet Coatings and Filters Using Innovative Materials Deposited by ALD

Prepared by: Paul Scowen (PI; Arizona State University, ASU); Brianna Eller, Robert J. Nemanich, and Hongbin Yu (ASU); Tom Mooney (Materion); and Matt Beasley (Planetary Resources)

Summary

The goal of this work is to use plasma-enhanced atomic layer deposition (PEALD) to synthesize mirrors and filters compatible with near-ultraviolet (UV) and far-UV optics. The development of this technology will ultimately provide diagnostic tools to access a range of topics for study, including protostellar and protoplanetary systems, intergalactic-medium (IGM) gas from galactic star formation, and the most distant of objects in the early universe. Since the beginning of the project, our team, from the School of Earth and Science Exploration and the Physics Department at ASU, Materion, and Planetary Resources, has been working to initiate this research. Our most significant progress to date has been to design, develop, and build the equipment necessary to complete this research.

Background

Atomic layer deposition (ALD) is a layer-by-layer deposition technique that synthesizes ultra-thin, uniform, and conformal films as shown in Fig. 1. The high quality of these films has consequently resulted in augmented coatings and optical elements. At the same time, major advances have been made in optical designs and detector technologies. As a result, measurement of far-UV and near-UV bands has improved dramatically. The development of this technology ultimately allows access to emission and absorption lines in the UV, which are emitted from a range of targets, including protostellar and protoplanetary systems, IGM gas from galactic star formation, and the most distant of objects in the early universe. These diagnostic tools require the implementation of stable optical layers, including high-UV-reflectivity coatings and UV-transparent films [1].

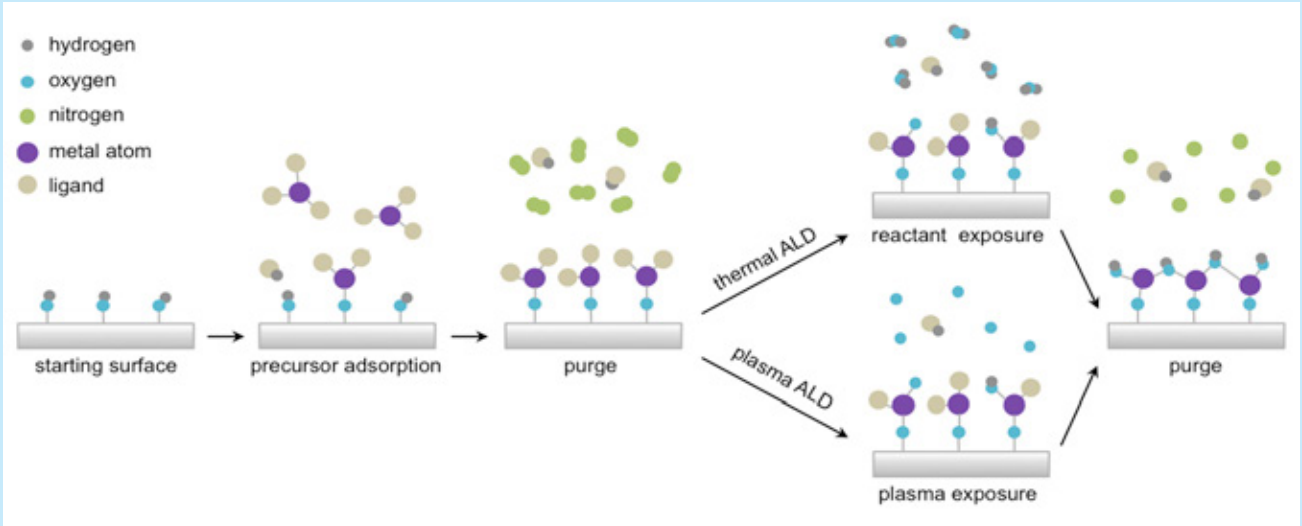

Fig. 1. *Schematic representation of the layer-by-layer deposition process of the thermal and PEALD. During the reactant or plasma exposure, the surface is exposed to a reactant gas or plasma.*

In this work, we will use a range of materials to implement stable protective overcoats with high UV reflectivity and unprecedented uniformity, and use that capability to leverage innovative UV/optical filter construction to enable the science mentioned above. The materials we will use include aluminum oxide and silicon oxide (as an intermediary step for development only) and a range of fluoride-based compounds (for production). These materials will be deposited in a multilayer format over a metal base to produce a stable construct. Specifically, we will use PEALD for deposition and construction of reflective layers that protect bare aluminum for mirror use in the UV. Our designs indicate that by using PEALD we can reduce adsorption and scattering in the optical films as a result of the lower concentration of impurities and increased control over the stoichiometry, yielding vastly superior quality and performance over comparable traditional thermal ALD techniques [2-17] currently being developed by other NASA-funded groups [18]. These capabilities will allow us to push the blue edge in usable UV reflectivity for magnesium-fluoride-protected aluminum below the current 115-nm limit.

This work will demonstrate for the first time whether loss-free oxides of materials such as Al, Hf, and Si can be deposited using ALD to lower cutoff reflectivities in the UV to as low as 92 nm. We will also demonstrate the use of PEALD to deposit low-loss thin films of fluoride-based materials, and aluminum metal. Using these techniques, we will then demonstrate our proof of concept of using these techniques together to construct thin-film, multilayer, metal-dielectric cavities with a reflective surface as the foundation, that can be tuned to isolate specific emission lines of astronomical importance. The resulting optical technologies will advance the coating stability, thickness, and performance of thin films in the far-UV sought by NASA, to match recent UV detector advances. Such improvement will enable next-generation space-based far-UV missions, opening access to the wealth of diagnostic information the far-UV offers for exoplanet, star formation, and cosmological/IGM science.

Objectives and Milestones

Our research seeks to demonstrate several objectives:

- Films of material can be deposited to demonstrate the approach using PEALD techniques to produce loss-free films of e.g. silicon and aluminum oxide; the resulting coatings will be of a thickness and a purity far higher than can be delivered by current techniques that involve sputtering deposition;
- Using the same deposition techniques, PEALD can deposit thin (tens of nm) low-loss films of fluorides of aluminum and magnesium as well as e.g. lithium, lanthanum-calcium, and beryllium, that can serve as protective overcoats for materials which would otherwise be easily oxidized by exposure to air;
- Aluminum deposition, protective-layer deposition, and characterization can be completed in-situ in a controlled environment that minimizes contamination, improving the reflectivity of the resulting films and their interfaces by reducing scattering and adsorption;
- Deposition of such protective overcoats over aluminum metal can be achieved with PEALD to provide a sufficiently crystalline, uniform, and stable structure, pushing blueward the currently observed 115-nm cutoff in efficient reflectivity from atomic sputtering deposition of magnesium fluoride, thereby extending the range of diagnostic emission and absorption lines available for science;
- Extend the metal-dielectric overcoat process to concave mirrors to demonstrate the performance of the reflective surfaces in an optical test bed environment;
- Use our PEALD approach to apply alternating layers of metals and dielectrics, producing multi-cavity structures exhibiting very high performance; this goal is currently limited by the inability to deposit very thin layers with great accuracy, while demonstrating film toughness and 'bulk' thin-film material losses;
- Apply the multilayer approach to the construction of multi-layer dielectric mirrors to act as reflection filters or high reflectors in narrow-band systems; and
- Similarly construct multi-layer broadband mirrors, thought to exhibit higher performance than metal-based mirrors (using a short-wave extension to prototype dichroics our group is already developing for space applications).

Table 1 summarizes the timeline to achieve these objectives, modified to accommodate equipment fabrication.

Activity Name	Duration (Days)	Start Date	Finish Date
Upgrade in-situ reflectivity to 120 nm			Completed
PEALD of oxides on evaporated aluminum			Completed
PEALD of Al_2O_3 and SiO_2 on aluminum			Completed
Upgrade PEALD for aluminum deposition	242	1/1/17	8/31/17
PEALD of aluminum	183	7/1/17	12/31/17
Install precursors for PEALD of fluorides	91	8/31/17	11/30/17
Oxides on PEALD aluminum	89	10/3/17	12/31/17
Upgrade in-situ reflectivity to 90 nm	151	8/2/17	12/31/17
PEALD of aluminum fluoride on aluminum	80	10/23/17	12/31/17
PEALD of magnesium fluoride on aluminum	80	10/23/17	12/31/17
PEALD of aluminum and magnesium fluoride	60	12/2/17	1/31/18
Magnesium fluoride/aluminum filters	260	2/1/18	9/28/18
Oxide-fluoride multilayers and protective layers	261	4/1/18	12/31/18
Multi-layer broadband mirrors	261	4/1/18	12/31/18

Table 1. *Timeline for objectives and milestones.*

Progress and Accomplishments

The initial state of this research has largely focused on developing the equipment necessary to synthesize and characterize the oxygen-free structures required to achieve the aforementioned objectives. Modifications to the system are well under way, where the chambers to be added to the ultra-high-vacuum system are summarized in Fig. 2. Specifically, two new systems are being added to the setup:

- A fluoride PEALD system for both the aluminum metal and metal fluorides needed for this work; and
- A visible and UV (VUV) optical system, which will be used to characterize the films deposited without atmospheric contamination.

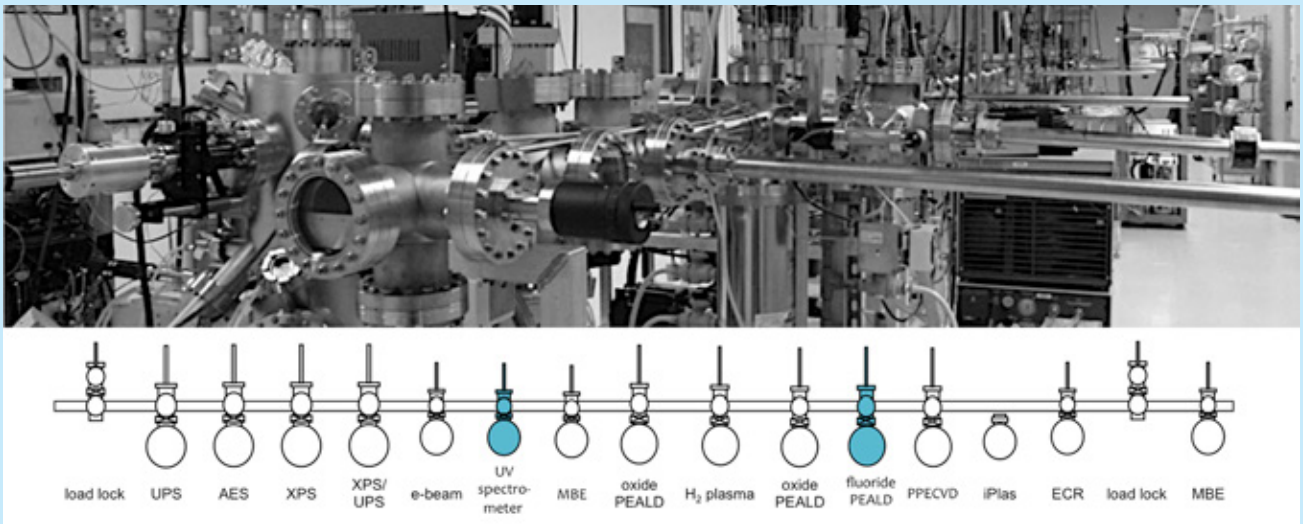

Fig. 2. *Photo (top) and schematic (bottom) of ASU in-situ ultra-high-vacuum system; blue shows new systems in progress (UPS, UV Photoelectron Spectroscopy; AES, Auger electron Spectroscopy; XPS, X-ray Photoelectron Spectroscopy; MBE, Molecular Beam Epitaxy; iPlas, Innovative Plasma Chemical Vapor Deposition; ECR, Electron Cyclotron Resonance).*

A key component of this work is related to the in-situ nature of the deposition and characterization soon to be enabled. Since oxidation of aluminum has presented a significant challenge in previous research [18], this work will allow for the deposition of aluminum and metal fluorides without exposure to atmosphere.

1. Plasma-Enhanced Atomic Layer Deposition

The new PEALD system is in the initial stages of assembly based on the previous oxide system available in the lab, with only a few alterations. Specifically, the plasma was designed with a remote configuration, helping reduce ion bombardment of the sample, mitigating potential ion damage. Plasma will be ignited with 13.56-MHz RF-excitation applied at ~200 W to a helical copper coil wrapped around a 32-mm-diameter quartz tube, and maintained at a pressure of ~100 mTorr with a flow rate of ~35 sccm (standard cubic centimeters per minute). This system must achieve a background pressure of $<5\times10^{-8}$ Torr and processing pressures of ~10 mTorr. The pumping requirements, therefore, vary during transfer and deposition. To assist with transfer, the system is equipped with a Pfeiffer turbo with pumping speed of 300 liters/sec and a dry backing pump, enabling lower pressures; however, the chemicals used during deposition are often too harsh, reducing the lifetime of the turbo pumps. Therefore, when operating, the turbo is isolated with a gate valve, and a two-state dry pump with a pumping speed of ~7000 liters/sec is used. The pumping stage is vented with nitrogen gas during operation to further ensure system longevity. In addition, the gas-flow mechanisms are designed to deliver the precursors to the chamber with the correct timing sequence using mass-flow controllers (MFCs), nitrogen valves, and a custom LabView program. Metering valves were also added to the gas lines to further control the amount of precursor released into the chamber. Lastly, a butterfly valve before the two-stage dry pump is used to maintain the required pressures during processing. The system is in mid-assembly as shown in Fig. 3.

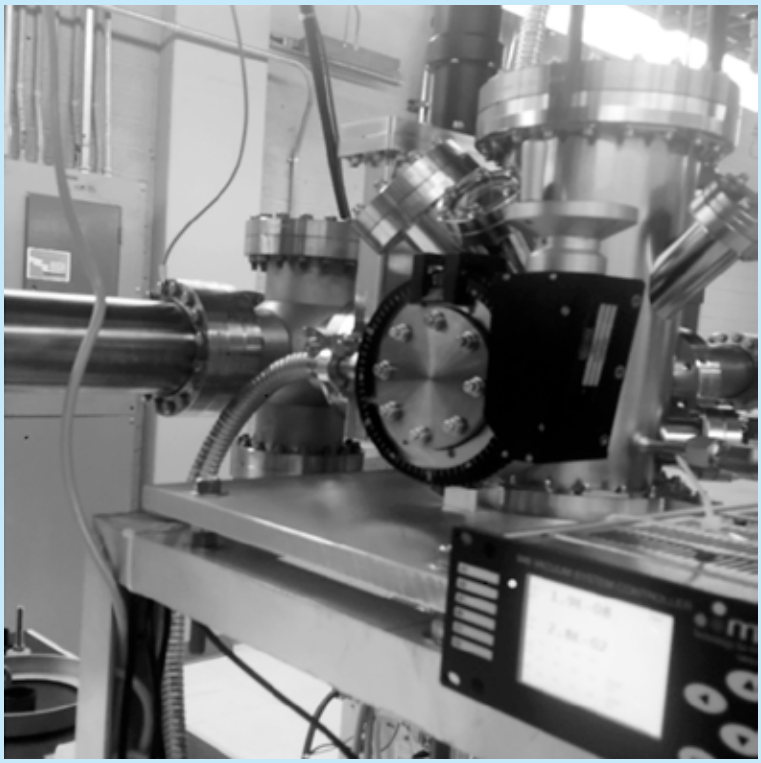

Fig. 3. *Image of a new metal and fluoride PEALD system in progress. Vacuum has been achieved and is maintained at ~10^{-8} Torr.*

To facilitate assembly, the fabrication has been completed in stages where the first stages are as follows:

- ☑ ***Stage 1. Vacuum and transfer mechanisms***. This includes system and chamber design, as well as installation of the equipment needed to achieve and maintain vacuum and transfer the samples from the in-situ vacuum system. Some additional electrical work to support this new equipment is scheduled.
- ☐ ***Stage 2. Plasma generation and gas delivery***. The plasma generating system will be added to the PEALD system. This work is in progress now, where the rack to support the equipment is being fabricated. In addition, the gas delivery system for nitrogen and hydrogen will need to be plumbed.
- ☐ ***Stage 3. Aluminum PEALD process and gas delivery***. Fortunately, some work was done on PEALD of aluminum, using trimethylaluminum and hydrogen plasma [19]; therefore, this process will be used. Additional modifications to the system will include installation of gas lines, MFCs, bubblers, and a customized Labview program for system operation.
- ☐ ***Stage 4. Modification for fluorides***. Unfortunately, the corrosiveness and toxicity of hydrogen fluoride (HF) raise safety concerns that must be carefully considered for this process. To address these concerns, the following precautions will be implemented:
  - Storing the HF in a bubbler as an HF-pyridine mixture, which is less volatile than HF;
  - Electroplating the bubbler with gold, to prevent corrosion;
  - Replacing the quartz tube with sapphire, to prevent etching;
  - Introducing a dry-air abatement system following the two-stage dry pump, to remove waste by-products; and
  - Coating the chamber with a thick aluminum layer prior to using HF to prevent etching the chamber.
- ☐ ***Stage 5. Fluoride precursors***. Fluoride processes have not been developed extensively. In fact, to date, there are no published processes for fluoride PEALD. However, there has been some work on thermal ALD processes, which use HF [20, 21], TiF_4 [22-25], and TaF_4 [26] as the fluorine source. While TiF_4 and TaF_4 come with significantly less severe safety hazards, the films deposited with these materials are typically characterized by some metal contamination, which will likely cause absorption in the desired wavelengths. A fluoride-based plasma was also considered for this work but dismissed due to concerns that it might lead to etching rather than deposition. Therefore, an HF-pyridine mixture seems to be the best option at this point. To take advantage of the desirable properties of PEALD, the HF step will be coupled with a hydrogen-plasma step to ensure film purity. For aluminum and magnesium fluoride, trimethylaluminum and bis(ethylcyclopentadienyl) magnesium have been chosen as the respective metal precursors.

2. Visible and Ultraviolet Optical System

We have also established in-situ reflectivity to 120 nm in order to characterize PEALD oxides and aluminum. In addition, the VUV optical system will need to be upgraded for lower wavelengths (> 90 nm) in the future. This system (Fig. 4) has also been designed, fabricated, and tested.

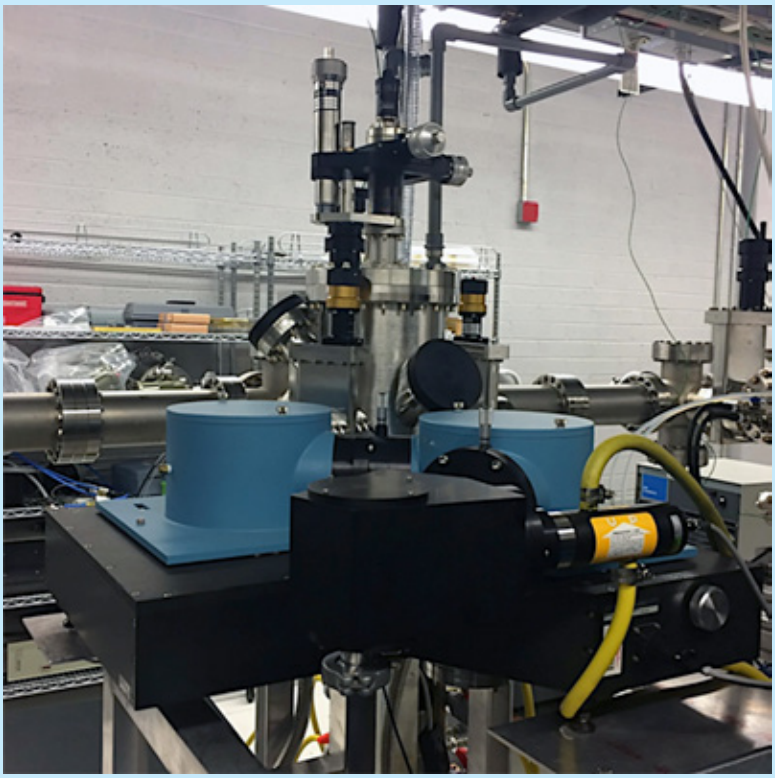

Fig. 4. *Images of the custom-designed UV spectrometer unit, which can currently deliver reflectivity measurements down to 115 nm.*

2.1 Thermally evaporated aluminum coated in PEALD oxides

Some testing of PEALD Al_2O_3 has been explored as well, as a means to test and establish protocols for the system. This testing will continue while the aluminum and fluoride PEALD system is in progress. Some initial results show, as expected, that the thickness of the Al_2O_3 layers influences the reflectivity at lower wavelengths as shown in Fig. 5.

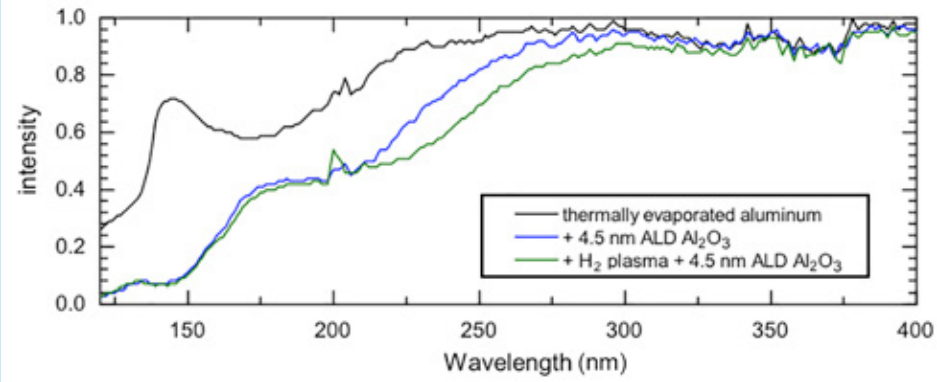

Fig. 5. *UV reflectance of PEALD Al_2O_3 on thermally evaporated Al. Some additional work is needed to ensure consistency.*

2.2 UV reflectance of additional mirrors

Additional mirrors have been purchased – including gold, silver, aluminum, UV aluminum, and MgF_2-coated aluminum – to test, develop, and implement rigorous protocols to ensure reliable and consistent measurements in this system. In particular, small variations in position and vacuum level influence the measured intensity. Therefore, some additional work is needed to ensure the system provides reliable measurements. Using samples with known reflectance is helping isolate these issues.

Path Forward

The plan of work is structured around the goals and milestones stated above. In general, the plan is to focus on timely assembly of the PEALD system, and to continue to use the UV spectrometer. This will enable use and fabrication of bandpass filters. More specifically, the following will be necessary:

1. Demonstrate the use of PEALD to deposit loss-free oxides of silicon and aluminum on evaporated and e-beam-deposited aluminum surfaces. These oxides were selected based on their promise for stable, high-performance oxides. This is motivated because current methods produce lossy films, which are not usable below 190 nm.
2. Establish the capability for PEALD aluminum films and characterize the UV reflectivity of the films and the surface contamination using in-situ characterization tools. These aluminum surfaces will be the basis of the structures pursued in this program.
3. Demonstrate the feasibility of using PEALD to deposit low-loss films of fluoride compounds on ALD aluminum. The fluorides of interest include most significantly aluminum and magnesium fluoride, but others will be considered as well. We will need to demonstrate stability, uniformity, and performance before advancing.
4. Extend the reflectivity characterization to 90 nm and characterize the fluoride-aluminum structures. This is a critical step, as the aluminum-oxide/fluoride layer will serve as the foundation not only for simple reflective surfaces. For filters, we intend to show proof of concept in the next segment. The quality of aluminum and interface will define the required performance, which will be verified before advancing to the next stages.

This first phase of work will be conducted by Dr. Nemanich and his team, focusing on developing processes that result in optimized films. This first round of work and demonstrations are expected to be completed within the first 18 months of the project, i.e. by December 2017.

Before moving on to the next sequence, Dr. Scowen, Dr. Mooney, and Dr. Beasley will revisit the demonstrated performance of the three classes of product (above) and compare them to the models that initiated the work. Stability will be measured using vacuum exposure and spectral retest, and similarly humidity exposure followed by spectral retest. If there are differences in stability and reflectivity, we need to understand their origins before we can build prototype filters, since these parameters are critical for tuning an individual filter for a particular bandpass. Once this has been done, we will implement the techniques used above for the deposition of multilayer construction.

The next phase will then address the following goals:

5. Optimize far-UV reflectivity of fluorides on aluminum, to deliver a wide bandpass, far-UV-optimized mirror. The optimization will focus on minimizing interface contamination and optimizing material-growth parameters and film thickness for far-UV reflectivity. We will demonstrate performance as far as possible into the far-UV with our new VUV system.

6. Construct metal-dielectric Fabry-Perot bandpass filters using aluminum and magnesium fluoride, leading to multi-cavity structures that will exhibit very high performance–based on our models. This design approach is currently limited by the ability to deposit very thin layers with great accuracy, film toughness, and 'bulk' thin-film material losses. We believe only two to five layers will be needed to demonstrate proof of concept, with each layer ~10-nm thick.
7. Fine-tune approach and models to produce designs for multi-layer dielectric (narrowband) mirrors to act as reflection filters or high reflectors in narrowband systems. We will demonstrate construction and performance.
8. Demonstrate the construction of multi-layer broadband mirrors, which we believe–based on models–will exhibit higher performance than metal-based mirrors.
9. We expect this second round of work to occupy most of 2017 and 2018. To achieve all this work, we will demonstrate our approach, designs, and methodologies to deliver the necessary improvements in thickness control, lower 'bulk' losses, absence of color centers, smoother films (lower scatter), ability to deposit very thin films (with bulk-like optical properties), durability, and lower stress. The above plan, executed in this manner, will demonstrate all these goals.

References

[1] J.M. Shull and C.W. Danforth, "*Identifying the Baryons in a Multiphase Intergalactic Medium*," *arXiv1208.3249S* (2012)

[2] O.K. Kwon, S.H. Kwon, H.S. Park, and S.W. Kang, "*PEALD of a ruthenium adhesion layer for copper interconnects*," J. Electrochem. Soc. **151**, C753 (2004)

[3] O.K. Kwon, S.H. Kwon, H.S. Park, and S.W. Kang, "*Plasma-enhanced atomic layer deposition of ruthenium thin films*," Electrochem. Solid-State Lett. **7**, C46 (2004)

[4] J.W. Lim, S.J. Yun, and J.H. Lee, "*Low temperature growth of SiO_2 films by plasma-enhanced atomic layer deposition*," ETRI J. **27**, 118 (2005)

[5] W.J. Maeng, S.J. Park, and H. Kim, "*Atomic layer deposition of Ta-based thin films: Reactions of alkylamide precursor with various reactants*," J. Vac. Sci. Technol. B **24**, 2276 (2006)

[6] M.K. Song and S.W. Rhee, "*Phase formation in the tantalum carbo-nitride film deposited with atomic layer deposition using ammonia*," J. Electrochem. Soc. **155**, H823 (2008)

[7] J.S. Park, M.J. Lee, C.S. Lee, and S.W. Kang, "*Plasma-enhanced atomic layer deposition of tantalum nitrides using hydrogen radicals as a reducing agent*," Electrochem. Solid-State Lett. **4**, C17 (2001)

[8] J.S. Park, H.S. Park, and S.W. Kang, "*Plasma-enhanced atomic layer deposition of Ta-N thin films*," J. Electrochem. Soc. **149**, C28 (2002)

[9] J.Y. Kim, K.W. Lee, H.O. Park, Y.D. Kim, H. Jeon, and Y. Kim, "*Barrier Characteristics of TaN Films Deposited by Using the Remote Plasma Enhanced Atomic Layer Deposition Method*," J. Korean Phys. Soc. **45**, 1069 (2004)

[10] J.Y. Kim, Y. Kim, and H. Jeon, "*Characteristics of TiN Films Deposited by Remote Plasma-Enhanced Atomic Layer Deposition Method*," Jpn. J. Appl. Phys., **42** Part 2, No. 4B, L414 (2003)

[11] Y. Kim, J. Koo, J. W. Han, S. Choi, H. Jeon, and C.G. Park, "*Characteristics of ZrO_2 gate dielectric deposited using Zr t–butoxide and $Zr(NEt_2)_4$ precursors by plasma enhanced atomic layer deposition method*," J. Appl. Phys. **92**, 5443 (2002)

[12] J. Koo, Y. Kim, and H. Jeon, "*ZrO_2 Gate Dielectric Deposited by Plasma-Enhanced Atomic Layer Deposition Method*," Jpn. J. Appl. Phys., **41** Part 1, No. 5A, 3043 (2002)

[13] B. Hoex, J. Schmidt, P. Pohl, M.C.M. van de Sanden, and W.M.M. Kessels, "*Silicon surface passivation by atomic layer deposited Al_2O_3,*" J. Appl. Phys. **104**, 044903 (2008)

[14] J. Koo, S. Kim, S. Jeon, H. Jeon, Y. Kim, and Y. Won, "*Characteristics of Al_2O_3 Thin Films Deposited Using Dimethylaluminum Isopropoxide and Trimethylaluminum Precursors by the Plasma-Enhanced Atomic-Layer Deposition Method*," J. Korean Phys. Soc. **48**, 131 (2006)

[15] P.K. Park and S.W. Kang, "*Enhancement of dielectric constant in HfO_2 thin films by the addition of Al_2O_3*," Appl. Phys. Lett. **89**, 192905 (2006)

[16] P.K. Park, E.S. Cha, and S.W. Kang, "*Interface effect on dielectric constant of HfO_2 /Al_2O_3 nanolaminate films deposited by plasma-enhanced atomic layer deposition*," Appl. Phys. Lett. **90**, 232906 (2007)

[17] P.K. Park, J.S. Roh, B.H. Choi, and S.W. Kang, "*Interfacial Layer Properties of HfO_2 Films Formed by Plasma-Enhanced Atomic Layer Deposition on Silicon*," Electrochem. Solid-State Lett. **9**, F34 (2006)

[18] J. Hennessy, A.D. Jewell, F. Greer, M.C. Lee, and S. Nikzad, "*Atomic layer deposition of magnesium fluoride via bis(ethylcyclopentadienyl)magnesium and anhydrous hydrogen fluoride*," J. Vac. Sci. Technol. A **33**, 01A125 (2015)

[19] J.-H. Park, D.-S. Han, Y.-J. Kang, S.-R. Shin, and J.-W. Park, "*Self-forming Al oxide barrier for nanoscale Cu interconnects created by hybrid atomic layer deposition of Cu-Al alloy*," J. Vac. Sci. Technol. A **32**, 01A131 (2014)

[20] Y. Lee and S.M. George, "*Atomic Layer Deposition of Metal Fluorides using Various Precursors and Hydrogen Fluorides*," ALD conference (2015)

[21] J. Hennessey, B.K. Balasubramanian, A. Jewell, S. Nikzad, C.S. Morre, and K. France, "*Thin ALD fluoride films to protect and enhance Al mirrors in Far UV*," ALD conference (2015)

[22] T. Pilvi, T. Hatanpää, E. Puukilainen, K. Arstila, M. Bischoff, U. Kaiser, N. Kaiser, M. Leskelä, and M. Ritala, "*Study of novel ALD process for depositing MgF_2 thin films*," J. Mater. Chem. **17**, 5077 (2007)

[23] M. Mäntymäki, J. Hämäläinen, E. Puukilainen, F. Munnik, M. Ritala, and M. Leskelä, "*Atomic Layer Deposition of LiF Thin Films from Lithd and TiF_4 Precursors*," Chem. Vap. Dep. **19**, 111 (2013)

[24] M. Mäntymäki, M. J. Heikkilä, E. Puukilainen, K. Mizohata, B. Marchand, J. Räisänen, M. Ritala, and M. Leskelä, "*Atomic Layer Deposition of AlF_3 Thin Films Using Halide Precursors*," Chem. Mater. **27**, 604 (2015)

[25] T. Pilvi, K. Arstila, M. Leskelä, and M. Ritala, "*Novel ALD process for depositing CaF_2 thin films*," Chem. Mater. **19**, 3387 (2007)

[26] T. Pilvi, E. Puukilainen, U. Kreissig, M. Leskelä, and M. Ritala, "*Atomic Layer Deposition of MgF_2 Thin Films Using TaF_5 as a Novel Fluorine Source*," Chem. Mater. **20**, 5023 (2008)

For additional information, contact Paul Scowen: *paul.scowen@asu.edu*

Advanced UVOIR Mirror Technology Development for Very Large Space Telescopes

Prepared by: H. Philip Stahl, PhD (NASA/MSFC)

Summary

The Advanced Mirror Technology Development (AMTD) project is in Phase 2 of a multi-year effort initiated in Fiscal Year (FY) 2012, to mature toward the next Technology Readiness Level (TRL) critical technologies required to enable 4-m-or-larger monolithic or segmented ultraviolet, optical, and infrared (UVOIR) space telescope primary-mirror assemblies for general astrophysics and ultra-high-contrast observations of exoplanets.

In 2012, AMTD-2 defined three major milestones. During 2016/17, AMTD-2 successfully accomplished half of the work on these (fully completing the first):

- ✓ Harris Corp fabricated a ~150-Hz 1.5-m Ultra-Low Expansion (ULE®) mirror (1/3 scale of a 4-m mirror) substrate using the stacked-core method, demonstrating lateral scalability of the stacked-core technology.
- ○ MSFC characterized the mechanical and thermal performance of the Schott-owned 1.2-m Zerodur® mirror (polished and integrated into an assembly by Arizona Optical Systems).
- ○ MSFC validated by test its integrated Structural-Thermal-Optical-Performance (STOP) model prediction of the 1.2-m Zerodur® mirror's mechanical and thermal performance; including verification of coefficient-of-thermal-expansion (CTE) homogeneity.

The balance is scheduled for completion in the fourth quarter of FY 2017:

- ○ Characterizing the mechanical and thermal performance of the Harris 1.5-m ULE® mirror.
- ○ Validating by test MSFC's integrated STOP model prediction of the 1.5-m ULE® mirror's mechanical and thermal performance; this testing also includes verification of CTE homogeneity.

Additionally, lessons learned about low-temperature-slumping (LTS) of large stiff mirror substrates from fabricating the 1.5-m ULE® mirror are being incorporated into various current and planned NASA and National Interest missions. An AMTD-3 proposal to resolve the issues was submitted to the Research Opportunities in Space and Earth Sciences (ROSES) 2016 Strategic Astrophysics Technology (SAT) Program. Finally, MSFC is using integrated design tools developed on AMTD-2 to design candidate optical telescope assemblies for the potential Habitable Exoplanet Imager Mission (HabEx).

The foundation of AMTD's success continues to be its integrated team of government/industry scientists, systems engineers, and technologists executing a science-driven systems-engineering approach to technology development. Additionally, AMTD continues mentoring the next generation of scientists and engineers as interns, co-ops, and volunteers. In this cycle AMTD hosted two undergraduate student interns: Samantha Hansen of Rutgers University and Mary Elizabeth Cobb of the University of Alabama in Huntsville.

AMTD results were presented at Mirror Tech Days 2016 and published in proceedings of the 2016 SPIE Astronomy Conference [1] and the 2017 SPIE Optics and Photonics Conference [2, 3].

Background

"*Are we alone in the universe?*" is probably the most compelling science question of our generation.

Per the 2010 *New Worlds, New Horizons* (NWNH) Decadal Report [4]: "*One of the fastest growing and most exciting fields in astrophysics is the study of planets beyond our solar system. The ultimate goal is to image rocky planets that lie in the habitable zone of nearby stars*." NWNH recommended, as its highest priority, medium-scale activity such as a "New Worlds Technology Development (NWTD) Program" to "*lay the technical and scientific foundations for a future space imaging and spectroscopy mission*." The National Research Council (NRC) report, "*NASA Space Technology Roadmaps and Priorities*" [5], states that the second-highest technical challenge for NASA regarding expanding our understanding of Earth and the universe in which we live is to "*develop a new generation of astronomical telescopes that enable discovery of habitable planets, facilitate advances in solar physics, and enable the study of faint structures around bright objects by developing high-contrast imaging and spectroscopic technologies to provide unprecedented sensitivity, field of view, and spectroscopy of faint objects*." NASA's "*Enduring Quests, Daring Visions*" [6] called for a Large Ultraviolet/Optical/Infrared (LUVOIR) Surveyor mission to "*enable ultra-high-contrast spectroscopic studies to directly measure oxygen, water vapor, and other molecules in the atmospheres of exoEarths*," and "*decode the galaxy assembly histories through detailed archeology of their present structure*." As a result, NASA will study in detail the LUVOIR Surveyor and HabEx concepts for the 2020 Decadal Survey [7, 8]. Additionally, the Association of Universities for Research in Astronomy (AURA) report "*From Cosmic Birth to Living Earths*" [9] details the potential revolutionary science that could be accomplished from "*directly finding habitable planets showing signs of life*."

Directly imaging and characterizing habitable planets requires a large-aperture telescope with extreme wavefront stability. For an internal coronagraph, this requires correcting wavefront errors (WFEs) and keeping that correction stable to a few picometers root mean square (rms) for the duration of the science observation. This places severe specification constraints on the performance of the observatory, telescope, and primary mirror. One important problem is dynamic WFE. For either large monolithic mirrors (for HabEx) or smaller mirror segments (for LUVOIR), mechanical disturbances create rigid-body motion of the mirror on its mount. These inertial motions introduce dynamic WFE when the mirror distorts (or bends) as it reacts against its mount. Achieving wavefront stability is a systems-engineering trade between mirror stiffness and vibration isolation. Per Lake [10], WFE is proportional to the rms magnitude of the applied inertial acceleration divided by the square of the structure's first mode frequency. Therefore, to achieve <10 pm rms requires either a very stiff system or very low acceleration loads. It is easier to improve performance by increasing stiffness rather than increasing isolation. For a given stiffness mirror, a 10× reduction in acceleration results in a 10× WFE reduction. For a given acceleration level, a 10× increase in stiffness results in a 100× WFE reduction. While systems-engineering analysis is still preliminary, the HabEx program estimates that it needs a 4-m monolithic primary mirror with a first mode frequency greater than 100 Hz and maybe as high as 200 Hz. The LUVOIR program estimates that it needs 1.5-m segments with a first mode frequency greater than 220 Hz (James Webb Space Telescope, JWST) and maybe as high as 500 Hz.

Before AMTD, the state of the art (SOTA) for lightweight stiff glass mirror substrates was defined by the Advanced Mirror System Demonstrator (AMSD) and Advanced Technology Telescope (ATT). For their sizes (AMSD, 1.5 m×50 mm; ATT, 2.5 m×150 mm) both mirrors have >150 Hz first mode required for stable on-orbit mechanical performance. But neither has sufficient structural depth for >100 Hz at 4 m. The easiest way to increase stiffness is to increase thickness. AMTD-1 advanced TRL by successfully

demonstrating a new process (stacked-core low-temperature fusion) that extended the previous SOTA for deep-core substrates from <300 mm to >400 mm. This was done by making a 43-cm-diameter full-scale 'cut-out' of a 4-m mirror. AMTD-2 continued this advance by making a 450 Hz, 1.5-m×165-mm mirror.

Objectives and Milestones

AMTD's objective is to mature toward TRL 6 technologies to enable large monolithic or segmented UVOIR space telescopes. Phase 1 advanced technology readiness of six key technologies required to make an integrated primary mirror assembly (PMA) for a large-aperture UVOIR space telescope.

- Large-Aperture, Low-Areal Density, High-Stiffness Mirror Substrates;
- Support System;
- Mid/High-Spatial Frequency Figure Error;
- Segment Edges;
- Segment-to-Segment Gap Phasing; and
- Integrated Model Validation

Phase 2 is continuing the efforts in high-stiffness substrates, support systems, segment-to-segment gap phasing, and integrated model validation with three clearly defined milestones:

- Fabricate a 1/3-scale model of 4-m class 400-mm thick deep-core ULE® mirror substrate to demonstrate lateral scaling of the deep-core process (successfully completed in 2016);
- Characterize two candidate primary mirrors (the 1/3-scale mirror and a 1.2-m extreme-lightweight Zerodur® Mirror, ELZM, owned by Schott) by measuring their modal and optical performance from 250 K to ambient (Schott 1.2-m Zerodur® mirror successfully characterized in 2016; 1.5-m ULE® Harris mirror is schedule for characterization in 2017); and
- Add capabilities and validate integrated design and modeling tools to predict the mechanical and thermal behavior of the candidate mirrors, validate models, generate Pre-Phase-A point designs, and predict on-orbit optical performance (Schott 1.2-m Zerodur® mirror mechanical and thermal performance models were successfully validated by test in 2016; 1.5-m ULE® Harris mirror models are scheduled for validation by test in 2017; additionally, MSFC is using integrated design and modeling tools on the potential HabEx mission concept).

Progress and Accomplishments

Large-Aperture, Low-Areal-Density, High-Stiffness Mirror Substrates

Need: To achieve ultra-stable mechanical and thermal performance required for high-contrast imaging, either (4-m to 8-m) monolithic or (8-m to 16-m) segmented mirrors require thicker, stiffer mirrors.

Milestone 1: Fabricate a 1/3-scale model of 4-m-class 400-mm thick deep-core ULE® mirror substrate to demonstrate lateral scaling of the deep-core process.

Accomplishment: During FY 2016/17, AMTD-2 advanced this technical area by fabricating a 450-Hz 1.5-m substrate to accomplish its defined milestone and learning lessons from turning that substrate into a mirror.

High-Stiffness Mirror Substrates: Previously, AMTD-1 advanced TRL by successfully demonstrating the ability to make a 40-cm-thick subscale mirror substrate via the stacked-core low-temperature fusion (LTF) process. This extended the previous SOTA for deep-core substrates from <300 mm to >400 mm. This was done by making a 43-cm-diameter, 40-cm-thick, full-scale 'cut-out' of a 4-m mirror. In 2016, AMTD-2 achieved its major milestone for this technology when Harris Corp successfully fabricated through LTF a 1.5-m-diameter×165-mm-thick 5-layer ULE® mirror substrate with a 450-Hz first-mode frequency. In 2016/17, Harris Corp used LTS to fabricate the mirror substrate to a 3.5-m radius of

curvature (ROC) then ground, polished, coated it with protective aluminum, and integrated it into a flight-like mount (Fig. 1). In 2017, the mechanical and thermal performance of this mirror assembly will be characterized at MSFC.

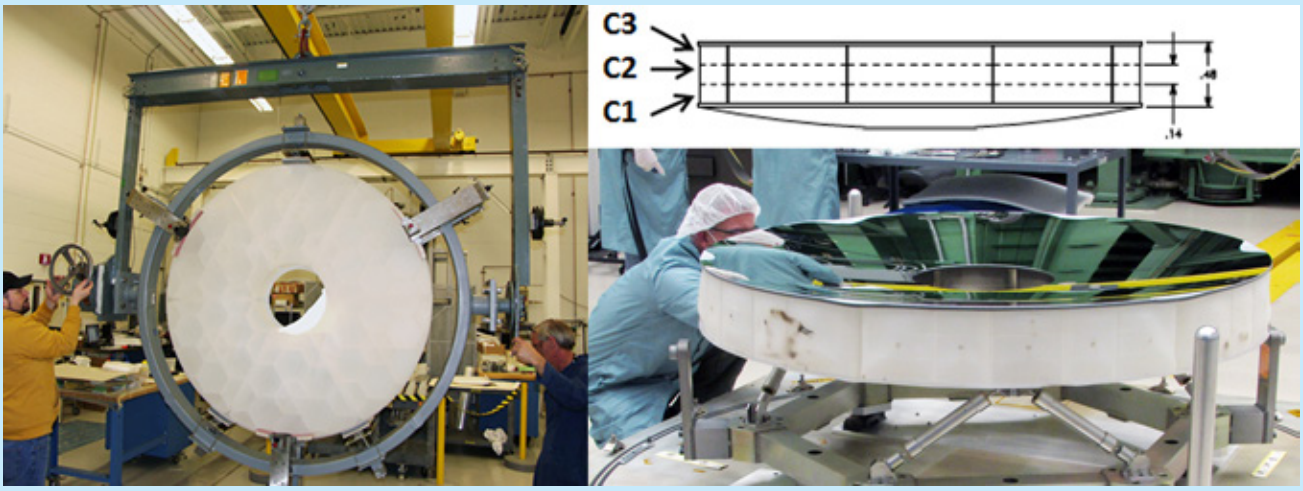

Fig. 1*:* Left: *LTF mirror substrate.* Top Right: *5-layer design.* Bottom Right: *Completed mirror assembly.*

During AMTD-1, when the 43-cm deep-core mirror was slumped from 5.0-to-2.5-m ROC, there was noticeable deformation in the core walls. To quantify the magnitude of this bending, MSFC imaged the mirror's internal structure via X-ray tomography. A small amount of bending was expected because slumping places the concave surface in compression and stretches the convex surface; this places the core elements in shear stress. The measured deformation exceeded that expectation. Fortunately, analysis indicated that such core-wall bending had a limited effect on the mirror's strength.

In designing the 1.5-m 1/3-scale model of a 4-m mirror, Harris Corp used proprietary modeling tools to predict the visco-elastic performance of the mirror (Fig. 2). The spacing between the wedge-shaped core elements was specifically increased to prevent adjacent core walls from touching. While the core walls never touched, they did get within 0.25 mm at four locations (Fig. 2). In 2017, MSFC plans to image the internal structure of the mirror via X-ray computed tomography, use that data to create an as-built 3D model of the mirror to predict its mechanical and thermal performance, and characterize that performance.

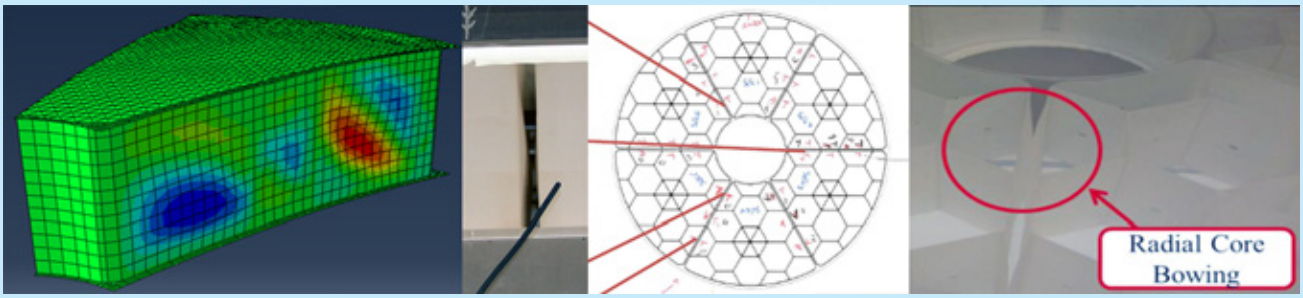

Fig. 2. Left: *predicted visco-elastic deformation used to design mirror substrate.* Center Left to Right *(3 images): actual visco-elastic deformation; four locations had gaps of less than 0.25 mm.*

Explaining core-wall bending is complicated. Previous to AMTD, the only mirrors fabricated via LTS replication were AMSD and Multi-Mirror System Demonstration (MMSD). Neither of these mirrors exhibited core-wall bending. Preliminary analysis indicates that the effect depends on the shear stress in the radial core walls. The greater the amount of shear stress, the greater the amount of viscous flow of the glass during LTS replication, and the greater the core-wall bending. Preliminary analysis indicates that this shear stress is proportional to the unsupported radial core-wall length divided by the ROC (independent of core thickness and independent of whether the core is composed of a single layer or multiple layers). The AMTD-1 2.5-m-ROC 0.43-m-diameter×400-mm-thick mirror had significantly larger core cells than the AMTD-2 3.5-m-ROC 1.5-m-diameter×165-mm-thick mirror; and thus, less bending. An AMTD-3 proposal to resolve this issue was submitted to the ROSES 2016 SAT.

Arnold Mirror Modeler: the Arnold Mirror Modeler (AMM) was developed under AMTD to rapidly create and analyze detailed mirror designs. The AMM creates a complete analysis stream, including model, loads (static and dynamic), plots, and a summary file of input variables and results suitable for optimization or trade studies. Values of all settings can be archived and recalled to continue or redo any configuration. In FY 2016/17, an updated AMM was released, which is being used to perform point-design trade studies for HabEx closed-back ULE® and open-back Zerodur® mirror systems.

Support System

Need: Large-aperture mirrors require large support systems to ensure they survive launch and deploy on-orbit, stress-free, and undistorted. Additionally, segmented mirrors require large structure systems that establish and maintain the mirror's shape.

Accomplishment: During FY 2016/17, AMTD-2 advanced this technical area by continuing to develop mount capabilities in the AMM and use it to perform trade studies of candidate mirror mount systems for HabEx. The emphasis of these trade studies has been on understanding and specifying dynamic primary-mirror WFE.

Dynamic WFE is produced when a mirror is placed in inertial acceleration by a mechanical disturbance, causing it to react (i.e., bend) against its mounts. A 'static' example is gravity sag. The acceleration of gravity causes a mirror to bend on its mount. Assuming that no resonant mode is excited, a mirror's dynamic WFE has the same shape as its gravity sag with an amplitude proportional to the disturbance's 'G-acceleration.' Assuming that the mirror substrate's first-mode stiffness is higher than the mechanical disturbance frequencies, the biggest accelerations occur when the mechanical disturbance excites a mount resonance mode. AMTD-2 has studied dynamic WFE for various mirror substrates on both 3-point and 6-point mounts attached to the substrate at the edge, as well as 80% and 50% radial points (Fig. 3).

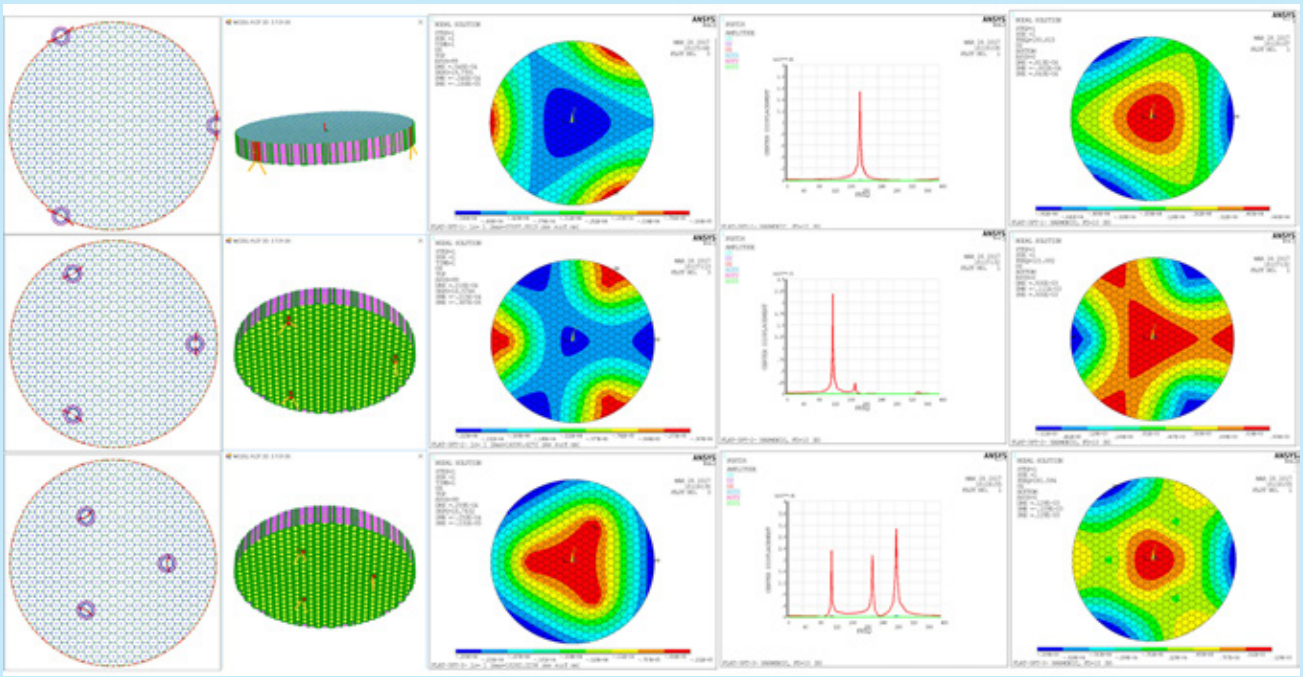

Fig. 3. *Static gravity sag and dynamic deformation of 180-Hz 4-m-diameter closed-back mirror on three-point mount attached at edge, as well as 80% and 50% radial locations.*

Mid/High-Spatial-Frequency Error

Need: High-contrast imaging requires mirrors with very smooth surfaces (<10 nm rms). While deformable mirrors can correct low-order errors, they cannot correct mid- and high-spatial-frequency errors. Such errors can arise from the fabrication process or CTE inhomogeneity, and can introduce artefacts into the dark hole.

Milestone 2: Characterize thermal-induced surface figure error (SFE) of two candidate primary mirrors (1.5-m ULE® mirror and 1.2-m Zerodur® mirror owned by Schott) from 250 K to ambient.

Accomplishment: During FY 2016/17, AMTD-2 advanced this technical area by characterizing the thermal performance of the 1.2-m ELZM owned by Schott. This test accomplishes half of this major milestone. Anticipated testing of the 1.5-m ULE® mirror in 2017 will complete this milestone. Previously, AMTD-1 had demonstrated the ability of the Harris Corp's ion polishing process to produce a 5.4-nm-rms surface.

Thermal Characterization: In 2016/17, MSFC enhanced its 23-m×7-m thermal vacuum test chamber by adding a pressure-tight enclosure that allows test equipment to be placed at the center of curvature of short-ROC mirrors (Fig. 4). This new capability enabled testing of the Schott 1.2-m ELZM mirror from ambient to 250 K. No thermal-deformation-induced high-spatial quilting associated with the lightweight was measured. The test did measure 9.4 nm rms of mid-spatial error associated with CTE inhomogeneity (Fig. 4).

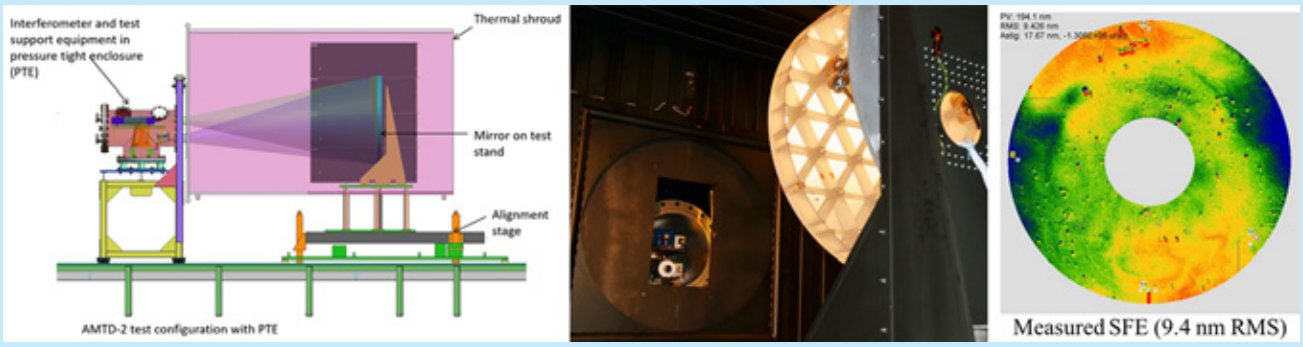

Fig. 4. Left: *Short-ROC mirror test setup with pressure-tight enclosure.* Center: *Schott ELZM in test setup.* Right: *Measured thermal SFE from 250 K to ambient.*

Segment-to-Segment Gap Phasing

Need: To avoid speckle noise which can interfere with exoplanet observation, internal coronagraphs require an ultra-stable wavefront.

Accomplishment: During FY 2015/16, AMTD-2 advanced this technical area by continuing the systems-engineering effort to understand the interaction between optical telescope wavefront stability and coronagraph contrast leakage.

Contrast-Leakage WFE Tolerances: In our previous studies, we evaluated the contrast leakage over specific regions of interest (ROI). These studies showed a correlation between numbers of segment rings and noise in a dark-hole ROI. These studies also provided preliminary tolerance values for the allowed amounts of different WFEs. Because of the asymmetric nature of the ROI, the tolerance results were misleading. Therefore, in FY 2016/17 we implemented a new method that decomposes contrast leakage into average radial (photometric noise) and azimuthal (systematic noise) components as defined by Shaklan [11]. The new method confirms our previous conclusions that segment-to-segment co-phasing (piston and tip/tilt) errors must be stable in the 10- to 20-pm peak-to-valley (PV) range. The new method was used to evaluate the contrast leakage in annular ROI for 50 random trials of global Seidel and Zernike aberration produced by rigid-body motion of the primary and/or secondary mirror assemblies. The maximum allowance for static aberration and contrast leakage for aberration exhibiting sinusoidal variation was also studied. Table 1 lists the maximum amount of random WFE that a 4th-order radial coronagraph can tolerate while keeping the photometric noise less than 10^{-10} and the systematic noise less than 5×10^{-11} over an annular ROI from 1.5 to 2.5 λ/D.

Aberration (Random)	WFE (pm) for 1×10^{-10} of Photometric Noise	WFE (pm) for 5×10^{-11} of Systematic Noise
Tip/Tilt	9,600	35,000
Seidel Power	1,100	22,000
Zernike Astigmatism	6,800	49,000
Zernike Trefoil	6,800	44,000
Zernike Hexafoil	9,600	78,000
Seidel Spherical	300	11,000
Seidel Coma	6,800	840

Table 1. *PV aberration amplitude tolerance for contrast leakage over an annular ROI from 1.5 to 2.5 λ/D.*

Clearly, photometric noise (radial average) is more sensitive to Seidel spherical than Seidel power. It is equally apparent that systematic noise is more sensitive to rotationally asymmetric aberrations, such as Seidel coma, than to rotationally symmetric aberrations like Zernike astigmatism.

Integrated Model Validation

Need: On-orbit performance is driven by mechanical stability (both thermal and dynamic). As future systems become larger, compliance cannot be fully tested; performance verification will rely on results from a combination of sub-scale tests and high-fidelity models. It is necessary to generate and validate as-built models of representative prototype components to predict on-orbit performance for transmitted wavefront, point spread function (PSF), pointing stability, jitter, thermal stability, and vibro-acoustic and launch loads.

Milestone 3A: Add capabilities to integrated design and modeling tools to predict the mechanical and thermal behavior of candidate mirrors; use these tools to generate Pre-Phase-A point designs and predict on-orbit optical performance.

Milestone 3B: Validate by test the integrated design and modeling tools to predict the mechanical and thermal behavior of candidate mirrors.

Accomplishment: During FY 2016/17, AMTD-2 accomplished Milestone 3A by continuing to develop its integrated design and modeling tools and by using these tools to conduct point-design trade studies for the HabEx primary mirror, including on-orbit performance predictions. Additionally, during FY 2016/17, AMTD-2 accomplished half of major Milestone 3B by using its integrated modeling tools to predict the mechanical and thermal behavior of the Schott 1.2-m ELZM mirror assembly, then validating those predictions by test. AMTD-2 expects to complete major Milestone 3B in 2017 by validating by test its performance predictions for the 1.5-m ULE® mirror assembly.

Mechanical and thermal models were made of the Schott 1.2-m ELZM mirror. The mechanical model predicted a gravity sag deformation of 125 nm rms and a first free-free-resonant-bending mode of 207 Hz. The thermal model predicted a 21 nm rms total SFE change (from 294 K to 250 K) consisting of contributions from its athermal mount, through-thickness thermal gradient, and bulk CTE homogeneity. The largest contributor of this shape-change error is from an assumed CTE homogeneity of 10 ppb (based on Schott catalog data) (Fig. 5).

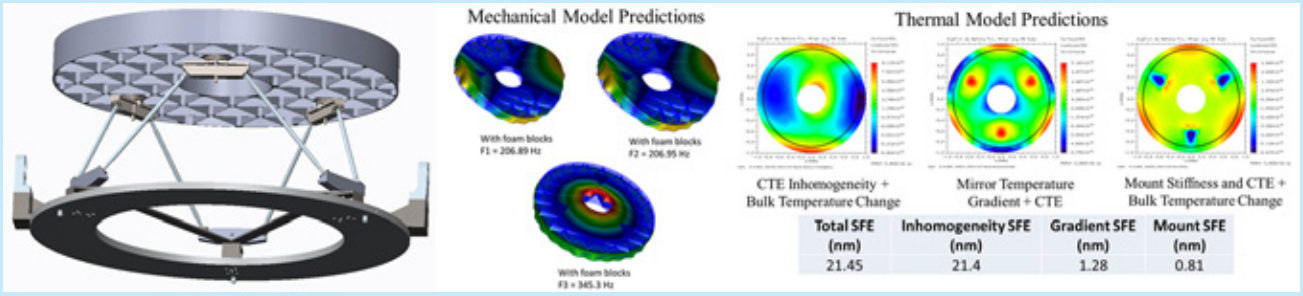

Fig. 5. Left: *Schott 1.2-m ELZM assembly.* Center: *Predicted first-mode frequency.* Right: *Predicted thermal SFE.*

The models were validated by test in the MSFC X-ray and Cryogenic Facility (XRCF). First-mode frequency was measured via tap test on foam blocks to be 196 Hz (5% agreement). Gravity sag was measured by rotation test to be 142 nm rms; with a 31 nm rms difference between predicted and measured (Fig. 6). This difference could be caused by a 2-mm error between the model and the 'as-built' mount pad locations.

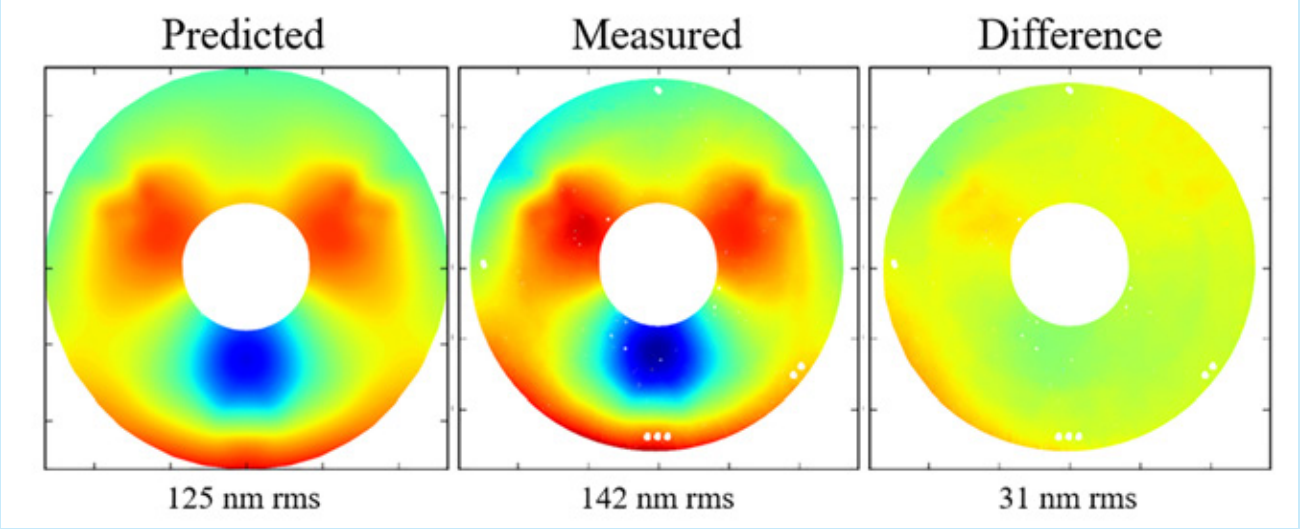

Fig. 6. *Predicted vs. measured ELZM gravity sag.*

Thermal-model predictions are validated by measuring how the mirror shape deforms from 294 K to 250 K. For input into the thermal model, the mirror assembly is fully instrumented with thermal sensors to measure its bulk temperature and thermal gradients. Using the Schott catalog specification of 10 ppb CTE homogeneity, the predicted thermal SFE change is 21 nm rms. But, the measured SFE change is 9.4 nm rms. After consulting with Schott, we were informed that the 1.2-m ELZM mirror has a CTE homogeneity of 5 ppb. With this new CTE specification, the predicted SFE change is 9.55 nm rms (Fig. 7).

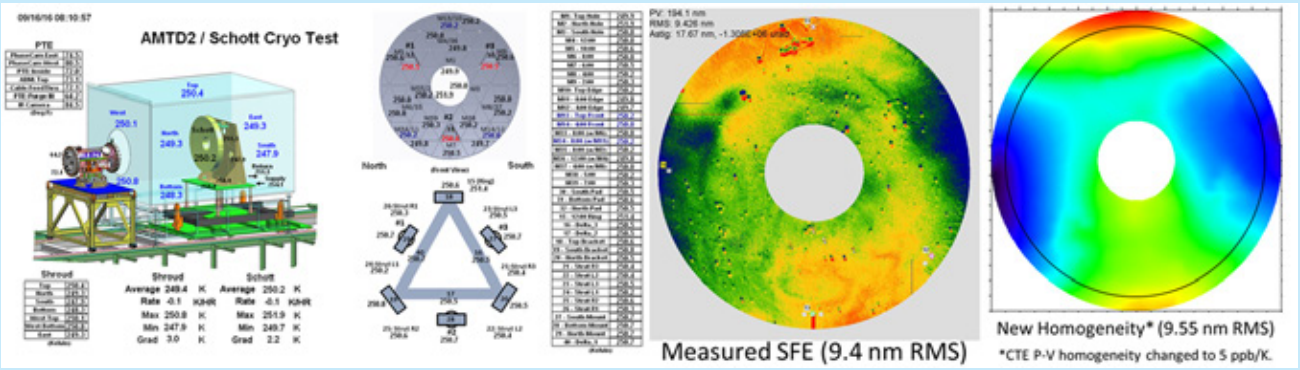

Fig. 7. Left: *Instrumented thermal test monitors temperature at multiple locations.* Center: *Measured thermal SFE change.* Right: *Predicted thermal SFE change with corrected CTE homogeneity.*

Path Forward

AMTD has quantifiable milestones for each technology. Figure 8 shows the Phase 2 schedule. The primary tasks for FY 2017 are to predict the mechanical and thermal performance of the 1.5-m ULE® mirror and validate those predictions by test at the XRCF.

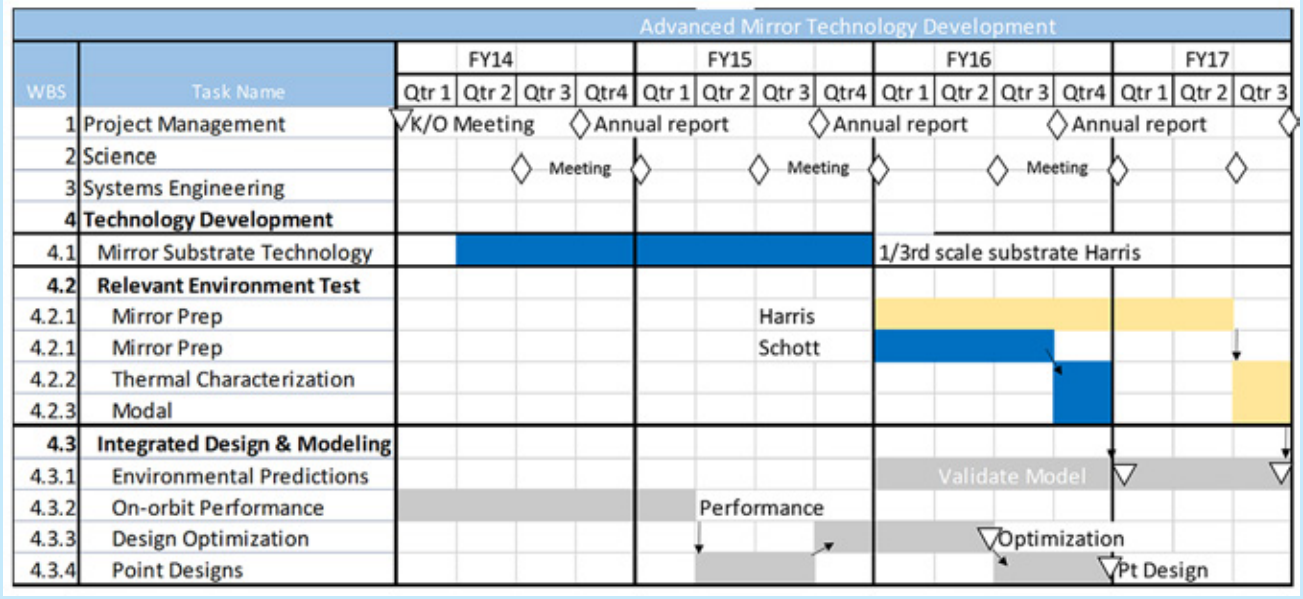

Fig. 8. *AMTD Phase 2 schedule.*

References

[1] H.P. Stahl, "*Advanced mirror technology development (AMTD) project: year five status*," Proc. SPIE **10401** (2017)

[2] T. Brooks, T. Hull, R. Eng, and H.P. Stahl, "*Modeling the extremely lightweight Zerodur mirror (ELZM) thermal soak test*," Proc. SPIE **10374** (2017)

[3] H.P. Stahl, "*Advanced mirror technology development (AMTD) project: overview and year four accomplishments*," Proc. SPIE **9912**, Advances in Optical and Mechanical Technology for Telescopes and Instrumentation II; doi:10.1117/12.2234082 (2016)

[4] Committee for a Decadal Survey of Astronomy and Astrophysics; National Research Council, "*New Worlds, New Horizons in Astronomy and Astrophysics*," The National Academies Press, Washington, D.C. (2010)

[5] "*NASA Space Technology Roadmaps and Priorities: Restoring NASA's Technological Edge and Paving the Way for a New Era in Space*," NRC Report (2012)

[6] C. Kouveliotou et al., "*Enduring Quests, Daring Visions: NASA Astrophysics in the Next Three Decades*," arXiv:1401.3741 (2014)

[7] P. Hertz, "*Planning for the 2020 Decadal Survey: An Astrophysics Division White Paper*," available at science.*nasa.gov/astrophysics/documents/* (2015)

[8] NASA Town Hall, AAS Winter Meeting, Kissimmee, FL (2016)

[9] J. Dalcanton et al., "*From Cosmic Birth to Living Earths: The Future of UVOIR Space Astronomy*," Association of Universities for Research in Astronomy, (2015) *www.hdstvision.org/report/*

[10] M.S. Lake, L.D. Peterson, and M.B. Levine, "*Rationale for defining Structural Requirements for Large Space Telescopes*," AIAA Journal of Spacecraft and Rockets, Vol. **39**, No. 5 (2002)

[11] S.B. Shaklan, L. Marchen, J. Krist, and M. Rud, "*Stability error budget for an aggressive coronagraph on a 3.8m telescope*," SPIE Proceedings **8151** (2011)

For additional information, contact Philip Stahl: *h.philip.stahl@nasa.gov*

Predictive Thermal Control Technology to Enable Thermally Stable Telescopes

Prepared by: H. Philip Stahl, PhD (NASA/MSFC)

Summary

The Predictive Thermal Control (PTC) technology development project is a multi-year effort initiated in Fiscal Year (FY) 2017, to mature the Technology Readiness Level (TRL) of critical technologies required to enable thermally ultra-stable telescopes for exoplanet science. PTC has defined three objectives:

1. Validating thermal-optical-performance models.
2. Deriving thermal-system stability specifications.
3. Demonstrating Predictive Thermal Control.

To achieve our objectives, we have defined a detailed technical plan with five quantifiable milestones. While PTC is still in its initial stage, progress is being made on Milestones 1-3 (below). PTC is a joint effort between NASA/MSFC and Harris Corporation.

Background

"*Are we alone in the universe?*" is probably the most compelling science question of our generation.

Per the 2010 *New Worlds, New Horizons* (NWNH) Decadal Report [1]: "*One of the fastest growing and most exciting fields in astrophysics is the study of planets beyond our solar system. The ultimate goal is to image rocky planets that lie in the habitable zone of nearby stars.*" NWNH recommended, as its highest priority, medium-scale activity such as a "*New Worlds Technology Development (NWTD) Program*" to "*lay the technical and scientific foundations for a future space imaging and spectroscopy mission.*" The National Research Council (NRC) report, "*NASA Space Technology Roadmaps and Priorities,*" [2] states that the second-highest technical challenge for NASA regarding expanding our understanding of Earth and the universe in which we live is to "*develop a new generation of astronomical telescopes that enable discovery of habitable planets, facilitate advances in solar physics, and enable the study of faint structures around bright objects by developing high-contrast imaging and spectroscopic technologies to provide unprecedented sensitivity, field of view, and spectroscopy of faint objects.*" NASA's "*Enduring Quests, Daring Visions*" [3] called for a Large Ultraviolet/Optical/Infrared (LUVOIR) Surveyor mission to "*enable ultra-high-contrast spectroscopic studies to directly measure oxygen, water vapor, and other molecules in the atmospheres of exoEarths,*" and "*decode the galaxy assembly histories through detailed archeology of their present structure.*" As a result, NASA will study in detail a LUVOIR Surveyor and a Habitable Exoplanet Imaging Mission (HabEx) concept for the 2020 Decadal Survey [4, 5]. Additionally, the Association of Universities for Research in Astronomy (AURA) report "*From Cosmic Birth to Living Earths*" [6] details the potential revolutionary science that could be accomplished from "*directly finding habitable planets showing signs of life.*"

Per the 2015 Cosmic Origins (COR) Program Annual Technology Report (PATR) [7], a "*Thermally Stable Telescope*" is a critical, highly desirable technology for a strategic mission. "*Wavefront stability is the most important technical capability that enables 10^{-10} contrast exoplanet science with an internal coronagraph.*

State of art for internal coronagraphy requires that the telescope must provide a wavefront that is stable at levels less than 10 pm for 10 minutes (stability period ranges from a few minutes to tens of minutes depending on the brightness of the star being observed and the wavefront-sensing technology being used)."

Thermal wavefront error (WFE) occurs because of thermal expansion; slewing the telescope relative to the sun causes its structure or mirrors to change temperature. Thermal-heat-load changes cause the structure holding the mirrors to expand/contract and the mirrors themselves to change shape. Fortunately, thermal drift tends to be slow, i.e., many minutes to hours. It is assumed that any drift that is longer than the Wavefront Sense and Control (WFSC) control cycle will be corrected by a deformable mirror. Thus, it is only necessary to actively control stability errors that are shorter than 10 to 120 minutes.

No previous mission has ever required a telescope with a wavefront that is stable at levels of less than 10 pm per 10 minutes. State of the art (SOTA) for ambient-temperature space telescopes are 'cold-biased' with heaters required for 'operational' temperature. The telescope is insulated from solar load such that, for all orientations relative to the sun, it would passively be at a 'cold' temperature (for example, 250 K). The telescope is then warmed to an ambient temperature via heater panels on the forward stray-light baffle tube as well as behind and beside the mirror. SOTA thermal control systems have demonstrated ~1-K stability for a 1-m-class telescope using a 'bang/bang' controller. Analysis indicates that ~100 mK should be possible with a proportional integral differential (PID) controller.

Hubble Space Telescope (HST), NextView, the Wide Field Infrared Survey Telescope (WFIRST), and the James Webb Space Telescope (JWST) illustrate the challenge. When the JWST (which will reside behind a sun shade) slews from its coldest to its warmest pointing, its temperature is predicted to change by 220 mK and its WFE is predicted to change by 31 nm root mean square (rms). While not designed to pursue exoplanet science, it would take JWST over 14 days to 'passively' achieve stability better than 10 pm per 10 min [8]. HST is a heated telescope, but its temperature is not controlled. The HST's temperature changes by nearly 20°C as it orbits [9]—moving in and out of the Earth's shadow. This change causes the structure between the primary and secondary mirrors to change (typically ±3 µm) resulting in WFE changes of 10–25 nm every 90 min (1–3 nm per 10 min) [10]. Assuming linear performance, HST could be used for exoplanet science if its thermal variation were controlled to < 20 mK. To solve the HST focus problem, the commercial NextView telescope system manufactured by PTC partner Harris Corporation has a 'bang/bang' system that controls its temperature to ~±1 K. WFIRST plans to use proportional thermal control that may achieve stability in the 200-to-100-mK range.

PTC plans to advance the SOTA in thermal control by demonstrating a control logic called Model Predictive Control (MPC). MPC places a physics-based model into the control loop to determine control variables (heater power levels) based on state variables (temperature measurements). MPC determines heater-power levels using a completely different logic than proportional control. Proportional control adjusts heater power in proportion to the difference between measured and desired temperatures at one location. MPC uses multiple control zones and takes into account the interdependency between all control zone temperatures and heater power. Preliminary analysis indicates that (assuming that thermal performance is linear) it is possible to achieve picometer wavefront stability by either controlling the shroud to a tight temperature range (within 10 mK) or by rapidly correcting the temperature. Given that mirrors and telescope have a finite thermal response time, the best way to achieve picometer-level stability is to sense and correct for changes in the thermal environment faster than the telescope can respond. Additional stability can be achieved by increasing the system's thermal mass. Based on this analysis, we assess the current TRL of such a system to be 3. PTC will advance this TRL by test using the 1.5-m Ultra-Low Expansion (ULE®) mirror fabricated by Advanced Mirror Technology Development (AMTD-2).

Objectives and Milestones

PTC has defined three objectives to significantly mature the technology needed for an exoplanet-science thermally stable telescope by developing "*thermal design techniques validated by traceable characterization testing of components*":

1. Validating models that predict thermal-optical performance of real mirrors and structure based on their structural designs and constituent material properties, i.e., distribution of coefficients of thermal expansion (CTEs), thermal conductivity, thermal mass, etc.
2. Deriving thermal-system stability specifications from wavefront stability requirements.
3. Demonstrating utility of a Predictive-Control thermal system for achieving thermal stability.

To achieve our objectives, we have defined a detailed technical plan with five quantifiable milestones:

- Milestone 1: Develop a high-fidelity traceable model of the 1.5-m ULE® AMTD-2 mirror, including 3D CTE distribution and reflective coating, that predicts its optical-performance response to steady-state and dynamic thermal gradients;
- Milestone 2: Derive thermal-control system specifications as a function of wavefront stability;
- Milestone 3: Design and build a PTC system for a 1.5-m ULE® mirror that senses temperature changes and actively controls the mirror's thermal environment;
- Milestone 4: Validate model by testing the 1.5-m ULE® mirror in a relevant thermal-vacuum environment at the MSFC X-ray and Cryogenic Facility (XRCF); and
- Milestone 5: Use a validated model to perform trade studies determining how thermo-optical performance can be optimized as a function of mirror design, material selection, mass, etc.

Progress and Accomplishments

Objective 1: Validated High-Fidelity Structural-Thermal-Optical-Performance (STOP) Model

Need: Designing a telescope to have 10-pm-per-10-minute WFE stability using model predictive control requires a validated high-fidelity STOP model.

Milestone 1: Develop a high-fidelity STOP model of the 1.5-m ULE® AMTD-2 mirror, including 3D CTE distribution and reflective coating, that predicts its optical performance response to steady-state and dynamic thermal gradients.

Milestone 4: Validate high-fidelity STOP model by testing the 1.5-m ULE® mirror in a relevant thermal-vacuum environment at the XRCF.

Accomplishment: During FY 2017, PTC is advancing technology for Milestone 1. MSFC created a preliminary STOP model of the 1.5-m ULE® AMTD-2 mirror to make an initial assessment of the mirror's thermal performance in the XRCF (Fig. 1). This assessment was needed to assist in the design and specification of the modifications to XRCF needed to impose axial and lateral thermal gradients into mirror assemblies and characterize the ability of PTC algorithms to sense and correct the effects of such gradients. This preliminary model assumes a uniform CTE distribution and internal core structure without any visco-elastic deformations. Note that the mirror actually has visco-elastic deformations caused by low-temperature-slumping the mirror to a very fast 3.5-m radius of curvature (~f/1.15).

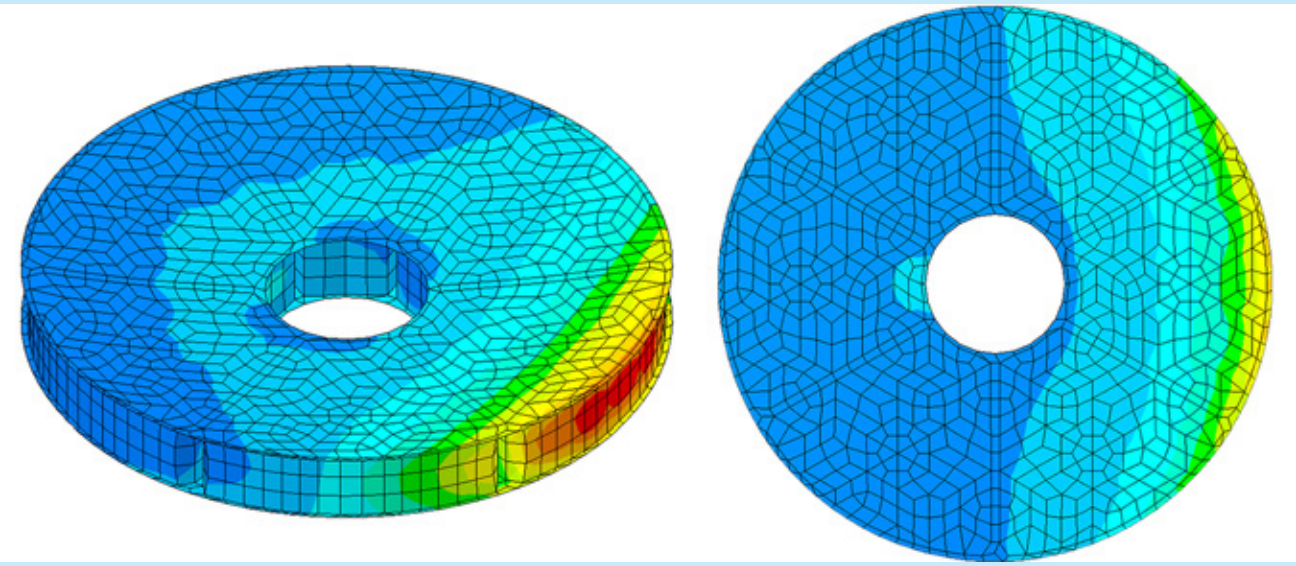

Fig. 1. *Potential thermal-gradient response.*

To improve the fidelity of MSFC's model, Harris Corporation delivered through-thickness and radial CTE maps (generated by Corning Corporation) of each ULE® face-sheet and core boule used to make the 1.5-m ULE® AMTD-2 mirror. These maps are critical to producing a high-fidelity STOP model. High-fidelity STOP models require knowledge of the CTE match between the front and back face-plates, where in the boules each core element was cut, and where each core element was placed in the mirror's core (Fig. 2). Finally, PTC coated the 1.5-m ULE® AMTD-2 mirror with protected aluminum to produce a test article with flight-traceable front-surface thermal emissivity (Fig. 3).

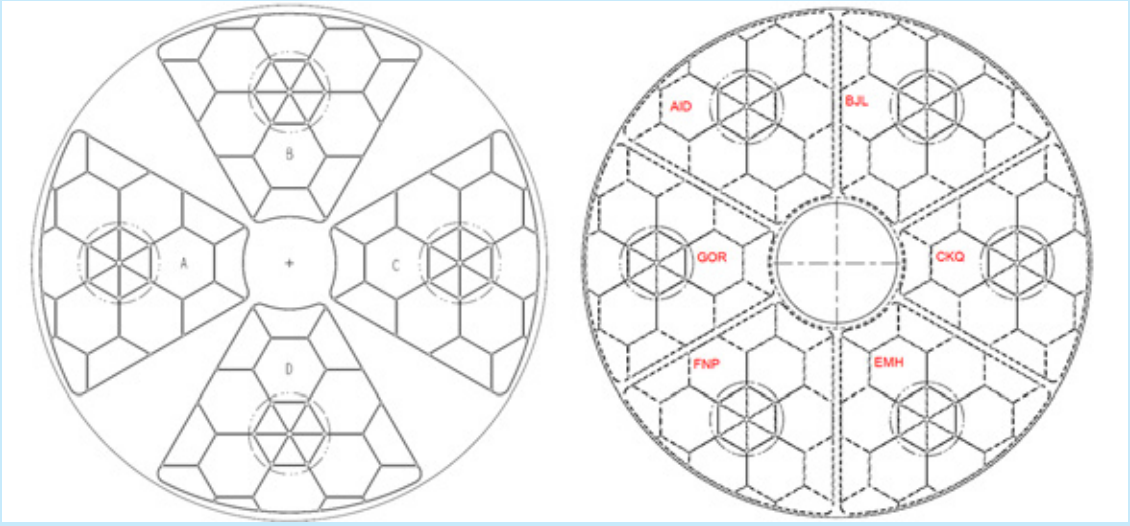

Fig. 2. *Boule CTE mapping to mirror.*

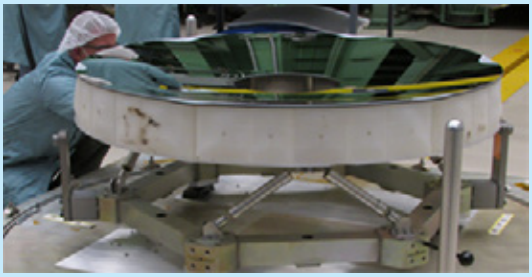

Fig. 3. *Coated 1.5-m ULE® AMTD-2 mirror.*

In FY 2017/18, PTC will further advance technology for Milestone 1 by using X-ray computed tomography to image the internal structure of the mirror and produce a 3D structural model of the 'as-built' mirror. The MSFC high-fidelity STOP model will investigate integrating this 3D structure with the CTE maps to produce predictions of the 1.5-m ULE® AMTD-2 mirror's mechanical (first-mode frequency and gravity-sag deformation) and thermal (static thermal deformation) performance. Additionally, in FY 2017/18, PTC will advance technology for Milestone 4 by testing in the XRCF the 1.5-m ULE® AMTD-2 mirror's response to static thermal gradient loads. This test will be conducted jointly with the planned AMTD-2 static thermal soak test.

Objective 2: Traceable Specifications for an Active Thermal Control System

Need: Designing a telescope to have 10-pm-per-10-minute WFE stability via active thermal control requires a validated STOP model. Such a model is required to derive the active thermal control system's performance specifications, such as sensing resolution (1 mK or 10 mK), control accuracy (10 mK or 50 mK), control period (1 min or 5 min), number and distribution of sense and control zones, etc.

Milestone 2: Derive thermal-control-system specifications as a function of wavefront stability.

Milestone 5: Use validated model to perform trade studies to determine how thermo-optical performance can be optimized as a function of mirror design, material selection, material properties (i.e., CTE), mass, etc.

Accomplishment: During FY 2017, PTC is advancing technology for Objective 2 by working with the HabEx engineering team to determine the sensitivities of candidate coronagraphs to potential WFEs. Once this sensitivity is defined, MSFC will use its high-fidelity model to determine what thermal conditions might produce errors to which candidate coronagraphs are sensitive.

Objective 3: Demonstrate Utility of a Predictive Control Thermal System for Achieving Thermal Stability

Need: A telescope with 10-pm-per-10-minute WFE stability requires an active thermal control system that is beyond the current SOTA (i.e., bang-bang or proportional control).

Milestone 3: Design, build, and test a PTC system for the 1.5-m ULE® AMTD-2 mirror that demonstrates the utility of a physics-based model in the control loop to determine control variables (heater-power levels) based on state variables (temperature measurements).

Milestone 3 has two goals. First, provide data needed by Milestone 4 to validate Milestone 1's thermal model. Second, demonstrate PTC. PTC will be considered demonstrated if it can correct for externally imposed thermal gradients (i.e., radial, lateral, and axial gradients). Other goals of Milestone 3 include self-tuning of less-well-known thermal parameters in the thermal model to improve the PTC's veracity, informing the design of hardware such as heated bathtubs and thermal shrouds to enable controllability, and directly imposing measurable thermally induced WFE into the mirror.

Accomplishment: During FY 2017, PTC advanced technology for Objective 3 by modifying the XRCF to be able to impose into mirror systems axial and lateral thermal gradients. Axial thermal gradients are produced by placing heaters behind the mirror and a cold wall in front of the mirror (Fig. 4). Lateral thermal gradients are produced using a side-wall of solar lamps.

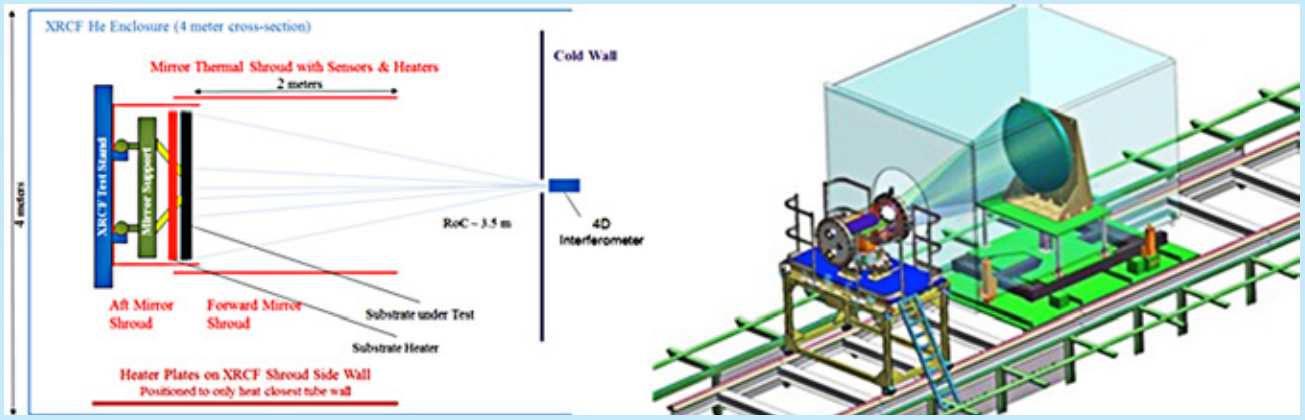

Fig. 4. *XRCF thermal test environment (ROC, Radius of Curvature).*

In FY 2017, the lateral heat source was designed, fabricated, and tested. An array of 24 lamps connected in a 3-phase delta configuration was developed using residual hardware from a previous XRCF project. Stands were designed and fabricated to provide support for the lamp fixtures, which are to be subjected to cryogenic temperatures. The system utilizes a phase controller with zero crossing. A control system was designed for safe operation at temperature and vacuum extremes. Safety features for over-temperature, loss of signal, shorted silicon controlled rectifier (SCR), corona, and over-current were incorporated into the design. Manual Control (0 to 100% power), as well as automatic PID control to a set temperature, were included as part of the system design. The complete system was tested to below the PTC operating temperature (< 200 K) with a test article instrumented with 14 temperature sensors across an area of 2 m × 3 m. The lateral-heat-source operation at cryogenic temperature increased the test-article average temperature by more than 115 K in 10 minutes, without significant impact on chamber pressure or shroud temperature (Fig. 5). By comparison, the proposed Milestone 3 test plan for the 1.5-m ULE® AMTD-2 mirror has 33 diodes: 24 on the mirror, three on the bond pads, and six on the delta-frame structure.

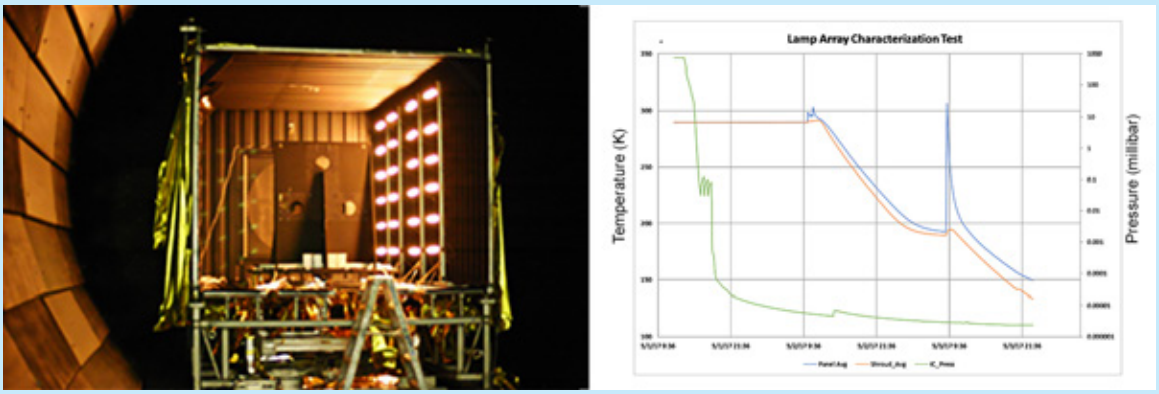

Fig. 5. Left: *XRCF solar lamp array for lateral thermal gradient.* Right: *Lamp-array characterization test results.*

Path Forward

PTC has quantifiable milestones for each technology. Figure 6 shows the 'as-proposed' Phase 1 schedule. However, this is not the current baseline schedule. PTC was required to stretch its schedule to four years due to lack of funding. Significant funds needed to perform tasks in FY 2018 were moved to FY 2020, resulting in growth of total cost and schedule. Unfortunately, at present PTC's baseline funding profile for FY 2020 is insufficient to complete all tasks.

WBS	Task Name	Start
1.0	**Program Management**	1/2/17
2.0	**Systems Engineering**	1/2/17
	Milestone #2 Specifications for Predictive Thermal Control System	2/3/17
	Milestone #5 Trade Study Analysis	9/20/19
3.0	**Predictive Thermal Control Technology Development**	4/10/17
3.1	**Opto-Thermal Modeling**	4/10/17
	Milestone #1 High Fidelity AMTD-2 Model with 3D CTE Distribution	1/26/18
3.2	**Predictive Thermal Control (PTC) Algorithm Development**	5/8/17
3.3	**Testing in XRCF with AMTD-2 Mirror**	1/28/19
3.4	**Model and PTC Algorithm V&V**	3/25/19
	Milestone #4 Validated by Test Model of AMTD-2 Mirror	7/26/19
4.0	**Test Support**	9/11/17
4.1	**Design and Build Thermal Control System**	9/11/17
	Milestone #3 Predictive Thermal Control System Test Setup	1/25/19
4.2	**Metrology Equipment**	9/11/17
4.3	**XRCF Test Environment**	1/15/18

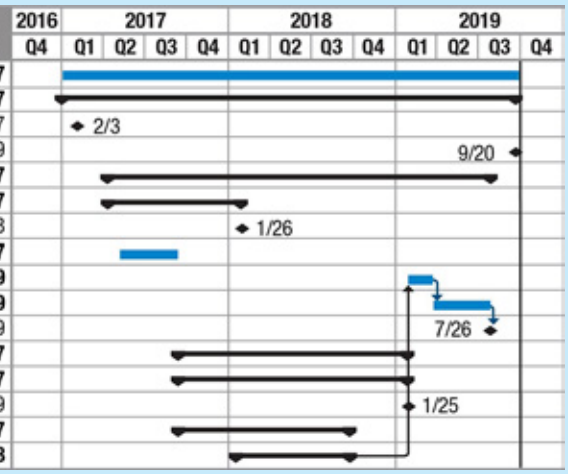

Fig. 6. *PTC 'as-proposed' Phase 1 schedule.*

References

[1] Committee for a Decadal Survey of Astronomy and Astrophysics; National Research Council, "*New Worlds, New Horizons in Astronomy and Astrophysics,*" The National Academies Press, Washington, D.C. (2010)

[2] "*NASA Space Technology Roadmaps and Priorities: Restoring NASA's Technological Edge and Paving the Way for a New Era in Space,*" NRC Report (2012)

[3] C. Kouveliotou et al., "*Enduring Quests, Daring Visions: NASA Astrophysics in the Next Three Decades,*" arXiv:1401.3741 (2014)

[4] P. Hertz, "*Planning for the 2020 Decadal Survey: An Astrophysics Division White Paper,*" available at https://science.nasa.gov/astrophysics/documents/ (2015)

[5] NASA Town Hall, AAS Winter Meeting, Kissimmee, FL (2016)

[6] J. Dalcanton et al., "*From Cosmic Birth to Living Earths: The Future of UVOIR Space Astronomy,*" Association of Universities for Research in Astronomy, www.hdstvision.org/report (2015)

[7] "*Cosmic Origins Program Annual Technology Report*" (2015)

[8] 13-JWST-0207 F (2013)

[9] C. Cox and M. Lallo, "*Keeping the Hubble Space Telescope in focus,*" Proc. of SPIE **8442**, 844237, doi: 10.1117/12.924900 (2012)

[10] M. Lallo, "E*xperience with the Hubble Space Telescope: 20 years of an archetype,*" Opt. Eng. Vol. **51**, 011011, doi: 10.1117/1.OE.51.1.011011 (2012)

For additional information, contact Philip Stahl: *h.philip.stahl@nasa.gov*

Development of Large-Area (100 cm^2) Photon-Counting UV Detectors

Prepared by: John Vallerga (Space Sciences Laboratory, UC Berkeley)

Summary

Micro-Channel-Plate (MCP) detectors have been an essential imaging technology in space-based NASA ultraviolet (UV) missions for decades, and have been used in numerous orbital and interplanetary instruments. The Experimental Astrophysics Group (EAG) at the University of California (UC) Berkeley's Space Sciences Laboratory (SSL) was awarded an Astrophysics Research and Analysis (APRA) grant in 2008 to develop massively parallel cross-strip (XS) readout electronics. These laboratory XS electronics have demonstrated spatial resolutions of 12 µm full-width at half-maximum (FWHM), global output count rates of 2 MHz, and local count rates of 100 kHz; all at gains a factor of ~20 lower than existing delay-line readouts [1]. They have even been deployed in biomedical and neutron-imaging labs but are presently too bulky and high-powered for space applications, though a current version was successfully flown on a rocket flight in 2014 [2].

EAG has been awarded two Strategic Astrophysics Technology (SAT) grants to develop XS technology for large, photon-counting UV detectors: the first in 2012 for a 50-mm square detector, and more recently (2016) scaling this technology to a 100-mm square design. The goal of these SAT programs is to raise the Technology Readiness Level (TRL) of this XS technology by:

1. Developing new Application Specific Integrated Circuits (ASICs) that combine optimized faster amplifiers and associated Analog-to-Digital Converters (ADCs) in the same chip(s).
2. Developing a Field-Programmable-Gate-Array (FPGA) circuit that will control and read out groups of these ASICs so that XS anodes of many different formats can be supported.
3. Developing a spaceflight-compatible 100-mm XS detector that can be integrated with these electronics and tested as a system in flight-like environments. This detector design can be used directly in many rocket, satellite, and interplanetary UV instruments, and could be easily adapted to different sizes and shapes to match various mission requirements. Having this detector flight design available will also reduce cost and development risk for future Explorer-class missions. New technological developments in photocathodes (e.g., GaN) or MCPs (e.g., low-background, surface-engineered, borosilicate-glass MCPs) could be accommodated into this design as their TRLs advance.

Since the start of our project in April 2012, we have designed and constructed a 50-mm XS detector with a new low-noise anode, and have demonstrated its excellent performance using our best laboratory electronics. The second versions of our ASICs have been designed, fabricated, and tested, and are now being integrated into a full 160-channel (for 80×80 strips) electronic system that supports our 50-mm detector in full flight-like environmental tests. We recently started a follow-on SAT project that scales up the detector to 100 mm × 100 mm (320 channels) including a new version of our ASIC, fabricated in a 130-nm CMOS process that combines the functions of the previous two versions to reduce board complexity while maintaining similar performance.

Background

The 2010 Decadal Survey, "*New Worlds, New Horizons in Astronomy and Astrophysics*" (NWNH), commenting on UV astronomy, noted, "*Key advances could be made with a telescope with a 4-meter-diameter aperture with large field of view and fitted with high-efficiency UV and optical cameras/spectrographs*." Further, it recommends to "*invest in essential technologies such as detectors, coatings, and optics, to prepare for a mission to be considered by the 2020 decadal survey*." Many of the White Paper submissions to the Decadal Survey on UV astrophysics missions require large fields of view (detector formats >10 cm), and high spatial and/or spectral resolution recorded with high efficiency over a large wavelength range [3, 4]. Our SAT program plans to take our successful XS technology that achieves the performance goals above in the laboratory, and raise its TRL by lowering its mass and power, and qualifying it for space use.

XS readouts collect the charge exiting from a stack of MCPs with two sets of coarsely spaced and electrically isolated orthogonal conducting strips (Fig. 1). When the charge collected on each strip is measured, a centroid calculation determines the incident location of the incoming event (photon or particle). This requires many (e.g., 80, 160) identical amplifiers whose individual outputs must all be digitized and analyzed. The advantage of this technique over existing and previous MCP readout techniques (wedge and strip, delay-line, intensifiers) is that the anode capacitance per amplifier is lower, resulting in lower noise. This allows (factor of ~20) lower MCP gain operation while still achieving better spatial resolution compared to the delay-line MCP readouts of current space missions [5], thereby increasing the dynamic range of MCP detectors by up to two orders of magnitude. This can also be scaled readily to large (>100 mm × 100 mm) or unique formats (e.g., circular for optical tubes, rectangular for spectrographs, and even curved anodes to match curved MCP focal planes). The XS readout technology is mature enough to be presently used in the field in many laboratory environments producing quality scientific results [6, 7] and is ready for the next step of development – preparing for an orbital or deep-space-mission implementation.

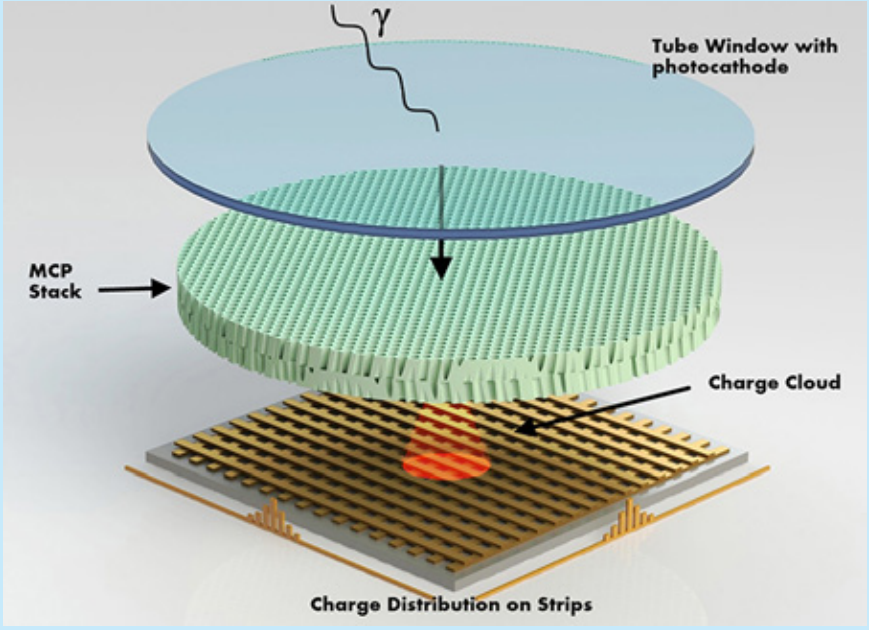

Fig. 1. *Schematic of a XS readout behind an MCP stack.*

Our laboratory XS readout electronics, called the Parallel XS (PXS) electronics, consist of a preamplifier board placed near the MCP anode and a boxed set of electronics containing ADCs and FPGAs. The PXS electronics performance presently meets or exceeds all of the specifications of the previous flight systems mentioned above. However, the PXS laboratory electronics are too bulky and massive, and use relatively high power and therefore are not currently suitable for a long-term space mission. One important goal of the present effort is to replace the PXS electronics with ASICs that combine the functionality of the preamp board and the downstream ADCs into one or two low-power, low-mass chip(s). When a set of these chips is combined with an FPGA and XS anode, we expect the performance to exceed the higher-power PXS electronics due to the noise improvement expected for the smaller-scale components.

In addition to space-flight-appropriate ASIC development, our first SAT program planned to construct a flight prototype 50-mm XS MCP detector with a XS readout using our new ASICs. The new ASICs and FPGA control electronics are being integrated into a compact package so the performance of the whole detector system can be qualified in space-like environments (e.g., thermal and vibration tests). This standard detector design will become the baseline XS detector, which could be used in many proposed rocket and satellite missions. We note that many UV sounding-rocket programs (e.g., at Johns Hopkins University and the University of Colorado) currently use MCP detectors. In fact, we expect this detector to be the baseline of many Explorer-class mission proposals in the future. This XS design can also be scaled easily to other useful formats required by specialized instruments. For example, doubling the length of one detector dimension entails adding more strips to the anode and more ASICs to read them out, but not a redesign of the ASIC.

Objectives and Milestones

As the 50-mm detector development winds down and the 100-mm detector follow-on SAT program begins, we will reiterate the milestones of the first project and include additional milestones of the second, which scales up the first by a factor of four in area.

1. Design and fabricate ASICs to amplify and digitize cross-strip signal charges

A major thrust of our 50-mm program was developing new ASICs that can overcome the limitations on the front end of our laboratory electronics. We designed and fabricated input ASICs that had the following features:

a. An optimized front-end charge-sensitive amplifier (CSA) matched to the anode-strip load capacitance with fast signal rise and fall times to minimize event "collision."
b. Fast (~GHz) analog sampling to fully characterize both amplitude and arrival time of the intrinsically fast input charge pulse.
c. Digital conversion of the analog samples in the ASIC, avoiding complex, bulky, and high-power discrete ADCs downstream.
d. ASIC self-triggering capabilities to select and transfer only event data across long cables to the FPGA, where the centroiding and timing calculations take place.

The original 50-mm detector proposal called for an ASIC that included a multichannel preamp and an analog sampling and digitization circuit controlled externally by an FPGA. We soon realized that optimization of the analog amplifiers and digital circuits was best done using different fabrication technologies (IBM 130-nm 1.2-V CMOS process, 250 nm for the digital). The noise performance would also improve by not mixing the digital and front-end analog signals on the same piece of silicon. The original name for the combined ASIC (never built) was Gigasample Recorder of Analog Waveforms from a Photodetector ("GRAPH") but after separation of the amplifiers, the sampling digitizer was named the "HalfGRAPH."

After demonstrating two working ASICs (the CSAv3 and the HalfGRAPH2 ASIC described below), and continuing their integration into the 50-mm readout electronics, we now plan in our 100-mm effort to return to the original concept of combining the CSA with the fast sampling ADC. As the new digitizer/sampler will now be in the same CMOS process as the CSAv3, we can realize the original "GRAPH" ASIC concept, combining both on a single die. There are many reasons for doing this, but the two most important are a faster digital readout in the 130-nm process, and reduced layout space and power afforded by combining the ASIC designs into a single die. We also have methods to protect the low-noise analog amplifier from induced noise from the digital circuit. We have now characterized the first two separate ASICs in realistic radiation environments (total ionizing dose, TID) consistent with MIL STD 833 TM1019 for low Earth orbit (~10 krad), interplanetary missions (~30 krad), and the higher doses associated with Jupiter missions (100 krad behind shielding), since we have placed MCP detectors in all such environments. These successful radiation tests of the CSAv3 and HalfGRAPH2 will inform the design of the GRAPH, and we have an opportunity to improve its robustness to radiation dose by using standard industry design techniques for radiation hardness.

2. FPGA system to read out HalfGRAPH ASICs

Our proposed parallel XS readout system was not simply comprised of the new ASICs. New board assemblies had to be designed, laid out, and constructed to couple these ASICs to our existing XS anodes, minimizing stray load capacitances. These boards also included control FPGAs that not only have a new input interface, but also a new output interface to couple to the high-bandwidth computer interface required for our ultimate event rates.

3. Design of 50-mm and 100-mm XS MCP detectors incorporating new electronics

Key issues for large-area XS MCP detector implementations include low-mass and robust construction schemes that can accommodate the capability for a high-vacuum sealed-tube configuration. Without incurring excessive costs, a reasonable format to accomplish this first was the 50-mm detector. This detector achieved spatial resolutions of ~20 µm FWHM, background rates < 0.1 events cm^{-2} sec^{-1}, low fixed-pattern noise, long lifetime, multi-MHz rate capability with low dead time, and detector mass of a few hundred grams. The design and construction of brazed-body assemblies provides for the best packaging and diversity of applications, so this was one of the core tasks. The overall configuration is a device compatible with many current sounding-rocket experiments, and was qualified in vibration and thermal-cycling tests in a straightforward manner. This was a good stepping-stone for implementing much-larger-format devices for large optics/missions.

In the 100 mm × 100 mm effort, we scaled up the brazed-body assembly, detector backplate, XS anode, and number of channels by a factor of 2 in each dimension (320 electronic channels total), with the goal of maintaining the performance parameters achieved with the 50-mm assembly. We then plan to test them in appropriate flight-like environments (thermal and vibration), along with the eventual radiation testing of the GRAPH ASIC.

Progress and Accomplishments

Three parallel efforts came together in the final year of the 50-mm program and the first year of the 100-mm effort: ASIC design, fabrication, and test at the University of Hawaii; FPGA control electronics at UC Berkeley; and 50-mm and 100-mm XS detector design, also at UC Berkeley. Two versions each of the ASICs have been fabricated and tested, as has the 50-mm detector (albeit using the PXS readout electronics). The 160-channel FPGA-controlled amplifier and digitizer boards were fabricated along with their electronics boxes, and photon events are now being read out, albeit at a low event rate, while

we develop fast algorithmic firmware to increase this rate to the MHz level. Radiation testing of both the CSAv3 and the HalfGRAPH2 has been completed successfully up to 460-kRad TID level. The 100-mm brazed body and backplate design was completed, and the detector was fabricated and will soon be tested in vacuum with UV photons.

ASIC Design

We have successfully fabricated and tested two working ASIC designs: the 16-channel CSA called "CSAv3" (Fig. 2) and the 16-channel analog sampling and digitizing HalfGRAPH2. The sections below discuss these designs and their testing to date.

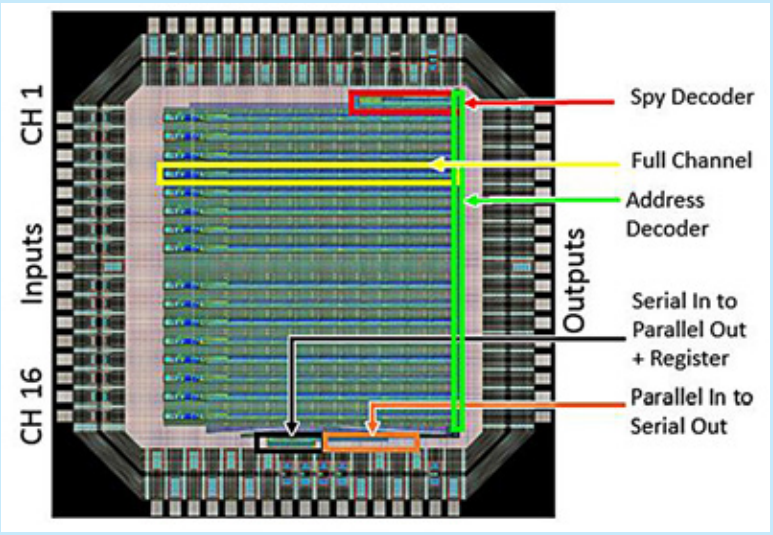

Fig. 2. *CSAv3 die layout showing 16 channels along with the regions of control circuitry including Digital-to-Analog Converters (DACs) and registers.*

CSAv3

Our goal for the ASIC preamp CSAv3 was to maintain the noise figure of the existing laboratory "PreShape32" amplifiers of around 1000 e- root mean square (rms), but also to narrow the waveform, halving the rise-time to 20 ns and decreasing the return to baseline to under 100 ns. This significantly reduces the pileup at high event rates. In addition, the chip does not require external components for biasing, reducing overall footprint on the printed circuit board.

At an MCP gain of 10^6 (160 fC), the largest signal expected on a single strip is ~50 fC. We chose the number of channels per die to be 16 to help with the fan-in from the 50-mm anode's 80 inputs. The CSAv3 amplifier was designed to drive the input of the HalfGRAPH2, including the short trace between them. We designed the amplifier to have linear output swings of ±600 mV.

The components of a single amplifier stage (Fig. 3) consist of a charge-sensitive preamp followed by a pole-zero cancellation (PZC) network, a shaper, an optional polarity inverter, and a buffer amp to drive the downstream HalfGRAPH2. The preamp is an inverting folded-cascode integrator, with the feedback-circuit time constant controlled by a PMOS (P-type metal-oxide-semiconductor) transistor operating as a voltage-controlled resistor. The PZC circuit cancels the pole of the preamp, removing the long baseline recovery. Additional programmable shaping and buffering circuits allow us to optimize the gain and noise of the amplifier. Programming the chip is required prior to operation, and is carried out through a 4-wire serial port to set 16 registers that either control switches to set up signal paths in the chain, or set the 10 (12-bit) DAC values to bias the circuits.

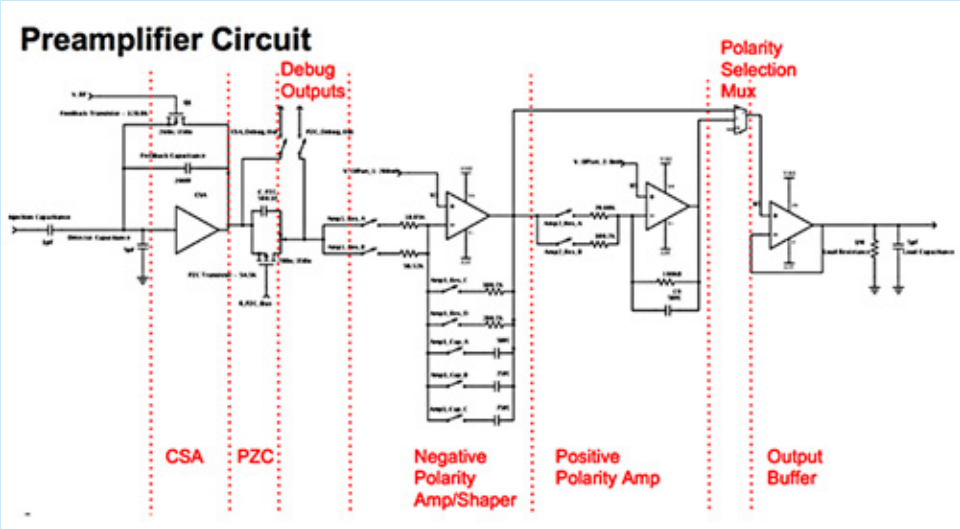

Fig. 3. *A generalized schematic of the new CSAv3.*

Initial performance tests with the amplifier show that it meets the specifications for gain, noise, rise-time, and fall-time [8]. In summary, the overall gain is ~9.5 mV/fC over a range of 0 to 60 fC input charge. Within this range, the gain linearity is within 7%, and the output pulse width is confined within 100 ns. The rms noise was estimated from a fit of noise measurements for different input load capacitances, and results in a noise equivalent of $586\,e^- + 96\,e^-/\mathrm{pF}$ input load. The spread in gain between channels for the same bias settings was found to be minimal, but can be fine-tuned if required. An example of a measured waveform for a charge injection of 50 fC is shown in Fig. 4. Details of the design, simulation, and fabrication of CSAv3 can be found in [8].

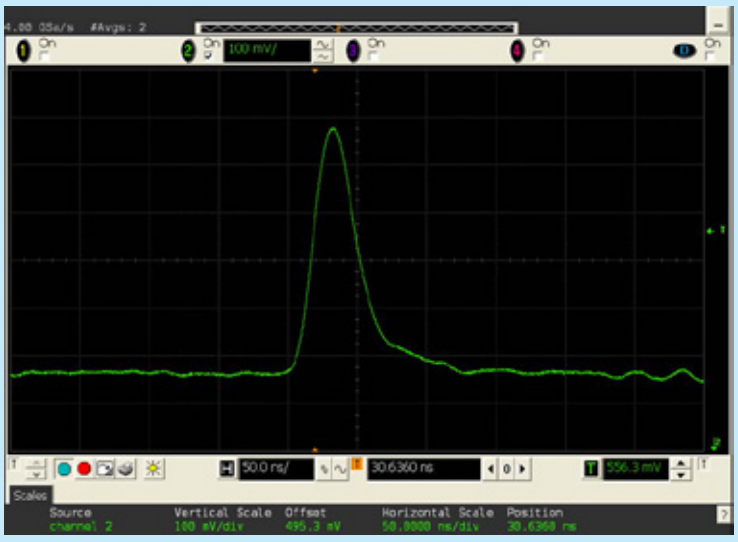

Fig. 4. *Amplifier response to a 50-fC input pulse with a 5-pF load. Note the 20-ns rise time and a return to baseline in 75 ns while retaining a noise value of ~1000 e^- rms.*

HalfGRAPH ASIC

HalfGRAPH2 is a 16-channel, 1 giga-sample-per-second waveform digitizing chip with 12-bit resolution (Figs. 5 and 6). It is being designed in the Taiwan Semiconductor Manufacturing Company (TSMC) 0.25-µm CMOS technology, using Tanner EDA design and simulation tools. The circuit's heritage is the TeV Array

Readout with GSa/s sampling and Event Trigger (TARGET) ASIC used for photomultiplier waveform sampling in the Cherenkov Telescope Array [9]. Each channel of this digitizer chip has a two-stage analog storage mechanism. In the first stage, a short sampling array is subdivided into two sample windows, each with 32 switched-capacitor storage cells. In the second stage, in a ping-pong fashion, as one sample window is filling, the other is transferred into a larger storage array. This storage array has 8192 cells, organized as two banks of 64 rows of 64 samples each (also called a storage window) for every channel. This results in a continuous sample of 8.192-μs length before being overwritten in a circular buffer.

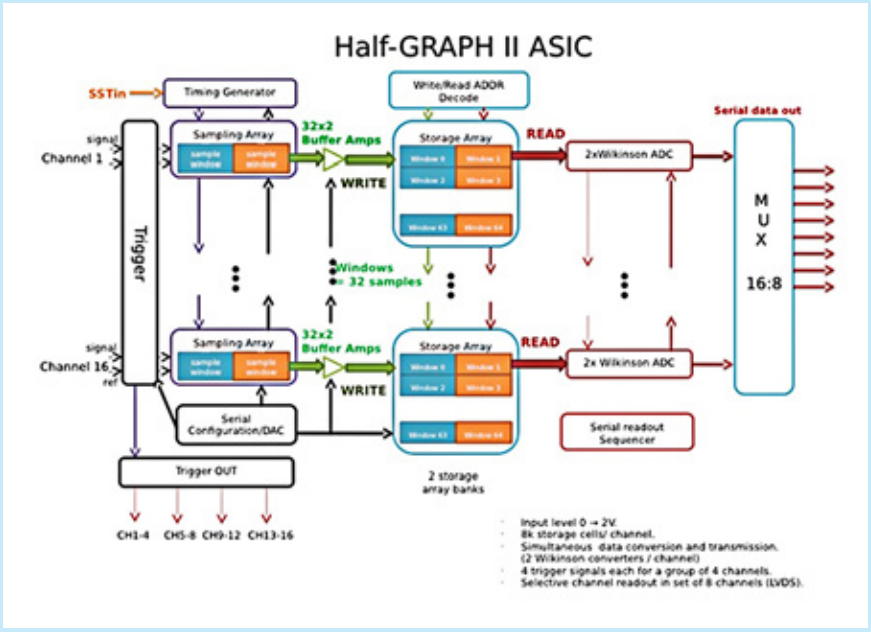

Fig. 5. *Functional schematic of the HalfGRAPH2 ASIC design (described in detail in the text).*

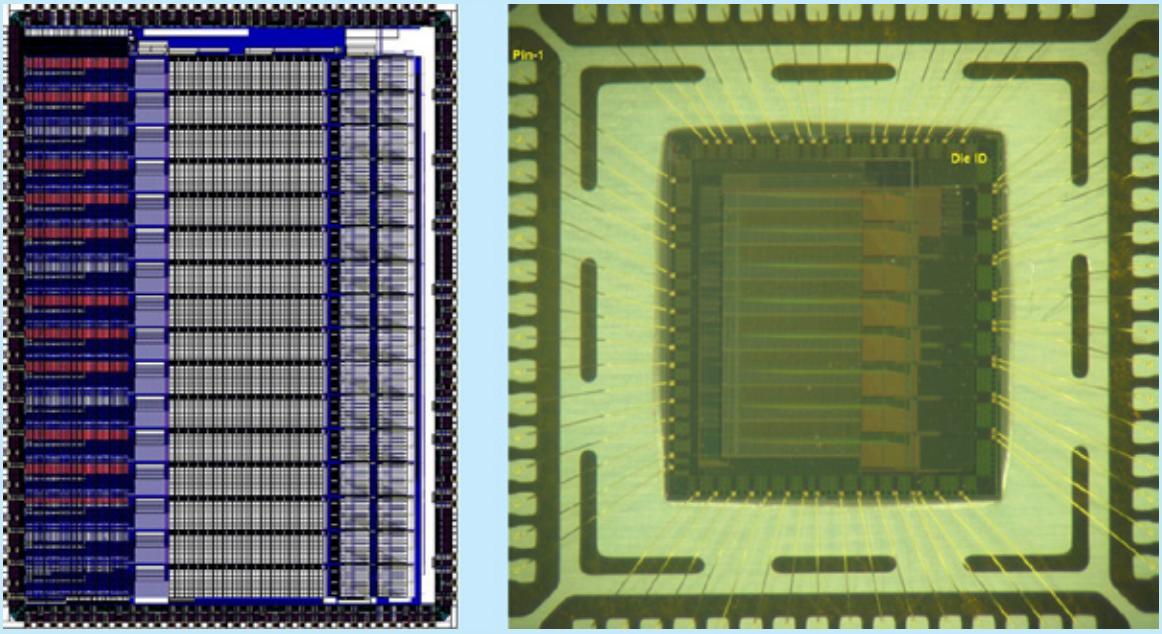

Fig. 6. *HalfGRAPH2 16-channel ASIC layout (left) and die mounted in carrier (right).*

The input analog trigger circuit has four digital output lines that notify a control FPGA of a new event. A trigger pulse is set in place if the measured signal on a channel is higher than a preset threshold. Trigger lines are organized to cover channels 1-4, 5-8, 9-12, and 13-16. This allows finer localization of the strip where the event occurred. The trigger arrival into the FPGA marks the address in the storage array of the samples for that event.

A DC input is applied to the input of the HalfGRAPH in all channels to bias the signal chain so that it is in range of the ADC. This pedestal must be subtracted out after digitization, so the ability to force synchronous triggers allows the pedestal to be measured for all channels and all 8192 samples (Fig. 7). Routines must be developed to measure and accumulate the average pedestal per memory location so that its subtraction can become a noiseless calculation.

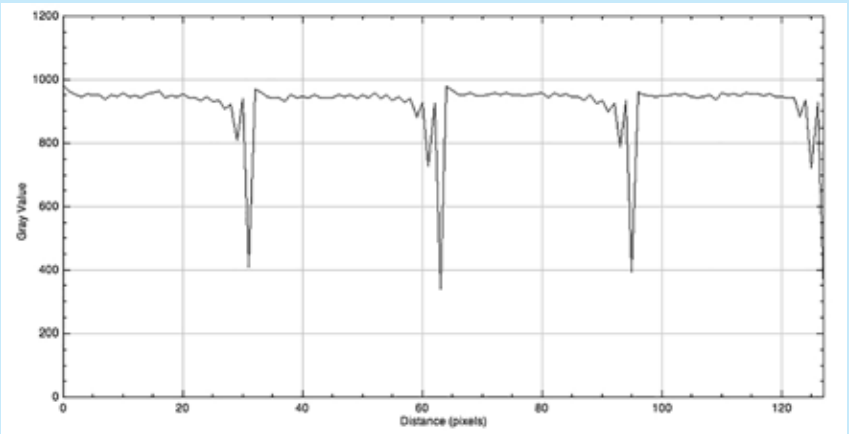

Fig. 7. *Single-channel HalfGRAPH2 output of a 128-sample (128 ns) subset, each measured 20 times, of the 8192 samples of the baseline of the CSAv3 output (no input pulse), showing the distributions of fixed DC pedestal per sample that must be stored and subtracted. The repetitive DC levels seen in the last couple of samples of each group of 32 are believed to be due to high via-contact resistance on long bus lines. This should be fixed in the GRAPH ASIC, but they do subtract out (e.g., Fig. 11).*

In order to digitize the acquired signal (e.g., Fig. 8), each channel uses two banks of 12-bit Wilkinson ADCs. An FPGA selects the storage window to be digitized. Thirty-two analog samples in parallel on all 16 channels of the storage window are converted concurrently into digital values using comparators, a voltage ramp, and counting (12-bit counter) with a 500-MHz dual-phase clock until the comparator fires when the ramp exceeds the analog value on the cell. It takes 4.1 µs to complete the digitization. At this point, the 32 time samples of 12-bit data are sent out serially over Low Voltage Differential Signal (LVDS) lines with a 250-MHz clock to the FPGA in 1.5 µs (=12×32/250 MHz). This is done for a subset of eight channels in parallel, chosen by the FPGA based on trigger information, allowing the centroid calculation using the properly filtered amplitude derived from the waveform. When the data transfer begins, the next window is digitized by the second Wilkinson converter, which takes over the next transmission, saving 1.5 µs.

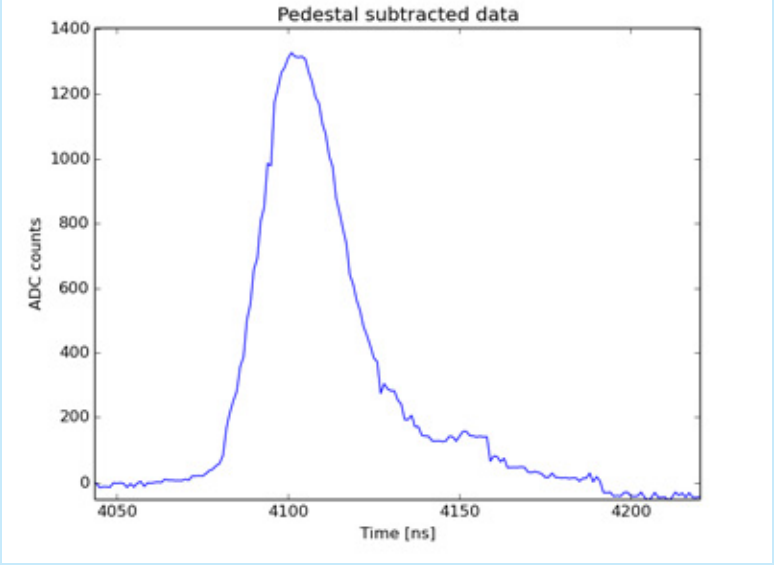

Fig. 8. *Single 50-fC pulse input to CSAv3 and digitized by the HalfGRAPH2 (pedestal subtracted). Residual high-requency noise is easily filtered with a simple 7-bin "top hat" filter kernel.*

As the FPGA has the address of the events in the storage array, it can prevent the overwriting of those cells. Therefore, the throughput of the system is limited by the 4.1-µs conversion time of the ADCs. The maximum throughput of one channel is 240 kHz, but there is no dead time at rates below this frequency due to the multiple buffering. With five independent ASICs per axis, the event rate that can be supported is 1.2 MHz. The readout rate can be greatly increased by decreasing the bit resolution. For a 10-bit conversion, the event rate could reach 5 MHz. As the event data will be digitally filtered by the FPGA processing, 10 bits will most likely be more than enough to achieve a high signal-to-noise ratio.

FPGA Controller and Integrated Readout Electronics for 50-mm Detector

In parallel with the ASIC testing described above, but slightly delayed to take advantage of what we learned, we designed the electronics layout for the full 160 channels of the 50 mm × 50 mm anode readout (Fig. 9). The sensitive preamps must be mounted close to the anode to minimize capacitance loading of the input, and the HalfGRAPH2 digitizing ASICs must be close to the preamp outputs to minimize their output load. Given these constraints, as well as the desire to fit the electronics into a small enclosure mounted directly to the detector backplate (Fig. 10), we decided to construct two printed circuit boards: an amplifier board with 10 CSAv3 chips and a digitizer board with 10 HalfGRAPH2 chips and two FPGAs (ArtixAX200), one for each axis, X and Y. The digitizer board will interface with a downstream FPGA development board (e.g., SP601) via 11 LVDS pairs.

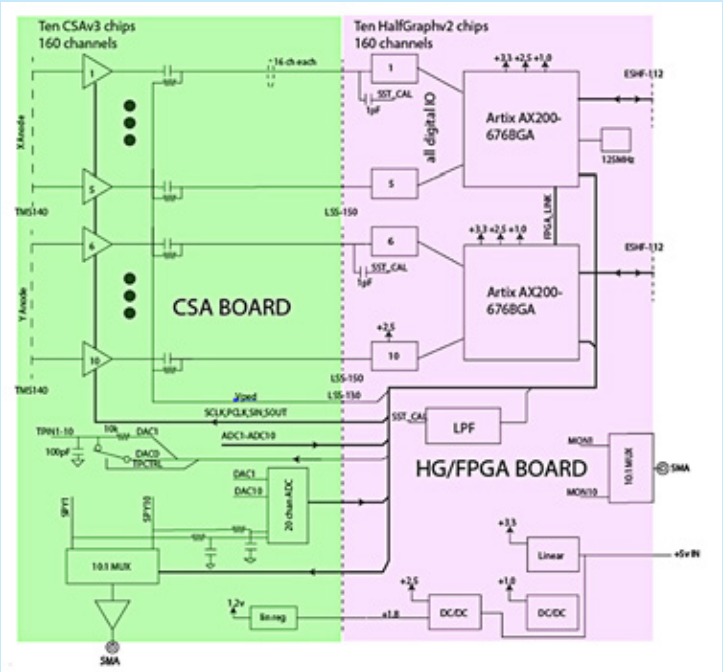

Fig. 9. *High-level schematic of 50-mm detector electronics, including a 160-channel amplifier board (left) and 160-channel digitizer board with two FPGAs to control ASICs and calculate event centroids (right).*

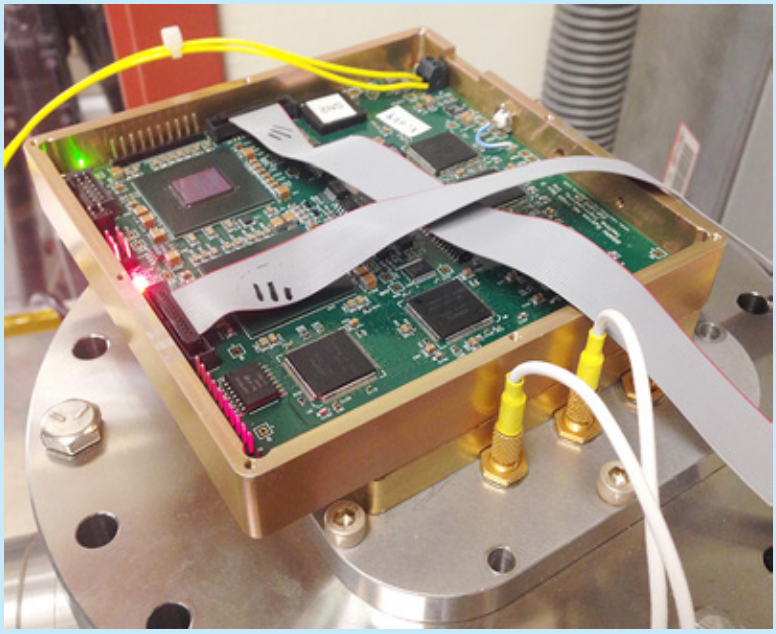

Fig. 10. *Amplifier (bottom) and digitizer (top) boxes mounted to 50-mm detector backplate.*

The 160 total anode channels (80×80) are input to a CSAv3 amplifier board using two Samtec TMS-140-01-S-D connectors, and the 160 amplified signals pass through an inter-board connector (Samtec LSS-150-02-F-DV-A) to the ten HalfGRAPH2 chips on the digitizer board. Additional connectors also exist for inter-board power, control, and command/data out.

The main data interface (using 11 LVDS lines running at 100 MHz double data rate, DDR, to the development board) communicates with both FPGAs, X and Y, and is controlled by the downstream host. Initially in raw output mode, we transmit all 160-channel samples of 128 ns duration just for triggered

events, achieving 8000 events/s using both X and Y interfaces. Eventually, when the internal FPGAs are tasked with calculating the centroids themselves, only one interface (X) will be needed, as the bandwidth of sending just X, Y, and pulse-height for each event is much smaller, so the rate can reach 16 Mevents/s.

The boards have been fabricated, installed in their boxes, and coupled to the 50-mm detector backplate (Fig. 10). We can test them either with test pulses capacitively coupled into their input or directly with photon events from the 50-mm detector. Learning to control the HalfGRAPH2 chip with the FPGA has been a long and laborious process, as the trigger timing of the analog gigasamples in the ring buffer is very sophisticated while maintaining synchronicity between the X and Y channels. We are now able to read out in full raw-data mode photon events into our computer at 180 Hz (limited by the "ZED" board to Ethernet interface), which will allow us to check our event centroiding algorithms and finite impulse response (FIR) filtering techniques. These can then be incorporated directly into the firmware to decrease the downstream bandwidth and thereby increase the output event rate to the MHz level.

We discovered three issues with the HalfGRAPH chip which we want to improve/fix in the GRAPH design. The two least significant bits (LSBs) of the Wilkinson ADC do not seem to function, so our pulses are sampled at 10 bits instead of 12. This is due to a race condition in the logic for the pseudo-synchronous counter used in the gray-code count generator, which has been reproduced in simulation. This probably won't affect the spatial resolution, since we will be combining many of the nanosecond samples with a FIR filter, effectively increasing the sample resolution. Second, the combined total power dissipation of the two boards comes to 11.4 W (including the two FPGAs and the voltage regulator inefficiencies). We have not yet designed a method to remove this power in vacuum, so we want to design the GRAPH chip to achieve a lower power level, and the 100-mm enclosure box and boards to extract this power to a better heat sink. We also want to correct the layout issue that causes the pedestal features seen in Fig. 11.

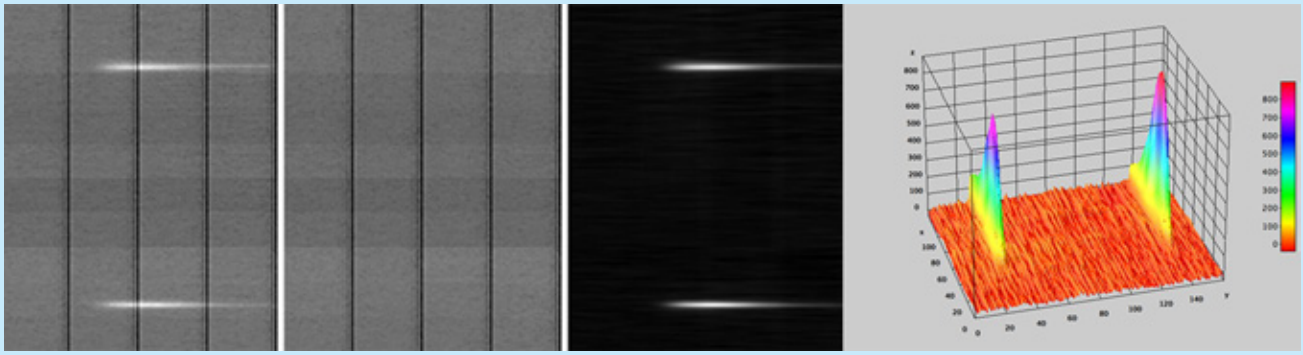

Fig. 11. *Examples of raw mode output from all 160 channels (vertical/spatial axis) of 128 ns of data (horizontal/temporal axis).* Left: *Raw data from a single amplified photon event showing detector X axis in the top set of 80 channels and detector Y axis in the bottom 80 channels.* Left center: *Pedestal of those memory locations.* Right center: *Pedestal-subtracted image showing just the photon data.* Right: *3-D representation of the right center image, with charge events occupying ~8 channels in both the X and Y axes.*

50-mm XS Detector

There are two key aspects to our flight-like 50-mm and 100-mm XS detector designs. The first is a photolithographic and laser-cut XS anode design made with polyimide. Polyimide's dielectric constant is lower than that of alumina ceramic by a factor of three, resulting in lower individual strip capacitance and thus lower amplifier noise. The top strip pattern is first etched in the copper, after which a laser ablates the material between the strips. This top layer is then bonded to the bottom strip pattern etched

on a much thicker polyimide substrate. The input side of the anode is shown in Fig. 12, installed in the 50-mm XS detector, with measured strip capacitances matching our design model. Outputs from the 80×80 strips go through a hermetic seal consisting of 2×80-pin connectors sealed with vacuum epoxy (Fig. 13). The other key aspect of our detector is using a Kovar and ceramic brazed body to mount the MCPs over the XS anode. This technique is used in vacuum-image-tube construction to make a strong, robust, and clean detector that can survive launch stress. Figure 12 shows the brazed body of the 50-mm detector mounted over our XS anode onto a vacuum backplate with three high voltage (HV) feedthroughs (MCPs removed to show the anode below).

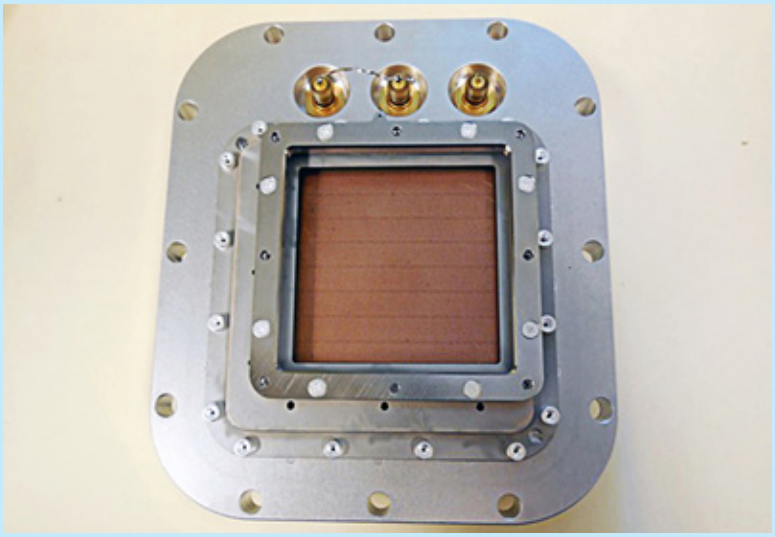

Fig. 12. *View of windowless 50-mm XS detector mounted on a vacuum flange with three HV feed-throughs showing the XS anode (MCPs removed).*

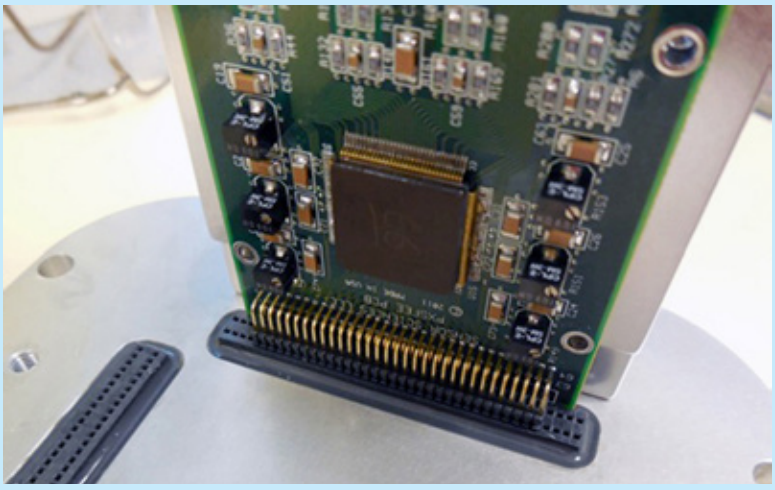

Fig. 13. *External side of detector showing 80-contact feed-throughs (×2) sealed with epoxy and a 64-channel preamp board plugged into one axis.*

Imaging Results with 50-mm Detector

Since the readout firmware is still being developed, we used our existing PXS2 electronics and 64-channel amplifier boards to read out the central 64×64 strips of this 80×80 XS anode. This corresponds to a central active area of 40 mm×40 mm. The results below use a stack of two MCPs from Photonis USA with 10-µm pores on 12.5-µm centers, 53.7 mm×53.7 mm, and 60:1 L/d ratio (600-µm-thick each). We measured the spatial resolution and linearity, and acquired flat fields to measure the UV response uniformity to 183-nm light from a Hg pen-ray lamp.

To measure the spatial resolution, we used a pinhole mask grid mounted directly on the input MCP. The pinholes are 10 µm in diameter and spaced 1 mm apart on a square grid (Fig. 14), an excellent method of sampling the Point Spread Function (PSF) across the field of view. To measure the spatial resolution, we had to bin the X, Y event data to 8192×8192 (5-µm pixels) to resolve the PSF. The inset of Fig. 14 shows the X dimension PSF (top strips) of a single pinhole. The average spatial resolutions in the X and Y dimensions were 17.5 µm FWHM and 22 µm FWHM, respectively.

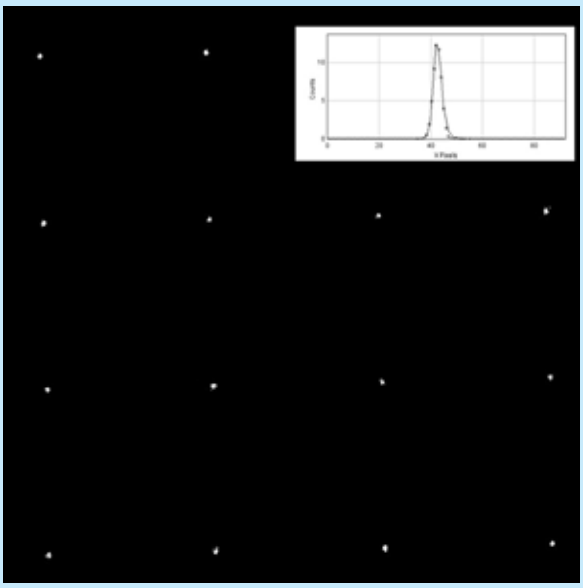

Fig. 14. *UV image of pinhole mask of 10-µm holes on 1-mm square grid. Inset shows the PSF of a single hole with resolution of ~4 pixels FWHM (20 µm).*

The detector linearity can also be measured with the pinhole mask data, as the pinholes are uniformly spaced at 1 mm. Figure 15 shows residuals (in µm) to a linear fit to pixel position of the pinhole vs. pinhole number. The ±15-µm deviation from zero is smaller than the detector spatial resolution measured above, and comparable to the hexagonal 12.5-µm pore spacing. This measurement attests to the accuracy of the photolithographic anode strip regularity.

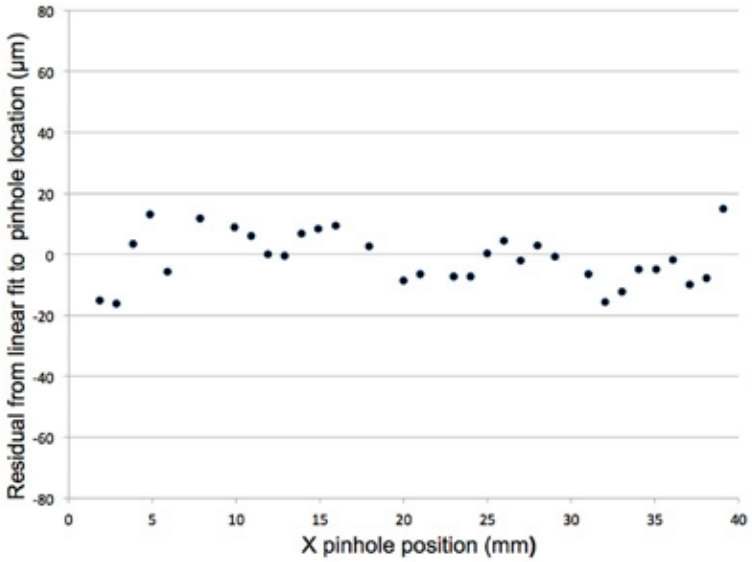

Fig. 15. *Residuals to linear fit of derived pinhole position across central 40 mm of the 50-mm XS detector.*

No detector has a perfectly flat response. For MCP detectors, a uniform input illumination can reveal MCP sensitivity variations plus nonlinearities in the X, Y determination of the charge cloud centroid by the anode. To measure response flatness, we collected more than 30 billion counts to achieve 460 counts per 5-µm pixel. Figure 16 is a small, 2.5 mm × 2.5 mm section of a UV flat field. There is a hint of fixed-pattern noise, and compressing the data in both dimensions reveals the presence of a differential nonlinearity at the strip spacing in the Y (bottom) dimension. The effect is at the 3% level peak-to-peak, and can be corrected with a lookup table. We used this flat field to divide another flat field taken the next day (140 counts per 5-µm pixel) and binned to 20-µm pixels. The second flat had only 34% of the counts of the first flat, but the resultant divided image, Fig. 17, shows no fixed pattern, and is consistent with Poisson statistics expected from the two images. The image pixel values histogram (Fig. 17 inset) has a standard deviation of 2.3%.

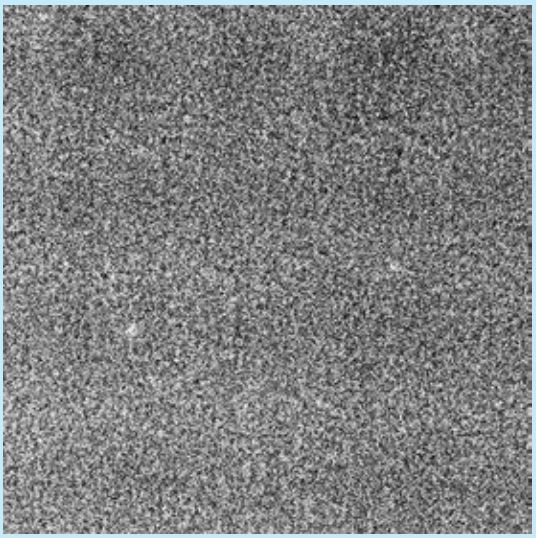

Fig. 16. *Small section of very deep (2500 cts/pxl) flat field showing a small but noticeable fixed pattern noise.*

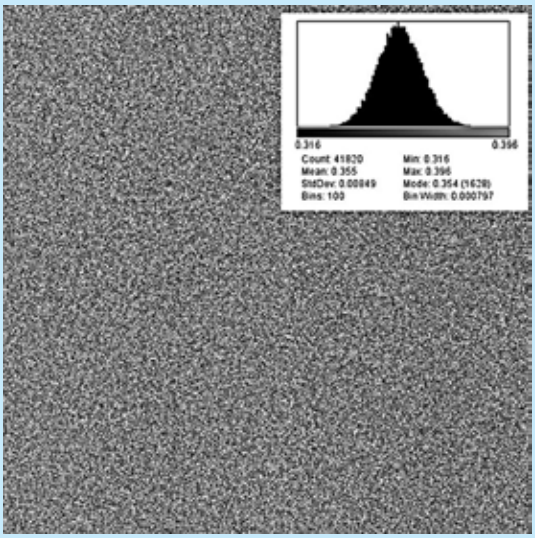

Fig. 17. *Image from Fig. 16 divided by deeper flat field. Residual variation consistent with expected Poisson statistics (2% standard deviation, inset).*

Environmental Testing of 50-mm Detector

One of the main goals of this SAT program was to advance the TRL of the 50-mm detector system. Since the new 50-mm detector on its backplate is a new design, we decided to go beyond testing its performance on the bench, and confirm its performance at temperature extremes, as well as its ability to survive the g-forces of standard rocket launches.

The detector and front-end electronics were mounted onto a vacuum housing inside a thermal chamber and cycled from –30°C to +45°C (Fig. 18). We measured detector performance from –15°C to +45°C, allowing the temperature to equilibrate for about one hour at each test level before taking a deep-UV flat-field image. Because we had a smattering of small dead spots on the detector that acted as spatial fiducials, we were able to notice a shift of ~30 microns in the image over a 60°C temperature swing. Since this shift was in the MCP-bias direction, we believe it was due to electron-cloud kinematics caused by thermally induced MCP gain variation. It speaks to the XS detector's excellent spatial resolution that we can even measure this effect and in all other measures – resolution, background rate, and dynamic range – the detector worked flawlessly.

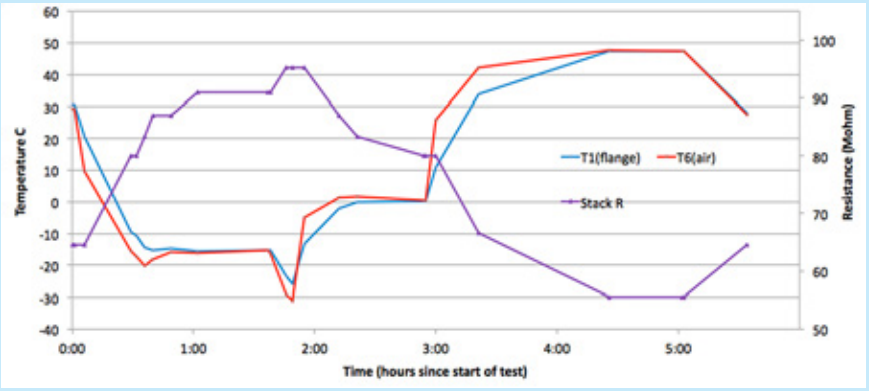

Fig. 18. *Detector temperature and MCP resistance during thermal test of XS detector.*

We also used the SSL vibration table to vibrate the detector (without the electronics) to 14.1 g (rms) as recommended in the GSFC General Environmental Verification Standard, GEVS (GSFC-STD-7000A). Figure 19 shows the detector backplate (air side) on the test fixture, and Table 1 shows the vibration spectrum levels applied to the detector. UV imaging performance was identical before and after vibration, showing this new detector design is ready for flight vibrations.

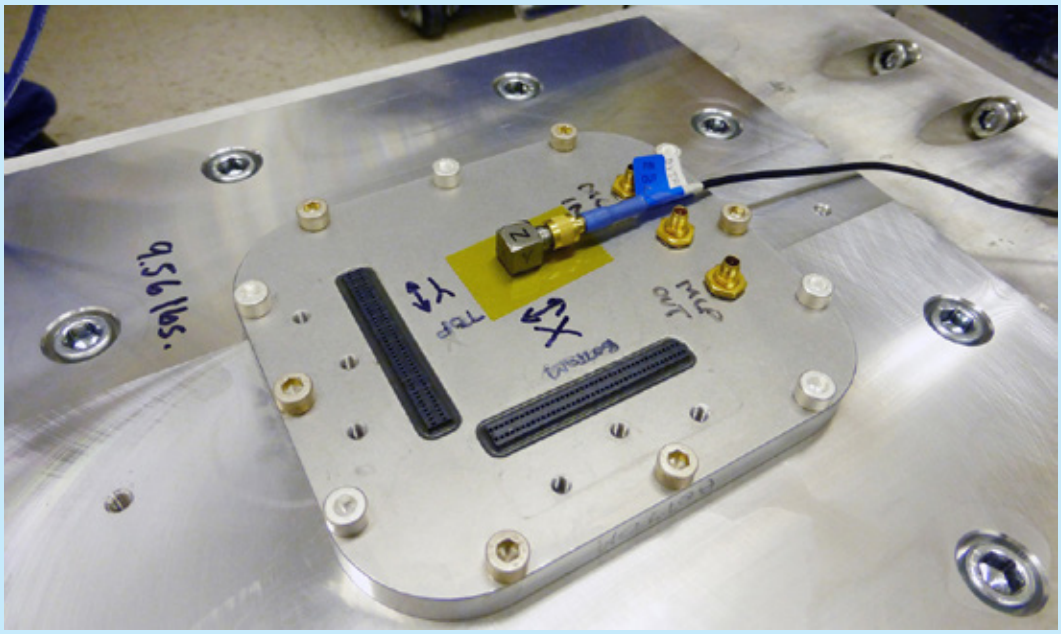

Fig. 19. *50-mm XS detector mounted on vibration table at SSL.*

Frequency (Hz)	g^2/Hz	dB/Octave
20	0.026	5.97
50	0.16	0
800	0.16	-5.97
2000	0.026	–

Table 1. *Vibration frequency spectrum (14.1 g rms).*

Radiation Testing of the CSAv3 and the HalfGRAPH2 ASIC

To test the resilience of the new ASICs to TID, we spent two days at the University of Massachusetts Lowell Radiation facility, which has the ability to expose microelectronics to ^{60}Co gamma rays at controllable rates and durations (Table 2), to achieve a calibrated dose traceable to NIST standards using a calibrated Bruker Biospin dosimeter. For the CSAv3, we tested the ASICs both unpowered and battery-powered during the exposure, first in steps of 25-kRad dose, with performance testing in between. We measured bias current, pulse gain, and noise of every channel of the eight chips and did not detect a change (Fig. 20) or failure up to a TID of 486 kRad, more dose than we would expect for a mission to Jupiter. For the separate exposure of the HalfGRAPH2, our performance test consisted of driving the input with a linear voltage ramp and measuring the linear increase in the digital output codes for all channels, and again, did not see a change in performance to 236 kRad. We have not yet tested either ASIC with energetic ions to see if they suffer from single-event upsets (SEUs) or latch-ups.

Date	Dose Rate Rad/sec	Distance (inches)	Sample ID#	Exposure Length hr:min:sec	Incremental Dose Rad (Si)	Cumulative Dose Rad (Si)
04/04/2017	53.3	14.5	#1, 3	0:07:53	25,187	25,187
	"	"		0:07:53	25,187	50,375
	"	"		0:07:53	25,187	75,562
	"	"		0:07:53	25,187	100,749
04/04/2017	53.3	14.5	#2, 4	0:07:53	25,187	25,187
	"	"		0:07:53	25,187	50,375
	"	"		0:07:53	25,187	75,562
	"	"		0:07:53	25,187	100,749
04/05/2017	102.9	9.5	#2, 4	0:07:27	45,996	146,745
	"	"		0:17:31	108,150	254,895
	"	"		0:33:22	206,000	460,895

Table 2. *Dose and dose rate applied to CSAv3 ASIC samples.*

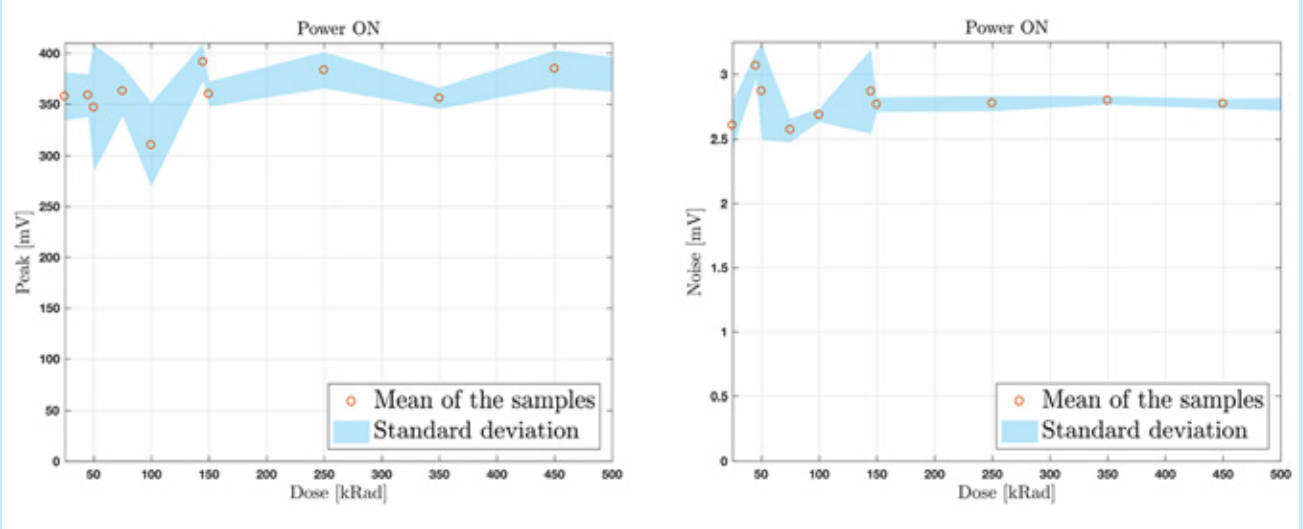

Fig. 20. *Gain (left) and rms noise (right) of the CSAv3 CSA ASICs vs. TID from ^{60}Co gamma rays. Six chips with 16 channels each were tested and the standard deviation was derived from the variation of the channels. Not all chips received the full dose.*

The 100 mm × 100 mm XS Detector

The latest SAT program is essentially continuing to scale the XS technology to larger format size plus other improvements to increase its TRL. We plan to double the size (quadruple the area) of a XS detector to 100 mm × 100 mm active area, while demonstrating high TRL with vibration and thermal tests. This larger size is not targeting a specific mission, but will demonstrate a large-format design that can be scaled easily to a similar format while reducing risk. Along with a new detector mechanical design, we plan to combine our working ASIC designs into a single ASIC (the "GRAPH" chip) using 130-nm CMOS technology to reduce readout volume, mass, and complexity. As such, we are converting all our sub-circuit libraries used in the 250-nm process HalfGRAPH2 to the TSMC 130-nm process, and then combining with the CSAv3 into the GRAPH ASIC (The CSAv3 was already designed in the 130-nm process). We also plan to continue and demonstrate the radiation hardness of the existing ASIC designs with energetic particles, and maintain this hardness in the new GRAPH ASIC.

The 100 mm × 100 mm Mechanical Design

The brazed-body design (Fig. 21) is scaled up by approximately a factor of two, having an output aperture below the MCPs of 103 mm while the active field of view is set by a 100 × 100 open mask of 25-µm thickness between the top and bottom MCPs. It is designed to hold square Photonis USA MCPs up to 110 mm in size. The XS anode design (Fig. 22) is also scaled to 160 strips per axis, but with a slight increase in strip pitch from the 635 µm of the 50-mm anode to 645 µm for the 100-mm anode. This results in a 103 mm × 103 mm anode with enough strips at the edges to sample the 100-mm field of view fully. The anode outputs are now distributed on all four corners of the anode in a "pinwheel" fashion so the mechanical cutouts through the vacuum backplate can be more symmetric for increased strength. It also facilitates the electronics board layout where the GRAPH chips can be spread out on the printed circuit board. The vacuum backplate is made of stainless steel and can be weight-relieved (Fig. 23).

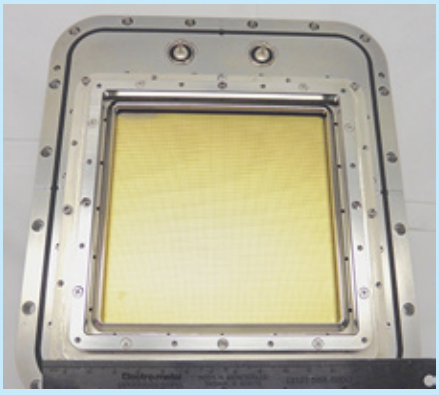

Fig. 21. *View of windowless 100-mm XS detector mounted on a vacuum flange with two HV feed-throughs showing the XS anode (MCPs removed).*

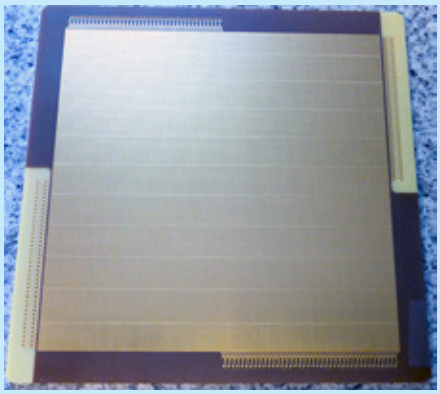

Fig. 22. *Fabricated 100-mm XS anode. Note the four distributed output connectors along the edges of the anode.*

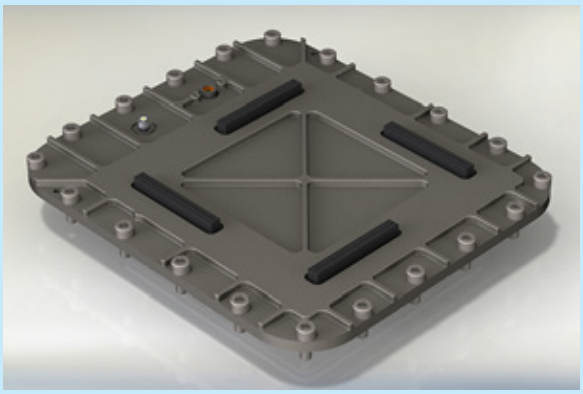

Fig. 23. *Rendering of a 100-mm detector stainless steel backplate (air side) showing the 4 × 80-channel anode connectors equally spaced around the anode perimeter with a possible weight-relieving scheme.*

103-mm XS Anode

We have fabricated the new 103-mm square anode with the new pinwheel output arrangement using the same techniques of laser cutting and bonding of a polyimide top layer as we did with the 50-mm anode. Resistance and capacitive measurements were as expected, with about a factor-of-two increase due to the doubling of the strip length. This should increase the readout noise of the CSAs from that of the 50-mm anode by only 50% given the baseline, no-load noise of the amps. Figure 22 shows the new, gold-coated anode.

100-mm Detector Brazed Body and Backplate

The brazed body design is mostly a scaled-up version of the 50-mm design, but the body is more symmetric as the signal outputs are now coming off all four sides of the anode, so this must be accommodated by adding the cantilevered shelf to mount the MCPs directly over the anode center. The backplate now has four cutouts to let the four signal connectors (80 channels each) through, again with an epoxied hermetic seal. The pinwheel design puts much more steel between the cutouts, increasing the strength of the backplate. Initially, we have not weight-relieved the first article, but plan to do that for the second backplate in hand after the vibration tests of the first. We have welded two commercial-off-the-shelf (COTS) safe HV (SHV) connectors to provide the MCP bias high voltage. Figure 21 shows the brazed body attached to the backplate with the XS anode showing (MCPs not installed).

GRAPH ASIC

Given our success with the CSAv3 in 130-nm technology and design libraries, we are planning to combine the amplifier and digital converter on the same chip using this technology. Design techniques will be employed to shield the low-noise inputs from the high-speed digital outputs. However, to hedge our bets, we are using multiplexors to allow bypassing of the GRAPH CSA circuit (Fig. 24) in case the induced noise proves problematic. The resulting ASIC would then act like an improved HalfGRAPH, which could be used with the existing CSAv3.

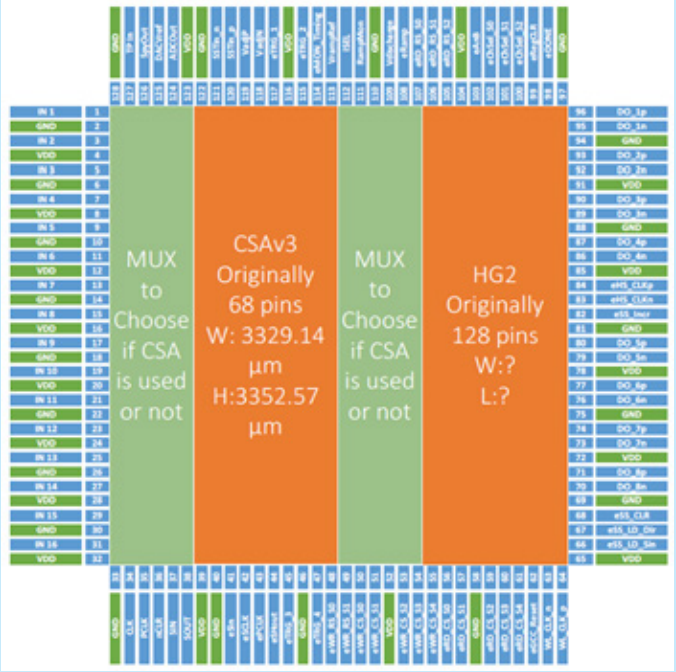

Fig. 24. *Proposed GRAPH ASIC layout with analog amplifiers on left and sampling/digital conversion on right. Multiplexers (MUXs) allow the amplifiers to be bypassed.*

As of June 2017, most sub-circuits have been designed using the Cadence software suite and 130-nm CMOS design rules of TSMC. One channel has been simulated end-to-end, and final layout of the 16 channels has begun. The initial power estimates are 500 mW per chip, so a 20-chip readout for the 100-mm detector (320 channels) should dissipate ~10 W plus the FPGA power and regulator inefficiencies. The comparators are a dominant contributor to the power budget, at ~200 mW per chip. Investigations are taking place to use a dynamic biasing scheme for the comparators by turning them on only when a channel is triggered. The channel trigger will be set low, many sigma above the noise threshold, while maintaining a separate threshold for events to not increase false event triggers. This should reduce the comparator power by a factor of ~5.

Path Forward

The 100-mm detector (with Photonis MCPs) has been fabricated and is ready to go into a special vacuum chamber matched to its size. Testing its imaging performance can start immediately using the laboratory PXS electronics, but not over its whole field of view. The readout electronics for the 50-mm detector have established that the HalfGRAPH and CSAv3 ASICs meet expectations and can provide the raw data to meet specifications. The next phase is to incorporate our triggering and centroiding algorithms into the FPGA firmware so that we can sparsify the extremely high data load to only transmit X and Y locations of photon events, and confirm the imaging performance meets or exceeds the performance demonstrated with the laboratory PXS2 electronics.

This effort is directly transferable to developing a 100-mm detector readout using the same logic as the 50-mm system scaled up by a factor of two in each dimension. In fact, some aspects are easier in that there are twice as many components, but four times the area. This might make the thermal design easier as well. Boards will have to be laid out and electronics boxes fabricated for the new size, this time incorporating methods for better heat extraction.

In parallel, the new GRAPH ASIC is being designed and is expected to undergo fabrication in fall 2017. Test boards will be built at the University of Hawaii to measure its performance, and readout boards that incorporate the new design will be started in Berkeley, taking advantage of the lower power and simplified layout, provided by the 2-for-1 decease in chip count.

References

[1] J. Vallerga, J. McPhate, A. Tremsin, O. Siegmund, R. Raffanti, H. Cumming, A. Seljak, V. Virta, and G. Varner, "*Development of a flight qualified 100×100 mm MCP UV detector using advanced cross strip anodes and associated ASIC electronics*," Proc. SPIE, **9905**, 99053F (2016)

[2] K. Hoadley, K. France, N. Nell, R. Kane, T.B. Schultz, M. Beasley, J.C. Green, J.R. Kulow, E. Kersgaard, and B.T. Fleming, "*The assembly, calibration, and preliminary results from the Colorado high resolution Echelle stellar spectrograph (CHESS)*," Proc. SPIE, **9144** (2014)

[3] P. Scowen et al., "*The Star Formation Observatory (SFO) mission to study cosmic origins*," Proc. SPIE, **7010**, 115 (2008)

[4] K. Sembach, M. Beasley, M. Blouke, D. Ebbets, J. Green, F. Greer, E. Jenkins, C. Joseph, R. Kimball, J. MacKenty, S. McCandliss, S. Nikzad, W. Oegerle, R. Philbrick, M. Postman, P. Scowen, O. Siegmund, H.P. Stahl, M. Ulmer, J. Vallerga, P. Warren, B. Woodgate, and R. Woodruff, "*Technology Investments to Meet the Needs of Astronomy at Ultraviolet Wavelengths in the 21st Century*," Astro2010: The Astronomy and Astrophysics Decadal Survey, Technology Development Papers, no. 54 (2009)

[5] J. Vallerga, R. Raffanti, A. Tremsin, O. Siegmund, J. McPhate, and G. Varner, "*Large-format high-spatial-resolution cross-strip readout MCP detectors for UV astronomy*," SPIE **7732** (2010)

[6] X. Michalet, R.A. Colyer, J. Antelman, O.H.W. Siegmund, A. Tremsin, J.V. Vallerga, and S. Weiss, "*Single-quantum-dot imaging with a photon-counting camera*," Current Pharmaceutical Biotechnology **10** (5), 543-558 (2009)

[7] F.B. Berendse, R.G. Cruddace, M.P. Kowalski, D.J. Yentis, W.R. Hunter, G.G. Fritz, O. Siegmund, K. Heidemann, R. Lenke, A. Seifert, and T.W. Barbee Jr., "*The joint astrophysical plasmadynamic experiment extreme ultraviolet spectrometer: resolving power*," SPIE Conference Series, **6266**, 31 (2006)

[8] H.S. Cummings, A. Seljak, G. Varner, J. Vallerga, R. Raffanti, and V. Virta, "*CSAv3, a fast, low-power and low-noise charge sensitive amplifier ASIC chip for a UV-imaging detector*," JINST, submitted (2016)

[9] K. Bechtol, S. Funk, A. Okumura, L.L. Ruckman, A. Simons, H. Tajima, J. Vandenbroucke, and G.S. Varner, "*TARGET: A multi-channel digitizer chip for very-high-energy gamma-ray telescopes*," Astroparticle Physics, **36**, 156-165 (2012)

For additional information, contact John Vallerga: *jvv@ssl.berkeley.edu*

Raising the Technology Readiness Level of 4.7-THz Local Oscillators

Prepared by: Qing Hu (MIT)

Summary

The 63-μm (4.744 THz) [OI] fine-structure line is an important spectral line for astrophysics observations. Despite the great potential, however, astrophysical observation of the [OI] line has rarely been performed because the 4.744-THz frequency is beyond the reach of most implemented local oscillators (LOs) in sensitive heterodyne receivers involving cryogenic mixers. In this three-year NASA Strategic Astrophysics Technology (SAT) project, we plan to raise the Technology Readiness Level (TRL) of THz quantum-cascade lasers (QCLs) for LO applications to 5 or beyond, bridging the "mid-TRL gap" between a promising enabling technology and a mission-ready component. The project started in March 2016 and is planned to conclude in February 2019.

The objective will be achieved by developing antenna-coupled 3rd-order distributed feedback (DFB) lasing structures, and in parallel, designing and growing high-performance quantum-cascade gain media with peak frequency around 4.7 THz. By the end of the project, we will develop single-mode DFB lasers with frequency within 10 GHz of the target 4.744-THz line, continuous wave (*cw*) output power of ~5 mW, wall-plug power efficiency (WPE) of ~0.5% at an operating temperature of ~40 K, and beam patterns narrower than 10×10 degrees^2.

The project will be carried out in the Principal Investigator's laboratory at MIT, with the molecular beam epitaxy (MBE) wafers provided by Dr. John Reno at Sandia National Laboratories through a user agreement.

During the previous year, we completed the design of antenna-coupled 3rd-order DFB structures, and generated fabrication masks based on the design. We also completed the design of quantum-cascade structures and based on this design grew three MBE wafers. We have started the microfabrication process based on these wafers and masks.

Background

The 63-μm (4.744 THz) [OI] fine-structure line is the dominant cooling line of warm, dense, neutral atomic gas. Because of its great intensity in high-UV photodissociation regions (PDRs) and shocks, the [OI] 63-μm line is superior for probing regions of massive star formation and the centers of galaxies. It is a unique probe of PDRs, shock waves from stellar winds/jets, supernova explosions, and cloud-cloud collisions. These radiative and mechanical interactions shape the interstellar medium of galaxies and drives galactic evolution. The size scale of the interactions can excite [OI] emission over many parsecs. Moreover, the emission regions are often complex, with multiple energetic sources processing the environment. Spectrally resolved observations of the [OI] line with a heterodyne receiver array will allow users to disentangle this convoluted interaction and permit the study of the energy balance, physical conditions, morphology, and dynamics of these extended regions. In this way, such a receiver array will provide new and unique insights into the interrelationship of stars and gas in a wide range of galactic and extragalactic environments.

This project mainly addresses NASA's Strategic Subgoal 3D, "*Discover the origin, structure, evolution, and destiny of the universe, and search for Earth-like planets*." It also addresses NASA's Strategic Subgoal 3A, "*Study planet Earth from space to advance scientific understanding and meet societal needs*"; and NASA's Strategic Subgoal 3C, "*Advance scientific knowledge of the origin and history of the solar system, the potential for life elsewhere, and the hazards and resources present as humans explore space*." The development will significantly reduce the risk of several proposed suborbital projects such as the Gal/Xgal U/LDB Spectroscopic/Stratospheric THz Observatory (GUSTO), a long-duration balloon (LDB) payload. The proposed systems this project will develop include a seven-element heterodyne receiver array for the 4.744-THz [OI] line.

DFB structures are required to generate robust single-mode lasing output. Currently, 1st-order, 2nd-order, and 3rd-order DFB lasers have been demonstrated (the grating period of an nth-order DFB grating is n times the half-wavelength in the gain medium). Among these, the 3rd-order DFB structures show the greatest promise for LO applications, because of their compact size and good beam patterns. Despite the promise of 3rd-order DFB lasers, the phase mismatch limits total length to less than 1 mm so the beam is still quite divergent. In addition, the low extraction efficiency yields a low WPE of 0.1%. In this SAT project, we plan to further develop this promising technology by developing the following.

- Perfectly phase-matched 3rd-order DFB lasers, to generate even narrower beam patterns and higher output power levels;
- Novel antenna-coupled 3rd-order DFB structure to increase WPE; and
- Better-performance gain medium, peaked at 4.74 THz.

Objectives and Milestones

The project objectives are to develop single-mode DFB lasers with frequency within 10 GHz of the target 4.744-THz line, *cw* output power level greater than 5 mW, WPE ≥0.5% at an operating temperature of ~40 K, and beam patterns narrower than 10×10 degrees^2. The annual milestones are listed in Table 1.

Year	Milestones
Year 1 (3/2016 – 2/2017)	• Complete the design of perfectly phase-matched 3rd-order DFB lasers aimed for ~4.7 THz • Develop a high-yield dry-etching process using inductive-coupled plasma (ICP) to achieve clean and smooth sidewalls with high aspect ratios • Grow ~3 MBE wafers based on improved QCL designs • Fabricate devices using a combination of dry and wet etching
Year 2 (3/2017 – 2/2018)	• Continue to improve the fabrication process for higher quality and higher yield • Grow ~3 MBE wafers based on improved designs • Develop perfectly phase-matched ($n_{eff} = 3.00 \pm 0.02$) 3rd-order DFB with a modest value of $\alpha_m \approx 2\,cm^{-1}$ to ensure a robust single-mode operation and $\eta_{WPE} \approx 0.1\%$ • Design phase-matched 3rd-order DFB structures integrated with half-wave antennas
Year 3 (3/2018 – 2/2019)	• Grow ~3 MBE wafers based on improved designs • Develop phase-matched 3rd-order DFB coupled with integrated antennae with a more aggressive value of $\alpha_m \approx 10\,cm^{-1}$, achieving $\eta_{WPE} \approx 0.5\%$ with ≥ 5 mW power at ~40 K. The phase matching should be good enough for a long device for the high output power and with beam divergence ≤ 10×10 degrees^2

Table 1. *Milestones of this SAT project.*

Progress and Accomplishments

Prior to the beginning date of the current SAT project, we successfully developed a single-mode 3rd-order DFB laser that lases within 3 GHz of the target 4.744-THz [OI] line [1]. Although the power level is lower than desired due to imperfect phase matching and the lack of integrated antennas (which as discussed above will be pursued in the SAT project), it is adequate to pump a single-element hot-electron bolometer (HEB) mixer. One device has been integrated with the Stratospheric Terahertz Observatory (STO-2) LDB observatory. Unfortunately, the control electronics of this device were damaged by the sun during the flight, so no data was obtained.

The design of novel antenna-coupled, perfectly phase-matched 3rd-order DFB structures requires clever analysis and accurate numerical validation, which is what we accomplished during the first year of the project. Fabrication of the designed structures will require a sophisticated combination of dry and wet etching, which started in the past three months. The design and growth of high-performance THz gain media is also a highly challenging process. Aided with sophisticated numerical packages including Schrödinger and Poisson solvers, we completed the design of quantum-cascade structures and three MBE wafers were grown. The growth was carried out by Dr. John Reno at Sandia National Laboratories. Sandia has all the required equipment, and Dr. Reno has a long track record in the growth of record-setting THz gain media.

The design of high-power and single-mode DFB lasers requires innovative thinking and detailed numerical simulations, and both have been accomplished following a long history of innovation and technical know-how in the PI's group. We completed the design of antenna-coupled 3rd-order DFB structures and generated fabrication masks based on the design. We also designed quantum-cascade gain structures with the center frequency around 4.7 THz. Three MBE wafers were grown based on the design. We do not anticipate any change of direction in the project. We are on track to achieve our milestones as shown above, and anticipate achieving our objectives.

Path Forward

At this stage, we expect our remaining work will closely follow the annual milestones listed above.

Reference

[1] J.L. Kloosterman, D.J. Hayton, Y. Ren, W. Kao, J.N. Hovenier, J.R. Gao, T.M. Klapwijk, Q. Hu, C.K. Walker, and J.L. Reno, "*Hot electron bolometer heterodyne receiver with a 4.7-THz quantum cascade laser as a local oscillator*," Appl. Phys. Lett. **102**, 011123 (2013)

For additional information, contact Qing Hu: *qhu@mit.edu*

High-Efficiency Continuous Cooling for Cryogenic Instruments and sub-Kelvin Detectors

Prepared by: James Tuttle (NASA/GSFC)

Summary

This is a three-year development effort, which began in January 2017. Its goal is to advance the Technology Readiness Level (TRL) of a multi-stage magnetic cooling system, which will continuously cool detectors to 0.05 K and reject heat to 10 K. The device, based on adiabatic demagnetization refrigerators (ADRs), will have high thermodynamic efficiency and will simultaneously cool optics continuously at 2–4 K. It will exceed the cooling requirements of all currently conceived future space missions with cryogenic detector arrays. With a heat-rejection temperature of 10 K, it will be compatible with recently demonstrated extremely-low-vibration mechanical coolers. Since ADRs have no moving parts, it will enable an essentially vibration-free 300-K-to-0.05-K cooling system.

The development team is a group of technologists at NASA/GSFC with a wealth of experience in spaceflight and laboratory ADRs. In fact, this group developed and demonstrated the technology being advanced here. During the first five months of this effort, they completed the 10-to-4-K component design and analysis and performed extensive testing on an existing 10-K magnet and 10-to-4-K heat switch. In addition, the longest-lead procurements have been initiated.

Background

Several past, and many future astronomical instruments require cooling to sub-Kelvin temperatures to obtain high sensitivity. Newer generations of detector arrays need several μW of cooling at temperatures of 0.05 K and lower. Previous long-life space missions used single-cycle cooling devices with modest cooling powers, but these sub-Kelvin refrigerators are no longer adequate. As the detector technology has matured and the array size grows larger, demand has increased for higher cooling power and lower operating temperatures. Presently, several astrophysics flagship mission concepts require cooling of large superconductor-based focal planes to sub-Kelvin temperatures, including the Origins Space Telescope (OST, formerly Far-IR Surveyor) and Lynx (formerly the X-ray Surveyor); as well as an Inflation Probe, Explorers, and international cosmic-microwave-background- (CMB) polarization and absolute-spectrum experiments. Sub-Kelvin energy-resolving detectors would enhance the Habitable Exoplanet (HabEx) Imaging Mission and Large UV, Optical, Infrared (LUVOIR) mission concepts. High-cooling-power, high-efficiency, high-duty-cycle sub-Kelvin coolers are required for the next generation of sensitive instruments. Both Cosmic Origins (COR) and Physics of the Cosmos (PCOS) Program Annual Technology Reports (PATRs) listed sub-Kelvin cooling as technology gaps ("*High Performance Sub-Kelvin Coolers*" and "*High-efficiency cooling systems covering the range from 20 K to under 1 K*", respectively).

Sub-Kelvin temperatures in space are produced by a combination of mechanical cryocoolers at the upper-temperature end and specialized sub-Kelvin coolers operating from a few K to less than 0.05 K. There are several ways to produce this low temperature: ADRs, dilution refrigerators, and a combination of sorption cooling and adiabatic demagnification. An ADR, having a thermodynamic efficiency close to Carnot, is the most efficient way to produce sub-Kelvin temperatures. It provides cyclic cooling by raising the magnetic field in a paramagnetic material, removing the resulting heat from the material, and then cooling it by reducing the field. Our team invented a method to produce high-heat-lift

continuous cooling with a multi-stage continuous ADR (CADR). We demonstrated a TRL-4 CADR with 6.5 μW of continuous cooling at 50 mK, a significant improvement over the 0.7 μW cooling provided for about 40 hours per cycle on Astro-H/Soft X-ray Spectrometer (SXS). That CADR can alternatively provide 31 μW at 100 mK compared to the 0.2 μW of cooling achieved on Planck. The CADR rejects its heat to a cryocooler at temperatures as high as 4.5 K.

In addition to detector cooling, several proposed far-IR space observatories require telescopes to be at 2–6 K to limit self-emission. This is much colder than the approximately 30 K that can be achieved via passive cooling, as in the James Webb Space Telescope (JWST). This technology need is listed in the COR PATR ("*Advanced Cryocoolers*"). The combination of a highly reliable mechanical cryocooler reaching 10 K and a CADR cooling from 10 to 4 K will provide a low-input-power solution to fill this technology gap.

Many space observatories require extremely stable pointing. The CADR, which has no moving parts, is vibration-free, but it is just part of a cooling chain. Currently, the CADR rejects its heat at 4 K, limiting the choice of upper stage coolers to linear piston cryocoolers. Jitter caused by such coolers has been a problem for recent astrophysics missions. Miniature turbo-Brayton coolers offer a solution to this problem, as was demonstrated by the 70-K cooler for the Hubble Space Telescope (HST) Near Infrared Camera and Multi-Object Spectrometer (NICMOS) instrument. There are difficulties extending this technology to 4 K, but an engineering unit has recently demonstrated significant cooling power at 10 K. Thus, extending the CADR heat rejection temperature from 4 to 10 K will enable sub-Kelvin detectors in observatories with tight pointing requirements.

Figure 1 shows our full CADR schematically. The left side of the image is the four-stage 4-to-0.05-K CADR. The stages are thermally connected in series via heat switches. The first stage, on the very left, remains continuously at 0.05 K. The other stage temperatures rise and fall as the heat switches open and close in a sequence that pumps heat from the cold source to the continuous 4-K stage. The 10-to-4-K CADR is on the right side. It consists of two parallel stages, which alternatively cool the 4-K stage and warm up to just above 10 K to dump heat to the cryocooler. Each magnet in the system has its own ferromagnetic shield to minimize its stray magnetic field and to enhance the field inside the magnet bore. The entire system is surrounded by a second shield, which further reduces any field fluctuations caused by the magnets. Figure 2 shows a preliminary conceptual design with the overall shield cut away for clarity, and insets illustrating sectioned views of some key components.

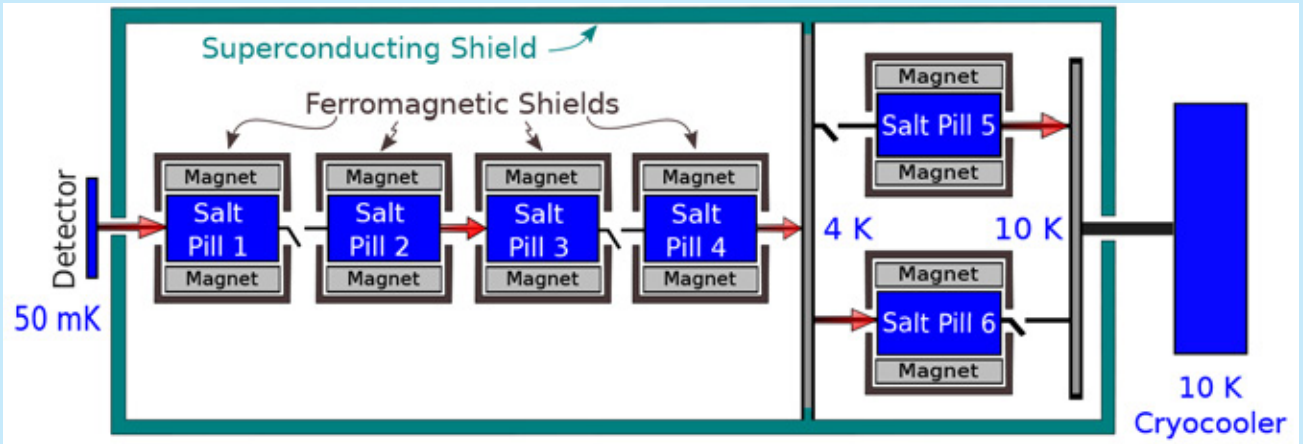

Fig. 1. *A schematic representation of our 10-to-0.05-K CADR.*

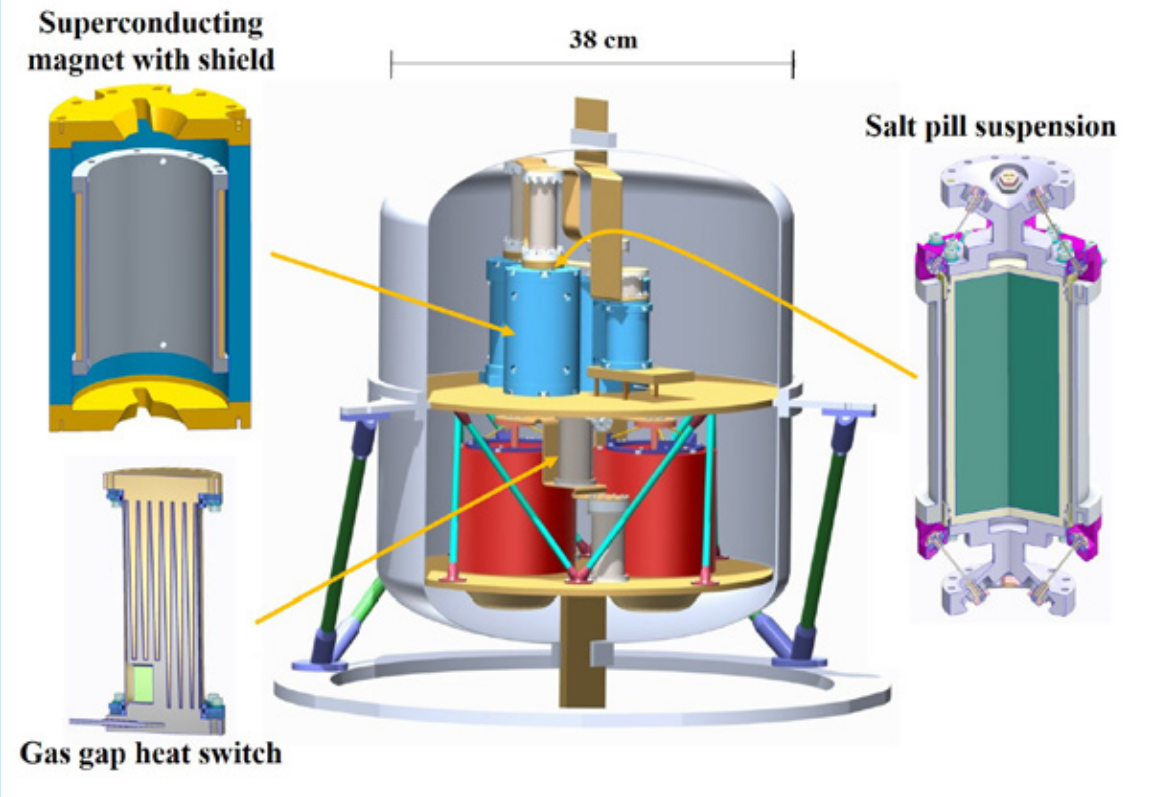

Fig. 2. *A preliminary conceptual design of the full CADR with the overall magnetic shield cut away for clarity. The insets show sectioned views of some key components.*

Our development plan is to demonstrate a single-stage 10-to-4-K ADR in Year 1, a two-stage 10-to-4-K CADR in Year 2, and a 10-to-0.05-K CADR in Year 3. In addition, we will develop an overall magnetic-shielding scheme which nearly eliminates any nearby field fluctuations caused by our CADR operation. The complete system will be tested before and after vibration in order to demonstrate TRL 6.

Objectives and Milestones

Our first major milestone will be met at the end of Year 1, when we will demonstrate a single-stage 10-to-4-K ADR. This device will include a unique 10-K magnet, developed several years ago under NASA's Small Business Innovative Research (SBIR) program. It will also include a passive gas-gap heat switch configured to work from 10 to 4 K, a ferromagnetic shield for the magnet, a paramagnetic salt pill inside a metal can, and a thermally isolating suspension system for the salt pill.

By the end of Year 2, we will meet our second major milestone by demonstrating continuous cooling at 4 K using a two-stage 10-to-4-K CADR. This will include two shielded 10-K magnets with salt pills suspended in them, two passive and two active gas-gap heat switches, and thermal straps connecting the pills and switches. It will require a customized control algorithm to keep the 4-K temperature constant to within 0.001 K. The target cooling at 4 K will be greater than 20 mW.

By the end of Year 3, we will assemble a flight-worthy version of our laboratory 4-to-0.05-K CADR and integrate it with the 10-to-4-K CADR. The resulting 10-to-0.05-K CADR will be surrounded by an overall magnetic shield to keep external field fluctuations below 5 μT. Our third major milestone will

be met in the third quarter of Year 3, when this assembly will be performance-tested, with a target of at least 5 μW of cooling at 0.05 K and better than 1 μK root-mean-square (rms) temperature stability at that temperature. We will then subject it to a vibration test chosen to envelope the acceptance levels expected for future cryogenic space missions. The final major milestone will be a successful post-vibration performance test by the end of Year 3.

Progress and Accomplishments

During the first five months of this effort, the team made significant progress toward the Year-1 goal, and also in addressing long-lead items critical to maintaining the schedule in Years 2 and 3.

A key enabling technology is the 10-K magnet (Fig. 3, left), developed via the SBIR program between 2002 and 2010. Early this year, we performed a detailed structural analysis on this magnet, identifying minor design details that need to be changed to make it flight-worthy. We also tested the performance of the prototype magnet that was delivered at the end of the SBIR effort. In addition to verifying the ability to ramp up its central magnetic field rapidly to 4 T, we carefully measured its internal resistance and the hysteretic heat generated in the magnet during the ramping process. Our test results showed that the magnet was suitable for use in our CADR, so we negotiated a purchase cost for three more of these magnets from the manufacturer. We initiated the procurement process, and these magnets should arrive at GSFC in Year 2 and early in Year 3. We will use the prototype unit for our Year-1 testing.

The right panel of Fig. 3 shows a passive gas-gap heat switch used in the 10-to-4-K CADR subsystem. One end of the switch is thermally linked to the salt pill that provides the cooling, while the other end is attached to a 10-K stage. When we ramp the magnetic field up to "re-charge" the salt pill, the pill temperature rises above 10 K. At this point, the switch automatically releases ^{3}He gas into its volume, creating a strong thermal link between its two ends. When we ramp the magnetic field down again, the pill cools below 10 K, the switch's gas is automatically adsorbed onto a charcoal "getter," and the salt pill is thermally de-coupled from the 10-K sink. The adsorption of the gas, which thermally "opens" the switch, must occur at an optimal temperature just below 10 K to achieve maximum ADR cooling. We achieve this by sealing the correct gas pressure inside the switch volume, and this pressure must ultimately be determined by trial and error. Before this effort, we used passive switches at lower temperatures but had never optimized one for use at 10 K. For our Year-1 testing, we obtained a spare heat switch left over from an earlier ADR effort. Using a combination of analysis and testing, we determined the optimum gas pressure for this switch. Its performance has been verified, and it is ready for use in the single-stage 10-to-4-K ADR.

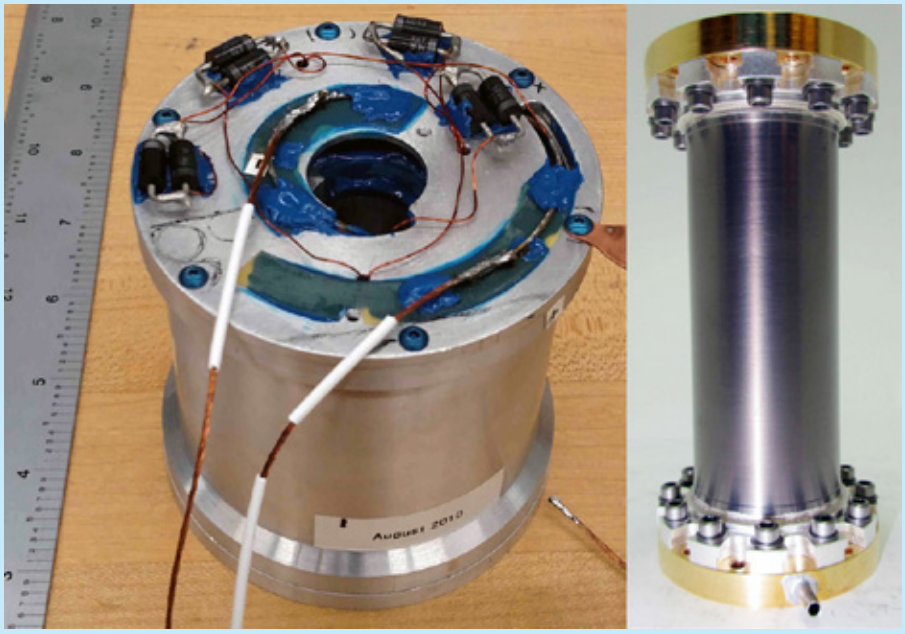

Fig. 3. Left: *The 10-K superconducting magnet, developed under NASA's SBIR program.* Right: *The 9-cm-tall passive gas-gap heat switch, configured for use in the 10-to-4-K ADR.*

We performed structural, thermal, and magnetic analyses on the 10-to-4-K magnet, magnetic shield, salt pill, and pill suspension to determine the optimum designs for these components. The left panel of Fig. 4 shows the magnetic field map produced by the magnetic modeling software. It verified for us that the salt pill length was optimized for maximum cooling capability and that the shield thickness was sufficient to avoid saturation at the maximum operating field. By extending the salt pill's length beyond the ends of the magnet coils, we were able to get significantly more cooling than our original hand-calculation predicted. Our modeling results enabled the final design of the 10-to-4-K subsystem (Fig. 4 right). Completing this design in early June allowed us to initiate the long-lead procurement of the gadolinium-gallium-garnet (GGG) salt pills. As of mid-June we are about to begin fabrication of the other parts needed for the single-stage 10-to-4-K ADR.

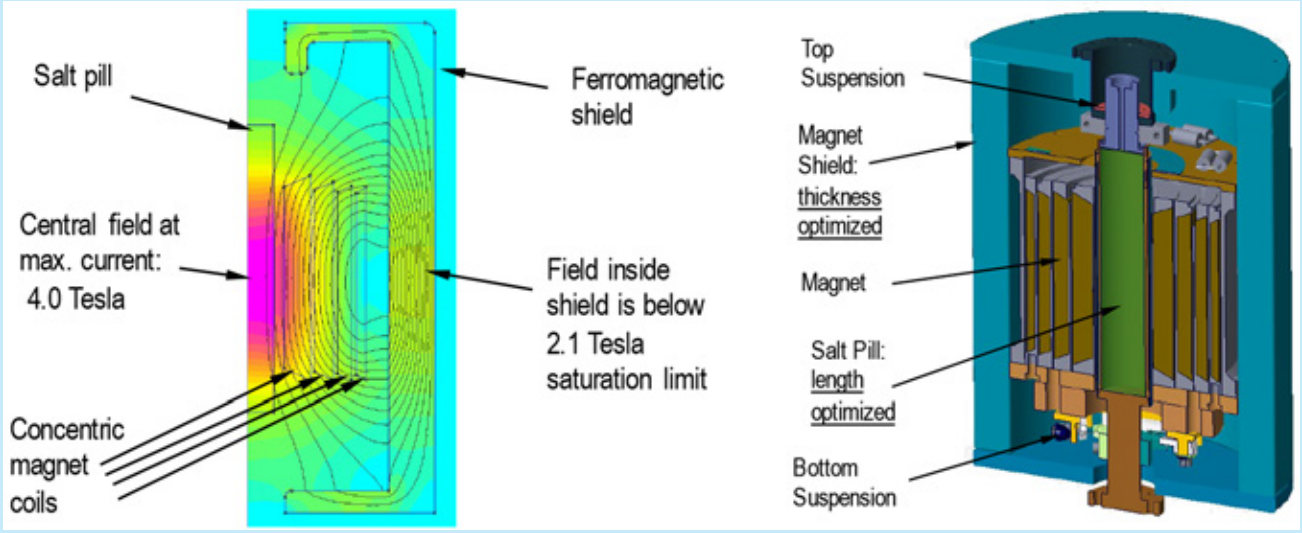

Fig. 4. Left: *The magnetic field map of our 10-to-4-K ADR's magnet, shield, and salt pill.* Right: *The final mechanical design model for a single 10-to-4-K ADR stage.*

Most of the components in the 4-to-0.05-K CADR will be exact duplicates of components in an existing laboratory CADR. This subsystem will not be assembled until Year 3, but we have already begun fabricating parts for it. Some of the more intricate parts must be cut using an electrostatic discharge machining (EDM) process. Our group has an EDM device, and we have an in-house machinist who used it to make ADR parts. We have prioritized the fabrication of these EDM-cut parts, since the machinist and facility will be available intermittently over the next two years. Most of the other parts will be machined by external shops, so their timing is less of a concern.

The Year-1 component and ADR testing is being performed in a small cryostat, but the CADR subsystems and full system would not fit in this facility. After some negotiations with ongoing flight projects, we identified and took control of a test cryostat large enough to accommodate our full 10-to-0.05-K CADR with its overall shield. Figure 5 shows this facility in use in our lab.

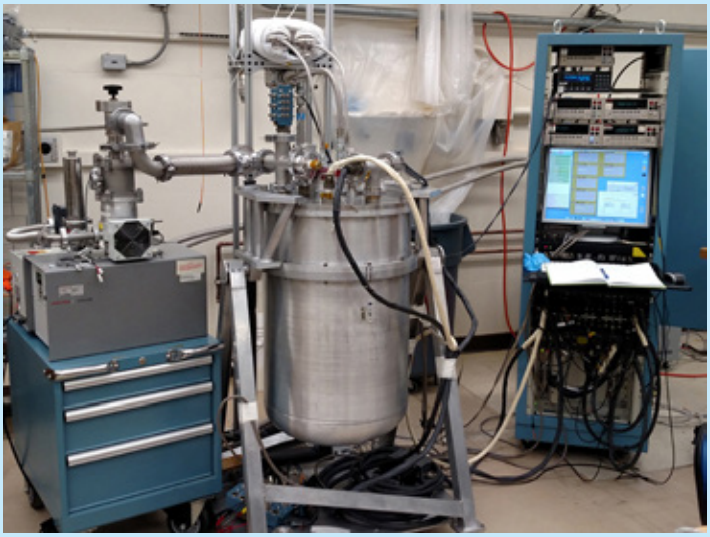

Fig. 5. *The cryostat which will be used for testing our full 10-to-4-K CADR.*

In May and June, two members of our team participated in preliminary design studies for future instruments for OST and Lynx. The three instruments studied will include CADRs very similar to our 4-to-0.05-K subsystem, so we were able to get insight into which specific aspects of our design are most important to future customers. We learned that for these instruments, maximizing cooling power is more important at the 2-to-4-K optics stage than at the 0.05-K detector stage. In addition, at this time our planned CADR size and mass are acceptable for all three potential customers. It was encouraging to get specific confirmation that the CADR we will bring to TRL 6 will meet the needs of specific instruments on future missions.

Path Forward

In the second half of Year 1, we will produce drawings and fabricate the remaining parts for the single-stage 10-to-4-K ADR. These include the magnetic shield, the salt pill containment can, and the salt-pill-suspension system parts. We will make duplicates of each part, since we will need a second, identical stage for the CADR in Year 2. Once the shield is completed, we will install it on the existing

10-K magnet and measure the performance of the shielded magnet. Later in the year, we will assemble the single-stage ADR and performance-test it to meet our Year-1 milestone. In parallel, we will continue to fabricate parts needed for the 10-to-4-K CADR in Year 2 and the 4-to-0.05-K CADR in Year 3. If time and resources allow, we will fabricate the overall magnetic shield and test its effectiveness in Year 1. In Years 2 and 3, we will proceed with our original development plan, as described above.

For additional information, contact James Tuttle: *james.g.tuttle@nasa.gov*

Ultra-Sensitive Far-IR Bolometers

By: Charles Bradford (JPL)

We propose to demonstrate flight readiness with the world's most sensitive bolometers: transition-edge-sensed (TES) devices which meet the requirement for zodical-light-limited far-IR spectroscopy on cold space telescopes. Building on our success with single pixels and small arrays, we will fabricate and characterize TES bolometer arrays which:

1. Demonstrate a per-pixel noise equivalent power (NEP) less than 1×10^{-19} W/$\sqrt{}$(Hz).
2. Provide sufficient speed of response (f_{3dB} >10 Hz (requirement), 15 Hz (goal)) to be useful in a range of instrument configurations.
3. Are read out with a frequency-domain multiplexing scheme which is scalable to enable a mission with tens of thousands of detectors at 50 mK.
4. Can maintain high duty cycle in the face of cosmic-ray interactions in space.

This work on low-NEP detector development is directly applicable to future far-IR space missions such as SPICA and the Origins Space Telescope (OST). These missions feature cryogenic telescopes, which when combined with dispersive spectrographs at the background limit (hereafter referred to as BLISS-type) create powerful spectroscopic facilities with 1–4 orders of magnitude sensitivity improvement over the current state of the art. This advance will bring far-IR sensitivities into parity with those of the powerful flagship programs at shorter and longer wavelengths: JWST and ALMA, but providing unique access to the most dust-enshrouded star formation and black hole growth in the universe's first billion years.

We will build on our broad experience in all of these aspects from ground-based instrumentation, Herschel, and Planck; and our work on the BLISS-specific bolometer technology to design and demonstrate a full focal-plane array system and testbed to verify performance against the requirements. While NASA's TRL definitions are broad and subject to interpretation, we submit that the current state of the technology is TRL 4, and our proposed system-level advances will position this far-IR detector + readout technology at TRL 6, 'system demonstration in a relevant end-to-end environment.'

Development of Digital Micromirror Devices for Far-UV Applications

By: Zoran Ninkov (RIT)

We propose to develop commercially available digital micromirror devices (DMDs) for use in the far ultraviolet (FUV) and near ultraviolet (NUV) regimes of 100 nm – 400 nm, using recently developed FUV mirror coatings. DMDs can be used as rapidly reconfigurable "slit mask" object-selectors in space-based UV multi object spectrometers (MOS). Currently, DMDs are the only alternative to microshutter arrays, which were developed for the infrared MOS on the James Webb Space Telescope. The need for an efficient UV MOS has been identified as a Priority 1 Technological Gap by the general community, according to the Cosmic Origins 2016 Program Annual Technology Report. There are several missions currently in the planning process, which are developing concepts for multi-object spectrometers. For example both LUVOIR and HabEx plan to include such an instrument, working into the UV. Several smaller dedicated spectroscopic survey missions based around a highly multiplexed spectrometer have also been proposed. The choice of slit selector for such instruments is limited. While microshutter arrays are currently viewed as the frontrunner, the previous generation of microshutters has limitations and the next generation is still in early development. We have worked extensively on space qualification of the Texas Instruments DMDs and have shown the current generation of these devices to be ideal for space applications. However the deep UV (100 nm - 300 nm) reflectivity of such devices needs to be substantially higher. We will re-coat commercially available DMDs (which use aluminum alloy mirrors) with high reflectivity aluminum, which is protected by an overcoat using recently developed FUV-enhanced thin films (LiF and AlF_3). These protected aluminum coatings were developed to have a high reflectivity in the FUV range of 100 nm – 300 nm by two recent SAT projects. This work will build on our own previous SAT-funded efforts to determine the usability of DMDs in space and to extend their use into the NUV range of 200 nm – 400 nm. As part of this work we will produce re-coated DMDs with a high reflectivity in the FUV (with and without a protective window) and investigate the susceptibility of these devices to damage due to long exposures to highly energetic FUV photons. DMDs that operate in the FUV range will provide an alternative to microshutter arrays and help close a critical technology gap in FUV/NUV astronomy.

High Performance Sealed Tube Cross Strip Photon Counting Sensors for UV-Vis Astrophysics Instruments

By: Oswald Siegmund (U.C. Berkeley)

The objective of this program is to exploit the developments in atomic layer deposited (ALD) microchannel plates (MCPs), photocathodes and cross strip (XS) readout techniques to provide a new generation of enhanced performance sealed tube photon counting sensors that span the 115 nm to 400 nm regime. Efforts in all the subcomponent areas have achieved considerable technical development and heritage, but putting them into a robust integrated package with advanced TRL for the next UV-Vis Astrophysics instruments has not been done to date. Component developments include ALD MCP formats up to 127 × 127 mm with 10 µm pores, background rates of ~0.05 events/cm^2/sec, and extended lifetimes to >10 C/cm^2. XS anodes and electronics have shown spatial resolutions of <18 µm FWHM over formats of 100 mm × 100mm and event handling rates of 5 MHz at <15% dead time. Photocathodes in the FUV can achieve 50% quantum efficiency at ~115 nm and 30% at 200 nm – 300 nm with cutoffs above 400 nm. Combining these developments has a significant impact to potential future NASA sub-orbital and satellite instruments. These advancements will enable high spatial resolution improvements to MCP based spaceflight detectors for imaging and spectroscopic instruments from small to large (>10 cm) formats in the UV to Visible regimes. The smaller pore sizes (~ 10 µm) and high resolution XS readouts will facilitate higher spatial resolutions over the large formats. At the same time the reduced (÷3) detection efficiency for high-energy background events demonstrated by use of ALD MCPs will also improve observational sensitivities. The chemical compatibility of the new MCP borosilicate glass and the ALD materials has the potential to provide further improvements in the stability and lifetime of these detectors due to the rigorous pre-conditioning steps for sealed tubes. In addition, improvements in fabrication processes provide the opportunity to reduce the imaging fixed pattern modulation and thermal resistance changes. XS readouts integrated into sealed tube packages can also fully take advantage of the efforts currently taking place to establish high performance, spaceflight compatible, low power-mass-volume ASIC readout electronics. These developments will together provide a significant step in the realization of high performance, robust, MCP detectors for the next generations of UV Astrophysics instruments.

Development of a Robust, Efficient Process to Produce Scalable, Superconducting kilopixel Far-IR Detector Arrays

By: Johannes Staguhn (JHU)

We propose to develop and streamline the fabrication processes required to produce background limited large far-infrared arrays with large pixel numbers n ~ 10^5. We will achieve this goal by combining mature detector and readout technologies from our previous work, to fabricate a robust, close packed high sensitivity bolometer array with reliable high-quantum efficiency absorbers that operates over the entire FIR range and can be efficiently and reliably produced. The simplified process will integrate detector arrays through superconducting bonds to a cold readout multiplexer. It is very versatile in its applications, since it will allow the mating of TES detectors to time domain, frequency domain, microwave and code division multiplexers.

The main objectives will be achieved by meeting the following goals:

a) Develop a novel BUG architecture in which the superconducting through via process is separated from the detector production, improving production speed and reducing risk; and
b) Production of background-limited 5-kilopixel arrays suitable for the FIR spectrometer Super-HIRMES.

For the latter we will additionally:

c) Refine our AlMn process for quickly and reliably fabricating TES with highly predictable and uniform transition temperatures (better less than 5% variation) across the entire wafer; and
d) Refine a standard process for reliably fabricating impedance- matched and robust absorbers for the entire FIR wavelength range, which are not susceptible to room temperature aging.

Appendix D
Acronyms

A

AAS . . . . . American Astronomical Society
ADC. . . . . Analog-to-Digital Converter
ADR. . . . . Adiabatic Demagnetization Refrigerator
AES . . . . . Auger Electron Spectroscopy
AFM. . . . . Atomic Force Microscope/Microscopy
AFRC . . . . . Armstrong Flight Research Center
AGN. . . . . Active Galactic Nuclei
AIP . . . . . Astrophysics Implementation Plan
ALD . . . . . Atomic Layer Deposition
ALE . . . . . Atomic Layer Etching
ALMA. . . . . Atacama Large Millimeter/submillimeter Array
AMM . . . . . Arnold Mirror Modeler
AMSD . . . . . Advanced Mirror System Demonstrator
AMTD . . . . . Advanced Mirror Technology Development
AOS . . . . . Arizona Optical Systems
APD. . . . . Astrophysics Division
APD. . . . . Avalanche Photo Diode
APL . . . . . Applied Physics Laboratory, Johns Hopkins
APRA. . . . . Astrophysics Research and Analysis
AR . . . . . Anti-Reflection
ARC. . . . . Ames Research Center
ASIC . . . . . Application-Specific Integrated Circuit
ASU . . . . . Arizona State University
ATLAST . . . . . Advanced Technology Large-Aperture Space Telescope
ATT . . . . . Advanced Technology Telescope
AURA. . . . . Association of Universities for Research in Astronomy

B

BETTII. . . . . Balloon Experimental Twin Telescope for Infrared Interferometry
BLAST-TNG . . . . . Balloon-borne Large-Aperture Sub-millimeter Telescope - The Next Generation

C

CADR. . . . . Continuous Adiabatic Demagnetization Refrigerator
CCD. . . . . Charge-Coupled Device
CFRP . . . . . Carbon Fiber Resin Epoxy
CGI . . . . . Coronagraph Instrument
CHESS . . . . . Colorado High-Resolution Echelle Stellar Spectrograph
CMB . . . . . Cosmic Microwave Background
CME. . . . . Coronal-Mass Ejection
CMOS . . . . . Complementary Metal-Oxide Semiconductor
COPAG . . . . . Cosmic Origins Program Analysis Group
COR. . . . . Cosmic Origins
COS . . . . . Cosmic-Origins Spectrograph
COTS . . . . . Commercial-Off-the-Shelf
CSA . . . . . Charge-Sensitive Amplifier
CTE . . . . . Coefficient of Thermal Expansion

cw . . . . . Continuous wave
CWI . . . . . Cosmic Web Imager

D

DAC . . . . . Digital-to-Analog Converter
DARE . . . . . Dark Ages Radio Explorer
DARPA . . . . . Defense Advanced Research Projects Agency
DDR . . . . . Double Data Rate
DFB . . . . . Distributed Feedback
DLR . . . . . Forschungszentrum der Bundesrepublik Deutschland fu_r Luft- und Raumfahrt (German Aerospace Research Center)
DM . . . . . Deformable Mirror
DMD . . . . . Digital Micro-mirror Device

E

EAG . . . . . Experimental Astrophysics Group
ECR . . . . . Electron Cyclotron Resonance
EDA . . . . . Electronic Design Automation
EDM . . . . . Electrostatic Discharge Machining
ELZM . . . . . Extreme-Lightweight Zerodur® Mirror
EMCCD . . . . . Electron-Multiplying Charge-Coupled Device
EoR . . . . . Epoch of Reionization
ESA . . . . . European Space Agency
ExEP . . . . . Exoplanet Exploration Program

F

Far-IR . . . . . Far Infrared
Far-UV . . . . . Far Ultraviolet
FGS . . . . . Fine Guidance Sensor
FIR . . . . . Far IR
FIR . . . . . Finite Impulse Response
FIREBall . . . . . Faint Intergalactic medium Redshifted Emission Balloon
FOV . . . . . Field of View
FPA . . . . . Focal-Plane Array
FPC . . . . . Flexible Printed Circuit
FPGA . . . . . Field Programmable Gate Array
FTS . . . . . Fourier Transform Spectroscopy
FUSE . . . . . Far-Ultraviolet Spectroscopic Explorer
FUV . . . . . Far Ultraviolet
FWHM . . . . . Full-Width at Half-Maximum
FY . . . . . Fiscal Year

G

GALEX . . . . . Galaxy Evolution Explorer
GEVS . . . . . General Environmental Verification Standard
GGG . . . . . Gadolinium-Gallium-Garnet
GOLD . . . . . Global-scale Observations of the Limb and Disk
GRAPH . . . . . Gigasample Recorder of Analog waveforms from a PHotodetector
GSFC . . . . . Goddard Space Flight Center
GUSTO . . . . . Galactic/Extragalactic ULDB Spectroscopic Terahertz Observatory
GUSSTO . . . . . Galactic/Xtragalactic ULDB Spectroscopic Stratospheric Terahertz Observatory
GW . . . . . Gravitational Wave

H

HabEx . . . . . Habitable Exoplanet (Imaging Mission)
HAWC . . . . . High-resolution Airborne Wide-bandwidth Camera
HDST. . . . . High-Definition Space Telescope
HEB. . . . . Hot Electron Bolometer
HEM . . . . . Heat Exchanger Method
HEMT . . . . . High Electron Mobility Transistor
HF . . . . . Hydrogen Fluoride
HIRMES . . . . . HIgh-Resolution Mid-infrarEd Spectrometer
HQ . . . . . Headquarters
HSO. . . . . Herschel Space Observatory
HST . . . . . Hubble Space Telescope
HV. . . . . High Voltage

I

IBM . . . . . International Business Machines Corp.
ICON . . . . . Ionospheric Connection Explorer
ICP . . . . . Inductive-Coupled Plasma
IF. . . . . Intermediate Frequency
IGM . . . . . Intergalactic Medium
IISW . . . . . International Image Sensor Workshop
iPlas. . . . . Innovative Plasma Chemical Vapor Deposition
IR . . . . . Infrared
IWA . . . . . Inner Working Angle

J

JATIS . . . . . Journal of Astronomical Telescopes, Instruments, and Systems
JAXA . . . . . Japanese Aerospace eXploration Agency
JHU . . . . . Johns Hopkins University
JPL. . . . . Jet Propulsion Laboratory
JVST. . . . . Journal of Vacuum Science and Technology
JWST . . . . . James Webb Space Telescope

L

LBL . . . . . Lawrence Berkeley National Laboratory
LDB . . . . . Long-Duration Balloon
LET . . . . . Linear Energy Transfer
LIGO . . . . . Laser Interferometer Gravitational-Wave Observatory
LISA Pathfinder . . . . Laser Interferometer Space Antenna Pathfinder
LISM . . . . . Local Interstellar Medium
LN . . . . . Liquid Nitrogen
LO . . . . . Local Oscillator
LRA . . . . . Lunar Radio Array
LSBs . . . . . Least Significant Bits
LTF . . . . . Low-Temperature Fusion
LTS . . . . . Low-Temperature-Slumping
LUVOIR . . . . . Large UV/Optical/IR
LVDS . . . . . Low-Voltage Differential Signaling
L3ST . . . . . L3 Study Team

M

MBE. . . . . Molecular Beam Epitaxy
MCP. . . . . Micro-Channel Plate
MFC. . . . . Mass-Flow Controller

MIDEX . . . . . Medium-Class Explorer
MIRI . . . . . Mid-Infrared Instrument
MIT . . . . . Massachusetts Institute of Technology
MKID . . . . . Microwave Kinetic Inductance Detector
MMSD . . . . . Multi-Mirror System Demonstration
MMSD . . . . . Multiple Mirror System Demonstrator
MPC . . . . . Model Predictive Control
MOS . . . . . Multi-Object Spectrograph/Spectroscopy
MSFC . . . . . Marshall Space Flight Center
MUXs . . . . . Multiplexers

N

NA . . . . . National Academies
NASA . . . . . National Aeronautics and Space Administration
NDAs . . . . . Non-disclosure Agressments
Near-IR . . . . . Near Infrared
NEP . . . . . Noise-Equivalent Power
NICMOS . . . . . Near Infrared Camera and Multi-Object Spectrometer
NIR . . . . . Near-infrared
NIRISS . . . . . Near-Infrared Imager and Slitless Spectrograph
NIS . . . . . Normal Insulator Superconductor
NIST . . . . . National Institute of Standards and Technology
NPR . . . . . NASA Procedural Requirements
NRC . . . . . National Research Council
NSF . . . . . National Science Foundation
NUV . . . . . Near Ultraviolet
NWNH . . . . . New Worlds, New Horizons in Astronomy and Astrophysics (2010 Decadal Survey)
NWTD . . . . . New Worlds Technology Development

O

OCT . . . . . Office of the Chief Technologist
OD . . . . . Outer Diameter
OST . . . . . Origins Space Telescope (formerly the Far-IR Surveyor)

P

PAG . . . . . Program Analysis Group
PATR . . . . . Program Annual Technology Report
PCOS . . . . . Physics of the Cosmos
PDR . . . . . Photo-Dissociation Region
PDR . . . . . Preliminary Design Review
PEALD . . . . . Plasma-Enhanced Atomic Layer Deposition
PI . . . . . Principal Investigator
PID . . . . . Proportional Integral Differential
PMA . . . . . Primary Mirror Assembly
PMOS . . . . . P-type Metal-Oxide-Semiconductor
PSF . . . . . Point Spread Function
PTC . . . . . Predictive Thermal Control
PV . . . . . Peak-to-Valley
PVD . . . . . Physical Vapor Deposition
PXS . . . . . Parallel Cross Strip
PZC . . . . . Pole-Zero Cancellation
PZTs . . . . . Piezoelectric Actuators

Q

QCL . . . . . Quantum-Cascade Laser
QE . . . . . Quantum Efficiency
QSO . . . . . Quasi-Stellar Object

R

RAL . . . . . Rutherford Appleton Laboratory
RF . . . . . Radio Frequency
RFI . . . . . Request for Information
RH . . . . . Relative Humidity
RIT . . . . . Rochester Institute of Technology
rms . . . . . Root mean square
ROC . . . . . Radius of Curvature
ROI . . . . . Regions of Interest
ROLSS . . . . . Radio Observatory on the Lunar Surface for Solar Studies
ROSES . . . . . Research Opportunities in Space and Earth Sciences

S

SAO . . . . . Smithsonian Astrophysical Observatory
SAT . . . . . Strategic Astrophysics Technology
SB . . . . . Solar-Blind
SBIR . . . . . Small Business Innovative Research
sCMOS . . . . . Scientific Complementary Metal-Oxide-Semiconductor
SCR . . . . . Silicon Controlled Rectifier
SEE . . . . . Single Event Effect
SEU . . . . . Single Event Upset
SFE . . . . . Surface Figure Error
SFO . . . . . Star Formation Observatory
SGT . . . . . Stinger Ghaffarian Technologies
SHV . . . . . Safe High Voltage
SIG . . . . . Science Interest Group
SL . . . . . Superlattice
SLAR . . . . . SL-doped, AR-coated
SMD . . . . . Science Mission Directorate
SMEX . . . . . Small Explorer
SNR . . . . . Signal-to-Noise Ratio
SOFIA . . . . . Stratospheric Observatory for Infrared Astronomy
SOTA . . . . . State of the Art
SPICA . . . . . Space Infrared Telescope for Cosmology and Astrophysics
SPIE . . . . . Society of Photo-optical Instrumentation Engineers
SPUD . . . . . Solid-state Photon-counting Ultraviolet Detector
SR&T . . . . . Supporting Research and Technology
SRON . . . . . Space Research Organization Netherlands
SSL . . . . . Space Sciences Laboratory
STDT . . . . . Science and Technology Definition Team
STM . . . . . Science Traceability Matrix
STMD . . . . . Space Technology Mission Directorate
STO . . . . . Stratospheric Terahertz Observatory
STOP . . . . . Structural-Thermal-Optical-Performance
STScI . . . . . Space Telescope Science Institute
SXS . . . . . Soft X-ray Spectrometer

T

TARGET . . . . . TeV Array Readout with GSa/s sampling and Event Trigger
TCOR. . . . . Technology development for Cosmic Origins
TI . . . . . Texas Instruments
TID . . . . . Total Ionizing Dose
TIG . . . . . Technology Interest Group
TMA. . . . . Trimethylaluminum
TMB. . . . . Technology Management Board
TRL . . . . . Technology Readiness Level
TSMC. . . . . Taiwan Semiconductor Manufacturing Company

U

UC . . . . . University of California
UHV . . . . . Ultra-High Vacuum
ULDB. . . . . Ultra-Long-Duration Balloon
ULE® . . . . . Ultra-Low Expansion
UNM . . . . . University of New Mexico
UPS . . . . . Ultraviolet Photoelectron Spectroscopy
US . . . . . United States
USA . . . . . United States of America
UV . . . . . Ultraviolet
UVOIR . . . . . UV/Optical/IR

V

VUV. . . . . Visible and UV

W

WaSP . . . . . Wafer-Scale Imager for Prime instrument
WFE. . . . . Wavefront Error
WFIRST . . . . . Wide-Field Infrared Survey Telescope
WFSC. . . . . Wavefront Sense and Control
WISE . . . . . Wide-field Infrared Survey Explorer
WPE. . . . . Wall-plug Power Efficiency

X

XGA. . . . . eXtended Graphics Array
XPS . . . . . X-ray Photoelectron Spectroscopy
XRCF . . . . . X-Ray and Cryogenic Facility
XS . . . . . Cross-Strip